ISSN: 2153-1196 Volume 13, Number 5, May 2022

Scientific Research Publishing

Journal of Modern Physics

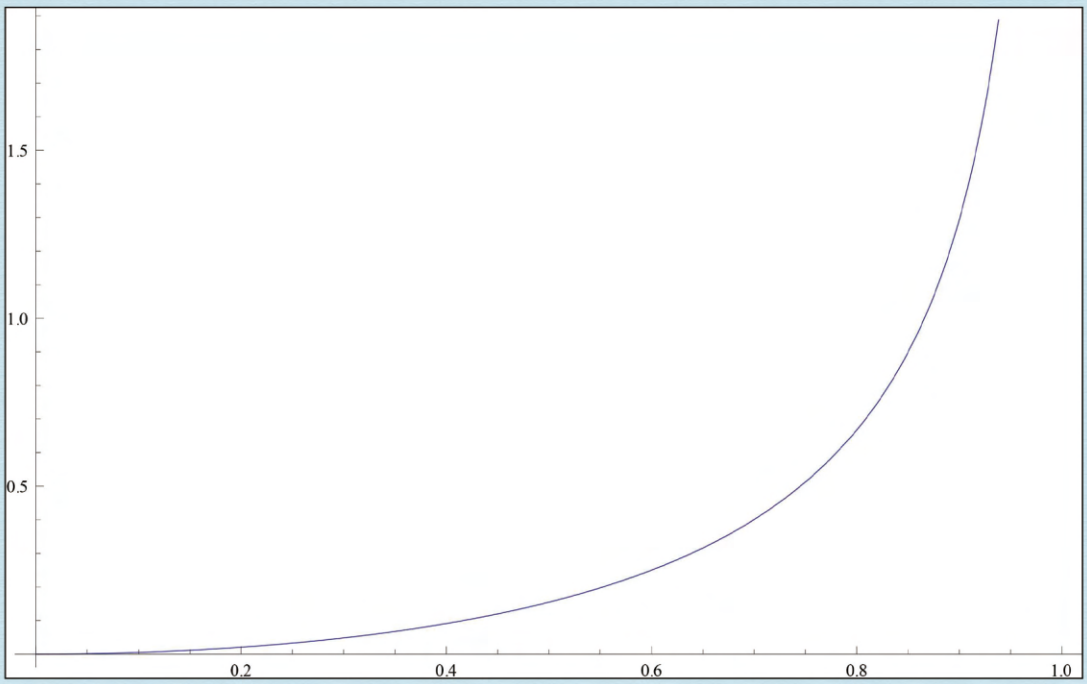

ISSN: 2153-1196
9 772153 119007 05

https://www.scirp.org/journal/jmp

Journal Editorial Board

ISSN: 2153-1196 (Print) ISSN: 2153-120X (Online)
https://www.scirp.org/journal/jmp

Editor-in-Chief

Editorial Board

Scientific Research Publishing

Journal of Modern Physics, 2022, 13, 671-838
https://www.scirp.org/journal/jmp
ISSN Online: 2153-120X
ISSN Print: 2153-1196

Table of Contents

Volume 13 Number 5 May 2022

The figure on the front cover is from the article published in Journal of Modern Physics, 2022, Vol. 13, No. 5, pp. 671-681 by Gustavo V. López.

Journal of Modern Physics (JMP)
Journal Information

SUBSCRIPTIONS

The *Journal of Modern Physics* (Online at Scientific Research Publishing, https://www.scirp.org/) is published monthly by Scientific Research Publishing, Inc., USA.

Subscription rates:
Print: $89 per issue.
To subscribe, please contact Journals Subscriptions Department, E-mail: sub@scirp.org

SERVICES

Advertisements
Advertisement Sales Department, E-mail: service@scirp.org

Reprints (minimum quantity 100 copies)
Reprints Co-ordinator, Scientific Research Publishing, Inc., USA.
E-mail: sub@scirp.org

COPYRIGHT

PRODUCTION INFORMATION

For manuscripts that have been accepted for publication, please contact:
E-mail: jmp@scirp.org

Journal of Modern Physics, 2022, 13, 671-681
https://www.scirp.org/journal/jmp
ISSN Online: 2153-120X
ISSN Print: 2153-1196

About Quantum Mechanics without Hamiltonians

Gustavo V. López

Departamento de Física, CUCEI, Universidad de Guadalajara, Guadalajara, Mexico
Email: gulopez@udgserv.cencar.udg.mx

How to cite this paper: López, G.V. (2022) About Quantum Mechanics without Hamiltonians. *Journal of Modern Physics*, **13**, 671-681.
https://doi.org/10.4236/jmp.2022.135037

Received: March 20, 2022
Accepted: May 6, 2022
Published: May 9, 2022

Abstract

An extension of Shrödinger's quantization on the space $(\mathbf{x},\mathbf{p})$, where the Hamiltonian approach is needed, is made on the space $(\mathbf{x},\mathbf{v})$ where the Hamiltonian approach is not needed at all. The purpose of this paper is to give a possible extension of the actual formulation of the Quantum Mechanics, and this is achieved through a function $K(\mathbf{x},\mathbf{v},t)$ which takes the place of the Hamiltonian on the Shrödinger's equation and has units of energy. This approach allows us to include the quantization of classical velocity depending problems (dissipative) and position depending mass variation problems. Some examples are given.

Keywords

Quantization in the Space $(\mathbf{x},\mathbf{v})$, Mass Positiondepending, Shrödinger's Equation

1. Introduction

Despite the enormous success of the Hamilton formulation of the Quantum Mechanics [1] [2] [3] [4], there are still some problems in the Hamiltonian Classical Mechanics formalism with ambiguities which become evident when one tries to make their quantization, for example, dissipative [5] and mass variation [6] problems. In addition, even some simple problems [7] can have the ambiguity of having two different Hamiltonians describing the same classical dynamics, but when their quantization is made, they describe different quantum dynamics [8]. These are the main reasons that one would like to study the possibility of making a quantization of systems without the Hamiltonian formulation [9]. Another reason would be that this different formulation could represent a possible exten-

sion of the same Quantum Mechanics Theory, and this will be carried out here for the first time.

In this work, it is proposed to make the quantization in terms of the variables $(\mathbf{x},\mathbf{v})$, where $\mathbf{v}=\dot{\mathbf{x}}$, instead of the variables $(\mathbf{x},\mathbf{p})$, where $\mathbf{p}$ is the generalized linear momentum deduced from a Lagrangian of the system, $p_j=\partial L/\partial \dot{x}_j$ $j=1,2,3$, in fact, this was done firstly by Heisenberg at his beginning of the matrix theory quantization. In this way, one can get rid of the Hamiltonian formulation, and the goal is to obtain a function $K(\mathbf{x},\mathbf{v},t)$ (having the energy as units) that can take the place of the Hamiltonian $H(\mathbf{x},\mathbf{p},t)$ in the Schrödinger's equation.

2. Classical Function *K*(x, v, *t*)

In this section, the analysis of several classical examples and cases will be made to obtain a function $K(\mathbf{x},\mathbf{v},t)$ that can be used for quantization of the classical system in terms of its variables $\mathbf{x}$ and $\mathbf{v}$.

2.1. Conservative Systems

Consider a conservative system which describes the motion in the space of a particle of mass position depending, $m(\mathbf{x})$, under a position depending force $\mathbf{F}(\mathbf{x})$. Its Newton's equation of motion is

$$\frac{\mathrm{d}}{\mathrm{d}t}(m_0\mathbf{v})=\mathbf{F}(\mathbf{x}). \tag{1}$$

This type of systems are invariant under Galileo's transformations, as it is well known, and the so called energy is a constant of motion of the system,

$$K(\mathbf{x},\mathbf{v})=\frac{1}{2}m_0\mathbf{v}^2-\int\mathbf{F}(\mathbf{x})\cdot\mathrm{d}\mathbf{x}, \tag{2}$$

where the first term represents the kinetic energy, and the second one is the potential energy.

2.2. Conservative Systems with Position Depending Mass

Consider a conservative system which describes the motion in the space of a particle of mass position depending, $m(\mathbf{x})$, under a position depending force $\mathbf{F}(\mathbf{x})$. Its Newton's equation of motion is

$$\frac{\mathrm{d}}{\mathrm{d}t}(m(\mathbf{x})\mathbf{v})=\mathbf{F}(\mathbf{x}). \tag{3}$$

One must point out that this type of systems are not invariant under Galileo's transformation [10], and Sommerfeld's invariant formulation [11] is not satisfactory [12]. However, one can still keep (3) as the right description of the problem [13]. Therefore, multiplying on both side of this expression by $m(\mathbf{x})\mathbf{v}$, rearranging terms, and integrating with respect the time, one gets

$$\frac{1}{2}(m(\mathbf{x})\mathbf{v})^2=\int m(\mathbf{x})\mathbf{F}(\mathbf{x})\cdot\mathbf{v}\mathrm{d}t+C, \tag{4}$$

where C is the integration constant. Knowing that one has the relation $\mathbf{v}\mathrm{d}t = \mathrm{d}\mathbf{x}$, and dividing the above expression by a characteristic mass m_0, the following constant of motion is gotten

$$K(\mathbf{x},\mathbf{v}) = \frac{\left(m(\mathbf{x})\mathbf{v}\right)^2}{2m_0} - \frac{1}{m_0}\int m(\mathbf{x})\mathbf{F}(\mathbf{x})\cdot \mathrm{d}\mathbf{x}. \tag{5}$$

The mass m_0 is that one that whenever $m(\mathbf{x}) = \text{constant}$, this constant is m_0. For example, for the 1-D harmonic oscillator ($F(x) = -m_0\omega_0 x^2$) with mass variation $m(x) = m_0 + m_1 x$, and at first order in gradient m_1, one would have the 1-D constant of motion

$$K(x,v) = \frac{1}{2}m_0 v^2 + \frac{1}{2}m_0\omega_0^2 x^2 + m_1\left[xv^2 + \frac{m_0\omega_0^2}{3}x^3\right], \tag{6}$$

which will be a good approximation on the region $|m_1 x| \ll m_0$.

2.3. Liniar Dissipation 1-D Case

Consider the 1-D motion of a particle of constant mass m under the Hook's force $-kx$ in a dissipative medium which produces a velocity depending force of the form $-\alpha v$, where k is the spring constant, and α is the dissipative constant. The associated dynamical system is given by the pair of equations

$$\frac{\mathrm{d}x}{\mathrm{d}t} = v, \quad \frac{\mathrm{d}v}{\mathrm{d}t} = -\omega^2 x - \frac{\alpha}{m}v, \tag{7}$$

where $\omega = \sqrt{k/m}$ represents the natural spring angular frequency. It has been shown [14] that the constant of motion associated to this system is given by

$$K(x,v) = \frac{m}{2}\left(v^2 + 2\omega_\alpha xv + \omega^2 x^2\right)\mathrm{e}^{-2\omega_\alpha G_\alpha(v/x,\omega)}, \tag{8}$$

where ω_α and G_α are defined as

$$\omega_\alpha = \alpha/m, \text{ and } G_\alpha = \begin{cases} \dfrac{1}{2\Omega_\alpha}\ln\left(\dfrac{\omega_\alpha + v/x - \Omega_\alpha}{\omega_\alpha + v/x - \Omega_\alpha}\right), & \text{if } \omega < \omega_\alpha \\ \dfrac{1}{\omega_\alpha + v/x}, & \text{if } \omega = \omega_\alpha, \\ \dfrac{1}{\sqrt{\omega^2 - \omega_\alpha^2}}\arctan\left(\dfrac{\omega_\alpha + v/x}{\sqrt{\omega^2 - \omega_\alpha^2}}\right), & \text{if } \omega > \omega_\alpha \end{cases} \tag{9}$$

where $\Omega_\alpha = \sqrt{\omega_\alpha^2 - \omega^2}$, and corresponding to strong, critical, and weak dissipation cases. Of course, when dissipation is zero ($\alpha = 0$) one gets the usual energy of the harmonic oscillator.

2.4. Quadratic Dissipation 1-D Case

Consider the motion of a particle with position mass depending $m(x)$ under gravitational force, $-m(x)g$, in a dissipative medium where the force depende quadratically on its velocity, $-\alpha v^2$ (with $v < 0$). The equation of motion is given by

$$\frac{\mathrm{d}\left(m(x)v\right)}{\mathrm{d}t} = -m(x)g - \alpha v^2, \tag{10}$$

where α is a non negative constant. This equation can be written as

$$m(x)\frac{\mathrm{d}v}{\mathrm{d}t} = -m(x)g - (\alpha + m_x)v^2, \tag{11}$$

where m_x is the variation of the mass with respect the position, $m_x = \mathrm{d}m/\mathrm{d}x$. Integrating this equation, it is not difficult to see that one gets the following function

$$K(x,v) = \frac{\left(m(x)v\right)^2}{2m_0}\mathrm{e}^{2\alpha\int^x \frac{\mathrm{d}\sigma}{m(\sigma)}} + \frac{g}{m_0}\int^x \mathrm{d}\sigma m^2(\sigma)\mathrm{e}^{2\alpha\int^\sigma \frac{\mathrm{d}s}{m(s)}} \tag{12}$$

which is a constant of motion ($\mathrm{d}K/\mathrm{d}t = 0$) of the system with energy units. The mass m_0 has been chosen such that if $m(x) = \text{constant}$, this constant has the value m_0.

2.5. Electromagnetic Case

The motion of a charged particle of charge q and mass m under an electric and magnetic fields $\mathbf{E}$ and $\mathbf{B}$ is governed by Lorentz's equation of motion [12] (non relativistic case and CGS units)

$$\frac{\mathrm{d}(m\mathbf{v})}{\mathrm{d}t} = q\mathbf{E} + \frac{q}{c}\mathbf{v}\times\mathbf{B}, \tag{13}$$

where c is the speed of light. This equation can be written in terms of the scalar potential Φ and vector potential $\mathbf{A}$, where $\mathbf{B} = \nabla\times\mathbf{A}$ and $\mathbf{E} = -\nabla\Phi - \partial\mathbf{A}/\partial(ct)$, as

$$\frac{\mathrm{d}}{\mathrm{d}t}\left(m\mathbf{v} + \frac{q}{c}\mathbf{A}\right) = -\nabla\left(q\Phi - \frac{q}{c}\mathbf{A}\cdot\mathbf{v}\right). \tag{14}$$

Defining the new quantity of motion $m\mathbf{V}$ as

$$m\mathbf{V} = m\mathbf{v} + q\mathbf{A}/c, \tag{15}$$

and knowing that the function K associates to the equation $\mathrm{d}(m\mathbf{V})/\mathrm{d}t = -\nabla\phi$ is just $K = m\mathbf{V}^2/2 + \phi$, where $V^2 = V_x^2 + V_y^2 + V_z^2$, one can define the function K for this system as

$$K(\mathbf{x},\mathbf{v},t) = \frac{m}{2}\left(\mathbf{v} + \frac{q}{mc}\mathbf{A}\right)^2 + q\Phi - \frac{q}{c}\mathbf{A}\cdot\mathbf{v}. \tag{16}$$

For most of the cases, one has that $\mathbf{A}\cdot\mathbf{v} = 0$. So, the function K is given by

$$K(\mathbf{x},\mathbf{v},t) = \frac{m}{2}\left(\mathbf{v} + \frac{q}{mc}\mathbf{A}\right)^2 + q\Phi. \tag{17}$$

2.6. Relativistic Conservative Case

This case is given as a good example for completeness of the concept of a constant of motion. The equation of motion of a relativistic particle of constant mass m on a conservative force $\mathbf{F}(\mathbf{x})$, with potential function $V(\mathbf{x}) = -\int\mathbf{F}(\mathbf{x})\cdot\mathrm{d}\mathbf{x}$, is

given by

$$\frac{\mathrm{d}(\gamma m\mathbf{v})}{\mathrm{d}t} = F(\mathbf{x}), \tag{18}$$

where the function γ is $\gamma = \left(1-|\mathbf{v}|^2/c^2\right)^{-1/2}$. It is well known [15] that this system has the following constant of motion

$$K(\mathbf{x},\mathbf{v}) = (\gamma-1)mc^2 + V(\mathbf{x}), \tag{19}$$

where the function $V(\mathbf{x})$ represents the potential energy of the system, $V(\mathbf{x}) = -\int \mathbf{F}(\mathbf{x})\cdot \mathrm{d}\mathbf{x}$.

3. Quantization in the Space (x, v)

The main idea is to assign a linear operator to the energy function $K(\mathbf{x},\mathbf{v},t)$ in order to have an equation that can be identify with Schrödinger's equation. Firstly one needs to point out that in the case of Hamilton approach, if the generalized linear momentum, $p_j = \partial L/\partial v_j$ with $L(\mathbf{x},\mathbf{v},t)$ being a Lagrangian of the system, is related with the velocity of the form $p_j = mv_j$ (m is the constant mass), the function K is exactly a Hamiltonian of the system, $H(\mathbf{x},\mathbf{p},t)$. Therefore, the quantization (Schrödinger's equation) done with the function K can represent an extension of the theory of Quantum Mechanics. To do this, operators associated to the variables "$\mathbf{x}$" and "$\mathbf{v}$" are introduced, and as one could expect, the operators associated to these variables are postulated as

$$\mathbf{x} \to \hat{\mathbf{x}} \quad \text{and} \quad \mathbf{v} \to \hat{\mathbf{v}} = -i\frac{\hbar}{m(\mathbf{x})}\nabla, \tag{20}$$

where $\hbar$ is as usual the Planck's constant divided by 2π. In addition, one has the following commutation relation between the components of these operators

$$\left[x_k, \hat{v}_l\right] = -i\frac{\hbar}{m(\mathbf{x})}\delta_{kl} I, \tag{21}$$

where "I" is the identity operator and the component $\hat{v}_l$ is

$$\hat{v}_l = -i\frac{\hbar}{m(\mathbf{x})}\frac{\partial}{\partial x_l}. \tag{22}$$

One needs to point out that the operator (20) would be an Hermitian operator if and only if the mass does not depend on the position. The square, or self composition of this operator, has the following expression

$$\hat{\mathbf{v}}^2 = -\frac{\hbar^2}{m(\mathbf{x})}\left(-\frac{1}{m^2(\mathbf{x})}\nabla m\cdot\nabla + \frac{1}{m(\mathbf{x})}\nabla^2\right). \tag{23}$$

Then, using the above definitions, one associates and operator to the energy function $K(\mathbf{x},\mathbf{v},t)$ as $\hat{K}(\mathbf{x},\hat{\mathbf{v}},t) = i\hbar\partial/\partial t$ and defines the Schrödinger-like equation in the space $(\mathbf{x},\mathbf{v})$ as

$$i\hbar\frac{\partial\Psi}{\partial t} = \hat{K}(\mathbf{x},\hat{\mathbf{v}},t)\Psi, \tag{24}$$

where $\Psi = \Psi(\mathbf{x},t)$ is the wave function. If one has position depending mass problem, the operator $\hat{K}$ may be not Hermitian ($\hat{K}^{\dagger} \neq \hat{K}$) and there would not be conservation of the probability since the system is not invariant under Galileo's transformation,

$$i\hbar \frac{\mathrm{d}}{\mathrm{d}t}\int_{\Re^3} \left|\Psi(\mathbf{x},t)\right|^2 \mathrm{d}^3\mathbf{x} = \left\langle \Psi, \hat{K}\Psi \right\rangle - \left\langle \hat{K}^{\dagger}\Psi, \Psi \right\rangle, \tag{25}$$

where the inner product has the usual definition, $\langle \phi, \psi \rangle = \int \phi^{\dagger}(\mathbf{x})\psi(\mathbf{x})\mathrm{d}\mathbf{x}$.

However, for the case of position depending mass problems, one can construct a Schrödinger equation with Hermitian operator in the following way

$$i\hbar \frac{\partial \Psi}{\partial t} = \left[\hat{K}(\mathbf{x},\hat{\mathbf{v}},t) + \hat{K}^{\dagger}(\mathbf{x},\hat{\mathbf{v}},t)\right]\Psi. \tag{26}$$

In addition, although there might be some doubts where the function $K(\mathbf{x},\mathbf{v},t)$ can not be a constant of motion [16], this statement is not necessarily a request, but it is necessary that this function must have units of energy. Let us see few examples of Schrödinger-like equations for the classical systems shown before. However, one needs to point out that the dissipation force on a motion of a body in the classical system appears as the result of the average collisions of the body with the particles of the medium where this body is moving, meanwhile in quantum mechanics this collisions are much more complicated and depends strongly of the energy of the particle and the particle itself ($e^-, e^+, p, \overline{p}, \mu^-, \mu^+, n, \Lambda$, etc.) [17], therefore, it is not so direct to make the identification and transition of the classical problem to the quantum problem. However, from the mathematical point of view, the quantum theory must be able to address these types of problems. The same situation is presented with the mass position depending problem.

3.1. Quantization of Mass Variation of Conservative Systems

Using (20) and (24) in (5), and assigning to the function $f(\mathbf{x})^2 v^2$ (for any arbitrary function f) the operator

$$\widehat{f^2 v^2} = \frac{1}{3}\left(\hat{v}^2 f^2 + f^2 \hat{v}^2 + \hat{v} f^2 \hat{v}\right), \tag{27}$$

one can get the operator for the function $m^2\mathbf{v}^2$ as

$$\widehat{m^2\mathbf{v}^2} = -\frac{\hbar^2}{3m}\left[\left(-\frac{1}{m^2}\nabla m\cdot\nabla + \frac{1}{m}\nabla^2\right)m^2 + 2m\nabla^2\right]. \tag{28}$$

Therefore, it follows that the Scrödinger-like equation is

$$i\hbar\frac{\partial\Psi}{\partial t} = -\frac{\hbar^2}{6m_0 m(\mathbf{x})}\left[\left(-\frac{1}{m(\mathbf{x})}\nabla m(\mathbf{x})\cdot\nabla + \frac{1}{m(\mathbf{x})}\nabla^2\right)m^2(\mathbf{x}) + 2m(\mathbf{x})\nabla^2\right]\Psi$$
$$-\left[\frac{1}{m_0}\int m(\mathbf{x})\mathbf{F}(\mathbf{x})\cdot\mathrm{d}\mathbf{x}\right]\Psi. \tag{29}$$

If one makes the approximation to an Hermitian operator $\hat{\mathbf{v}} = -(i\hbar/m_0)\nabla$, the operation $\widehat{m^2\mathbf{v}^2}$ would be given instead by

$$\widehat{m^2(\mathbf{x})v^2} = -\frac{\hbar^2}{3m_0^2}\Big[3m(\mathbf{x})^2\nabla^2 + 5m(\mathbf{x})\nabla m(\mathbf{x})\cdot\nabla + 2\nabla m(\mathbf{x})\cdot\nabla m(\mathbf{x}) + 2m(\mathbf{x})\big(\nabla^2 m(\mathbf{x})\big)\Big], \tag{30}$$

and the wave equation would be given by

$$i\hbar\frac{\partial\Psi}{\partial t} = -\frac{\hbar^2}{6m_0^3}\Big[3m(\mathbf{x})^2\nabla^2 + 5m(\mathbf{x})\nabla m(\mathbf{x})\cdot\nabla + 2\nabla m(\mathbf{x})\cdot\nabla m(\mathbf{x}) + 2m(\mathbf{x})\big(\nabla^2 m(\mathbf{x})\big)\Big]\Psi - \left[\frac{1}{m_0}\int m(\mathbf{x})\mathbf{F}(\mathbf{x})\cdot\mathrm{d}\mathbf{x}\right]\Psi. \tag{31}$$

3.2. Quantization of a Charged Particle Motion under Electromagnetic Forces and Pauli-Like Equation

From the expression (17) and since the mass is constant, the quantization of these systems can be carried out with the following Shrödinger-like equation

$$i\hbar\frac{\partial\Psi}{\partial t} = \left\{\frac{m}{2}\left(-\frac{i\hbar}{m}\nabla + \frac{q}{mc}\mathbf{A}\right)^2 + q\Phi\right\}\Psi, \tag{32}$$

where $\Psi = \Psi(\mathbf{x},t)$ is an scalar function. Here again there is conservation of probability, and if the system has dipole electric and magnetic moments $\mathbf{P}$ and $\mathbf{m}$, the interaction with the electric and magnetic fields can be added in the usual way [18] by adding the terms $-\mathbf{P}\cdot\mathbf{E}$ and $-\mathbf{m}\cdot\mathbf{B}$. Now, it is well known Pauli's matrix, σ_k, properties [19], and their relation with the spin-1/2, $\mathbf{S}$ of a charged particle,

$$\left[\sigma_k,\sigma_j\right] = i2\varepsilon_{kj}^l\sigma_l, \quad \sigma_j^2 = I, \quad (\vec{\sigma}\cdot\mathbf{a})(\vec{\sigma}\cdot\mathbf{b}) = \mathbf{a}\cdot\mathbf{b}I + i(\mathbf{a}\times\mathbf{b})\cdot\boldsymbol{\sigma}, \quad \mathbf{S} = \frac{\hbar}{2}\vec{\sigma}, \tag{33}$$

where I is the 2×2 identity matrix, $\vec{\sigma} = (\sigma_x,\sigma_y,\sigma_z)$, $a,b\in\Re^3$ are arbitrary vectors, and Einstein's convention was used. Thus, the Pauli's equation in the quantum space $(\boldsymbol{x},\boldsymbol{v})$ for a charged particle of spin one-half can be written as

$$i\hbar\frac{\partial\Psi}{\partial t} = \left\{\frac{m}{2}\left[\vec{\sigma}\cdot\left(-\frac{i\hbar}{m}\nabla + \frac{q}{mc}\mathbf{A}\right)\right]^2 + q\Phi\right\}\Psi, \tag{34}$$

where Ψ is an spinor (a two components vector of scalar complex functions)

$$\Psi(\mathbf{x},t) = \begin{pmatrix}\psi_1(\mathbf{x},t)\\ \psi_2(\mathbf{x},t)\end{pmatrix}. \tag{35}$$

3.3. Quantization of 1-D Dissipative-Mass Variable Problem

From the expression (12), one notices that it will appear the product of $f(x)v^2$ where the this function is given by

$$f(x) = m^2(x)\mathrm{e}^{2\alpha\int\mathrm{d}\sigma/m(\sigma)}. \tag{36}$$

So, using the same expression (27) for 1-D, the Shcrödinger-like equation can be given as

$$i\hbar\frac{\partial\Psi}{\partial t}=\left\{-\frac{\hbar^2}{6m_0}\left[\left(\frac{-1}{m^2(x)}\frac{\partial}{\partial x}m(x)\frac{\partial}{\partial x}+\frac{1}{m(x)}\frac{\partial^2}{\partial x^2}\right)m^2(x)\lambda(x)\right.\right.$$
$$\left.+\lambda(x)\left(-\frac{\partial}{\partial x}m(x)\frac{\partial}{\partial x}+m(x)\frac{\partial^2}{\partial x^2}\right)+\frac{\partial}{\partial x}m(x)\lambda(x)\frac{\partial}{\partial x}\right] \quad (37)$$
$$\left.+\frac{g}{m_0}\int \mathrm{d}\sigma m^2(\sigma)\lambda(\sigma)\right\}\Psi,$$

where the function $\lambda(x)$ has been defined as

$$\lambda(x)=\mathrm{e}^{2\alpha\int \mathrm{d}s/m(s)}. \quad (38)$$

If the mass of the system is constant ($m(x)=m_0$), one would have that $\hat{v}=-(i\hbar/m_0)\partial/\partial x$ is an Hermitian operator, the function λ would be $\lambda(x)=\mathrm{e}^{2\alpha x/m_0}$, and the wave equation would be

$$i\hbar\frac{\partial\Psi}{\partial t}=\left\{-\frac{\hbar^2\lambda(x)}{3m_0}\left[3\frac{\partial^2}{\partial x^2}+\left(\frac{6\alpha}{m_0}\right)\frac{\partial}{\partial x}+\left(\frac{2\alpha}{m_0}\right)^2\right]+\frac{gm_0^2}{2\alpha}(\lambda(x)-1)\right\}\Psi. \quad (39)$$

3.4. Quantization of the Relativistic Scalar Case

For completeness, for the system characterized by the expression (19), let us make first some algebraic manipulation. Let us write this expression in the form

$$K-V(\mathbf{x})+mc^2=\gamma mc^2,$$

let us take the square of this expression and pass the velocity dependence to the left hand side. So, one gets

$$\left(1-\frac{v^2}{c^2}\right)\left(K-V(\mathbf{x})+mc^2\right)^2=m^2c^4. \quad (40)$$

In this way, using the identification of the operators for different variables and the function K, it follows that

$$\left(1+\frac{\hbar^2}{m^2c^2}\nabla^2\right)\left(-i\hbar\frac{\partial}{\partial t}-V(\mathbf{x})+mc^2\right)^2\Psi=m^2c^4\Psi. \quad (41)$$

4. Some Particular Solutions on the Space (x, v)

In this section, two simple solutions of the above approach are presented for illustration.

4.1. 1-D harmonic Oscillator with Position Depending Mass

Using the approximated constant of motion (6), one can write this expression of the form

$$K(x,v)=K_0(x,v)+W(x,v), \quad (42)$$

where K_0 represents the usual harmonic oscillator with constant mass m_0, and W represents the term of the variation of mass at first approximation in

Taylor expansion,

$$K_0(x,v)=\frac{1}{2}m_0v^2+\frac{1}{2}m_0\omega_0^2x^2,\quad W(x,v)=m_1\left[xv^2+\frac{m_0\omega_0^2}{3}x^3\right]. \tag{43}$$

Of course, for $m_1=0$, one has that $p=mv$, and K_0 represents the Hamiltonian $H(x,p)=p^2/2m_0+m_0\omega_0 2x^2/2$, and one knows that the solution of the Schrödinger's equation would be $\Psi_0(x,t)=\sum_{n=0}c_n\exp(-iE_nt/\hbar)\Phi_n(x)$, where the set $\{E_n=\hbar\omega_0(n+1/2),\Phi_n(x)\}$ is the solution of the eigenvalue problem $\hat{H}\Phi=E\Phi$ [2]. This solution is exactly the solution of Schrödinger-like equation

$$i\hbar\frac{\partial\Psi_0}{\partial t}=\hat{K}(x,\hat{v})\Psi_0. \tag{44}$$

For $m_1\neq 0$, one considers that W is a perturbation of the system and uses perturbative theory to find the modification of the energy levels of the system. Since W contains odd monomials order, there is not contribution a first order perturbation, $\langle n|\hat{W}|n\rangle$ with $\langle x|n\rangle=\Phi_n(x)$. It is not difficult to calculate that up to second order in perturbation theory, the eigenvalues are of the form

$$E_n\approx\hbar\omega_0(n+1/2)+\frac{m_1^2\hbar^2}{2m_0^3}\left(\frac{39(2n^2+2n)}{18}+\frac{7}{6}\right). \tag{45}$$

4.2. Free Relativistic Particle

Just to have some idea what the relativistic case would be, let us consider the quantization in the space (x,v) of the relativistic free particle motion. In this case, one makes $V(\mathbf{x})=0$ on the expression (41) and propose a plane wave solution of the form

$$\psi(\mathbf{x},t)\sim e^{i(\mathbf{k}\cdot\mathbf{x}-\omega t)}, \tag{46}$$

on the resulting equation

$$\left(1+\frac{\hbar^2}{m^2c^2}\nabla^2\right)\left(-i\hbar\frac{\partial}{\partial t}+mc^2\right)^2\Psi=m^2c^4\Psi. \tag{47}$$

Thus, one gets the dispersion relation given by

$$\omega(k)=\frac{mc^2}{\hbar}\left[\frac{1}{\sqrt{1-\frac{\hbar^2k^2}{m^2c^2}}}-1\right]. \tag{48}$$

See following figure (**Figure 1**) where it has been plotted this relativistic dispersion relation.

The general solution would be the superposition of all the solutions,

$$\Psi(\mathbf{x},t)=\int_{\Re^3}A(\mathbf{k})e^{i(\mathbf{k}\cdot\mathbf{x}-\omega(k)t)}d^3\mathbf{k}, \tag{49}$$

where, due to conservation of probability, the function $A(\mathbf{k})$ is such a

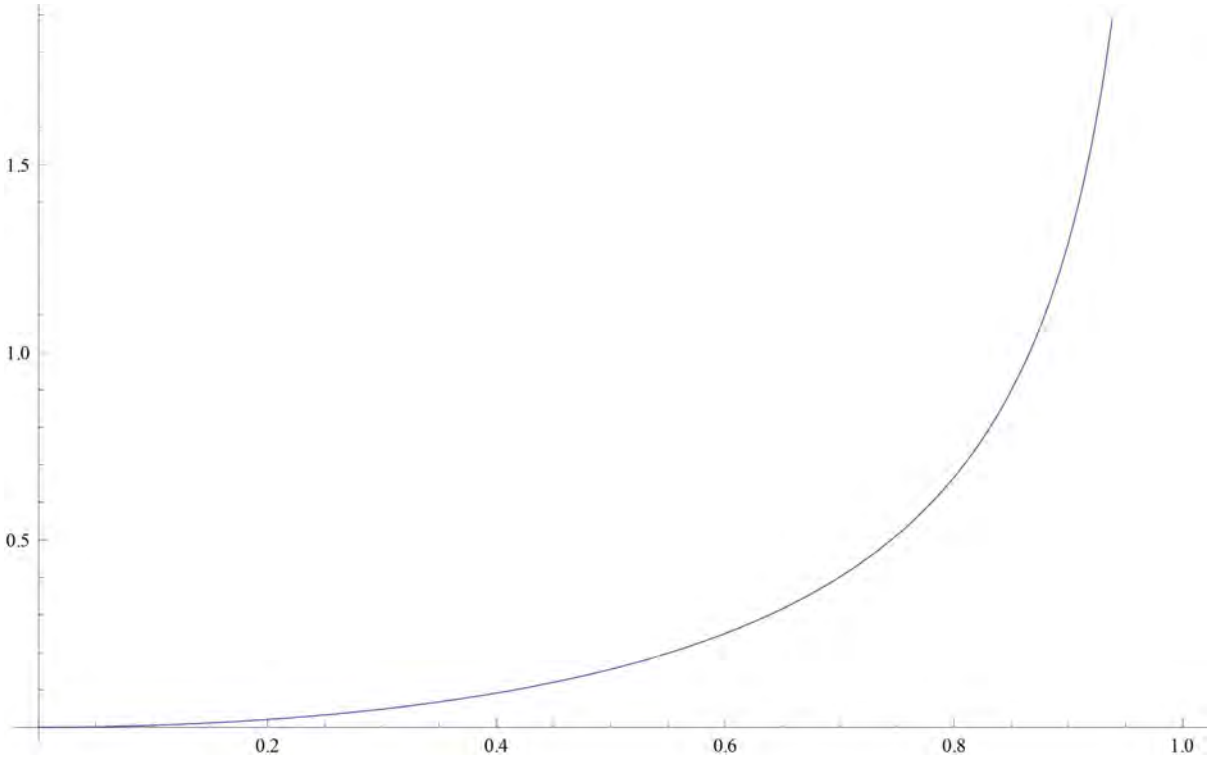

Figure 1. $\omega/\left(mc^2/\hbar\right)$ (vertical) vs. $k^2c^2/\left(mc^2/\hbar\right)^2$ (horizontal) with $mc^2/\hbar = 1.42\times10^{24}\,\text{sec}$.

$$\int_{\Re^3}\left|A(\mathbf{k})\right|^2 \mathrm{d}^3\mathbf{k} = 1. \tag{50}$$

5. Conclusions and Comments

It has been done an extension of the Shrödinger's quantization approach to the quantization on the space $(\mathbf{x},\mathbf{v})$ through the function $K(\mathbf{x},\mathbf{v},t)$ which has energy units. Within this approach, the Hamiltonian notion is not needed, and the quantization of conservative systems is the same with this approach and the Hamiltonian approach (in fact, it must be the same whenever the generalized linear momentum is of the form $\mathbf{p} = m\mathbf{v}$). The possibility to include the quantization of mass variation problems and velocity depending problems (dissipation) is clearly stablished. In addition, the quantization of non relativistic interaction of charged particles with electromagnetic field is also stablished.

Conflicts of Interest

The author declares no conflicts of interest regarding the publication of this paper.

References

[1] Shrödinger, E. (1926) *Annalen der Physik*, **81**, 109-139. https://doi.org/10.1002/andp.19263861802

[2] Cohen-Tannoudji, C., Diu, B. and Laloe, F. (1977) Quantum Mechanics, I, II. Wi-

ley-Interscience, Hoboken.

[3] Dirac, P.A.M. (1976) The Principles of Quantum Mechanics. Oxford University Press, Oxford.

[4] Messiah, A. (1995) Quantum Mechanics. Dover Publications, Inc., Mineola.

[5] Dodonov, V.V., Man'kov, V.I. and Skarzhinsky, V.D. (1981) *Hadronic Journal*, **4**, 1734.

[6] López, G.V. and Prieto, C.R.M. (2014) *Journal of Modern Physics*, **5**, 900-907.

[7] López, G.V., López, P. and López, X.E. (2011) *Advanced Studies in Theoretical Physics*, **5**, 253-268.

[8] López, G.V., Griselda, A. and Prieto, C.R.M. (2018) *Journal of Applied Mathematics and Physics*, **6**, 1382. https://doi.org/10.4236/jamp.2018.66115

[9] López, G.V., López, P. and López, X.E. (2007) *International Journal of Theoretical Physics*, **46**, 1100. https://doi.org/10.1007/s10773-006-9260-7

[10] Plastino, A.R. and Muzzio, J.C. (1992) *Celestial Mechanics and Dynamical Astronomy*, **53**, 227-232. https://doi.org/10.1007/BF00052611

[11] Sommerfeld, A. (1964) Lectures on Theoretical Physics, I. Academic Press, Cambridge.

[12] López, G.V. and Juárez, E.M. (2013) *Journal of Modern Physics*, **4**, 1638-1646. https://doi.org/10.4236/jmp.2013.412204

[13] Spivak, M.D. (2010) Physics for Mathematicians, Mechanics I. Publish or Perish.

[14] López, G.V. (2012) Partial Differential Equations of First Order and Their Applications to Physics. World Scientific, Singapore, 120.

[15] Møller, C. (1955) The Theory of Relativity. Oxford University Press, Oxford.

[16] López, G.V. and Bravo, O.J.P. (2021) *Journal of Modern Physics*, **12**, 284-294. https://doi.org/10.4236/jmp.2021.123021

[17] Olive, K.A., *et al.* (2014) (Particle Data Group) Particle Physics Booklet. Chapter 32.

[18] Jackson, J.D. (1974) Classical Electrodynamics. John Wiley& Sons Inc., Hoboken.

[19] Pauli, W. (1927) *Zeitschrift fr Physik*, **43**, 601-623. https://doi.org/10.1007/BF01397326

Journal of Modern Physics, 2022, 13, 682-699
https://www.scirp.org/journal/jmp
ISSN Online: 2153-120X
ISSN Print: 2153-1196

Highly Accurate Relations between the Fine Structure Constant and Particle Masses, with Application to Its Cosmological Measurement

Frank R. Tangherlini

San Diego, CA, USA
Email: frtan96@gmail.com

How to cite this paper: Tangherlini, F.R. (2022) Highly Accurate Relations between the Fine Structure Constant and Particle Masses, with Application to Its Cosmological Measurement. *Journal of Modern Physics*, **13**, 682-699.
https://doi.org/10.4236/jmp.2022.135038

Received: March 25, 2022
Accepted: May 6, 2022
Published: May 9, 2022

Abstract

Highly accurate algebraic relations between the fine structure constant α and a wide range of particle masses are given, ranging from $\Delta\alpha/\alpha = (2.1 \pm 0.1)\times 10^{-7}$ to $\Delta\alpha/\alpha = (-2.7 \pm 0.3 \pm 0.6)\times 10^{-8}$, and with a very large standard deviation, ranging to $\Delta\alpha/\alpha = -5.5\times 10^{-9}$. The analysis is based on empirical relations that exist among some particle masses, and also on several theoretical assumptions, of which the most significant is that the electromagnetic contribution to the electron's mass is finite, and given by $f\alpha m_{eb}$, where f is a dimensionless parameter that is shown to be equal to 1.032409810 (63), and where m_{eb} is the electron's "bare mass." The relations for α and f are homogeneous degree zero in the particle masses. The relations for f in terms of particle masses are found by trial and error. A quadratic equation is given relating α to f and m_e/m_p. This equation is used in the application to cosmological measurements of α, and $\mu \equiv m_p/m_e$, where it is shown that, to a few percent accuracy, $\delta\alpha/\alpha \approx -\delta\mu/\mu$. This relation can serve to test the validity of measurements of α and μ.

Keywords

Fine Structure Constant, Particle Masses, Proton-Electron Mass Ratio, Cosmological Measurement

1. Introduction

There is a long standing interest in the underlying basis of the dimensionless fine structure constant $\alpha \equiv e^2/\hbar c$ (Gaussian units) following its appearance in Sommerfeld's [1] special relativistic correction to the Bohr orbit model of the

hydrogen atom that gave the fine-structure splitting of the energy levels in agreement with experiment. This result, followed by the quantum mechanically and relativistically correct derivation of the fine-structure splitting from the Dirac equation [2] [3] [4] led to numerous efforts to derive α from first principles, of which the attempt by Eddington, summarized in [5], in which the emphasis is on the value of $\alpha^{-1} \approx 137$, is the most well-known. Later considerations to investigate or comment on the significance of the fine structure constant include those of Born [6], Teller [7], Landau [8], Peebles and Dicke [9], Pauli [10], Wyler [11], Peres [12], Isham, *et al.* [13], MacGregor [14], Rozenthal [15], Barrow and Tipler [16], Good [17], and Várlaki *et al.* [18]. As yet another effort to study α, the purpose of this paper is to derive relations of very high accuracy between α and some of the masses of the elementary particles. This approach will be based on two empirical relations, and several theoretical assumptions that are eventually falsifiable. In Section 2, the two empirical observations, based on the work of Nambu [19], and the author [20], are shown to lead to an approximate empirical value for the fine structure constant, denoted by α_{emp} that depends on the ratio of the electron mass m_e to the charged pion mass $m_{\pi^\pm}$, and that results in an agreement given by $\left(\alpha_{emp} - \alpha\right)/\alpha = 3.4 \times 10^{-3}$. Although it is possible to proceed further working with the ratio $m_e/m_{\pi^\pm}$, because the value of the charged pion mass is not known sufficiently to deal with the very high accuracy that will be achieved below for the theoretical value of α denoted by α_{th}, and also because of the interest in the value of the ratio of the electron mass to the proton mass m_e/m_p (although usually expressed in terms of its reciprocal), as well as the fact that m_p is known to very high accuracy, subsequent work makes use of the ratio m_e/m_p. In Section 3, several theoretical assumptions are given that involve introducing the so-called "bare mass" of the electron, *i.e.* the mass of the electron that it would have in the absence of its interaction with the electromagnetic field. In addition, there are the assumptions that the electromagnetic self-energy of the electron is finite and small, and, in terms of mass, is given by $f\alpha m_e$, where f is a dimensionless parameter that, in the course of the analysis, turns out to be slightly greater than unity. These assumptions lead to an expression for the bare mass that is eventually falsifiable. The next assumption involves replacing m_e in the ratio m_e/m_p with the electron's bare mass. This yields a quadratic equation for α_{th} whose solutions are examined, first for $f = 1$, that leads to an agreement given by $\left(\alpha_{th} - \alpha\right)/\alpha = 2.3 \times 10^{-4}$. A further expression for f, that was obtained through trial-and-error, that involves the masses of a suitable number of elementary particles, and that maintains the homogeneous degree zero in the masses behavior of m_e/m_p, yields a substantially greater agreement of $\left(\alpha_{th} - \alpha\right)/\alpha = -2.1^{+0.6}_{-0.5} \times 10^{-8}$. With further trial-and-error in the choice of particle masses used in f, it is possible to improve the agreement for α_{th} still further, albeit with a larger standard deviation. Thus, with a suitable choice of masses in f, one obtained $\left(\alpha_{th} - \alpha\right)/\alpha = 1.4^{+1.6}_{-1.8} \times 10^{-8}$. The standard deviation is due to that in the particle masses used in f. However, the homogeneous degree zero in the masses behavior for f, and more generally

that of α_{th}, is still maintained. In Section 4, since the values for the masses in f involved hadrons that only contained the up, down, and strange quarks, expression for f are extended to include the masses of mesons and baryons that contain the charm quark, and masses of mesons that contain the bottom quark. For the case of f containing the mass of the charmed $D^{\pm}$ meson, among the other masses involved, one obtained $(\alpha_{th}-\alpha)/\alpha = 3.3^{+0.6}_{-0.4}\times 10^{-8}$. While, for the case of f containing the mass of the charmed lambda baryon Λ_c^+, the result was $(\alpha_{th}-\alpha)/\alpha = -5.5^{+6.9}_{-8.2}\times 10^{-9}$. For f containing masses of the bottom B^0 and $B^{\pm}$ mesons $(\alpha_{th}-\alpha)/\alpha = (-2.7\pm 0.3\pm 0.6)\times 10^{-8}$. For the bottom baryon Λ_b^0, the best value was $(\alpha_{th}-\alpha)/\alpha = 1.8^{+0.5\ +0.5}_{-0.6\ -0.7}\times 10^{-8}$. In all these cases in which f is a function of the various particle masses, the standard deviations in the value of $(\alpha_{th}-\alpha)/\alpha$ are due to the standard deviations in the particle masses. In Section 5, the analysis is extended to include the gauge bosons W and Z, and the Higgs H^0 boson, with agreements comparable to those found above. In Section 6, there is an application to the cosmological measurement of α, where it is pointed out that, since α_{th} is homogeneous degree zero in the particle masses, any change in the particle masses of the form $m_i \to \phi(z, RA, \delta)m_i$ where z is redshift, RA is right ascension, and δ is declination, would leave α_{th} invariant, and hence α itself, to the level of agreement found in the previous sections. Hence, it is noted that if there were a change in α, some of the masses would have to change differently than the others; a requirement that would be even more difficult to reconcile with the standard model than the above change of the form, $m_i \to \phi m_i$, but it cannot be ruled out on the basis of present knowledge. Since, as pointed out above, that because of the accurate agreements involved, the expression for α_{th} can be regarded as holding for α, and since the above quadratic equation, that under these circumstances holds for α, involves the ratio m_e/m_p, and since the reciprocal of this ratio is defined as μ, it follows that a cosmological variation in α is not independent of a cosmological variation in μ. It is shown that $\delta\alpha/\alpha \approx -\delta\mu/\mu$, the departure from strict equality being of the order of a few percent. This relation provides the possibility of an important test of such measurements that presently does not exist, since α and μ are treated as independent, In Section 7, there are concluding remarks.

2. Empirical Relations

It is well-known that the mass of the muon is related to the mass of the electron in the form

$$m_\mu \approx \frac{3}{2}\alpha^{-1}m_e . \tag{1}$$

This relation leads the empirical list of particle masses given by Nambu [19] that are of the form, integer or half-integer times $\alpha^{-1}m_e$. It is also known empirically, and that also follows from Nambu's list that the mass of the charged pion satisfies

$$m_{\pi^\pm} \approx \frac{4}{3}m_\mu . \tag{2}$$

Such a relation was also found by the author [20] to hold for two classical electron models that were compensated differently, one with the Poincaré pressure, and the other with transverse stress, so that the energy and momentum of these two models transformed properly under a Lorentz transformation. The former was identified with the charged pion, and the latter with the muon. The relation (2) emerged later in the form $m_\mu = (3/4)m_{\pi^\pm}$ in the author's [21] empirical extension of Nambu's list [19] to include particle masses m_i that are approximately of the form, $m_i = (a_i + (b_i/4))m_{\pi^\pm}$ where a_i are suitable integers, and $b_i = 0,1,2,3$; for example, the proton mass satisfies $m_p \approx 6\frac{3}{4}m_{\pi^\pm}$. However, for the purposes of this work (2) is to be regarded as a purely empirical relation. Upon inserting the value of m_μ from (1) into (2) and rewriting it as a relation for α, one has

$$\alpha \approx 2m_e/m_{\pi^\pm}. \tag{3}$$

This purely empirical result yields an approximate value for α, denoted by α_{emp}, with the value $\alpha_{emp} = 0.007322$, for $m_e = 0.511$ MeV/c^2 and $m_{\pi^\pm} = 139.57$ MeV/c^2 [22]. More accurate values for these masses from [22] will be used below. Hence an agreement with $\alpha = 0.007297$ given by

$$(\alpha_{emp} - \alpha)/\alpha \approx 3.4\times 10^{-3}, \tag{4}$$

A more accurate value for α will be used below. Although one can continue working with (3). It turns out that the standard deviation in the mass of the charged pion, as given by $m_{\pi^\pm} = 139.57039 \pm 0.00018$ MeV/c^2, yields too great a standard deviation in the theoretical values for α in some of the examples that will be found below, consequently, it turns out to be desirable to replace (3) with the ratio of the electron mass to the proton mass. From Nambu's second hint empirical mass list in [19], the proton mass obeys the relation.

$m_p \approx 13.5\alpha^{-1}m_e$, and since the list also gives $m_{\pi^\pm} \approx 2\alpha^{-1}m_e$, one has $m_p \approx 6\frac{3}{4}m_{\pi^\pm}$, as does the neutron mass, and, as was found later, the tauon mass satisfies $m_\tau \approx 12\frac{3}{4}m_{\pi^\pm} = m_n + 6m_{\pi^\pm}$. Hence, substituting for $m_{\pi^\pm}$ with m_p in (3), one has

$$\alpha_{emp} \approx 13.5\, m_e/m_p. \tag{5}$$

With $m_p = 938.272$ MeV/c^2, this yields the value $\alpha_{emp} \approx 0.007352$, and hence an agreement of

$$(\alpha_{emp} - \alpha)/\alpha \approx 7.5\times 10^{-3} \tag{6}$$

Although this agreement is clearly poorer than in (4), it will turn out from the theoretical work in the next section that considerably more exact agreements will be obtained.

3. Theoretical Assumptions and Improved Agreements

The above expressions for α are of a purely empirical nature: no theoretical

assumptions went into obtaining them, However, in the following analysis much more accurate expressions relating α to particle masses will be obtained, that are based on several theoretical assumptions that are all eventually falsifiable. The first assumption is that instead of m_e in the numerators of (3) and (5), one should have the bare mass of the electron m_{eb}, that is defined by

$$m_{eb} = m_e - \Delta m_e , \tag{7}$$

where Δm_e is the addition to the bare mass of the electron due to its interaction with the quantized electromagnetic field. According to current ideas, the bare mass would arise as a consequence of the electron's interaction with the expectation value of the Higgs field [23], although there are no generally accepted results in the literature, and in any case, it is irrelevant to this work as to just how the bare mass arises. As is well-known, Δm_e diverges logarithmically in a first order perturbation expansion, as obtained by Weisskopf [24] using hole-theory, in which he acknowledged it to have been found by Furry as a correction to his previous work, Weisskopf [25]. In contrast, in QED, the logarithmic divergence follows from the one-loop Feynman diagram [26], and is removed by renormalization [27]-[33], that regrettably fails to give a value for Δm_e, since all the final answers are in terms of m_e, and hence the electromagnetic self-mass never appears. Here, in contrast, it will be assumed, secondly, that the self-mass is finite, and thirdly, that it is given by

$$\Delta m_e = f \alpha m_{eb} , \tag{8}$$

where the factor f is of order unity, and will be determined below. A non-rigorous justification for assuming that Δm_e is a small contribution to the mass of the electron can be made by appeal to the quark model. The u and d quarks have masses comparable to that of the electron, but since the electric charge of the u quark is $2e/3$ while that of the d quark is $-e/3$, if the electromagnetic contribution to the masses of these quarks were dominant, then since it would behave as the square of the charges, one would expect $m_u/m_d \approx 4$, but instead it has been found that $m_u/m_d \approx 0.5$ [22]. Further justification follows from Feynman's [34] remark that he suspected, "renormalization is not mathematically legitimate." A possible reason for such a suspicion is that the subtraction of one infinity from another infinity is mathematically ambiguous: the difference need not vanish, it could be a finite quantity such as (8). However, as emphasized above, the basic justification for using (8) is the highly accurate results that are obtained below using it. Upon inserting the value of Δm_e from (8) in (7), and solving for m_{eb}, one obtains

$$m_{eb} = \frac{m_e}{1 + f \alpha} , \tag{9}$$

from which, using (7) one has that $\Delta m_{eb} = f \alpha m_e / (1 + f \alpha)$. Upon replacing m_e in (5) with the value of m_{eb} from (9) one obtains the following quadratic equation

$$\alpha^2 + \frac{\alpha}{f} - \frac{13.5}{f}\frac{m_e}{m_p} = 0. \tag{10}$$

The physically desired solution is the positive root that will be denoted by α_{th}, and is given by

$$\alpha_{th} = \left(\sqrt{1+\left(f\,54\,m_e/m_p\right)}-1\right)\Big/2f\ . \tag{11}$$

The physical significance of the negative root, if any, is left unresolved at this writing.

As a first approximation for the value of α_{th}, it will be assumed that $f = 1$. With more exact values of the masses from [22], $m_e = 0.51099895000(15)$ MeV/c^2 and $m_p = 938.27208816(29)$ MeV/c^2, one obtains, rounding off, $\alpha_{th} = 0.007299054$, so that in comparison with the present full value of α that will be needed further on, *i.e.* $\alpha = 0.0072973525693(11)$, [22], one has

$$\left(\alpha_{th} - \alpha\right)/\alpha = 2.3\times10^{-4}. \tag{12}$$

It is clear that there is already an improvement in accuracy over that given in (4) and (6) by more than an order of magnitude. Equation (10) can alternatively be used to determine m_p/m_e in terms of α and f. For $f = 1$, $m_p/m_e = 1836.58$ in comparison with its empirical value of 1836.15, hence with the same accuracy as above, 2.3×10^{-4}. Of interest is the fact that the value for α_{th} given in (11), with $f = 1$, is homogenous, degree zero in the masses, so that $\alpha_{th}\left(\varphi m_e, \varphi m_p\right) = \alpha_{th}\left(m_e, m_p\right)$, and hence

$$\frac{\partial\alpha_{th}}{\partial m_e}m_e + \frac{\partial\alpha_{th}}{\partial m_p}m_p = 0\,. \tag{13}$$

To proceed further, it will be necessary to determine the value of f more accurately. It will be assumed that f is a function of particle masses, and that it maintains the homogeneous degree zero character of α in (5). In order to assist in the determination of f, which will be by trial and error, it is helpful to know the value of f that would lead to the current value of the fine structure constant that is given above. One has from (10)

$$f = -\frac{1}{\alpha} + \frac{13.5}{\alpha^2}\frac{m_e}{m_p}, \tag{14}$$

from which one obtains

$$f = 1.032409810(63), \tag{15}$$

where the standard deviation in f is due mainly to the standard deviations in the masses of the proton and the electron, and less to that in α. Note also that (14) provides an upper bound on α since on empirical grounds $\alpha > 0$, and on physical grounds $f > 0$, hence one has $\alpha < 13.5\ m_e/m_p$, thus, rounding off, $\alpha < 0.00735233 = 1/136.0113$. In what follows, approximations to f will be made that involve a suitable choice of particle masses. As the first example, guided by the fact that m_e/m_p involves a lepton mass divided by a hadron mass, it seemed

reasonable to try a ratio involving the muon mass divided by a suitable sum of hadron masses. The following expression for f is the result of such a trial and error search

$$f = 1 + \frac{m_\mu}{\Sigma_i m_i} = 1 + \frac{m_\mu}{m_{\Xi^-} + m_n + m_{K^0} + m_{K^\pm}}. \tag{16}$$

From [22], with $m_\mu = 105.6583745(24)$ MeV/c^2, $m_{\Xi^-} = 1321.71 \pm 0.07$ MeV/c^2, $m_n = 939.56542052(54)$ MeV/c^2, $m_{K^0} = 497.611 \pm 0.013$ MeV/c^2, and $m_{K^\pm} = 493.677 \pm 0.016$ MeV/c^2, one has

$$\Sigma_i m_i = 3252.563 \pm 0.073 \text{ MeV/c}^2. \tag{17}$$

Hence, after obtaining f = 1.03248465 (72), and using (11), one has $\alpha_{th} = 0.00729734864(4)$, and hence an agreement given by

$$(\alpha_{th} - \alpha)/\alpha = (-5.4 \pm 0.1) \times 10^{-7}. \tag{18}$$

Thus, by the above assumption about f, one has achieved nearly a thousand-fold improvement over the agreement in (12). One can make a modest improvement to the above agreement in (18) by introducing in the denominator in (16) a different set of masses, consisting of the mass of the τ lepton, that of the proton, and that of the η meson, so that one has

$$f = 1 + \frac{m_\mu}{\Sigma_i m_i} = 1 + \frac{m_\mu}{m_\tau + m_p + m_\eta}. \tag{19}$$

From which, with $m_\tau = 1776.86 \pm 0.12$ MeV/c^2, $m_\eta = 547.862 \pm 0.017$ MeV/c^2, and m_p given above, one has

$$\Sigma_i m_i = 3262.994 \pm 0.121 \text{ MeV/c}^2. \tag{20}$$

After obtaining $f = 1.0323808(12)$, and again using (11), one has $\alpha_{th} = 0.00729735409(06)$, and hence an agreement given by

$$(\alpha_{th} - \alpha)/\alpha = (2.1 \pm 0.1) \times 10^{-7}. \tag{21}$$

With a somewhat different choice of masses in the denominator of (16), it is possible to improve the agreement by an order of magnitude over that in (21). Thus with f given by

$$f = 1 + \frac{m_\mu}{\Sigma_i m_i} = 1 + \frac{m_\mu}{m_{\Sigma^+} + m_n + m_{K^0} + m_{K^\pm} + m_{\pi^\pm}}, \tag{22}$$

with $m_{\Sigma^+} = 1189.370 \pm 0.07$ MeV/c^2, $m_{\pi^\pm} = 139.57039$ MeV/c^2, and the other masses as given above, one has

$$\Sigma_i m_i = 3259.793 \pm 0.073 \text{ MeV/c}^2. \tag{23}$$

After obtaining $f = 1.03241260(72)$, and using (11), one has that $\alpha_{th} = 0.00729735242(4)$, hence an improved agreement given by

$$(\alpha_{th} - \alpha)/\alpha = -2.1^{+0.6}_{-0.5} \times 10^{-8}, \tag{24}$$

where the standard deviation is due primarily to that in the mass of the Σ^+, while the standard deviation in (18) is due primarily to that in the mass of the

Ξ^-.

It is possible to obtain comparable agreement for α_{th}, albeit with a larger standard deviation, if in (16) one replaces m_μ in the numerator by $m_{\pi^\pm}$, and introduces another set of masses, that are found, as before, by trial and error, one has

$$f = 1 + \frac{m_{\pi^\pm}}{\Sigma_i m_i} = 1 + \frac{m_{\pi^\pm}}{m_{\Xi^0} + m_{\Sigma^0} + m_\Lambda + m_\eta + m_{\pi^0}}. \tag{25}$$

With $m_{\Xi^0} = 1314.86 \pm 0.2$ MeV/c², $m_{\Sigma^0} = 1192.642 \pm 0.024$ MeV/c², $m_\Lambda = 1115.683 \pm 0.006$ MeV/c², $m_{\pi^0} = 134.9768 \pm 0.0005$ MeV/c², and with the value of m_η as given above, one has

$$\Sigma_i m_i = 4306.024 \pm 0.202 \text{ MeV/c}^2. \tag{26}$$

Since the values of *f*, when the uncertainties in $\Sigma_i m_i$ are taken into account, are significantly different, they are given separately; for $\Sigma_i m_i = 4306.024$, f = 1.03241282, for $\Sigma_i m_i = 4306.206$, f = 1.03241275, and for $\Sigma_i m_i = 4305.822$, f = 1.03241434, from which $\alpha_{th} = 0.00729735241$, $\alpha_{th} = 0.00729735248$, and $\alpha_{th} = 0.00729735233$, respectively. Hence, one has

$$(\alpha_{th} - \alpha)/\alpha = -2.2^{+1.0}_{-1.1} \times 10^{-8}. \tag{27}$$

In the above analysis, the standard deviation in $m_{\pi^\pm}$ has been ignored. When this is taken into account, and that in $\Sigma_i m_i = 4306.024 \pm 0.202$ MeV/c² is ignored, one finds $f = 1.03241282(04)$, and with this small standard deviation in *f*, the value for α_{th} remains the same as above.

One need not replace m_μ in the numerator in *f* with $m_{\pi^\pm}$, one can instead replace it with, say m_{π^0}, and to be sure, a different set of masses in the denominator, as the following example shows. One has

$$f = 1 + \frac{m_{\pi^0}}{\Sigma_i m_i} = 1 + \frac{m_{\pi^0}}{m_{\Omega^-} + m_{\Sigma^-} + m_{\Sigma^+} + m_\mu}. \tag{28}$$

With $m_{\Omega^-} = 1672.45 \pm 0.29$ MeV/c², $m_{\Sigma^-} = 1197.449 \pm 0.03$ MeV/c², and the other two masses as given previously, one obtains

$$\Sigma_i m_i = 4164.927 \pm 0.30 \text{ MeV/c}^2. \tag{29}$$

Once again the values of *f* are sufficiently different, that they will be presented separately, for the different values of $\Sigma_i m_i$ associated with its standard deviation. For $\Sigma_i m_i = 4164.927$ MeV/c², one has $f = 1.032407963$, for $\Sigma_i m_i = 4165.227$ MeV/c², $f = 1.0324056288$, and for $\Sigma_i m_i = 4164.627$, $f = 1.0324102975$, from which one has $\alpha_{th} = 0.00729735267$, $\alpha_{th} = 0.00729735279$, and $\alpha_{th} = 0.00729735254$, respectively. Hence one has

$$(\alpha_{th} - \alpha)/\alpha = 1.4^{+1.6}_{-1.8} \times 10^{-8}. \tag{30}$$

The above analysis does not include the standard deviation in m_{π^0}. However, it turned out to be negligible, when compared with that for $\Sigma_i m_i$ in (29). Since the hadron masses used above only involved the *u, d,* and *s* quarks, in the next

section expressions for α_{th} will be given that involve the charmed *c*, and bottom *b* quarks. In what follows in the next section, one will work with $m_{\pi^{\pm}}$ in the numerator of the expression for *f*, except for the case involving the bottom particles.

4. Relations for α_{th} That Include Particles Containing Either a Charmed or Bottom Quark

Following the example of the previous section, but in which one now introduces the charmed $D^{\pm}$ meson, one has

$$f = 1 + \frac{m_{\pi^{\pm}}}{\Sigma_i m_i} = 1 + \frac{m_{\pi^{\pm}}}{m_{D^{\pm}} + m_{\Xi^-} + m_{\Lambda}}. \tag{31}$$

From which, with $m_{D^{\pm}} = 1869.65 \pm 0.05$ MeV/c^2, with m_{Ξ^-} and m_{Λ} as given previously, one has

$$\Sigma_i m_i = 4307.043 \pm 0.086 \text{ MeV}/c^2 . \tag{32}$$

Again, since the values of *f*, when the standard deviation in $\Sigma_i m_i$ is taken into account, are significantly different, they are given separately: for $\Sigma_i m_i = 4307.043$, $f = 1.03240515$, for $\Sigma_i m_i = 4307.139$, $f = 1.03240443$, and for $\Sigma_i m_i = 4306.957$, $f = 1.03240580$, so that one has, $\alpha_{th} = 0.00729735281$, $\alpha_{th} = 0.00729735285$, and $\alpha_{th} = 0.00729735278$, respectively. Hence, since the contribution of the standard deviation thin $m_{\pi^{\pm}}$ is negligible, one has

$$(\alpha_{th} - \alpha)/\alpha = 3.3^{+0.6}_{-0.4} \times 10^{-8}. \tag{33}$$

As yet another example involving a charmed particle, the charmed baryon Λ_c^+ will be introduced. One has

$$f = 1 + \frac{m_{\pi^{\pm}}}{\Sigma_i m_i} = 1 + \frac{m_{\pi^{\pm}}}{m_{\Lambda_c^+} + m_{\Sigma^-} + m_{\eta} + m_{\pi^{\pm}} + m_{\pi^0}}, \tag{34}$$

from which, with $m_{\Lambda_c^+} = 2286.46 \pm 0.14$ MeV/c^2, $m_{\Sigma^-} = 1197.449 \pm 0.0030$ MeV/c^2, and the other masses that have been given previously, one has

$$\Sigma_i m_i = 4306.318 \pm 0.144 \text{ MeV}/c^2 . \tag{35}$$

From which $f = 1.03241061(108)$, for the mean one has $\alpha_{th} = 0.00729735253$, and for $\Sigma_i m_i = 4306.462$ MeV/c^2, $\alpha_{th} = 0.00729735258$, and for $\Sigma_i m_i = 4306.174$ MeV/c^2, $\alpha_{th} = 0.00729735247$, so that finally one has

$$(\alpha_{th} - \alpha)/\alpha = -5.5^{+6.9}_{-8.2} \times 10^{-9}. \tag{36}$$

The contribution from the standard deviation of $m_{\pi^{\pm}}$ is $\pm 0.3 \times 10^{-9}$, and hence negligible.

For the case of a particle containing the b quark, one will work here with the masses of the $B^{\pm}$ and B^0 mesons, and then with the bottom baryon Λ_b^0. Because of the large mass involved in the denominator of $f - 1$, one has to choose a larger mass in the numerator than $m_{\pi^{\pm}}$, and m_{K^0} will be chosen., This choice in turn leads to an increased number of masses in the denominator, which will

also include the mass of a particle containing the charm quark, and since f will also include the masses of particles containing the three lighter quarks, all the quarks will be represented in the masses in f, except that of the top quark. One has

$$f = 1 + \frac{m_{K^0}}{\Sigma_i m_i} = 1 + \frac{m_{K^0}}{m_{B^0} + m_{B^\pm} + m_{D^\pm} + m_n + m_p + m_\eta + m_{K^0}}. \tag{37}$$

From which, with $m_{B^0} = 5279.65 \pm 0.12$ MeV/c^2, $m_{B^\pm} = 5279.34 \pm 0.12$ MeV/c^2, and the masses of the other particles in the sum given previously, one has

$$15351.95 \pm 0.18 \text{ MeV}/\text{c}^2 . \tag{38}$$

Just taking into account the standard deviation in the above sum, one has $f = 1.03241354(38)$, and hence $\alpha_{th} = 0.00729735237(2)$. Next. just taking the standard deviation into account in m_{K^0} in the numerator, since its contribution to the standard deviation in $\Sigma_i m_i$ is negligible, $f = 1.03241354(85)$, and $\alpha_{th} = 0.00729735237(4)$. One therefore has

$$(\alpha_{th} - \alpha)/\alpha = (-2.7 \pm 0.3 \pm 0.6) \times 10^{-8}, \tag{39}$$

where the first standard deviation in (39) is due to that in $\Sigma_i m_i$, and the second is due to the that of m_{K^0} in the numerator.

Next, one will take up the case when there is the mass of the bottom baryon Λ_b^0 in the denominator of $f - 1$. One has

$$\begin{aligned} f &= 1 + \frac{m_{K^0}}{\Sigma_i m_i} \\ &= 1 + \frac{m_{K^0}}{m_{\Lambda_b^0} + m_\tau + m_{\Xi^-} + m_{\Xi^0} + m_{\Sigma^-} + m_\Lambda + m_n + m_p + m_{K^0} + m_{K^\pm} + m_{\pi^\pm}} \end{aligned} \tag{40}$$

From which, with $\Lambda_b^0 = 5619.60 \pm 0.17$ MeV/c^2, and other masses as given previously, one has

$$\Sigma_i m_i = 15354.853 \pm 0.30 \text{ MeV}/\text{c}^2 . \tag{41}$$

Again, just taking into account the standard deviation in the sum, one finds $f = 1.03240741(63)$. From which one obtains for the mean $\alpha_{th} = 0.00729735270$, for the plus standard deviation, $\alpha_{th} = 0.00729735274$, and for the minus, $\alpha_{th} = 0.00729735266$. The standard deviation from that in m_{K^0} in the numerator is not the same at that above, hence one has

$$(\alpha_{th} - \alpha)/\alpha = 1.8^{+0.5\ +0.5}_{-0.6\ -0.7} \times 10^{-8} \tag{42}$$

where, as above, the first deviations are due to the standard deviation in the mass sum, and the second is due to that in m_{K^0} in the numerator. For brevity values of f and α_{th} are omitted.

In all the cases considered above, the denominator in $f - 1$ has only involved a sum of masses, based on the possibility that in a future theory, the denominators would arise as a consequence of a quantum theoretical mass sum

rule. However, in the present absence of such a theory, there is no obvious objection to having some of masses appear with a minus sign, so that the sum $\Sigma_i m_i$ gets replaced with $\Sigma_i (\pm)_i m_i$. For brevity only one case will be considered involving the baryon Λ_b^0. One has

$$f = 1 + \frac{m_{\pi^\pm}}{\Sigma_i (\pm)_i m_i} = 1 + \frac{m_{\pi^\pm}}{m_{\Lambda_b^0} - m_{\Omega^-} + m_{K^\pm} - m_{\pi^0}}. \tag{43}$$

From which, with $m_{\Lambda_b^0} = 5619.60 \pm 0.17$ MeV/c^2, and the masses of the other particles that have been given previously, one has

$$\Sigma_i (\pm)_i m_i = 4305.85 \pm 0.34 \text{ MeV}/c^2 . \tag{44}$$

Since the values of f and α_{th} are sufficiently different when the standard deviation is taken into account, they will be presented separately. However, the change in α_{th} due to the standard deviation in $m_{\pi^\pm}$ in the numerator is negligible. For the mean, one has f = 1.03241413, for the plus standard deviation, f = 1.03241157, and for the negative, f = 1.03241669, so that one has $\alpha_{th} = 0.00729735234$, $\alpha_{th} = 0.00729735247$, and $\alpha_{th} = 0.00729735221$, respectively. Hence, one has

$$(\alpha_{th} - \alpha)/\alpha = -3.2^{+1.8}_{-1.7} \times 10^{-8} . \tag{45}$$

Another issue is whether one could add or subtract the mass of the electron to the denominators to possible improve the agreement. For example, in the above case, if one adds m_e to the denominator, one gets f = 1.03241029, and hence $\alpha_{th} = 0.007297352544$, and hence an agreement $(\alpha_{th} - \alpha)/\alpha = -3.4 \times 10^{-9}$. But the standard deviation in the result is an order of magnitude greater, and makes the result questionable. But again, in absence of a proper theory, one cannot rule out such a contribution to the denominator.

Although the most accurate agreement for α_{th} up to now has been of order 10^{-9}, albeit with a large standard deviation, and most agreements are of order 10^{-8}, one could actually improve agreements by one to two orders of magnitude were it not for the large standard deviations in many of the particle masses. Therefore, it seems reasonable that with further improvement in particle mass measurements, it will be possible to fit the value of α given in [22] to within its experimental standard deviation of $\pm 1.5 \times 10^{-10}$. Interestingly, as this work was in the process of being completed, Morel *et al.* [35] presented an even more precise value of α, with a standard deviation of $\pm 0.81 \times 10^{-10}$. Since this is only about a factor of two increase in accuracy over α in [22], if with improved particle mass measurements one will be able to fit α in [22], one should also be able to fit this new value in [35]. In any case, the majority of the agreements found here, of the order of several parts in one hundred million, are more than sufficient to deal with the application to the cosmological measurement of α in section 6. However, for completeness, before going on to this application, it will be shown in the next section that the above analysis applies to the gauge W and Z bosons, and the Higgs H^0 boson.

5. Relations for α_{th} with Gauge W and Z, and Higgs H^0 Bosons

With the numerator of $f-1$ given by the bottom meson, B_1^0, and for brevity, rather than dealing with them individually, just the sum of the masses of W and Z, will be utilized in the denominator, along with earlier used particle masses. One has

$$f=1+\frac{m_{B_1^0}}{\Sigma_i m_i}=1+\frac{m_{B_1^0}}{m_Z+m_W+m_{\Omega^-}+m_n+m_p+m_{K^0}+m_{K^\pm}+m_\eta}. \tag{46}$$

From which, with $m_z=91.1876\pm0.0021$ GeV/c^2 and $m_W=80.379\pm0.012$ GeV/c^2, and with the other masses given previously, one has

$$\Sigma_i m_i=176.656\pm0.012\ \mathrm{GeV/c^2}. \tag{47}$$

With $m_{B_1^0}=5.7261\pm0.0013$ GeV/c^2, one obtains for the mean, $f=1.03241384$, for the plus standard deviation, $f=1.03241164$, and for the negative, $f=1.03241605$, and hence $\alpha_{th}=0.00729735236$, $\alpha_{th}=0.00729735247$, and $\alpha_{th}=0.00729735224$, respectively, so that one has

$$\left(\alpha_{th}-\alpha\right)/\alpha=-2.9^{+1.5}_{-1.6}\times10^{-8}. \tag{48}$$

The standard deviations in the masses of the Z and B_1^0 were negligible compared to that of the W. For the case of the Higgs H^0 boson, the numerator of $f-1$ will be taken to be the mass of the χ_{c1} $c\bar{c}$ meson, so that one has

$$f=1+\frac{m_{\chi_{c1}}}{\Sigma_i m_i}=1+\frac{m_{\chi_{c1}}}{m_{H^0}+m_{D^0}+m_{K^0}+m_{K^\pm}}. \tag{49}$$

From which, with $m_{H^0}=125.1\pm0.14$ GeV/c^2, $m_{D^0}=1864.83\pm0.05$ MeV/c^2, and $m_{\chi_{c1}}=4146.8\pm2.4$ MeV/c^2, and the values of the other masses given previously, one has

$$\Sigma_i m_i=127.956\pm0.14\ \mathrm{GeV/c^2}. \tag{50}$$

From which one obtains for the mean, $f=1.03240802$, for the plus standard deviation in (50) (that in $m_{\chi_{c1}}$ will be evaluated separately) one has $f=1.03240447$, and for the minus, $f=1.03241156$, and hence, $\alpha_{th}=0.00729735266$, $\alpha_{th}=0.00729735285$, and $\alpha_{th}=0.00729735248$, respectively. Next, the same evaluations will be made for the standard deviation in $m_{\chi_{c1}}$. For the plus, one has, $f=1.03242677$, and for the minus, $f=1.03238926$, and hence, one has $\alpha_{th}=0.00729735168$, and $\alpha_{th}=0.00729735365$, respectively. From the above one arrives at the following agreement

$$\left(\alpha_{th}-\alpha\right)/\alpha=1.2^{+2.6\ +14}_{-2.4\ -11}\times10^{-8}, \tag{51}$$

where the first standard deviation is due to that in the mass of the H^0, and the second, to that in the mass of the χ_{c1}.

6. Application to the Cosmological Measurement of α

Over the years there has been an interest in whether the fundamental constants,

such as the fine structure constant, vary with time, so that α would become $\alpha(z)$, where z is the redshift back to an earlier epoch. More generally, there is the question as to whether α would vary spatially as well, because of possible spatial anisotropy, so that one would have $\alpha=\alpha(z,RA,\delta)$, where RA is right ascension, and δ is declination. The following is a reduced list of references to this much researched subject: [7] [36]-[56]. For a detailed discussion, see, e.g., [16] and [50]. The present work has shown the dependency of α_{th} on particle masses has an accuracy given by $(\alpha_{th}-\alpha)/\alpha$ in the range 10^{-7} to 10^{-9}, and since current astronomical determinations α are of the order 10^{-5}, e.g., in [54], Wilczynska, *et al.* give $(\alpha_z-\alpha)/\alpha=(-2.18\pm 7.27)\times 10^{-5}$, while in [46], Reinhold *et al.* give for a weighted fit, $\Delta\mu/\mu=(2.4\pm 0.6)\times 10^{-5}$, it follows that statements here, based on the properties of α_{th}, can be taken to hold for the properties of α as they exist physically, and are determined astronomically. Thus, in what follows, the subscript "th" on α can be dropped, and one can assume the properties of α are the same as those of α_{th}. This leads to two interesting consequences. First, since α is homogeneous degree zero in the particle masses, since $\alpha=\alpha(f,\mu)$, and both f and μ are homogeneous degree zero in the particle masses of which they are functions, it follows that any change of the particle masses m_i of the form $m_i\to\phi(z,ra,d)m_i$, necessarily leaves α invariant, so that

$$\alpha\left(\phi(z,ra,d)m_i\right)=\alpha(m_i), \tag{52}$$

which entails that

$$\Sigma_i\frac{\partial\alpha}{\partial m_i}m_i=0. \tag{53}$$

Thus, for there to be a change in α, not all the masses of which α is a function can change in the same way. Consequently, there would have to be one or more changes in particle mass ratios, of which the simplest would be a change in the ratio that is the most accurately determined astronomically, *i.e.*, $\mu\equiv m_p/m_e$. Needless to say, such changes are not expected according to the standard model, since it is based on special relativity for which there is invariance under time and space translations.

To determine how a small change in α is related to a small change in μ it is convenient to rewrite (11) as

$$\alpha=\left(\sqrt{1+f54\mu^{-1}}-1\right)/2f, \tag{54}$$

and expand, just keeping the first two terms, which yields

$$\alpha=13.5\mu^{-1}-f(182.25)\mu^{-2}+\cdots, \tag{55}$$

from which, upon varying α, one has

$$\delta\alpha=-13.5\mu^{-2}\delta\mu+f(364.5)\mu^{-3}\delta\mu-182.25\mu^{-2}\delta f. \tag{56}$$

Since one is going to divide $\delta\alpha$ by α, it is helpful to determine the relative

magnitude of the terms in these two equations, so as to see what can be neglected. With $\mu^{-1} = 5.446\times10^{-4}$ and $f = 1.03241$, (55) becomes

$$\alpha = 7.35\times10^{-3} - 5.58\times10^{-5}. \tag{57}$$

Since the second term is less than one percent of the first term, and since the measurements are not of this accuracy, it will be neglected in what follows. Therefore upon dividing $\delta\alpha$ in (56) by just the first term in (55), one has

$$\frac{\delta\alpha}{\alpha} = -\frac{\delta\mu}{\mu} + f27\mu^{-1}\frac{\delta\mu}{\mu} - 13.5\mu^{-1}\delta f. \tag{58}$$

Inserting the values for μ^{-1} and f into (58), it takes the form

$$\frac{\delta\alpha}{\alpha} = -\frac{\delta\mu}{\mu} + 0.015\frac{\delta\mu}{\mu} - 7.4\times10^{-3}\delta f. \tag{59}$$

Since one has already neglected two terms of order one percent, the second term on the right hand side can be neglected. Also, since $\delta f = (\delta f/f) f$, and since $f \approx 1$, $\delta f \approx \delta f/f$. Under the assumption that $\delta f/f$ is no greater in magnitude than $\delta\mu/\mu$ which according to the latest measurements, if it exists at all, would be of the order 10^{-5}, so that this third term is less than one percent of the first term, and hence can also be neglected. Thus, to within a few percent, one has

$$\frac{\delta\alpha}{\alpha} \approx -\frac{\delta\mu}{\mu}. \tag{60}$$

This relation should prove helpful in ruling out false determinations, such as the ones that have been made in the past: since if there is a report of, say, a decrease in α of a certain magnitude for a given cosmological location, then, according to (60), there should be a simultaneous report of an increase in μ of very nearly the same magnitude at the same location, and vice versa.

7. Concluding Remarks

This work shows that it is possible to fit the empirical value of the fine structure constant to several parts per 10^9, albeit with a large standard deviation, and very likely fit it to its current determination, by employing more accurately measured particle masses. These relations, that are homogeneous degree zero in the particle masses, were found partly by empirical considerations, partly by trial and error, and partly by several theoretical assumptions about the mass of the electron that lie outside the current realm of QED. Most importantly, it was assumed that the contribution to the mass of the electron from the electromagnetic field is finite, and of the form: $\Delta m_e = f\alpha m_{eb}$, where m_{eb} is the so-called "bare mass" of the electron, that is defined in Equation (7), and where f is a new parameter that is a homogeneous degree zero function of particle masses that are chosen by trial and error. It is shown to have the value $f = 1.032409810(63)$, where the standard deviation in f is due mainly to the standard deviation in the masses of the proton and electron that are involved in the determination of f ac-

cording to Equation (14). With Δm_e as above, the bare mass of the electron according to Equation (9) is given by $m_e/(1+f\alpha)$, and this value for m_{eb} should be falsifiable when a generally-accepted determination of the contribution to the mass of the electron from its interaction with the Higgs field becomes available. What would help in this investigation would be the experimental determination of Δm_e. However, a glance at the literature, e.g. [31], shows that although there have been substantial efforts over many years to deal with the logarithmic divergence of the electron's self-energy, of which renormalization is the prime example, little attention has been paid to the issue to how to measure Δm_e, or whether in principle it is measurable at all. Thus it is hoped that this work, as well as an earlier comment by the author [57] will serve to direct attention to this long neglected area.

As indicated in the previous section, this work has significant bearing on the cosmological determination of whether α depends on time and space. It was pointed out that since some of the expressions given here for α_{th}, with improved particle mass determinations, most likely can finally arrive at $\alpha_{th}-\alpha=0$, to within the empirical uncertainty of α itself, then, because the expression for α would be homogeneous degree zero in the particle masses determining it, any variation of the particle masses of the form $m_i \to \phi(z, RA, \delta)m_i$ would necessarily leave α unchanged, so that at least one mass would have to change differently than the other masses in the relation for α. Although this seems highly unlikely on the basis of the standard model, based as it is on special relativity, nevertheless, since the model does not predict the masses of the particles, such behavior cannot be ruled out, and therefore continuing efforts to look for possible cosmological changes in α are fully justified. With regard to such investigations, it was shown that because of the relation between α and μ, as given in Equation (54), such possible changes in α would be accompanied by changes in μ, which would satisfy the relation, $\delta\alpha/\alpha=-\delta\mu/\mu$, to within a few percent. Consequently, when possible changes in α and μ are reported, the determination of whether they satisfied this approximate relation would provide a critical test as to whether the reported changes were true, or whether they were due to some previously unrecognized source of error.

Finally, it is a prediction of this work that a new approach to QED is possible, in which the electron's self-energy is finite, and the value of α emerges from the theory, rather than being inserted from empirical measurement. In view of the relation of α to the particle masses found here, such a theory might shed new light on the particle mass spectrum as well.

Acknowledgements

I would like to thank my son Prof, Timothy Tangherlini for providing me with copies of Prof. Victor Weisskopf's two papers cited in the text. It is perhaps of historical interest that I first learned of the logarithmic divergence of the electron's self-energy at a Harvard physics colloquium given by Prof. Julian Schwinger

in the late fall of 1947. I was a physics student in my senior year at the time, and two of my professors were: in electrostatics, Prof. Wendell Furry, who discovered the logarithmic divergence, as mentioned in the text, and in quantum mechanics, Prof. Julian Schwinger. Some years later, in 1954, there was a brief correspondence with Prof. Richard Feynman dealing in part with the divergence problem. I would also like to thank the reviewer for several references.

Conflicts of Interest

The author declares that there are no conflicts of interest regarding the publication of this paper.

References

[1] Sommerfeld, A. (1916) *Annalen der Physik*, **51**, 125-167. https://doi.org/10.1002/andp.19163561802

[2] Dirac, P.A.M. (1928) *Proceedings of the Royal Society A*, **11**, 610-624.

[3] Darwin, C.G. (1928) *Proceedings of the Royal Society A*, **118**, 654-650. https://doi.org/10.1098/rspa.1928.0076

[4] Gordon, W. (1928) *Zeitschrift für Physik*, **48**, 11-14. https://doi.org/10.1007/BF01351570

[5] Eddington, A.S. (1946) Fundamental Theory. Cambridge University Press, Cambridge.

[6] Born, M. (1935) *Proceedings of the Indian Academy of Science A*, **2**, 533-861. https://doi.org/10.1007/BF03045991

[7] Teller, E. (1948) *Physical Review*, **73**, 801-802. https://doi.org/10.1103/PhysRev.73.801

[8] Landau, L. (1955) On the Quantum Theory of Fields. In: Pauli, W., Ed., *Niels Bohr and the Development of Physics*, McGraw Hill, New York, 52.

[9] Peebles, P.J.E. and Dicke, R.H. (1962) *Physical Review*, **128**, 2006. https://doi.org/10.1103/PhysRev.128.2006

[10] Pauli, W. (1958) Theory of Relativity. Field, G., Trans., Pergamon Press, London, 225.

[11] Wyler, A.N. (1969) *Comptes Rendus Academie Sciences*, *Paris*, *Series A*, **269**, 743.

[12] Peres, A. (1971) *Physics Today*, **24**, 9. https://doi.org/10.1063/1.3022455

[13] Isham, C., Salam, A. and Strathdee, J. (1971) *Physical Review D*, **3**, 1805-1817. https://doi.org/10.1103/PhysRevD.3.1805

[14] MacGregor, M.H. (1971) *Lettere al Nuovo Cimento*, **1**, 759-764. https://doi.org/10.1007/BF02770123

[15] Rozenthal, L.L. (1981) *Soviet Physics*, *JETP Letters*, **31**, 279.

[16] Barrow, J.D. and Tipler, F.J. (1986) The Anthropic Cosmological Principle. Oxford University Press, New York, 295-297, 358.

[17] Good, I.J. (1990) A Quantal Hypothesis for Hadrons and the Judging of Physical Numerology. In: Grimmett, G.R. and Welah, D.J.A., Eds., *Disorder in Physical Systems*, Oxford University Press, Oxford, 141.

[18] Várlaki, P., Nádai, L. and Bokor, J. (2008) *Acta Politechnica Hungarica*, **5**, 71-104.

[19] Nambu, Y. (1952) *Progress Theoretical Physics*, **7**, 595-596. https://doi.org/10.1143/PTP.7.5.595

[20] Tangherlini, F.R. (1971) *Lettere al Nuovo Cimento*, **2**, 109-114. https://doi.org/10.1007/BF02770096

[21] Tangherlini, F.R. (1972) *Progress Theoretical Physics*, **58**, 2002-2003. https://doi.org/10.1143/PTP.58.2002

[22] Zyla, P.A., *et al.* (Particle Data Group) (2020) *Progress Theoretical Experimental Physics*, **2020**, 083C01.

[23] Srednicki, M. (2007) Quantum Field Theory. Cambridge University Press, Cambridge, 550. https://doi.org/10.1017/CBO9780511813917

[24] Weisskopf, V. (1934) *Zeitschrift für Physik*, **90**, 817-818. https://doi.org/10.1007/BF01340744

[25] Weisskopf, V. (1934) *Zeitschrift für Physik*, **89**, 27-38. https://doi.org/10.1007/BF01333228

[26] Feynman, R.P. (1949) *Physical Review*, **76**, 769-789. https://doi.org/10.1103/PhysRev.76.769

[27] Dyson, F.J. (1949) *Physical Review*, **75**, 486-502. https://doi.org/10.1103/PhysRev.75.486

[28] Schwinger, J. (1949) *Physical Review*, **75**, 651-679. https://doi.org/10.1103/PhysRev.75.651

[29] Tomonaga, S. (1946) *Progress Theoretical Physics*, **1**, 1-13. https://doi.org/10.1143/PTP.1.27

[30] Brown, L.M. (1984) Ed. Renormalization. Springer-Verlag, New York.

[31] Schweber, S.S. (1994) QED and The Men Who Made It: Dyson, Feynman, Schwinger, and Tomonaga. Princeton University Press, Princeton, 595-605. https://doi.org/10.1063/1.2808749

[32] Weinberg, S. (1995) The Quantum Theory of Fields. Cambridge University Press, Cambridge, 1-48. https://doi.org/10.1017/CBO9781139644167

[33] Zee, A. (2010) Quantum Field Theory in a Nutshell. 2nd Edition, Princeton University Press, Princeton, 161-172, 356-368.

[34] Feynman, R. P. (1985) QED. Princeton University Press, Princeton, 128.

[35] Morel, L., Yao, Z., Cladé, P. and Guellati-Khélifa, S. (2020) *Nature*, **588**, 61-65. https://doi.org/10.1038/s41586-020-2964-7

[36] Dirac, P.A.M. (1937) *Nature*, **139**, 323. https://doi.org/10.1038/139323a0

[37] Gamow, G. (1967) *Physical Review Letters*, **19**, 759-761, 1000. https://doi.org/10.1103/PhysRevLett.19.759

[38] Bahcall, J. and Schmidt, M. (1967) *Physical Review Letters*, **19**, 1527-1539. https://doi.org/10.1103/PhysRevLett.19.1294

[39] Dyson, F.J. (1972) The Fundamental Constants and Their Time Variation. In: Dirac, P.A.M., Salam, A. and Wigner, E.P., Eds., *Aspects of Quantum Theory*, Cambridge University Press, Cambridge, 213-236.

[40] Bekenstein, J.D. (1982) *Physical Review D*, **25**, 1527-1539. https://doi.org/10.1103/PhysRevD.25.1527

[41] Damour, T. and Dyson, F.J. (1996) *Nuclear Physics B*, **480**, 37-54. https://doi.org/10.1016/S0550-3213(96)00467-1

[42] Murphy, M.T., Webb, J.K. and Flambaum, V.V. (2003) *Science*, **320**, 1611. https://doi.org/10.1126/science.1156352

[43] Lamoreaux, S.K. and Torgerson, J.R. (2004) *Physical Review D*, **69**, Article ID: 121701.

[44] Peik, E., *et al.* (2004) *Physical Review Letters*, **93**, Article ID: 170801. https://doi.org/10.1103/PhysRevLett.93.170801

[45] Barrow, J.D. (2005) *Physical Review D*, **71**, Article ID: 083520. https://doi.org/10.1103/PhysRevD.71.083520

[46] Reinhold, E., *et al.* (2006) *Physical Review Letters*, **96**, Article ID: 151101.

[47] Cahir, H., *et al.* (2020) Improved Access to the Fine-Structure Constant with the Simplest Atomic Systems. arXiv:2006.14261v1 [physics.atom-ph]

[48] Milaković, D. *et al.* (2020) A New Era of Fine Structure Constant Measurements at High Redshift. arXiv: 2008:10169 [astro-ph. CO]

[49] Murphy, M.T., Flambaum, V.V., Muller, S. and Henkel, C. (2008) *Science*, **320**, 1611. https://doi.org/10.1126/science.1156352

[50] Uzan, J.-P. (2011) *Living Review of Relativity*, **14**, 2-146. https://doi.org/10.12942/lrr-2011-2

[51] Webb, J.K., *et al.* (2011) *Physical Review Letters*, **107**, Article ID: 191101.

[52] Stadnick, Y.V. and Flambaum, V.V. (2015) *Physical Review Letters*, **115**, Article ID: 201301. https://doi.org/10.1103/PhysRevLett.115.201301

[53] Wei, H., Zou, X.-B., Li, H.-Y. and Xue, D.-Z. (2017) *European Physical Journal C*, **77**, 14. https://doi.org/10.1140/epjc/s10052-016-4581-z

[54] Wilczynska, M.R., *et al.* (2020) *Science Advances*, **6**, eaay9672.

[55] Auci, M. (2021) *European Physics Journal D*, **75**, 253. https://doi.org/10.1140/epjd/s10053-021-00253-x

[56] Murphy, M.T., *et al.* (2022) *Astronomy and Asrrophysics*, **658**, A123.

[57] Tsngherlini, F.R. (2018) *Physics Today*, **71**, 15. https://doi.org/10.1063/PT.3.3834

Journal of Modern Physics, 2022, 13, 700-706
https://www.scirp.org/journal/jmp
ISSN Online: 2153-120X
ISSN Print: 2153-1196

Selection Rules in Weak Interaction and Conservation of Fermion Quantum Number

Xinhua Ma[1,2]

[1]Key Laboratory of Particle Astrophysics, Institute of High Energy Physics, Chinese Academy of Sciences, Beijing, China
[2]TIANFU Cosmic Ray Research Centre, Chengdu, China
Email: maxh@ihep.ac.cn

How to cite this paper: Ma, X. H. (2022) Selection Rules in Weak Interaction and Conservation of Fermion Quantum Number. *Journal of Modern Physics*, **13**, 700-706.
https://doi.org/10.4236/jmp.2022.135039

Received: March 24, 2022
Accepted: May 8, 2022
Published: May 11, 2022

Abstract

Traditionally, in weak interaction, I_3, Y and four flavour quantum numbers are not conserved but several empirical selection rules work well. Recently, it was found that, in weak interaction, there are three levels of conservation of additive quantum numbers, and fermion quantum number F is conserved in all kinds of interactions. It is known that weak interaction has three types: fermionic, pure hadronic and pure leptonic, corresponding to the first and the second level of conservation of additive quantum numbers respectively. It is demonstrated in this paper that the selection rules in all types of weak interaction can be interpreted by conservation of F, and the formula of relation between Q/e, F and F_0 is more general than Gell-Mann-Nishijima formula. Description of weak interaction becomes simpler, If only we take Q, F_0 and F, based on the conserved physical quantities.

Keywords

Weak Interaction, Selection Rules, Fermion Quantum Number

1. Introduction

At the most elementary level, at present, fermions include quarks and leptons. Traditionally, isospin (I) with isospin projection (I_3) is assigned to u and d quarks, but the other four quarks have the flavour quantum numbers: S, C, B^* and T for s, c, b and t quarks respectively. All quarks have the baryon quantum number B and electric charge Q. Hypercharge Y is defined from I_3 and Q. Leptons, much simpler than quarks, have Q and lepton quantum number L. Q, B, L, I, I_3, Y and four flavour quantum numbers are additive quantum numbers. Q, B and L are conserved in strong interaction, electromagnetic interaction and weak interaction. I_3, Y and four flavour quantum numbers are conserved in strong interac-

tion and electromagnetic interaction, but not conserved in weak interaction. I is conserved in strong interaction, but not conserved in either electromagnetic interaction or weak interaction. On the other hand, in weak interaction, the systematic way in which symmetry related to conservation is broken leads to several empirical selection rules which may serve to check observations and to put constraint on models. It is conventional to refer to weak interaction events as being pure leptonic, pure hadronic (or nonleptonic) or fermionic (or semi-leptonic, semi-hadronic) depending on whether they involve leptons only, hadrons only, or both leptons and hadrons. Knowledge above is described in textbooks, e.g., [1] [2] [3] [4].

Recently, it was found that, in weak interaction, there are three levels of conservation of additive quantum numbers [5]: at the first (the highest) level, Q, B, L and fermion quantum number F are conserved including all kinds of fermions (both quarks and leptons). At the second level, quark quantum number H is only conserved including pure hadrons, and lepton quark-like quantum number H_L is only conserved including pure leptons. At the third (the lowest) level, I, I_3, Y and flavour quantum numbers are not conserved. Because realized that the types of weak interaction correspond to the first and the second level of conservation of the additive quantum numbers respectively, it is natural to consider if there is any relation between conservation of the additive quantum numbers and the selection rules in weak interaction.

2. Additive Quantum Numbers

Characteristics of additive quantum numbers are described in [5] and here are summarized in brief. Flavor quantum number D and U for d and u quark respectively are related to I_3 in

$$I_3 = \left(D+U\right)/2. \tag{1}$$

H is sum of all six flavor quantum numbers:

$$H = D+U+S+C+B^*+T = \begin{cases} -1: \text{quark is 'd' type} \\ +1: \text{quark is 'u' type} \end{cases} \tag{2}$$

Antiquarks have additive quantum numbers with the same absolute values as quarks but the opposite sign of quarks, except that antiquarks have same I as quarks. H of each lepton is zero.

H_L of leptons is similar with H of quarks:

$$H_L = \begin{cases} -1: \text{lepton is 'd' type} \\ +1: \text{lepton is 'u' type} \end{cases} \tag{3}$$

Antileptons have additive quantum numbers with the same absolute values as leptons but opposite sign of leptons. H_L of each quark is zero.

F for all fermions is combined from H and H_L:

$$F = H + H_L = \begin{cases} -1: \text{fermion is 'd' type} \\ +1: \text{fermion is 'u' type} \end{cases} \tag{4}$$

The formula of relation between electronic charge Q/e, F and F_0 is

$$Q/e = \left(F_0 + F\right)/2, \tag{5}$$

where F_0 is:

$$F_0 = \begin{cases} B = +1/3: \text{fermion is quark} \\ -L = -1: \text{fermion is lepton} \end{cases} \tag{6}$$

Values of additive quantum numbers of quarks and leptons are listed in Table 1 and Table 2 respectively. Comparing Equation (5) with Gell-Mann-Nishijima formula [6] [7] [8] (in extended form)

$$Q/e = I_3 + Y/2, \tag{7}$$

we can see that Equation (5) only includes conserved additive quantum numbers so as to express more general and more profound connotation than Equation (7) including not-conserved additive quantum numbers in weak interaction.

3. Selection Rules and Conservation of *F*

In the following paragraphs we check all three types of weak interaction one by one to verify if the selection rules are related to conservation of *F*. Firstly, hadrons composed by only u, d and s quarks are considered, so from Equation (2),

$$H = D + U + S. \tag{8}$$

After it, the relation is generalized to heavier quarks (Section 3.4).

3.1. Pure Hadronic Weak Interaction

From Equation (1) and (8),

Table 1. Additive quantum numbers of quarks.

quark	Q/e	B	I	I_3	D	U	S	C	B^*	T	Y	H	F
d	−1/3	+1/3	+1/2	−1/2	−1	0	0	0	0	0	+1/3	−1	−1
u	+2/3	+1/3	+1/2	+1/2	0	+1	0	0	0	0	+1/3	+1	+1
s	−1/3	+1/3	0	0	0	0	−1	0	0	0	−2/3	−1	−1
c	+2/3	+1/3	0	0	0	0	0	+1	0	0	+4/3	+1	+1
b	−1/3	+1/3	0	0	0	0	0	0	−1	0	−2/3	−1	−1
t	+2/3	+1/3	0	0	0	0	0	0	0	+1	+4/3	+1	+1

Table 2. Additive quantum numbers of leptons.

Lepton	Q/e	L	H_L	F
e^-	−1	+1	−1	−1
ν_e	0	+1	+1	+1
μ^-	−1	+1	−1	−1
ν_μ	0	+1	+1	+1
τ^-	−1	+1	−1	−1
ν_τ	0	+1	+1	+1

$$\Delta H = \Delta\left(S + D + U\right) = \Delta S + 2\Delta I_3 . \tag{9}$$

The pure hadronic weak interaction obeys selection rule

$$\Delta S = \mp 1,\ \ \Delta I = \pm 1/2,\ \ \Delta I_3 = \pm 1/2 . \tag{10}$$

Obviously, the selection rule (Equation (10)) can be deduced from $\Delta H = 0$ (Equation (9)), *i.e.*, conservation of H as well as conservation of F because in pure hadronic weak interaction $H_L = 0$ and then $F = H_L$ (Equation (4)). For example, in K^0 decay

$$\mathrm{K}^0 \to \pi^+ + \pi^- , \tag{11}$$

or in quark terms

$$\bar{\mathrm{s}}\mathrm{d} \to \bar{\mathrm{d}}\mathrm{u} + \bar{\mathrm{u}}\mathrm{d} , \tag{12}$$

we can see that $\Delta H = 0$ as well as $\Delta F = 0$ which leads to $\Delta S = -1$ and $\Delta I_3 = 1/2$.

Although lower probability than $\Delta S = \pm 1$, there exists the pure hadronic weak interaction with $\Delta S = \pm 2$. For example, in the decay

$$\Xi^- \to \mathrm{n} + \pi^- , \tag{13}$$

or in quark terms

$$\mathrm{ssd} \to \mathrm{ddu} + \bar{\mathrm{u}}\mathrm{d} , \tag{14}$$

the selection $\Delta S = 2$ and $\Delta I_3 = -1$ can still be deduced from $\Delta H = 0$ (Equation (9)) as well as $\Delta F = 0$.

In consequence, in the pure hadronic weak interaction including u, d and s quarks, the selection rules can be deduced from conservation of H as well as conservation of F.

3.2. Pure Leptonic Weak Interaction

In the pure leptonic weak interaction, because $S = 0$ and $H = 0$, there is no selection rule, but H_L as well as F is conserved. For example, in muon decay

$$\mu^- \to \mathrm{e}^- + \bar{\nu}_\mathrm{e} + \nu_\mu , \tag{15}$$

$\Delta H_L = 0$ as well as $\Delta F = 0$ is satisfied.

3.3. Fermionic Weak Interaction

The fermionic weak interaction, in which both hadrons and leptons are involved, obeys two selection rules:

1) The first selection rule is

$$\Delta S = 0,\ \ \Delta I = \pm 1,\ \ \Delta I_3 = \pm 1 . \tag{16}$$

From Equation (4) and Equation (9),

$$\Delta F = \Delta H_L + 2\Delta I_3 . \tag{17}$$

For example, in β decay

$$\mathrm{n} \to \mathrm{p} + \mathrm{e}^- + \bar{\nu}_\mathrm{e} , \tag{18}$$

or in quark terms

$$\mathrm{ddu} \to \mathrm{uud} + \mathrm{e}^- + \bar{\nu}_\mathrm{e}, \tag{19}$$

where s quark does not appear, we can see that $\Delta F = 0$ (Equation (17)) which leads to $\Delta I_3 = 1$ and $\Delta H_L = -2$.

Another example is that in Σ^+ decay

$$\Sigma^+ \to \Lambda^0 + \mathrm{e}^+ + \nu_\mathrm{e}, \tag{20}$$

or in quark terms

$$\mathrm{suu} \to \mathrm{sud} + \mathrm{e}^+ + \nu_\mathrm{e}, \tag{21}$$

where S is not changed as s quark so called "spectator" does not participate in the reaction, we can see that $\Delta F = 0$ (Equation (17)) which causes $\Delta I_3 = -1$ and $\Delta H_L = 2$.

2) The second selection rule is

$$\Delta S = \Delta Q_h = \pm 1, \ \Delta I = \pm 1/2, \ \Delta I_3 = \pm 1/2, \tag{22}$$

where ΔQ_h is change of electric charge of hadrons. From Equation (4) and Equation (9),

$$\Delta F = \Delta H_L + \Delta S + 2\Delta I_3. \tag{23}$$

For example, in decay

$$\Sigma^- \to \mathrm{n} + \mathrm{e}^- + \bar{\nu}_\mathrm{e}, \tag{24}$$

or in quark terms

$$\mathrm{sdd} \to \mathrm{ddu} + \mathrm{e}^- + \bar{\nu}_\mathrm{e}, \tag{25}$$

$\Delta S = \Delta Q_h = 1$, $\Delta I_3 = 1/2$, and $\Delta H_L = -2$. The selection can be deduced from $\Delta F = 0$ (Equation (23)).

A reverse case is that a reaction with $\Delta S = -\Delta Q_h$ is consistent with Gell-Mann-Nishijima formula Equation (7), but has not been observed. For example,

$$\Sigma^+ \to \mathrm{n} + \mathrm{e}^+ + \bar{\nu}_\mathrm{e}, \tag{26}$$

or in quark terms

$$\mathrm{suu} \to \mathrm{ddu} + \mathrm{e}^+ + \bar{\nu}_\mathrm{e}, \tag{27}$$

where $\Delta S = -\Delta Q_h = 1$ and $\Delta I_3 = -3/2$, but $\Delta H_L = 0$, so that $\Delta F = -2$. So, the reason why a reaction with selection $\Delta S = -\Delta Q_h$ has not been observed is clear: F is not conserved in the case.

In consequence, in the fermionic weak interaction including u, d and s quarks, the selection rules can be deduced from conservation of F.

3.4. Heavier Quarks

Relation between selection rules in weak interaction and F conservation can be extended to the other quarks including c, b and t quarks. For example, including c quark, from Equation (2), $H = U + D + S + C$ and then from Equation (1),

$$\Delta F = \Delta S + 2\Delta I_3 + \Delta C + \Delta H_L \tag{28}$$

D^+ decay is a fermionic weak interaction:

Table 3. Conserved additive quantum numbers and selection rules in different types of weak interaction. Hadrons composed by only u, d and s quarks are listed.

type of weak interaction	conserved additive quantum number	selection rule in weak interaction
pure leptonic	F, H_L	null
pure hadronic	F, H	1) $\Delta S = \mp 1$, $\Delta I = \pm 1/2$, $\Delta I_3 = \pm 1/2$.
		2) $\Delta S = \mp 2$, $\Delta I_3 = \pm 1$
fermionic	F	1) $\Delta S = \Delta Q_h = \pm 1$, $\Delta I = \pm 1/2$, $\Delta I_3 = \pm 1/2$
		2) $\Delta S = 0$, $\Delta I = \pm 1$, $\Delta I_3 = \pm 1$

$$\mathrm{D}^+ \to \bar{\mathrm{K}}^0 + \mathrm{e}^+ + \nu_\mathrm{e}, \tag{29}$$

or in quark terms

$$\mathrm{c}\bar{\mathrm{d}} \to \bar{\mathrm{d}}\mathrm{s} + \mathrm{e}^+ + \nu_\mathrm{e}, \tag{30}$$

we can see that $\Delta F = 0$ (conservation of F) leads to selection $\Delta S = -1$, $\Delta C = -1$, $\Delta I_3 = 0$ (Equation (28)). In consequence, conservation of F determines the selection rules of weak interaction including heavier quarks.

4. Conclusions

This Conservation of F determines the selection rules in all types of weak interaction. Especially, conservation of H, as the hadronic part of F, determines the selection rules in pure hadronic weak interaction, and conservation of H_L, as the leptonic part of F, determines the selection rules in pure leptonic weak interaction (Table 3). Compared with miscellaneous selection rules, conservation of F is more distinct and rather simpler for judgment on how fermions react in all types of weak interaction. Moreover, the reason why some selections, e.g., $\Delta S = -\Delta Q_h$ have not been observed can be explained by not conservation of F in the case, but cannot be explained by Gell-Mann-Nishijima formula Equation (7). Equation (5) is more general than Equation (7).

Conservation of F indicates that both hadrons and leptons must be considered together in weak interaction, but not separately. In fact, F due to its conservation gives a unified concept about both hadrons and leptons in weak interaction. If we only take Q, F_0 and F, description of weak interaction becomes simpler, only based on the conserved physical quantities. Conservation of F in weak interaction, strong interaction and electromagnetic interaction and a tight correlation among Q, F_0 and F should be utilized in quantum field theory.

Acknowledgements

This research was supported by National Natural Science Foundation (NSFC) grant number U2031103 in China.

Conflicts of Interest

The author declares no conflicts of interest regarding the publication of this paper.

References

[1] Zhang, N.S. (1986) Particle Physics (I). Science Press, Beijing, 302-305.

[2] Zhang, N.S. (1987) Particle Physics (II). Science Press, Beijing, 75-83.

[3] Kim, Q.H. and Pham, X.Y. (1998) Elementary Particles and Their Interactions. Springer, Verlag Berlin Heidelberg, 208-213.

[4] Nagashima, Y. (2010) Elementary Particle Physics, Volume 1: Quantum Field Theory and Particles. Wiley, Weinheim, 589-592. https://doi.org/10.1002/9783527630097

[5] Ma, X.-H. (2021) *Universe*, **7**, 317-321. https://doi.org/10.3390/universe7090317

[6] Nakano, T. and Nishijima, K. (1953) *Progress of Theoretical Physics*, **10**, 581-582. https://doi.org/10.1143/PTP.10.581

[7] Nishijima, K. (1955) *Progress of Theoretical Physics*, **13**, 285-304. https://doi.org/10.1143/PTP.13.285

[8] Gell-Mann, M. (1956) *Il Nuovo Cimento*, **4**, 848-866. https://doi.org/10.1007/BF02748000

Journal of Modern Physics, 2022, 13, 707-721
https://www.scirp.org/journal/jmp
ISSN Online: 2153-120X
ISSN Print: 2153-1196

Is Evolution a Causal, Yet Not-Predetermined Process?

Maria K. Koleva

Institute of Catalysis, Bulgarian Academy of Sciences, Sofia, Bulgaria
Email: mkoleva_1113@yahoo.com

How to cite this paper: Koleva, M.K. (2022) Is Evolution a Causal, Yet Not-Predetermined Process? *Journal of Modern Physics*, **13**, 707-721.
https://doi.org/10.4236/jmp.2022.135040

Received: March 15, 2022
Accepted: May 17, 2022
Published: May 20, 2022

Abstract

It is demonstrated that "survival of the fittest" approach suffers fundamental flaw planted in its very goal: reaching a uniform state starting from a minor random event. Simple considerations prove that a generic property of any such state is its global instability. That is why a new approach to the evolution is put forward. It conjectures equilibrium for systems put in an ever-changing environment. The importance of this issue lies in the view that an ever-changing environment is much closer to the natural environment where the biological species live in. The major goal of the present paper is to demonstrate that a specific form of dynamical equilibrium among certain mutations is established in each and every stable in a long-run system. Major result of our considerations is that neither mutation nor either kind dominates forever because a temporary dynamical equilibrium is replaced with another one in the time course. It will be demonstrated that the evolution of those pieces of equilibrium is causal, yet not predetermined process.

Keywords

Stable Evolution, Survival of the Fittest, Causality, Central Limit Theorem, Decomposition Theorem, Markov Process

1. Introduction

Despite great efforts undertaken recently, the issue about the general properties of evolution of eco-systems is far from establishing decisive solution. So far the dominant concept is based on the understanding that the most successful adaptations commence as a specific selection of random mutations that goes permanently among a given population and whose ultimate goal is spreading throughout the entire population. Put in other words, this approach, popular as "survival of the fittest", asserts that a non-causal individual (random in its origin) reason has

a long-term causal effect on the entire population. Further, the so established novel traits and features are open to novel type random mutations some of which again spread throughout the entire population and so on. However, since this scenario works for each and every kind of biological species and since the rate and intensity of those adaptations vary from one kind to another, most likely this scenario renders the corresponding eco-system permanently out of balance.

The quantification of the above scenario happens through the basic approach called fitness landscapes. The approach explores the major ideas of chaos theory, namely the sensitivity to initial conditions and the butterfly effect for achieving the goal about spreading of a local mutation throughout a system. All mutations are considered local and random in origin. The central point is assigning of a specific probability for survival, called fitness, to each and every mutation. Then, each fitness is currently modified under specific dynamical rules and novel values are assigned according to them. The ultimate goal is reaching a stationary state where a single constant fitness is established throughout the entire system. The parallel with the above mentioned suppositions of chaos theory is seen in the following: 1) the sensitivity to initial conditions is presented through permanent modifications of each local fitness; 2) the butterfly effect is substantiated through the ultimate goal, namely establishing a single steady cooperative state throughout the entire system starting from a small local random event.

One of the major flaws of the above approach is that the desired cooperative state is static not dynamical. The fundamental difference between the latter is that a static equilibrium implies that, on arrival at it, a system stays there forever while a dynamical equilibrium implies long-run balance between participating interactions. Indeed, as an immediate consequence of chaos theory, no dynamical correlations are established. This suggestion is supported by the fact that the power spectrum of each and every chaotic time series is white noise. The latter implies that there are no steady correlations among the power spectrum components. Thus, the ultimate steady state is uniform with regard to the victorious mutation.

Further, to the most surprise, the dominance of a single mutation over all others not only does not increase the strength of the corresponding system, but on the contrary, it weakens its stability by means of making the system vulnerable to a lager variety of hazardous events. To remind, the exclusive property of mutations is that each of them exerts specific robustness to a given environment. This issue is especially acute for systems put in an ever-changing environment. It is obvious that then, a single mutation is "fittest" only temporary: at the next instant another mutation turns more advantageous.

It is worth noting also that there is another cause for vulnerability of established uniform state: in general, all physical interactions between species in media, are short-ranged. Then, with a lack of long-range interactions, any uniform state is globally unstable, because any tiny local perturbation rapidly develops into a global one by means of excitation of the longest wave-length modes.

Then, the question becomes whether establishing of any form of equilibrium is ever possible for systems put in an ever-changing environment? The importance of this issue lies in the view that an ever-changing environment is much closer to the natural environment where the biological species live in. The major goal of the present paper is to demonstrate that a specific form of dynamical equilibrium among certain mutations is established in each and every stable in a long-run system. The generic characteristics of intra-kind and inter-kind dynamical equilibrium are subject of the present paper.

The major result of our considerations is that neither mutation nor either kind dominates forever because a temporary dynamical equilibrium is replaced with another one in the time course. It will be demonstrated that the evolution of those pieces of equilibrium is causal, yet not predetermined process.

Let us start with modeling of an ever-changing environment: we consider its major property to be diversification of impacts and responses, *i.e.* each of its components acts on different part of a system., e.g. sound acts on our hearing while heat on our skin. This renders mutations not only specific but diversified and qualitatively different. In turn, the latter renders all the probabilistic approaches inappropriate for the modelling the behavior of the corresponding system. This is so because the grounding idea of all probabilistic approaches is assigning a single number (current probability) to any variable, thus smearing out the qualitative difference among events (hearing and heat sensors in the skin in the above example). Even when a boundary separating qualitatively different events is established, it is quantitative and so does not allow emergence of a new quality.

This problem is so serious that its successful solution calls for fundamentally novel approach. The grounds for novel modelling is substantiated though the recently put forward by the author concept of boundedness [1]. It consists of the idea that a complex system put in an ever-changing environment operates steadily in a long run if and only if the rates and amplitudes of exchanging energy/matter/information never exceed specific margins. The exclusive property of that approach is the existence of a dynamical equilibrium for each and every system subject to boundedness. This is an immediate consequence of the central result of the concept of boundedness, proven by the author [1] [2]. It states that a dynamical equilibrium indeed comprises a specific steady pattern whose major generic property is that it is robust to the details of corresponding interactions. Rigorously speaking, the proven theorem, called by the author decomposition theorem, asserts that the power spectrum of each and every bounded irregular sequence (BIS) comprises additively two bands: 1) a specific discrete one, the position and intensity of whose components are robust to the details of the concrete interactions and to the minor variations of the environment; 2) a continuous band, the shape of whose envelope is also robust to the details of the concrete interactions and to the minor variations of the environment. The specific steady pattern is called by the author a homeostatic pattern. It is important to stress that it stands as an exclusive characteristic of a kind. It is obvious that the

homeostatic pattern of a single kind put in an ever-changing environment stays the same as long as the homeostatic pattern of the environment stays intact.

Next question asks whether inter-kind equilibrium is a generic property for every eco-system or its establishing needs meeting of additional constraints. The answer to this question is that establishing of an inter-kind equilibrium is not always available; it is available only for those eco-systems which are subject to the so called protocol of compatibility.

A general prerequisite of such protocol commences from the idea about hierarchical structuring of complex systems. It asserts that each and every complex system is hierarchically organized so that each and every hierarchical layer responses with bounded intensity to specific stimuli. The gain of such distribution of impacts is three-fold: 1) it strengthens the overall response; 2) it increases the types of stimuli to which a system respond in a controlled way; 3) it keeps the damages local as long as possible. The latter will become clear through considerations in Section 3. An exclusive for this type of hierarchy property is that the boundedness of the response renders the decomposition theorem to hold at each and every hierarchical level. Then the environment to a given hierarchical level comes from all other levels. Yet, the pre-dominant influence comes from the nearest lower level and higher level.

The evolution of an eco-system subject to that general protocol is driven by the perpetual motion in the state space sustained by means of orchestrating the directions of the development of the corresponding homeostatic patterns. It operates by means of two major implements: 1) the boundedness keep each and every homeostasis intact to the details of environment as long as the latter do not change it. 2) only changes in homeostasis of any current environment could provoke changes in homeostasis of the current hierarchical level; The far going consequence of this result, proven in Section 3, is that only causal correlations (encapsulated in those homeostatic patterns which participate to a given level as environments) could produce causal changes, *i.e.* changes in the current homeostatic pattern. The proof that the causal correlations are concentrated in homeostatic pattern is presented in [3] [4]. A simple explanation is grounded on the permutation sensitivity of the components which participate in any discrete pattern. Indeed, any change of positions and/or intensities of any components result a new pattern. Thus, all the discrete patterns share the exclusive property of causality, namely the permutation sensitivity of the order cause-effect. Yet, this form of causality is different from the traditional view on causality considered as a specific ordered sequence of binary relations cause-effect.

The fundamental role of the continuous band in each and every power spectrum which originates from minor individual responses compatible with the current homeostatic pattern [3] is that it renders the corresponding homeostatic pattern to be permanently bounded in size both in the space and in time. Figuratively speaking, its exclusive generic property is that it spontaneously sets specific constraints to the spread of any concrete dynamical equilibrium in the space and in time regardless to the details of the intra- and inter-kind interactions. As

a result the state space of any dynamical equilibrium turns partitioned into bounded in their spatio-temporal size domains of different homeostasis.

Thus, the fundamental novelty of the present model is that the evolution in the setting of the concept of boundedness is always a causal process both on the level of mutations (intra-kind interactions) and on the level of inter-kind interactions. A far going consequence of that result is that the established equilibrium is dynamical one so that neither mutation and neither kind dominates forever on the contrary to the survival of the fittest approach where a single mutation turns dominant over the entire system forever.

2. Decomposition Theorem and the Intra-Kind Equilibrium

The subject of the present section is to consider the major exclusive properties of an already established intra-kind equilibrium. Let us start with the consideration that each mutation commences from specific to its kind bounded set and it interacts both with its current environment and neighboring mutations. The interactions among mutations are specific to each mutation and the corresponding environment but generally they are of two types: synergetic ones, *i.e.* interactions which act in favor of all participants and competing interactions which act in favor of dominance of a single participant. It is important to stress that since the environment acts non-homogeneously over the corresponding system, the outcome of interactions varies throughout a system and in the time course. Then, I suggest the definition a dynamical equilibrium to be: the response from each and every spatio-temporal point of a system is permanently self-sustained to be bounded and well-defined.

Then, the major question becomes whether there exists general operational protocol insensitive to the details of interactions which provides existence of a dynamical equilibrium. The high non-triviality of the matter lies in the fact that no Hamiltonian-type description for systems which exert competing interactions is available [5]. Therefore, the positive answer to the above question calls for fundamentally novel approach. Next it is demonstrated that the recently introduced concept of boundedness and more precisely its central result, the decomposition theorem, are able to provide a positive solution to this issue and to delineate the exclusive characteristics of any dynamical equilibrium regardless to the details of intra-kind interactions.

The definition of the dynamical equilibrium, viewed as establishing of permanent boundedness of the response in a long-run, renders the mathematical description of any such response to be presented as a BIS. As it has already been mentioned, an exclusive generic property of any stable BIS is that it is subject to decomposition theorem. To remind, it proves that the power spectrum of any BIS is additively decomposed to a specific discrete pattern, called homeostasis, and a continuous band of a universal shape so that both the structure of the discrete pattern and the shape of the continuous band are robust to the details of environment as long as the homeostasis of the latter stays intact. To remind, ac-

cidental correlations are eliminated from the power spectrum because they are short-lived and thus their impact is averaged out. Put in other words, the power spectrum comprises only steady in a long-run correlations and thus appears as most appropriate characteristic of a dynamical equilibrium.

Let us now consider the exclusive generic properties of specific discrete patterns and universal continuous bands and to consider the highly non-trivial role of their persistent coexistence.

First in this line comes the exclusive generic property of discrete patterns to comprise only causal correlations. This assertion is an immediate consequence of the fact that positions and intensities of the components in each discrete pattern along with the ratios among the latter are permutation sensitive. It implies that any permutation and/or modification of the intensities, e.g. any switch between any two components, results in a new pattern. It should be stressed that this form of causality fundamentally differs from the traditional view on causality as a binary ordered relation cause-effect. The difference is best pronounced through the fact the novel form of causality is an emergent generic property from a sea of interplay among short-ranged and long-ranged interactions.

The generic role of the continuous band is also highly non-trivial: as considered in [3] [4] it originates from minor individual responses compatible with the current homeostatic pattern. Its fundamental role is that it renders the corresponding homeostatic pattern to be permanently bounded in size both in the space and in time. Figuratively speaking, its exclusive generic property is that it spontaneously sets specific constraints to the spread of any concrete dynamical equilibrium in the space and in time regardless to the details of the intra-kind interactions. As a result the state space of any dynamical equilibrium turns partitioned into bounded in their spatio-temporal size domains of different homeostasis.

As a consequence of the above generic properties an exclusive generic property commences. It is that neither mutation dominates both in a short and a long-run. Thus, in a short run a given spatio-temporal pattern, much resembling a landscape, is established and develops in the space and time like a living organism: from "birth" to "death". In a long run, the pattern development retains the same homeostasis on the "re-birth" as long as the environment keeps its homeostasis intact. Yet, on change of its current homeostasis, a new dynamical equilibrium, *i.e.* new pattern of mutations is established.

Next in the line of our considerations the matter why only changes in the homeostasis of the environment are able to cause changes in a dynamical equilibrium comes. Indeed, changes in environmental homeostasis are global in the sense that its impacts are spread throughout entire system in a persistent way. The latter implies that the impacts undermine the same critical points of any current equilibrium persistently on each "birth-death" cycle until the collapse of the latter happens. It is worth noting that this process is insensitive to the intensity of impacts. On the other hand, local accidental impacts, even of large inten-

sity, most probably remain local and short-lived. As it has been already mentioned, this is a direct consequence of the very notion of a power spectrum where accidental correlations are averaged out and thus do not participate in it. To remind, a power spectrum of a system in equilibrium comprises only steady reproducible correlations. It is worth noting that individual correlations which belong to a continuous band participate to the process as the major factor for constraining the size of the spatio-temporal domain for the operating of any equilibrium bounded. In turn, this renders equal evolutionary value of all mutations (all individuals) in a long run.

It is worth to consider the value of the existence of individual responses, despite their equal evolutionary value. To compare, suppose that all individual responses are identical. Then, the power spectrum in equilibrium would comprise only a discrete band. In turn, the dynamical equilibrium would turn into a periodic function spread throughout entire space and time. Therefore, the effect of any change in the environment would require infinite energy/matter/information for restoration of the equilibrium or for establishing a new one. Thus, the wisdom of confinement of the dynamical equilibrium into bounded spatio-temporal domains is three-fold: 1) it provides adaptability of the equilibrium to environmental changes; 2) it prevents the spread of a violation of an equilibrium by means of confining it to a local event; 3) it provides the evolution of a system to be substantiated by means of well-defined bounded jumps among different homeostatic patterns.

It is worth reminding that mathematical foundation for substantiating the above scenario is the use of BIS instead of until now dominant use of periodic functions.

3. Inter-Kind Equilibrium and General Protocol for Compatibility

It is obvious that a long-term coherent coexistence of different kinds is not always possible. That is why, the subject of the present section is establishing of the general characteristics of general operational protocol for compatibility of different kinds that constitute an eco-system.

The general prerequisite of such protocol commences from the idea about hierarchical structuring of complex systems. The latter asserts that each and every complex system is hierarchically organized so that each and every hierarchical layer along with its constituent responses with bounded intensity to specific stimuli. The gain of such distribution of impacts is three-fold: 1) it strengthen the overall response by means of an increase of the types of stimuli to which a system respond in a controlled way; 2) each and every unit should sustain its internal dynamical equilibrium, *i.e.* equilibrium among its mutations, intact; 3) keeps the damages local as long as possible. An exclusive for this type of hierarchy property is that though the response is specific and diversified, it is always bounded, the decomposition theorem holds at each and every hierarchical level.

Then the environment to a given hierarchical level comes from all other levels. Yet, the pre-dominant influence comes from the nearest lower and higher level. It is worth noting that this type of hierarchy is permanently bi-directional, *i.e.* it goes both bottom up and top-down unlike the pyramidal one which goes only top down and thus it turns vulnerable to tiny accidental perturbations.

As a result, each and every unit at each and every hierarchical level appears as a sub-system which has its specific internal structure and functionality and which is put in an ever-changing environment and whose behavior is subject to the concept of boundedness. Since each and every such sub-system has bounded "life-time", the state space of the entire hierarchy consists of a hierarchy of domains each and every of which is characterized by specific to it homeostatic pattern. The crucial for the further considerations fact is that the inter-unit interactions must meet a condition which consists of avoiding resonances among homeostatic patterns which come from different hierarchical levels. It is worth reminding that the avoidance of interference implies sustainability of the intra-structure of the corresponding unit while the avoidance of resonances implies maintenance of the boundedness of the response.

This requirement constitutes the foundation of the general protocol of compatibility. The need of compatibility commences from the need of avoidance resonances among homeostatic patterns that come from different hierarchical levels. This requirement implies that frequency domains that come from different hierarchical levels must not overlap. The non-overlapping of the frequency domains is necessary for avoiding interference and/or resonances with units that come from other hierarchical levels with the homeostatic pattern of any given one.

Then, eco-systems which meet the protocol of compatibility exert long-term stable behavior. The major exclusive property of the latter is that it consists of specific sequence of spatio-temporal intervals each of which is characterized by its homeostatic pattern. Thus, one causal pattern is replaced by other; after some time the latter is replaced with a new one and so on.

Yet, two major questions arise: 1) does this form of causality implies just a long-term predetermination of the evolution; 2) if not, how new patterns arise?

The answer to those questions commences as two aspects of the same fact which is that the motion of a stable hierarchy generically passes through bifurcation points. Here, we use the term bifurcation in a slightly modified way, namely: it represents the point where several units turn admissible for the further motion of a given unit. The generic existence of such points of bifurcation is set by the general structure of the state space which consists of its partitioning into bounded domains. Further, since controlled bounded response of the over-all system is available only when the behavior of all constituents and units at each and every hierarchical level is subject to boundedness of rate and amplitudes of exchanging matter/energy/information with the corresponding environment, the motion in the state space happens only among adjacent domains. Then, bifurcation points

present everywhere where there is more than one adjacent domain admissible.

The major question is whether this is a random choice among equally admissible alternatives? If so, does this randomness break the predetermination? Yet, though this choice seems random, it is a choice among causal alternatives and implies just a "jump" in the causality, *i.e.* one homeostatic pattern is replaced with another.

I assert that the choice among admissible alternative is a new type of a causal process which possesses the exclusive property of the randomness not to be exactly reproducible. To elucidate this matter let us consider how the process of choice develops. At the bifurcation point, the formation of clusters of different alternatives starts to appear and develop. Here again the interactions are specific of each alternative but they are of the types presented in the Introduction, namely synergetic and competitive. Yet, now the goal is different, namely it is establishing of complete dominance of one of the admissible alternatives. This goal is achieved by that alternative which establishes dominance first. Thus, this renders the choice among admissible alternatives path dependent and thus probabilistic-like in the sense that it is not reproducible in full details on repetition.

It is worth noting that, although the choice looks like a probabilistic process, its consideration in probabilistic terms is inappropriate because clusters of each alternative comprise different causality. However, an exclusive outcome of the decomposition theorem is that not only the difference in causality of both alternatives is qualitative, but they are algorithmically unreachable from one another. This is an outcome of the full proof of that theorem which states that a full power spectrum is algorithmically un-reachable in finite number of steps from any other although, at the same time it is physically reachable by means of involvement of bounded matter/energy/information [1].

It is very important to stress that establishing of a single alternative over the entire unit is fundamentally different from the survival of the fittest. Here, each alternative is advantageous and thus the dominance is of not that of the fittest one but of the first one that reaches global domination. Alongside the dominance of single "chosen" alternative has limited spatio-temporal span: it is established over bounded spatial area and has specific to it "life-time". On "re-birth", another alternative could be established. In turn, the dominance of a single selection is always temporary and confined.

Now the matter about the commencing of a new unit comes into consideration. It appears as a specific response to the path dependence of the choice among admissible selections at a bifurcation point. It could happen when a current configuration of clusters allows interference and/or local resonances among certain clusters.

Yet, the matter about the stable incorporation of a new unit into the entire hierarchy is apriori mathematically undecidable as it has been demonstrated in [3]. In general it either fit in the entire hierarchy or died out, or triggers a global

catastrophe. Let us start with considering in more details the case of incompatibility: it implies that in a short run the new pattern would be destroyed. Then, its effect on the entire evolution would appear as a constrained local accidental correlation. On the other hand, when the new pattern is compatible with the entire hierarchy, it provides new route of the evolution. The third alternative is substantiated when a local catastrophe drives a global one.

4. Non-Predetermination Viewed as New Reading of Central Limit Theorem

In general terms, not-predetermination of the evolution implies its behavior is to be described as a Markov process with non-constant, yet bounded memory radius. However, the question arises whether the evolution is a stable process and consequently how this matter is related to the behavior of the corresponding system. The criterion for the stability of a Markov process, under the mild condition of self-sustaining permanent boundedness of rates and amplitudes of exchanging matter/energy/information with an ever-changing environment, is the form of the shape of the power spectrum as established in [6 FNL]: whether it comprises continuous band of the shape $1/f^{\alpha(f)}$ or it is white noise. If the answer is positive for the first alternative two questions arises: what forms the spatio-temporal boundaries of the entire system and how to distinguish the physical correlations which come of the Markov process and the functional correlations which come from the boundedness of rates and amplitudes.

However the notion of Markovianity encounters highly non-trivial puzzle with regard to the up-to-date unforeseen fact that the probabilistic description is also subject to the decomposition theorem. This is because all probabilities, regardless to their origin and processes they describe, are bounded between zero and unity. Then what is independent event, e.g. tossing of a coin and how to describe it? Further, thus established constraint implies that any process described probabilistically is subject to the decomposition theorem. It is worth noting that the derivation of the decomposition theorem is explicitly grounded on the Lindeberg theorem [7]. Thus, since according to the latter each BIS has finite mean and variance, so does claim the Central Limit Theorem (CLT). Then, the following vicious circle arises: on the one hand, according to Lindeberg, each and every stable in a long run BIS has steady mean and variance. Then, according to current formulation of CLT, the asymptotic distribution tends to normal. However, according to the decomposition theorem, the asymptotic distribution is power dependent and has long tails. Its major property is insensitivity to the way of description of the characteristics of the members in a time series. Moreover, it is insensitive whether their formulation follows the same standard both in space and in time. Since all probabilistic approaches put recordings to the same frame of boundedness, the criterion which formulation of the CLT works for natural processes is the asymptotic shape of the statics: whether it tends to normal distribution or the power dependence. At that point again it is apriori mathematically undecidable whether the process makes an U-turn or bump into thresholds

at stage of rapid acceleration. Yet, if a statistics changes in a space-time course, it is mathematically undecidable apriori whether it would damp or accelerate. The mechanism of limitation of possible damages to local is the partitioning of the state space and the space time to bounded domains. Figuratively speaking, partitioning acts as a self-organized decentralized control over the evolution viewed as a stable in a long run process. Yet, the question arises: what are characteristics of a steady bounded spatio-temporal landscape: in power spectrum it appears as a specific discrete pattern where position and intensity of lines are reproducible in an ever-changing environment with constant characteristics. The time-translational invariance of that landscape is provided by the presence of accompanied continuous band of the shape $1/f^{\alpha(f)}$. To elucidate the smoothness of that band implies that metric-dependent specific structure is embedded in an underlying "see" of Euclidean metrics. Note that the metric of any landscape is specific and local in space-time to it while the metrics of the "see" is universal. In consequence the specific repeatable relations encapsulated in any discrete landscape are provided time-translational invariant in the sense that their operation does not depend on the choice of a reference frame and regardless to whether the latter is local or global.

Yet, the establishing of a stable functionality over a steady structure resolves in a highly non-trivial way: a structureless BIS is subject to universal distribution presented in [1]. It seems plausible to suggest that a specific steady spatio-temporal pattern would persist as a specific steady spikes embedded onto the universal distribution. Note that the shape and positions of these spikes are specific outcome of the interplay between the morphology of the active sites, the motion of relaxing species and the bounded velocity of any process. The novelty is that the characteristics of local events are interrelated by means of morphology-dependent factors. In turn, this transforms short-ranged interactions into long-ranged and makes the local dynamics global, for example see [8] [9]. The presence of continuous longe-range tail implies that the fluctuations from the steady pattern, though arbitrary, stay within the thresholds of stability. To compare, the normal distribution implies that the deviations from the mean are random yet unbounded events.

Thus, CLT suffers inherent contradiction: while the probability for any event is bounded, the outcome is that the deviations from the steady mean are independent and unbounded. However, the succession of random events implies that the corresponding transition rates define ill-defined velocity since there are no correlations between the successive transition rates which in turn renders that it is impossible to define velocity as an independent from the concrete particularities of succession of the transition rates. Further, it is impossible to define the notion of velocity as insensitive to partitioning variable. In turn, it renders corresponding system unstable: it is vulnerable to any large fluctuation and its occurring is unpredictable because the fluctuations are independent events. Further, this scenario renders impossible to define collective behavior because it is impossible to define collective variables which are independent from the way

of partitioning. Moreover, it is impossible to define any ecosystem because there is no way to synchronize their behavior because the velocity of all species is ill-defined.

In conclusion, it does not matter which one of both competing networks win, the result is total dominance of a single pattern and again its stability is subject of the CLT viewed in above meaning, namely a system becomes unstable under large enough fluctuation (or sequence of fluctuations) whose appearance is absolutely unpredictable.

Luckily, there is way out and it is the formation of a collective dynamics out of bounded in size and life-time landscapes each of which has its own dynamical equilibrium. The crucial step forward is the limitation both from below and above of the size and life-time for stable operation of any cluster regardless to the details of its dynamics [1] [10]. It is worth noting that the corresponding thresholds are specific for each landscape but their existence and boundedness are generic. The formation of a new collective dynamics happens again by means of motion, both ballistic and diffusion. Then the collective dynamics is highly specific yet stable when its behavior in the time course is BIS which exhibits time series invariants established in Chapter 1 [1]. Then, the route to evolution could go via hierarchical super-structuring instead of waiting for a new critical mutation appears.

The advantage of the new route lies in the fact that the partitioning of the state space into bounded domains renders the set of bifurcation points dense transitive one. However, at any bifurcation point the evolution path turns multi-valued and apriori it is undecidable which selection is stable. Note that each selection starts as formation of local clusters but some selections develops through percolation which eventually forms a dominant single state which however is globally unstable regardless to the details of any concrete dynamics. On the other hand, other selections goes via formation of a collective dynamic from the bounded is space-time domains by means of constraining the operation of each of them in specific for any cluster limited margins. It should be stressed that this operational protocol is general in the sense that it does not depend on the origin and nature of mutations and the way they interact.

Actually, the difference between CLT and the decomposition theorem is that the first ignores the rate of development of any process while the latter takes the boundedness of rates explicitly. To the most surprise ignoring the finite rate of development implies infinite velocity of development of any process regardless to the details physico-chemical characteristics.

The above considerations allow the following generalization of the Law of Large Numbers: a stable BIS transforms in a stable BIS after any form of coarse-graining. Note that the latter implies that the stability of this form of scale invariance implies insensitivity of the time series invariants of both original and offspring BIS to the way partitioning is made. The Layapunov coefficient could not serve as criterion for stability: if it follows power dependence with non-constant power, the fluctuations stay within thresholds of stability whereas for unlimited

grow the Lyapunov coefficient grows exponentially. However, practically it is impossible to discriminate a power dependence from an exponential one by any means of computing since both algorithmic and semantic computing operates with finite presentations: truncated and round-off Taylor series correspondingly. Since both of them are polynomials regardless to any concrete precision, the discrimination is mathematically undecidable. The latter is an argument for self-consistency of the previously obtained result that it is apriori mathematically undecidable whether any change of the status of a system is adaptation or destruction. In turn, does the latter imply that it is mathematically undecidable by any practical means whether a change brings about adaptation or destruction?

Yet, the role of scanning over partitioning implies that the synchronization of all constituents of a system is stable to small perturbations. In turn this provides arrow of time and constant speed of thus synchronized orchestra of "clocks" viewed as a single unit. It is worth noting that this arrow and speed is specific for any given unit. Thus, the question arises whether there is absolute time.

A criterion for synchronization of all processes in a unit is the development of an excursion: each excursion consists of steps produced by processes that operate at different spatio-temporal scales. The synchronization implies that all of them proceed with the same velocity. The latter provides the formation of a monotonic trend and the development of stretching at first because it is the only way to depart from the mean. However, any departure from the mean implies weakling the correlations. This provides a general shape of an excursion to be monotonic increase with gradual change of curvature. Eventually, the curvature reaches a critical point where it turns to zero. This is a point of bifurcation type: 1) the first scenario is to make an U-turn and to start development in the direction of gradual increase of correlations (folding); 2) the second scenario is to continue development and thus to bump into thresholds where it can either be damaged or destroyed. Yet, even if survives, the bumps into thresholds render the system to function unsteadily and eventually to stop functioning. It is worth noting that unlike the second scenario, the first one provides long-term stable functioning of a system. The high non-triviality of this type of bifurcation point is that the choice of a scenario is matter of the inherent functional organization not a random one. Note that if the choice was random, the unstable behavior would be the only alternative. Yet, for excursions below thresholds there is choice at the corresponding bifurcation point. Yet, the choice is not completely random, but it is a highly non-trivial interplay between current organization and the current environment provided by the nearest hierarchical levels.

The above scenario for synchronization is best revealed through the continuous part of the power spectrum where the shape ([1], chapter 1) implies that all scales contribute in a covariant manner, *i.e.* the spectrum does not signals out any specific spatio-temporal scale. In turn this sustains the idea about the proposed protocol of hierarchy to be that the latter goes both bottom up and top down.

It is worth noting that in order to provide permanence of the constant velocity

at synchronized systems the size and time interval of jumps should follow bell-type distribution. However, though it could be well-approximated by the Gaussian one, it is only in the sense that it has finite mean and finite variance. However, the latter is also what Lindeberg theorem says. The criterion for discrimination between normal distribution and the bell-type one whether the histograms are distributed at finite area while for normal distribution they should be scattered at very large areas. Other criterion is that normal distribution has only two moments: mean and variance while any stable BIS has infinite number of higher moments [1].

5. Conclusions

It is demonstrated that "survival of the fittest" approach suffers fundamental flaw planted in its very goal: reaching a uniform state starting from a minor random event. However, desired uniform state is globally unstable. The latter is unavoidable because this approach is grounded on the conjecture that a local random event, e.g. mutation, rapidly develops via eliminating all its rivals so that to reach its ultimate goal: spreading throughout entire system. Thus, on arrival at it, a system stays there forever.

Yet, the dominance of a single mutation over all others not only does not increase the strength of the corresponding system, but on the contrary, it weakens its stability by means of making the system vulnerable to a lager variety of hazardous events. To remind, the exclusive property of mutations is that each of them exerts specific robustness to a given environment. This issue is especially acute for systems put in an ever-changing environment. It is obvious that then, a single mutation is "fittest" only temporary: at the next instant another mutation turns more advantageous.

That is why a new approach to the evolution is put forward. It conjectures equilibrium for systems put in an ever-changing environment. The importance of this issue lies in the view that an ever-changing environment is much closer to the natural environment where the biological species live in. The major goal of the present paper is to demonstrate that a specific form of dynamical equilibrium among certain mutations is established in each and every stable in a long-run system. The major result of our considerations is that neither mutation nor either kind dominates forever because a temporary dynamical equilibrium is replaced with another one in the time course. It is demonstrated that the evolution of those pieces of equilibrium is causal, yet not predetermined process.

An important consequence of the view on evolution as a causal process provides another powerful argument in favor of the forwarded by the author ban over information perpetuum mobile [11]. To remind, it asserts that it is impossible to transform noise into information. Now this ban is confirmed through rendering new things to commence from a specific causality not from randomness.

Outlining, the long-term evolution is a causal though not predetermined process whose development is presented as a BIS. The far going consequences of

the latter are that any such eco-system is open to further hierarchical super-structuring the long-term evolution of which shares the same properties of being both causal and not predetermined.

Yet, the fundamental question is whether a long-run stability of any evolution is asymptotic. Moreover, is asymptotic stability ever possible and even if so; is it detectable by any means?

Conflicts of Interest

The author declares no conflicts of interest regarding the publication of this paper.

References

[1] Koleva, M.K. (2013) Boundedeness and Self-Organized Semantics: Theory and Applications. IGI Global. https://doi.org/10.4018/978-1-4666-2202-9

[2] Koleva, M.K. (2021) *Journal of Modern Physics*, **12**, 605-622. https://doi.org/10.4236/jmp.2021.125039

[3] Koleva, M.K. (2020) *Journal of Modern Physics*, **11**, 767-778. https://doi.org/10.4236/jmp.2020.116049

[4] Koleva, M.K. (2019) *Journal of Modern Physics*, **10**, 43-58. https://doi.org/10.4236/jmp.2019.101005

[5] Giampaolo, S.M., Hiesmayr, B.C. and Illuminati, F. (2015) Global-to-Local Incompatibility, Entanglement Monogamy, and Ground-State Dimerization: Theory and Observability of Quantum Frustration in Systems with Competing Interactions. arXiv: 1501.04642.

[6] Koleva, M.K. and Covachev, V. (2001) *Fluctuation and Noise Letters*, **1**, R131-R149. https://doi.org/10.1142/S0219477501000287

[7] Feller, W. (1970) An Introduction to Probability Theory and Its Applications. John Wiley & Sons, New York.

[8] Koleva, M. and Petrov, L. (1999) *Bulgarian Chemistry and Industrie*, **70**, 27-35. http://arXiv.org/cond-mat/0308616

[9] Koleva, M.K. and Petrov, L. (2018) *Emerging Trends in Kinetics and Thermodynamics*, **1**, 19-27. https://doi.org/10.36959/672/588 https://scholars.direct/Articles/kinetics-and-thermodynamics/etkt-1-003.php?jid=kinetics-and-thermodynamics

[10] Koleva, M.K. (2021) *Journal of Modern Physics*, **12**, 167-178. https://doi.org/10.4236/jmp.2021.123015

[11] Koleva, M.K. (2017) *Journal of Modern Physics*, **8**, 299-314. https://doi.org/10.4236/jmp.2017.83019

Journal of Modern Physics, 2022, 13, 722-729
https://www.scirp.org/journal/jmp
ISSN Online: 2153-120X
ISSN Print: 2153-1196

Quantum State Transfer between a Mechanical Oscillator and a Distant Moving Atom

Fu Zhang, Yanqing Guo, Guangyao Yang, Dianfu Wang*

School of Science, Dalian Maritime University, Dalian, China
Email: yqguo@dlmu.edu.cn, *wangdfu@dlmu.edu.cn

How to cite this paper: Zhang, F., Guo, Y.Q., Yang, G.Y. and Wang D.F. (2022) Quantum State Transfer between a Mechanical Oscillator and a Distant Moving Atom. *Journal of Modern Physics*, **13**, 722-729.
https://doi.org/10.4236/jmp.2022.135041

Received: April 10, 2022
Accepted: May 24, 2022
Published: May 27, 2022

Abstract

We propose a scheme for high fidelity quantum state transfer from a mechanical oscillator to a distant moving atom. In the scheme, two optical cavities connected by an optical fiber are interacted effectively through adiabatically eliminating fiber mode under large detuning limit. The quantum state transfer fidelity can be raised asymptotically to 100% by optimizing the Gaussian pulse $G(t)$, the maximum atom-cavity coupling strength $\Omega_{\max}$, and the atomic velocity v. We also show that the affect of dissipation can be obviously depressed by synchronously increasing $\Omega_{\max}$ and v.

Keywords

Quantum State Transfer, Mechanical Oscillator, Cavity QED

1. Introduction

It is well known that designing high fidelity quantum state transfer (QST) between spatially separated hybrid quantum systems plays a key role in quantum information process such as long range quantum communication [1] and distributed quantum computation [2]. By using shaped pulses method, QST can be implemented through quantum interface and map the state of a qubit onto another physically far apart [3]. Systems consist of optical cavity and mechanical oscillator [4], which can use photons to detect mechanical movement with high sensitivity in optical detecting process, is regarded as one of the important candidates for hybrid quantum systems to implement QST and has drawn a lot of research interest both theoretically and experimentally and may induce deep considerations for basic quantum problems [5]. A variety of fascinating schemes have been put forward to discuss QST from a stationary mechanical oscillator to another [6] [7] [8] or a cavity mode [9] [10]. It is shown that high transfer effi-

ciency can be achieved by using adjustable cavity quantum electrodynamics (QED) parameters. For example, in the work presented by Sete, a quantum state can be efficiently transferred from an optical cavity to a distant mechanical oscillator by adjusting cavity damping rates and destructive interference [9]. However, previous approaches to optomechanical QST mostly deal with state transfer between mechanical oscillators and cavity modes. Motivated by the fact that atoms are preferred as suitable candidate for entangled state transfer [11], universal quantum gate [2], and even for multiplexed quantum memory [12], it is reasonable to discuss QST between a mechanical oscillator and an atom. In the present paper, we propose a scheme for QST from a mechanical oscillator to a moving atom based on fiber-mediated cavity QED approach under real-time cavity QED condition. The advantage of the scheme is it works in a robust way since high fidelity can be reached through optimizing coupling parameters to against the dissipation of quantum channel.

2. Theoretical Model

We consider a theoretical model consisted of a mechanical oscillator, two identical optical cavities, and a moving atom, as is shown in **Figure 1**. Optical cavity 1 is coupled to mechanical oscillator. Optical cavity 2 interacts with the moving atom. Two cavities are connected by an optical fiber.

We start by analyzing the subsystem cavity-fiber-cavity and write the Hamiltonian $H_{\mathrm{c,f}}$ as [13]

$$H_{\mathrm{c,f}} = \omega_1 a_1^+ a_1 + \omega_2 a_2^+ a_2 + \omega_{\mathrm{f}} c^+ c + \nu\left(a_1^+ c + a_2^+ c + a_1 c^+ + a_2 c^+\right) \quad 1)$$

where $a_i\left(a_i^+\right)$ and $c\left(c^+\right)$ are the annihilation (creation) operators of cavity $i\left(i=1,2\right)$ and fiber, respectively. ω_i is the cavity frequency of cavity i (for convenience, we let $\omega_1=\omega_2=\omega_{\mathrm{c}}$ in the following discussions), ω_{f} is the fiber frequency. ν is the coupling strength. The subscriptc c and f indicate cavity and fiber modes. Under the rotation frame transformation $H'_{\mathrm{c,f}}=UH_{\mathrm{c,f}}U^+$, where $U=\mathrm{e}^{\frac{\nu}{\Delta}\left(a_1^+ c+a_2^+ c-a_1 c^+-a_2 c^+\right)}$, $\Delta=\omega_{\mathrm{c}}-\omega_{\mathrm{f}}$, we can adiabatically eliminate the transition between cavity and fiber in the large detuning limit $\Delta\gg\nu$ and obtain the effective Hamiltonian of subsystem cavity-fiber-cavity as

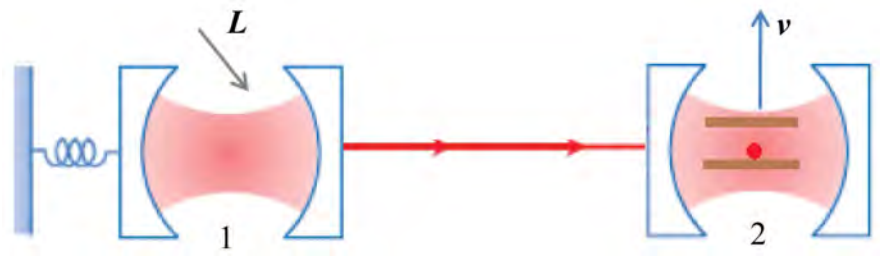

Figure 1. Schematic of proposed model. Optical cavity 1 is driven by a laser field *L*. A two-level atom moves along a direction perpendicular to cavity 2 mode with velocity *v*. Cavity waist $w=5\ \mu\mathrm{m}$.

$$H'_{\mathrm{c,f}} = \left(\omega_{\mathrm{c}} + \frac{2\nu^2}{\Delta}\right)a_1^+ a_1 + \left(\omega_{\mathrm{c}} + \frac{2\nu^2}{\Delta}\right)a_2^+ a_2 + \left(\omega_{\mathrm{f}} - \frac{4\nu^2}{\Delta}\right)c^+ c + \frac{2\nu^2}{\Delta}\left(a_1^+ a_2 + a_1 a_2^+\right) \tag{2}$$

Now we include the optomechanical subsystem and cavity-atom subsystem. The Hamiltonian of the global system without dissipation can be written as

$$H = \omega_{\mathrm{m}} b^+ b + \omega_{\mathrm{a}}\sigma^{\mathrm{z}} - \left(\delta - \frac{2\nu^2}{\Delta}\right)a_1^+ a_1 + \left(\omega_{\mathrm{c}} + \frac{2\nu^2}{\Delta}\right)a_2^+ a_2 + \frac{2\nu^2}{\Delta}\left(a_1^+ a_2 + a_1 a_2^+\right) - g_0 a_1^+ a_1\left(b + b^+\right) + \Omega\left(a_2\sigma^+ + a_2^+\sigma^-\right) \tag{3}$$

where $b\left(b^+\right)$ is the mechanical annihilation(creation) operator, σ_{z} and $\sigma^+\left(\sigma^-\right)$ are atomic spin and raising (lowering) operators. ω_{m} is the mechanical frequency, ω_{a} is the frequency of atomic internal transition. $\delta = \omega_{\mathrm{L}} - \omega_{\mathrm{c}}$ is the detuning of cavity 1 and the driving field. g_0 is the vacuum optomechanical coupling strength [14] [15]. Ω is the coupling strength of cavity to atom. For an atom moving along *x* scale perpendicular to the cavity mode with velocity *v*, the cavity-atom coupling strength can be represented by $\Omega(t) = \Omega_{\max}\mathrm{e}^{\frac{-(x_0+vt)}{w^2}}$, where $\Omega_{\max} = \Omega_0\cos(kz)$ is the maximum atom-cavity coupling strength, Ω_0 is Rabi frequency, x_0 is atomic initial position. The "c^+c" terms that does not influence the systematic transition is neglected.

3. Quantum State Transfer Protocol

The task of QST between two two-state ($|a\rangle_{1,2}$ and $|b\rangle_{1,2}$) systems is to accomplish the implementation $|\Psi_{\mathrm{in}}\rangle = (\alpha|a\rangle_1 + \beta|b\rangle_1)\otimes|b\rangle_2 \to |\Psi_{\mathrm{out}}\rangle = |b\rangle_1 \otimes (\alpha|a\rangle_2 + \beta|b\rangle_2)$ deterministically [11], where $|\Psi_{\mathrm{in}}\rangle$ and $|\Psi_{\mathrm{out}}\rangle$ are inputting initial state and outputting target state, α and β are normalized coefficients. The efficiency of QST can be illustrated by fidelity defined as $F = \left|\langle\Psi_{\mathrm{out}}|\Psi(t)\rangle\right|^2$. In our model, we assume that only the mechanical oscillator is initially excited, with initial system state $|\Psi_{\mathrm{in}}\rangle = |1\rangle_{\mathrm{m}}|0\rangle_1|0\rangle_2|0\rangle_{\mathrm{a}}$ and target state $|\Psi_{\mathrm{out}}\rangle = |0\rangle_{\mathrm{m}}|0\rangle_1|0\rangle_2|1\rangle_{\mathrm{a}}$. The system state $|\Psi(t)\rangle = \sum_i C_i(t)|\phi_i\rangle$ $(i = 1,2,3,4)$ is restricted within the Hilbert space spanned by basis vectors $|\phi_1\rangle = |1\rangle_{\mathrm{m}}|0\rangle_1|0\rangle_2|0\rangle_{\mathrm{a}}$, $|\phi_2\rangle = |0\rangle_{\mathrm{m}}|1\rangle_1|0\rangle_2|0\rangle_{\mathrm{a}}$, $|\phi_3\rangle = |0\rangle_{\mathrm{m}}|0\rangle_1|1\rangle_2|0\rangle_{\mathrm{a}}$, $|\phi_4\rangle = |0\rangle_{\mathrm{m}}|0\rangle_1|0\rangle_2|1\rangle_{\mathrm{a}}$, and is governed by Schrödinger equation $\frac{\partial|\Psi(t)\rangle}{\partial t} = -iH|\Psi(t)\rangle$, where $C_i(t)$ are normalized coefficients.

To accomplish high fidelity QST, the coupling strengthes are designed as follows. Initially, only the driving field is turned on. At time t_1, the driving field is turned off and the cavity-cavity interaction is turned on. At time t_2, the cavity-cavity interaction is turned off and the atom enters cavity with velocity *v*.

In the time $0 \le t \le t_1$, the QST implementation from mechanical oscillator to cavity 1 is only dominated by the Hamiltonian of optomechanical subsystem. By

using the standard "linearized approximation" procedure for optomechanics under the substitution $a_1 = \sqrt{\bar{n}_1} + A_1$ (where A_1 is the fluctuation of cavity 1 [15]) and considering dissipation, the subsystem is effectively described by a non-Hermitian Hamiltonian (under rotating wave approximation) as

$$H_{\mathrm{m},1} = \omega_{\mathrm{m}} b^{+} b - \delta A_1^{+} A_1 - G(t)\left(A_1^{+} b + A_1 b^{+}\right) - \frac{i}{2}\gamma_{\mathrm{m}} b^{+} b - \frac{i}{2}\kappa A_1^{+} A_1 \tag{4}$$

with mechanical decay rate γ_{m} and cavity leakage κ.

The pulsed many-photon optomechanical coupling is given by $G(t) = G_0 \mathrm{e}^{-(t-t_0)^2/2s^2}$ [9], where G_0 is the maximum optomechanical coupling strength. It has been experimentally demonstrated that optomechanical coupling is proportional to the mean number of the laser photons $\bar{n}_1$ [14], s represents the width of the Gaussian pulse. The designed coupling strengths sequence is shown in **Figure 2**, where $t_1 = \frac{4}{G_0}$, $t_2 = \frac{8}{G_0}$.

Obviously, in the time $0 \le t \le t_1$, the cavity-cavity coupling and cavity-atom interaction are negligible, and only the transition between mechanical oscillator and cavity 1 is considered. the coefficients C_i satisfy the equations

$$\begin{aligned} \dot{C}_1(t) &= -i\left[\omega_{\mathrm{m}} C_1(t) - G(t) C_2(t)\right] - \frac{\gamma_{\mathrm{m}}}{2} C_1(t) \\ \dot{C}_2(t) &= -i\left[-\delta C_2(t) - G(t) C_1(t)\right] - \frac{\kappa}{2} C_2(t) \end{aligned} \tag{5}$$

Under the condition $\omega_{\mathrm{m}} = -\delta$, and in a frame rotating with mechanical oscillator frequency ω_{m}, the equations can be simplified as

$$\begin{aligned} \dot{C}_1(t) &= iG(t) C_2(t) - \frac{\gamma_{\mathrm{m}}}{2} C_1(t) \\ \dot{C}_2(t) &= iG(t) C_1(t) - \frac{\kappa}{2} C_2(t) \end{aligned} \tag{6}$$

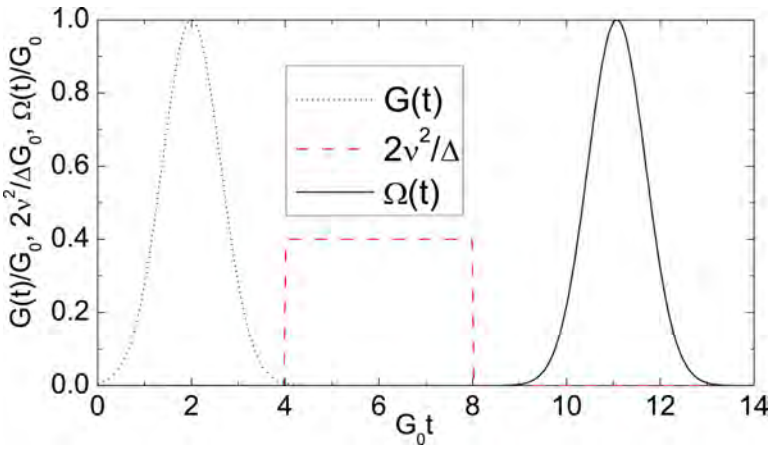

Figure 2. The time profiles of $G(t)$ (blue dotted line), $2\nu^2/\Delta$ (red dashed line), and $\Omega(t)$ (black solid line) normalized by G_0 as a function of normalized time $G_0 t$.

$G_0 = 2$ MHz, $\Omega_{\max} = G_0$, $\frac{\nu}{w} = 1.626\Omega_{\max}$, $\nu = 2G_0$, $\Delta = 10\nu$.

In the time $t_1 \le t \le t_2$, note that at the end of Gaussian pulse in cavity 1, $\bar{n}_1 = 0$, which leads to $a_1 = A_1$, we obtain equations:

$$\begin{aligned} \dot{C}_2(t) &= -i\frac{2\nu^2}{\Delta}C_3(t) - \frac{\gamma_m}{2}C_2(t) \\ \dot{C}_3(t) &= -i\frac{2\nu^2}{\Delta}C_2(t) - \frac{\gamma_m}{2}C_3(t) \end{aligned} \tag{7}$$

while in the time $t_2 \le t$, the coefficients satisfy:

$$\begin{aligned} \dot{C}_3(t) &= -i\Omega(t)C_4(t) - \frac{\gamma_m}{2}C_3(t) \\ \dot{C}_4(t) &= -i\Omega(t)C_3 - \frac{\gamma}{2}C_4(t) \end{aligned} \tag{8}$$

where γ is atomic decay rate (spontaneous emission rate).

The above equations can be solved numerically under the initial condition $C_1(0) = 1$, $C_2(0) = 0$. The excited state populations (ESP) of mechanical oscillator, cavity 1, cavity 2, and atom are represented by $|C_1(t)|^2$, $|C_2(t)|^2$, $|C_3(t)|^2$, and $|C_4(t)|^2$, respectively.

Figure 3(a) shows the ESP under characteristic experimental parameters without dissipation. The fidelity of QST can be calculated through the formula $F = \left|\left\langle \Psi_f \middle| \Psi(T+t_2)\right\rangle\right|^2$ for atomic transit time $T = \frac{L}{v}$ under the condition of atomic transit distance $L \gg w$. It can be proved that the fidelity turns out to be $|C_4(T+t_2)|^2$. Numerical results show that the quantum state initially encoded on mechanical oscillator can be transferred to atom with a fidelity 100% if the influence of dissipation is excluded. It is known that the system dissipation inevitably decreases the fidelity. However, the mechanical decay is not a big factor for maximum fidelity, which is 99.9% at $\frac{\gamma_m}{G_0} = 5\times10^{-4}$ (this result is obtained to demonstrate the affect of mechanical decay, all other decays are excluded).

Further more, **Figure 3(b)** shows the ESP in presence of system dissipation with specified decay rates [9] [14]. The maximum fidelity is 90.1%. One can see that the maximum fidelity strongly relies on cavity leakage and atom decay.

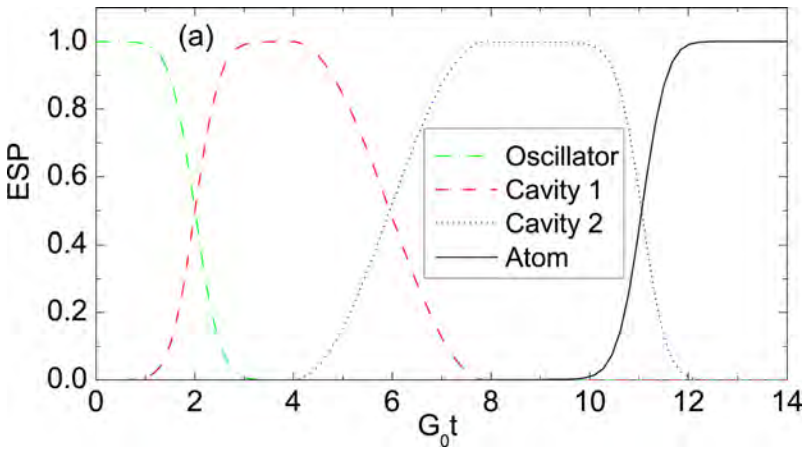

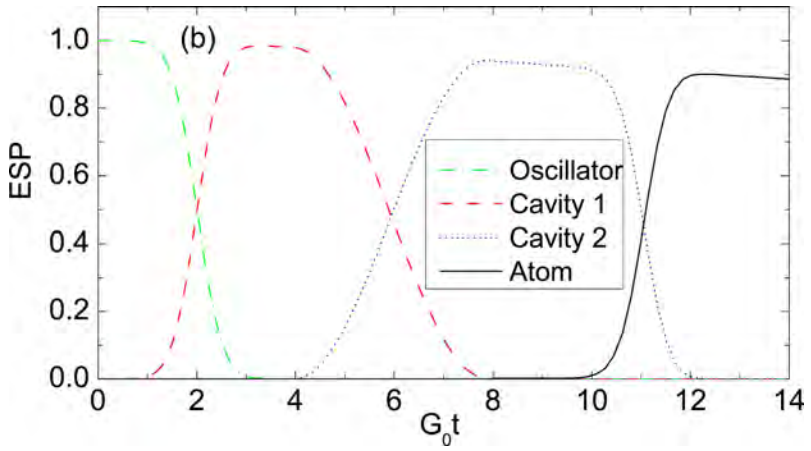

Figure 3. Excited state populations (ESP) of oscillator (green dash-dotted line), cavity 1 (red dashed line), cavity 2 (blue dotted line), atom (black solid line) versus G_0t. The quantum state initially encoded on oscillator is transferred to cavity 1, then to cavity 2 far apart via fiber, finally received by moving atom. The profiles of populations is modulated by parameters in **Figure 2** but for (a) without dissipation, (b) with dissipation, and the oscillator, cavity, and atom decay rates are characterized as $\gamma_m = 5\times10^{-4}G_0$, $\kappa = \gamma = 0.01G_0$, respectively [9] [14].

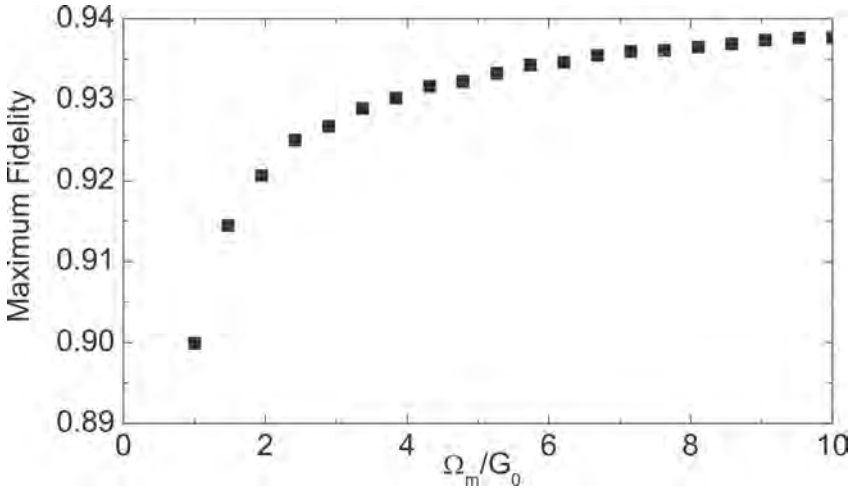

Figure 4. The maximum fidelity versus the maximum cavity-atom coupling strength Ω_m, where $v = 1.626\Omega_{max}w$.

Nevertheless, the fidelity can be obviously improved by optimal parameters. It is shown in **Figure 4** that synchronously increasing the maximum atom-cavity coupling strength Ω_{max} and atom velocity v increases maximum fidelity from 90.1% to 93.8%.

4. Conclusion

To summarize, we have analyzed a scheme to implement a quantum state transfer between a mechanical oscillator and a distant moving two-level atom mediated by cavity-fiber-cavity channel. By designing appropriate coupling strengths sequence within the experimental parameters range, a QST process is accom-

plished with fidelity 100%. We showed the scheme works in a robust way since the oscillator decay rate has very little impact on the fidelity and the affect of quantum channel has been reduced by adiabatically eliminating fiber mode. By synchronously increasing maximum atom-cavity coupling strength and atomic velocity, although the cavity leakage and atomic decay decrease the fidelity of QST, the maximum fidelity can be obviously raised to 93.8% from 90.1%. Furthermore, in the regime of "good cavity limits" with $\Omega_{\max} \gg \kappa, \gamma$ [16], the internal interaction of cavity-atom is much large than the dissipation that results in the decoherence of atom-cavity state, the affect of cavity leakage and atomic decay on QST can be effectively suppressed. Given the very successfully realized experimental real-time cavity QED technology [13] and strong-coupling optomechanical system [14], our scheme may be feasible and realizable.

Acknowledgements

Sincere thanks to the members of JMP for their professional performance.

Conflicts of Interest

The authors declare no conflicts of interest regarding the publication of this paper.

References

[1] Cirac, J.I., Zoller, P., Kimble, H.J. and Mabuchi, H. (1997) *Physical Review Letters*, **78**, 3221. https://doi.org/10.1103/PhysRevLett.78.3221

[2] Serafini, A., Mancini, S. Bose, S. (2006) *Physical Review Letters*, **96**, 010503. https://doi.org/10.1103/PhysRevLett.96.010503

[3] Xi, H.Z. and Pei, P. (2021) *Physical Review A*, **104**, 052401. https://doi.org/10.1103/PhysRevA.104.052421

[4] Oliveira, F. (2019) *Journal of High Energy Physics, Gravitation and Cosmology*, **5**, 935-940. https://doi.org/10.4236/jhepgc.2019.53049

[5] Kim, Y. (2021) *Journal of Modern Physics*, **13**, 138-165. https://doi.org/10.4236/jmp.2022.132012

[6] Molinares, H., Eremeev, V. and Orszag, M. (2011) *Physical Review A*, **105**, 033708. https://doi.org/10.1103/PhysRevA.105.033708

[7] Neto, G.D.M., Andrade, F.M., Montenegro, V. and Bose, S. (2016) *Physical Review A*, **93**, 062339. https://doi.org/10.1103/PhysRevA.93.062339

[8] Rao, S., Hu, X.M., Li, L.C. and Xu, J. (2015) *Journal of Physics B: Atomic, Molecular and Optical Physics*, **48**, 185501. https://doi.org/10.1088/0953-4075/48/18/185501

[9] Sete, E.A. and Eleuch, H. (2015) *Physical Review A*, **91**, 032309. https://doi.org/10.1103/PhysRevA.91.032309

[10] Hong, F.Y., Chen, L., Fu, J.L. and Zhu, Z.Y. (2015) *European Physical Journal D*, **69**, 122-127. https://doi.org/10.1140/epjd/e2015-60053-4

[11] Wu, J. and L, X.Y. (2011) *Optics Communications*, **284**, 2083-2088. https://doi.org/10.1016/j.optcom.2010.12.049

[12] Heller, L., Farrera, P., Heinze, G. and Riedmatten, H. (2020) *Physical Review Letters*, **124**, 210504. https://doi.org/10.1103/PhysRevLett.124.210504

[13] Hood, C.J., Chapman, M.S., Lynn, T.W. and Kimble, H.J. (1998) *Physical Review Letters*, **80**, 4157-4160. https://doi.org/10.1103/PhysRevLett.80.4157

[14] Gröblacher, S., Hammerer, K., Vanner, M.R. and Aspelmeyer, M. (2009) *Nature*, **460**, 724-727. https://doi.org/10.1038/nature08171

[15] Aspelmeyer, M., Kippenberg, T.J. and Marquardt, F. (2013) *Cavity Optomechanics*, **86**, 1319. https://doi.org/10.1007/978-3-642-55312-7

[16] Zhou, P. and Swain, S. (1998) *Physical Review A*, **58**, 1515-1530. https://doi.org/10.1103/PhysRevA.58.1515

Journal of Modern Physics, 2022, 13, 730-735
https://www.scirp.org/journal/jmp
ISSN Online: 2153-120X
ISSN Print: 2153-1196

Unification Might Be Achievable by a Hypothesis of Instantaneous Time-Jumps during Photon and Graviton Interactions (A Brief Note)

Eugene Terry Tatum

Independent Researcher, Bowling Green, USA
Email: ett@twc.com

How to cite this paper: Tatum, E.T. (2022) Unification Might Be Achievable by a Hypothesis of Instantaneous Time-Jumps during Photon and Graviton Interactions (A Brief Note). *Journal of Modern Physics*, **13**, 730-735.
https://doi.org/10.4236/jmp.2022.135042

Received: April 20, 2022
Accepted: May 24, 2022
Published: May 27, 2022

Abstract

Quantum theory according to the Copenhagen interpretation holds that, when a quantum interaction is observed (*i.e.*, "measured"), the observer's measuring devices temporarily become a part of the quantum system. Relativity theory holds that the event clock of the absorbed or emitted photon or graviton is frozen in time relative to all clocks outside the observed system. If we harmonize both theories, this would appear to imply that time continuity must be interrupted at each instant of observed photon or graviton interaction with matter. It is as if a segment of space-time is clipped out during each such observed interaction. If so, we must dispense with the notion of an absolutely smooth and continuous space-time and replace it with an observation-dependent, discontinuous, relativistic/quantum space-time. Mathematical physicists should be able to model this hypothesis (call it a "time-jump hypothesis") and its inherent discontinuous space-time in their further efforts at unification.

Keywords

Time-Jump Hypothesis, Unification, Relativity Theory, Quantum Field Theory, Relativistic/Quantum Space-Time, Instantaneous Energy Transition, Quantum Measurement Problem, Quantum Non-Locality

1. Introduction and Background

Philosopher Bertrand Russell once made the following remark in reference to quantum physics: "… its chief philosophical importance is that it regards physical phenomena as possibly discontinuous. It suggests that, in an atom, a certain

state of affairs persists for a certain time, and then suddenly is replaced by a finitely different state of affairs. Continuity of motion, which had always been assumed, appears to have been a mere prejudice… I suspect that (quantum theory) will demand even more radical departures from the traditional doctrine of space and time than those demanded by the theory of relativity [1]."

Previous attempts at the unification of relativity theory and quantum theory have failed, largely because the integration of gravity into quantum theory introduces unmanageable "infinities" into the mathematical models. Nevertheless, both physical theories work sufficiently well on their respective scales that they are enormously useful.

It has long been a subject of debate as to whether relativity theory or quantum theory must be comprehensively revised so that unification can be achieved. However, it may also be that both theories only need a small adjustment for them to become harmonious. The purpose of this brief note is to introduce the concept of a "time-jump" and to show by analogy how it might be understood. The key to this new understanding is to realize that relativistic considerations at the quantum scale must imply that we discard the long-held notion of an absolutely smooth and continuous space-time.

2. A Film-Editing Analogy of Time-Jumping

Movie films of the early 20th century had a jumpy time quality because there was poor camera/projector mechanization in conjunction with hand-cranking. Once this technology had sufficiently improved, a director's cut or editor's cut could be used to manipulate the time experience by actively creating a jump forward in the chronology of a story. In the editing room, the film could be spliced in such a way that a segment of time in an otherwise continuous sequence could be removed. The effect at sufficient film speed was an instantaneous jump in time; in other words, a time-jump.

3. How Relativistic Time-Jumping Might Work in the Quantum Realm

One of the concepts of special relativity theory is that faster relative motion slows the "moving" clock. Einstein's key conception was that, effectively, a photon's clock is timeless (*i.e.*, it is frozen it time) with respect to the reference frame clock of any outsider. With general relativity theory, the same can also be said of the clock of a graviton or a clock embedded exactly on the event horizon of a black hole (as perceived by the observer at any distance outside the event horizon). To put it another way, the clock of any outside observer, moving at any relative speed (short of speed of light c), ticks infinitely fast with respect to a photon, graviton, or black hole horizon clock.

But here's a key hypothetical point: the frozen clock of photon and graviton interactions pertains to the *entire* quantum frame (*i.e.*, "system" as defined by the Copenhagen interpretation). Any physical body, during the time of its emis-

sion or absorption of the energy of a photon or a graviton, is in the timeless reference frame of that speed-of-light particle. Thus, the emission or absorption of that relativistic energy is *instantaneous*. Furthermore, the same reference frame applies to the observer measuring devices during such an energy emission or absorption event. This is presumably how a quantum observation (*i.e.*, "measurement") can be defined. Thus, the quantum observer sees the energy interaction as instantaneous. When such an event is perceived as instantaneous, that means that no time elapses on the observer's clock during the event, and the space-time of the event can be represented as a finite point (*i.e.*, it has no space or time extension). When the observer is not observing (*i.e.*, not measuring) the quantum system, his own fast-ticking "outside" clock is his reference clock. This is perhaps why the "measurement problem" in quantum physics has been so perplexing. The relativistic concept of time-jumping, as described herein, wasn't formally a part of the Copenhagen interpretation.

4. Discussion

Several interesting theories about photon/graviton interactions with matter have been recently proposed [2] [3] [4] [5]. However, to this author's knowledge, recent and past theoretical work has not sufficiently explored the possibility of progress towards unification by incorporation of a relativistic instantaneous time-jump hypothesis into quantum theory.

The problem of unification could be somewhat analogous to viewing a pointillist painting from various distances. A sufficiently large separation between the viewer and the painting gives the impression of continuity in the landscape, whereas, a sufficiently short separation between the viewer and the painting gives the impression of discontinuity. Moreover, when the painting is sufficiently well-done, as in Seurat's "A Sunday Afternoon on the Island of La Grande Jatte", there is an intermediate distance which creates a certain level of cognitive dissonance, wherein one must inquire as to how something can appear to be both continuous and discontinuous at the same time. Nevertheless, the viewer can readily understand that this experience is merely one of clever illusion. Pointillism color theory, which was important to Seurat, is not germane to the present discussion.

The net effect of the instantaneous time-jump process described in this note is that its observer will never see an intermediate phase in the energy absorption. A photon-absorbing electron, in the temporary quantum system including its observer, effectively jumps instantaneously between atomic orbitals and can never be observed to be between them. It is as if there is no space-time distance between atomic orbitals during such energy transitions. Effectively, a space-time segment has been spliced out by the timeless photon or graviton clock. A similar instantaneous time-jumping process might also explain quantum non-locality between entangled quantum particles at great distances, so long as the emission/absorption messenger is absorbed and emitted by the intervening vacuum.

Distance as well as time is effectively eliminated, as if by a wormhole in space-time. Perhaps this sort of exchange is also a key to understanding dark energy within the vacuum, as recently theorized [6].

The following figures represent notions of energy transition by a seemingly smoothly-continuous process of energy absorption (Figure 1) and by a discontinuous process of quantum energy absorption (Figure 2). It may be helpful to imagine two different ways of representing the energy absorption of a body falling in a gravitational field. On the largest scale (Figure 1), the body appears to show a smoothly-continuous increase of energy. On the quantum scale (Figure 2), however, the body's energy gain is shown as representing instantaneous jumps in energy by graviton interactions at each time-jump. In an analogy to pointillism, both representations can be seen as useful, depending upon the scale needed at a given time. However, the greater and finer detail is obviously found in quantum Figure 2.

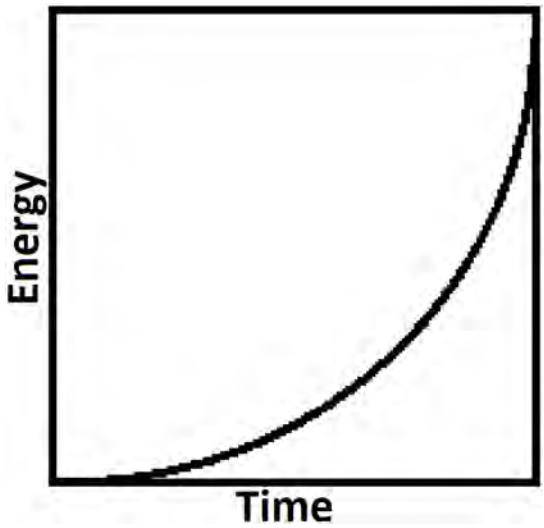

Figure 1. Classical energy transitions for a falling body.

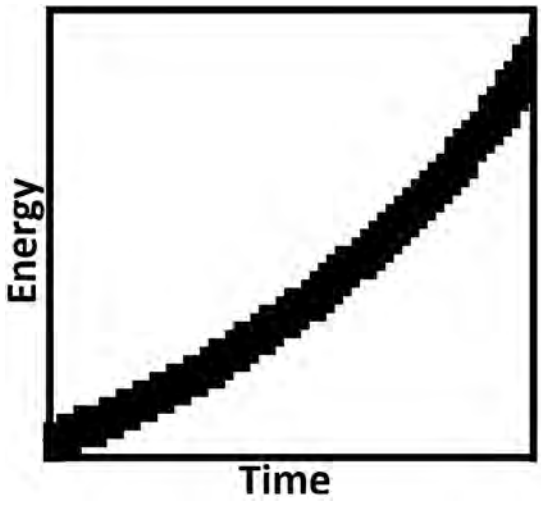

Figure 2. Quantum (graviton) energy transitions for a falling body.

With respect to this presentation, it is crucial to note that quantum time-jumps in Figure 2 are vertical (*i.e.*, having infinite slopes) because energy absorptions of gravitons are relativistically instantaneous. Perhaps, this correlates in some simplified way with the "infinities" found in previous attempts at unification. A rigid assumption of smoothly-continuous space-time will not allow for a notion of instantaneous events.

5. Conclusion and Summary

The present work is in the spirit of prior efforts to assist in unifying relativity with quantum theory. To our knowledge, the novelty of the present work is that the possibility of progress towards unification by incorporation of an instantaneous time-jump hypothesis has not been sufficiently explored. Future work is recommended along the lines of continuing to insert relativistic concepts of time and space into quantum theory.

The instantaneous energy jumps of the quantum world, wherein the energy-absorbing or energy-emitting particles are never found at an intermediate energy level (such as between atomic orbitals or within intervening space-time), might only be explainable by relativity, as discussed. One can think of the time clock of a photon or graviton as being frozen with respect to the infinitely fast-moving clock of the outsider. The particle absorbing or emitting a photon or graviton, as well as the observer measuring their energy transition, becomes temporarily part of the quantum system under observation and "sees" the event as instantaneous by the system's photon or graviton clock. Not only does a relativistic time-jump integration into quantum theory possibly alleviate the "infinities" problem in prior attempts at unification, it might also help us to better understand the instantaneous and space-eliminating nature of quantum non-locality, and the mystery of dark energy within the vacuum. If this time-jump hypothesis is correct, we must relinquish the long-held notion of an absolutely smooth and continuous space-time and replace it with an observation-dependent, discontinuous, relativistic/quantum space-time.

Dedications and Acknowledgements

This note is dedicated to Stephen Hawking and Roger Penrose for their groundbreaking work on black holes and their possible application to cosmology. Dr. Tatum sincerely thanks U.V.S. Seshavatharam for his co-authorship of the seminal Flat Space Cosmology papers and some of the more recent FSC publications. He also thanks Dr. Rudolph Schild of the Harvard-Smithsonian Center for Astrophysics for his past support and encouragement.

Conflicts of Interest

The author declares no conflicts of interest regarding the publication of this paper.

References

[1] Russell, B. (1945) A History of Western Philosophy. Simon & Schuster, New York,

832-833.

[2] Cheng, J. (2019) *Open Access Library Journal*, **6**, 1-9.

[3] Khairy Ahmed, A., Mohammed Yousif, M., Kurawa, Z., Allah Saad, Z., Makawy, S., Mohammed, M., Abd-Alla, M. and Elbadawi Mohamed, S. (2020) *Natural Science*, **12**, 588-598. https://doi.org/10.4236/ns.2020.128045

[4] Goray, M. and Annavarapu, R.N. (2020) *Results in Physics*, **16**, Article ID: 102866. https://doi.org/10.1016/j.rinp.2019.102866

[5] Athira, B.S., Susobhan, M. and Subhashish, B. (2021) *The European Physical Journal Plus*, **136**, Article No. 403. https://doi.org/10.1140/epjp/s13360-021-01361-8

[6] Tatum, E.T. and Seshavatharam, U.V.S. (2021) Flat Space Cosmology—A New Model of the Universe Incorporating Astronomical Observations of Black Holes, Dark Energy and Dark Matter. Universal Publishers, Irvine, California.

Journal of Modern Physics, 2022, 13, 736-760
https://www.scirp.org/journal/jmp
ISSN Online: 2153-120X
ISSN Print: 2153-1196

Can a Michelson-Morley Experiment Designed with Current Solar Velocity Distinguish between Non-Relativistic and Relativistic Theories?

Hector A. Munera

International Center for Theoretical Physics (CIF), Bogota, Colombia
Email: hmunera@hotmail.com

How to cite this paper: Munera, H.A. (2022) Can a Michelson-Morley Experiment Designed with Current Solar Velocity Distinguish between Non-Relativistic and Relativistic Theories? *Journal of Modern Physics*, **13**, 736-760.
https://doi.org/10.4236/jmp.2022.135043

Received: January 19, 2022
Accepted: May 27, 2022
Published: May 30, 2022

Abstract

If Michelson were to answer the question posed in the title, given the line of reasoning he used in 1881, Michelson would seat at his desktop computer to calculate the expected fringeshifts for several solar speeds around 400 km/s and various directions of motion. Present author did exactly the same in 2001 to plan his repetition of Michelson and Morley's (MM) 1887 experiment. The paper sketchedly summarizes the procedure to calculate expected fringeshifts in the MM interferometer for solar speeds available at Miller's epoch. In a pre-relativistic context, amplitudes of several fringeshifts may be expected in both MM and Miller experiments. However, all interferometer experiments up to 1930 were designed under the (incorrect from a modern viewpoint) assumption that fringeshifts would be smaller than one fringe-width. The inescapable conclusion is that those experiments were not appropriate to measure the true value of solar motion, always yielding a small, but lower than expected, value for solar speed. The ensuing "negative" interpretation led to the birth of relativity theory and to a new series of experiments implicitly designed to test the relativistic hypothesis of length-contraction, while the earlier "positive" experiments were designed to test a different hypothesis: whether the motion of Earth relative to some preferred frame can be measured using an interferometer of constant dimensions. With the benefit of hindsight this writer repeated the MM experiment, correcting main weaknesses identified up to the Michelson-Morley-Miller (MMM) measurements at Mount Wilson from April 1925 to February 1926. A new possible reinterpretation of the MMM data as a sequence of stationary measurements is pointed out. Our Michelson-Morley-Miller-Munera (MMMM) experiment at Bogota (Colombia) from January 2003 to June 2005 gave values for solar absolute velocity in

the same range as those obtained by astronomical means. Surprisingly, our results are compatible with modern third-party MM-type experiments designed and interpreted within relativistic contexts. Thus, a so far unexplored possibility arises: can interferometric experiments distinguish between pre-relativistic and relativistic theories? Our answer is negative.

Keywords

Michelson-Morley Experiment, Crucial Physics Experiments, Foundations of Physics, Absolute Solar Velocity, Absolute Motion of Earth, Correctness of MM Positive Experiments, Correctness of MM Negative Experiments

1. Introduction: CMB and Interferometer Experiments Are Non-Contradictory

In a recent paper Prilepskikh [1] correctly pinpointed the patent contradiction between two sets of empirical evidence related to the seat of electromagnetic phenomena. On one side, the conventional "negative" interpretation of the pioneering interferometric experiments by Michelson in 1881 [2] and Michelson and Morley in 1887 [3] (MM henceforth), and on the other side, the discovery reported in 1965 by Penzias and Wilson of cosmic microwave background radiation (CMB) [4], whose local anisotropy is interpreted as motion of solar system relative to a frame of reference attached to the CMB. Solar velocity approximately is 384 km/s, in the direction of galactic coordinates (264˚, 48˚) [5]. Since the Local Group of galaxies (including our Milky Way) seems to be moving with a higher speed, it is quite possible that the CMB-frame itself is also moving relative to something else, say a preferred frame, see [6] and references therein.

To solve the posited contradiction, Prilepskikh reinterprets Michelson's 1881 analysis [2] in terms of Doppler's effect and "*space-time* '*quantization*' *of radiation by wavelength-periods*", and concludes that the conventional "null" interpretation of Michelson's experiment is compatible with existence of motionless non-entrained ether. Thus, there is no contradiction with terrestrial and solar motion relative to CMB.

Technical details in Prilepskikh's paper [1] are not addressed here. Rather, it is noted that Doppler's effect was not a fully accepted theory in 1881 when Michelson was at Postdam carrying out his experiment under Helmholtz supervision. During the period 1872-1892 Vogel studied optical effects at the Observatory, also in Postdam, work that eventually led to the acceptance of Doppler's laws ([7], p 34). In the 19th century Riemann introduced the notion of four dimensions (space and time), while the current notion of spacetime is due to Einstein in the second decade of the 20th century.

From logical and historical considerations, this writer prefers to solve the contradiction, if any, with the technical, mathematical and philosophical means that Michelson had at his disposal in 1881 [8]. First thing to stress is that in the 1880s

relativity theory did not exist. This means that the analysis of Michelson's expectations has to be done without including relativistic effects. As clearly documented in [8], the historical facts are that both Lorentz length-contraction and Poincaré's principle of relativity were proposed to explain the null interpretation of Michelson's 1881 and MM's 1887 experiments.

Second point to stress is that, strictly speaking, there is no contradiction. Indeed, in all cases the data reduction process yielded a non-zero speed of Earth relative to the preferred frame that was lower than expected, but never zero [9] [10] [11] [12]—fact explicitly stated by Miller in several occassions [13]. This also applies both to the initial 1881 Postdam experiment [2], and to the short 1887 Michelson and Morley six-hour Cleveland experiment involving only 36 turns of the interferometer [3] (see Section 2). Furthermore, there are no error bars in the 1887 MM experiment, which had a significant error spread consistent both with a negative result, and with much larger values close to the expected 30 km/s [11] [12].

A third extremely significant aspect, usually overlooked, is that the vast majority of pretended "repetitions" of the MM experiment are not true repetitions in a strict sense. The reason is quite simple. After Einstein's formulated his special relativity in 1905, the data reduction process in those experiments incorporates corrections for the presumed length-contraction in the arms of the interferometer [9]. Thus, actually there are two different families of interferometric experiments, which have been treated so far as a single family, namely:

(A) Classical or pre-relativistic interferometric experiments, as Michelson's 1881 [2], MM's 1887 [3], and Morley-Miller and Miller's experiments [13], were all designed under the implicit premise that dimensions of the apparatus do not change as a result of absolute terrestrial motion (of course, dimensions may change by environmental or other causes). Since Earth's orbital and rotational motions are well-known, the problem reduces to testing for the value of solar motion [8]. For the value of solar velocity available in 1881 the expected fringeshifts were lower than one fringe-width (see Section 2.1). A variety of hypothesis were explicitly tested in Miller's work from 1902 to early April 1925 [13]. For his final campaign at Mount Wilson in April, August and September 1925, and February 1926, Miller finally tested for solar velocity without preconceived ideas (see Section 2.4), this will be called henceforth the Michelson-Morley-Miller (MMM) experiment. For the values of solar velocity available today, significant fringeshifts (*i.e.*, larger than one fringe-width) are expected in the large interferometers used in the MM and MMM-experiments [14] [15]. Our Michelson-Morley-Miller-Munera (MMMM) experiment also belongs to this category (see Section 3). Earth's velocity and the ensuing solar velocity are calculated from the observed large fringeshifts. These are the so-called "positive" experiments.

(B) Relativistic interferometric experiments assume that the Lorentz-Fitzgerald length-contraction is a physical phenomenon that continuously modifies the length of the arms of the apparatus (hence, the lengths of the two optical paths) as Earth moves in space. The so-called "negative" experiments are implicitly de-

signed to test the hypothesis that the outcome of the experiment is "null", that is, that the expected fringeshift is zero (exactly). Any deviation from the expected value (hopefully small, *i.e.*, less than one fringe-width) is attributed to experimental error. In the Kennedy and Thorndyke experiment [9] corrections for time dilation are also included during data reduction.

The distinction between the two families identified above has been missed because the apparatus and the experimental setup are the same in both cases. During the experimental phase, the only difference is in the recording of the observed fringeshift: the whole fringeshift (*i.e.*, an integer plus a fraction) in case (A), and in case (B) the fractional part of the fringeshift only. However, the process of data reduction is quite different: Earth's velocity is directly calculated from the observed large fringeshift in case (A), while in case (B) the observed fractional fringeshifts are interpreted as experimental errors relative to expected theoretical fringeshifts calculated with relativistic corrections for length of each arm moving at different velocity (orientation and speed) relative to some reference frame. Such velocity is obtained from external sources. Hence, the small observed residual error is attributed to: 1) accuracy of the value of speed used for the relativistic length-contraction corrections, 2) usual experimental errors, and 3) new unknown phenomena.

Turning now to the rhetorical question in the title of this paper: how would Michelson change the design of his 1881 and 1887 experiments with the information available today? Since Michelson was a top-class experimenter, we can answer in the same rhetorical mood that he would notice that the 1881 measurements at discrete positions of the apparatus requiring separate calibrations would not be appropriate, and he would implement continuous rotation of the interferometer relative to the preferred frame right since the initial 1881 experiment. Moreover, motion of reference fringe would be carefully monitored to identify shifts larger than one fringe-width. Furthermore, such large shifts would not be entirely attributed to usual experimental effects, say variation of temperature in the laboratory.

Returning to the historical record, it seems that Michelson's 1881 original assumption of recording only the fractional part of the shift was never revisited by Michelson, Morley or Miller. More than 40 years later, prompted by Nassau and Morse's work [16], Miller had a glimpse at the significant impact of solar motion ([13], pp 222-228), and implemented continuous 24 hr-measurement of fringeshifts for his MMM-experiment (see Section 2.4, and figures 1 and 2). Unfortunately, Miller continued recording the fractional-part of the fringeshift only.

Our own predictions take full account of solar motion as reported in 2002 [14] and 2006 [15]. Since Earth herself may provide a steady continuous slow rotation of the interferometer relative to the preferred frame, it follows that rotation of the apparatus relative to the laboratory is superfluous. Thus, the interferometer for our MMMM-experiment had short arms (2 meter long) and was, for the first time, stationary in the laboratory [15] [17] [18] [19] [20] (see Section 3).

Modern experiments based on different physical phenomena [21] [22] may ex-

hibit in the raw data exactly the same structure as our own positive results [18] [19] [20]. However, they are interpreted in the conventional negative context. For instance, in the well-controlled 2002 experiment at Stanford University using cryogenic resonant microwave cavities, the evident positive results were dismissed as unexplained "*mechanical disturbances*" that were subtracted from raw data, leading to a remaining white noise that was interpreted as their expected "null" result [21].

2. The Classical Pre-Relativistic Interferometric Experiments

In a general overview of the MM-type experiments [9] written by present author in 1998, some issues were not identified, and some weaknesses were not stressed enough, say, the lack of error analysis in MM experiment [11] [12]. Other issues as the possible existence of large fringeshifts (*i.e.*, larger than one wavelength) between two consecutive positions of the interferometer became obvious during the design in 2001 [14] and execution of our MMMM-experiment [15] [17]. All "positive" experiments are designed according to two classical postulates: (a) Light propagates isotropically with constant speed c relative to a preferred frame anchored to Newton's fixed stars, and (b) Velocity of a laboratory at Earth's surface (V_L) relative to the fixed stars frame is the vector addition of terrestrial velocity (V_E) and solar velocity (V_S). In turn, neglecting minor effects, V_E is the vector composition of orbital (V_O) and rotational (V_R) velocities, while V_S is formed by orbital motion around the center of our galaxy (speed V_G = 254 km/s), plus motion of Milky Way's center-of-mass relative to the fixed stars. Upper panel A in **Figure 1** illustrates the expected 24-hr periodic effect arising from terrestrial rotation V_R, while central panel B illustrates the expected annual periodic effect associated to V_O. Both periodicities were observed in the MMM and MMMM-experiments. At the time-scales of these experiments, solar velocity V_S is an unknown constant to be determined from the data. Lower panel C in **Figure 1** illustrates projections V_1 and V_2 of laboratory velocity V_L for different interferometer positions (angle relative to local east), as in the MM and MMM-experiments; panel C is not relevant for the MMMM-experiment, where the interferometer is at rest in the laboratory. In the context of "negative" experiments, panel C shows the time-dependent projections $V_1(t)$ and $V_2(t)$ upon arms A_1 and A_2 of the apparatus. $V_1(t)$ and $V_2(t)$ are used to calculate the respective relativistic length-corrections; laboratory velocity V_L is an outside datum.

2.1. The 1881 Michelson Experiment at Berlin and Postdam (Germany)

The arms of the interferometer used by Michelson in 1881 had a length L = 1.2 m, equivalent to approximately 2 E+6 wave-lengths of yellow light, chosen as the scale for his study. The theoretical basis for the experiment was: "*Assuming then that the ether is at rest, the earth moving through it, the time required for light to pass from one point to another on the earth's surface, would depend on the*

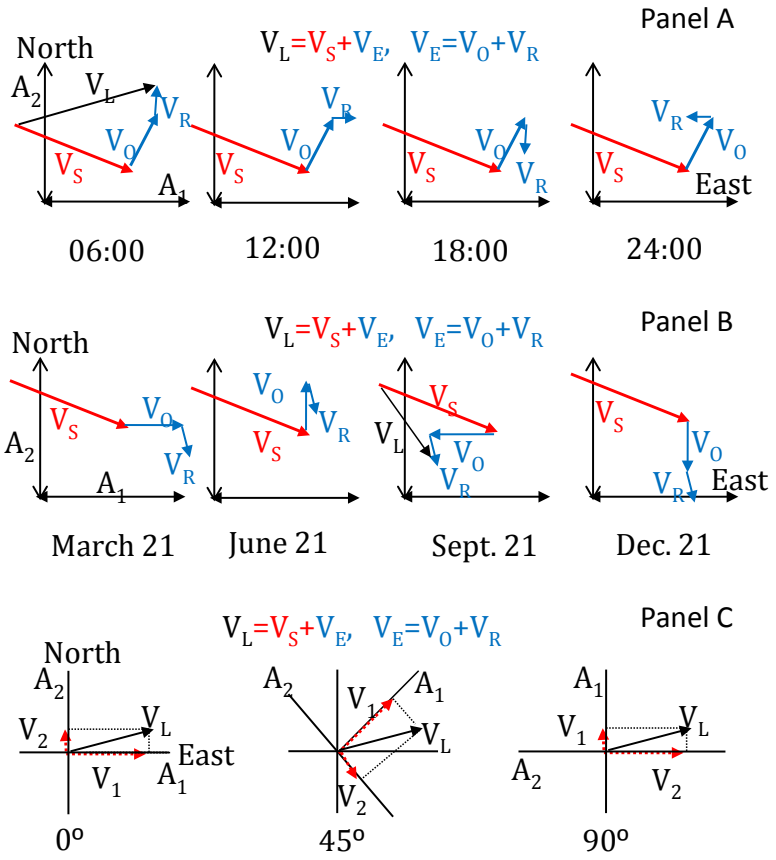

Figure 1. Illustration of diurnal and annual fringeshift periodic effects due to Earth's rotational ($\boldsymbol{V}_R$) and orbital ($\boldsymbol{V}_O$) motion (panels A and B respectively). Panel C: variation of projections V_1 and V_2 of absolute velocity $\boldsymbol{V}_L$ of a laboratory on Earth's surface upon arms 1 and 2 for different positions of an interferometer in rotation relative to the laboratory. Velocity arrows are not to scale: orbital speed V_O is 29.8 km/s, while V_S is at least one order of magnitude higher than V_O, and V_R is about two orders of magnitude lower than V_O.

direction in which it travels. Let c be the velocity of light, v = the speed of the earth with respect to the ether" ([2], p 120), underlining added, and the modern notation c for light velocity was used instead of Michelson's V. There are two tacit assumptions in previous statement: (a) Ether is at rest relative to something, that in 1881 most likely was Newton's absolute space, and (b) Light moves with speed c that is isotropic so that it has the same value any time of day at any epoch of the year, relative to some unspecified frame of reference, that may be Newton's preferred frame. Michelson continued: "*Suppose the direction of the line joining the two points to coincide with the direction of earth's motion*" ([2], p 120). Based on this direction (unknown in general), Michelson obtained equations for the time of light-travel along the arm of the interferometer aligned with this direction. As a numerical example Michelson calculated the time delay "*considering only the velocity of the earth in its orbit*" ([2], p 121). According to Michelson "*the actual distance the light travels in the first case is greater than in the second, by the quantity*" Δf given by

$$\Delta f = 2L\beta^2 \text{ where } \beta = v/c \quad (1)$$

Regarding the other arm of the interferometer Michelson stated: "*if, however, the light had traveled in a direction at right angles to the earth's motion it would be entirely unaffected*", and again at the end of same page: "*the other pencil being at right angles to the motion would not be afffected*" ([2], p 121), underlinings added. As independently noted by M. A. Potier in 1881 and by H. A. Lorentz in 1886, Michelson's analysis for the transverse arm is not correct regarding the underlined words above. Michelson acknowledged this error in his theory for the MM 1887 experiment ([3], p 334-336).

However, the final result presented in 1887, neglecting all terms above second order is exactly the same as in 1881. In Michelson words: "*if now the the whole apparatus be turned through* 90˚ *the difference will be in the opposite direction, hence the displacement of the interference fringes should be*" Δf given by equation (1) above ([3], p 336).

Michelson treated velocity of Earth's center of mass $V_{CM} = V_O + V_S$ as the vector addition of two components: (a) orbital motion with approximate speed V_O = 30 km/s along the plane of the ecliptic, plus (b) solar motion V_S toward constellation Hercules, that for early April 1881 was at an angle of 26˚ relative to Earth's terrestrial equatorial plane ([2], p 124). He explicitly stated that "*if the apparatus be so placed that the arms point north and east at noon, the arm pointing east would coincide with the resultant motion, and the other would be at right angles. Therefore, if at this time the apparatus be rotated* 90˚, *the displacement of the fringes should be twice* 8/100 *or* 0.16 *of the distance between the fringes*" emphasis in the original ([2], p 125).

Michelson also considered a second alternative: "*if on the other hand, the proper motion of the sun is small compared to the earth's motion the displacement should be* 6/10 *of* 0.08 *or* 0.048" ([2], p 125). And decided to average the two possibilities: "*taking the mean of these two numbers as the most probable, we may say that the displacement to be looked for is not far from one-tenth the distance between the fringes*" ([2], p 125).

Unfortunately, Michelson missed a third scenario, which is logically and physically possible, namely: solar speed $V_S >>$ 30 km/s, and/or the direction of solar motion is not towards Hercules. As accepted today, solar speed relative to a preferred frame is V_S = 384 km/s according to [5], or V_S = 390 km/s according to [23]. There are also higher estimates: V_S > 600 km/s [24] [25] [26]. This means that $\beta = v/c$ = 390/300,000,000 increases at least by a factor of 13 relative to Michelson's calculations. Thus Michelson's longitudinal fringe shift Δf = 0.16 becomes $\Delta f = 0.16 \times 13 \times 13 = 27$, *i.e.*, much larger than one fringeshift!

Thus, the three classical interferometric experiments [2] [3] [13] were designed under the (incorrect from a modern viewpoint) assumption that expected fringeshifts were smaller than one fringe-width.

For completeness, let us mention that the 1881 interferometer was a static apparatus that was aligned in 45˚ steps along different local directions North, North-

east, East, etc. Each measurement was independent of the next, and it was impossible for Michelson to know how many fringes shifted from a given position to the next. Thus, from the viewpoint of modern knowledge regarding the speed of solar motion, it is sad to say that Michelson's expectations (*i.e.*, a fringeshift about 0.1 fringe-widths, as quoted above) could not be determined from his experimental setup.

2.2. The 1887 MM-Experiment at Cleveland (Ohio)

For the MM-experiment there was a significant change in the design of the apparatus that was mounted upon a stone floating in mercury continuously rotating during the measurements. Length of the optical path along each arm was increased to L = 11 meters. Position of reference fringe was read by an observer continuously walking around the apparatus with same angular speed as the stone, and looking through a telescope every 22.5˚. As in the 1881 experiment, it was assumed (without any observational evidence) that the reference fringe always shifted by less than one fringe-width. This is an almost unbelievable assumption because in 1887 the 11-meter long arms of the apparatus were ten times longer than in 1881, so that in the case of motion toward Hercules only, the expected longitudinal fringeshift according to Equation (1) and Michelson's calculation mentioned in previous Section 2.1 would be $\Delta f = 0.16 \times 10 = 1.6$ fringes!

It is quite surprising that MM decided to ignore the small motion toward Hercules: "*only the orbital motion of the earth is considered. If this is combined with the motion of the solar system, concerning which but little is known with certainty, the result would have to be modified; and it is just possible that the resultant velocity at the time of the observations was small though the chances are much against it. The experiment will therefore be repeated at intervals of three months, and thus all uncertainty will be avoided*" ([3], p 341), undelinings added. However, the experiment never was repeated at the promised three-month intervals. From calculations in previous Section 2.1 without including solar motion (*i.e.*, with orbital motion only) the "expected" fringeshift would $\Delta f = 0.048 \times 10 = 0.48$ fringe-width. However, such value is just the lower limit in the set of all possible fringeshifts.

Granted, the true value of solar speed V_S was unknown in 1887, and even in 2022 it is not completely known. Instead of assuming $V_S = 0$, a standard and correct approach in experimental physics is to estimate possible outcomes of the experiment for different values of V_S, say {0, 30, 60, ..., 300, 600, ..., 3000 km/s}. Using Equation (1), values of Δf for each V_S were easy to calculate in 1881 and 1887. Evidently, for the majority of values of V_S the expected fringeshift would be larger than 1.

The time-dependent velocity of Earth's center of mass is $V_{CM} = V_O + V_S$, where orbital velocity V_O is a known time-dependent function, and solar velocity V_S is an (unknown) constant at the time-scale of the interferometric experiments

discussed here. At a laboratory located at longitude ϕ and latitude θ on the surface of Earth, velocity V_{CM} may be decomposed into a horizontal component $V_I(t; \phi, \theta)$ tangential to the surface of Earth (*i.e.*, parallell to the plane of the interferometer) and a vertical component $V_V(t; \phi, \theta)$, perpendicular to the floor.

Left panel in **Figure 2** shows the magnitude of V_I at a laboratory in Cleveland on July 8/1887 over the 24 hours of the day, for four different values of solar velocity: (a) $V_S = 30$ km/s in the direction of right ascension $\alpha = 270^\circ$, declination $\delta = 26^\circ$, which is used as an approximate representation of solar motion toward Hercules constellation as in the 1881 Postdam experiment. (b) $V_S = 0$, *i.e.*, only orbital motion of Earth as in the 1887 MM-experiment. (c) Miller-N: $V_S = 200$ km/s toward the northern galactic apex at $\alpha = 255^\circ$, $\delta = 68^\circ$ ([13], p 232). (d) Miller-S: $V_S = 208$ km/s toward the southern galactic apex at $\alpha = 73.5^\circ$, $\delta = -70.55^\circ$ ([13], p 234).

Left and central panels in **Figure 2** show that both V_I and fringeshift curves may have one or two cycles over a single day depending upon the speed and orientation of V_S. Examples for other values of V_s appear in ([14], fig 1, p 476). For the physically incorrect case with $V_S = 0$ there are two cycles (second row from top in left and central panels). As V_S increases the depth of one of the minima slowly evolves (first row in left and central panels for $V_S = 30$ km/s). As explained in [14] (see equation 32, p 480 in Section 4), there are values of V_S at which one of the minimum fringeshift values dissappears as it merges with the

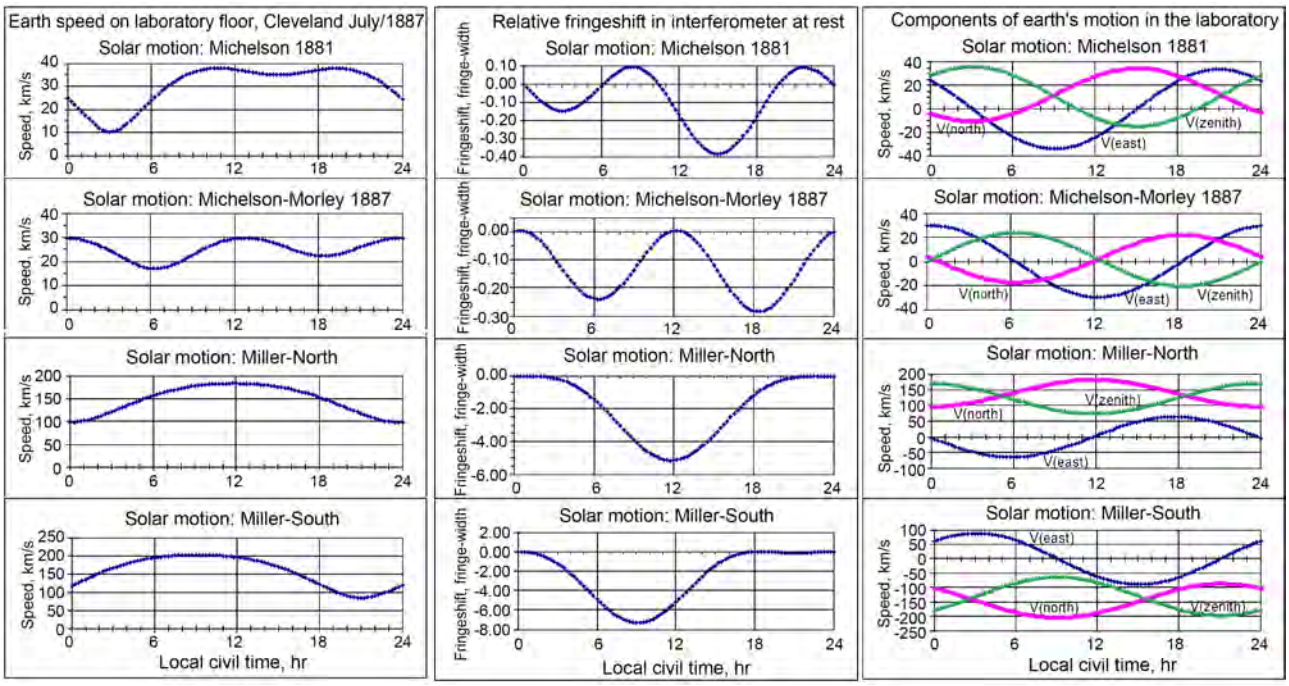

Figure 2. Effect of solar velocity (see text) upon a MM interferometer at rest in Cleveland (Ohio) on July 8/1887 during the MM-experiment. Left panel: magnitude of V_I the absolute motion of Earth's center-of-mass parallel to the floor of the laboratory. Central panel: relative fringeshift in fringe-widths. Right panel: daily variation of Cartesian components of V_{CM} at MM's laboratory. High values of solar speed (two lower rows) lead to fringeshifts larger than one fringe-width; maximum value is 8 fringe-width for Miller-S case (see central panel, bottom row).

two adjacent maxima (*i.e.*, three gradients of the curve become zero at same place). For such particular values of solar velocity the V_I and fringeshift curves have only one diurnal cycle. Also, location of maxima and minima significantly vary according to orientation of solar motion (α, δ).

Central panel in **Figure 2** shows the fringe shifts predicted in a MM interferometer at rest, *i.e.*, without rotation relative to the floor of a laboratory in Cleveland on July 8/1887. Of course, such predictions do not refer to MM-experiment where the interferometer was in rotation relative to the laboratory. There is, however, a connection between both types of experiments that is explained in Section 2.5. For an apparatus at rest, cases (a) and (b) in **Figure 2** calculated with the physically incorrect small solar speeds predict maximum and minimum amplitudes lower than one fringe-width. For solar speeds around 200 km/s predicted fringeshifts are significantly higher than one fringe-width. It may be recalled in passing that such speeds were obtained by Miller from his data by using a questionable ad hoc procedure. Of course, for higher solar speeds around 390 km/s, as currently accepted [5] [23], the expected fringeshifts are larger.

Shape of fringeshift curves in central panel of **Figure 2** is of paramount importance. Indeed, the only case showing a maximum at noon, and a minimum of equal magnitude at 6 p.m. corresponds to the physically incorrect assumption of a Sun at rest (*i.e.*, $V_S = 0$) as in case b. Since Michelson used such (incorrect) assumption in the derivation of Equation (1) above, it means that such expression is not physically correct, and invalidates its usage for the interpretation of the MM-experiment and for all the experiments carried out by Miller ([13], p 227). Further comments in next subsections.

For completeness, right panel in **Figure 2** shows the three Cartesian components of Earth's center of mass velocity V_{CM} relative to a laboratory on the surface of Earth: North, East and Zenith. V_I is the projection of V_{CM} upon the interferometer plane, given by the vector addition of V (North) and V (East). Magnitude of V_I is in the left panel of **Figure 2**.

2.3. Morley and Miller Experiments at Cleveland (Ohio) from 1902 to 1906

After Michelson left Cleveland for Chicago, Morley continued the experiments with Dayton C. Miller, a Princeton graduate. Altogether, Morley and Miller completed 995 turns of the interferometer from 1902 to 1906 ([13], pp 208-217), [27]. For the 260 turns in July 1904 the analysis "*was based upon the effect to be expected from the combination of the diurnal and annual motions of the earth, together with the presumed motion of the solar system towards the constellation Hercules*". Once again, this is the same small solar speed assumed in all classical interferometric experiments [2] [3] [13]. Morley and Miller found the "*two times of the day when the resultant of these motions, about* 33.5 *kilometers per second, would lie in the plane of the interferometer*, 11:30 *o'clock, A.M., and* 9:00 *o'clock, P.M.*" ([13], p 216, column 1), and, following Michelson, they averaged the A.M. and P.M. readings. However, the two lower graphs in central

panel of Figure 2 show that the method is incorrect for high values of solar speed. Miller discovered the error in the mid 1920s, and in his 1933 overview paper [13] he honestly stated that the "*procedure of* 1904 *was incorrect*" (see page 216, column 2 and figure 11 in page 217).

Despite the said gross errors in data gathering and data reduction, the experiments by Morley and Miller were "positive": "*the morning and evening observations each indicate a velocity of ether drift of about* 7.5 *kilometers per second*" ([13], p 217, column 1).

2.4. Miller's 1921-1926 Experiments at Cleveland (Ohio) and Mount Wilson (California)

Spurred by British observations during the 1919 solar eclipse (that were interpreted as supporting general relativity), Miller decided to resume his experiments, whose "null" interpretation was at the empirical foundations of special relativity ([13], p 217, column 2). Miller carried out measurements at Mount Wilson, near Pasadena (California) in 1921, at Cleveland during 1922-1924, and again at Mount Wilson during 1925-1926, for a grand total of 2327 turns of a steel interferometer.

After the Cleveland campaign Miller reports that "*at the end of year* 1924, *when a solution seemed impossible*, *a complete calculation of the then expected effects*, *for each month of the year*, *was made for the first time*. *This indicated that the effect should be a maximum about April* 1, *and further*, *that the direction of the effect should*, *in the course of the twenty-four hours of the day*, *rotate completely around the horizon*" underlinings added ([28], p 356). However, still following Michelson, only the apparent solar motion towards Hercules was considered ([13], p 221, column 2). A test at Mount Wilson from March 27 to April 10, 1925 finally demonstrated that absolute solar motion is not the same as the relative local motion towards Hercules ([13], p 222, column 1).

Thus, Miller realized at last that "*it is necessary to determine the variations in the magnitude and in the direction of the ether-drift effect throughout a period of twenty-four hours and at three or more epochs of the year*" emphasis in the original ([13], p 223, column 1). He then designed his new experiment with "*two sets of readings made in each hour through a working day*, *or night*, *of eight hours*" ([13], p 212, column 2). Miller's introduction of frequent readings over a 24-hr period, in experimental sessions of several days at different epochs of the year, was a significant improvement over MM-experiment.

Each set of readings at Mount Wilson lasted about sixteen (16) minutes for twenty turns of the interferometer mounted on a rotating stone floating in mercury, each turn taking forty eight seconds. Thus, every three (3) seconds "*the observer has only one single thing to do…announce the position of the central black fringe with respect to the fiducial point*, *plus or minus*, *in units of a tenth of a fringe width*, *at the instant of the click of the electric sounder*" ([13], p 213, column 1). However, this is easier said than done: the observer had to "*walk in a small circle*, *in the dark*" ([13], p 228, column 2), at the same angular speed as

the apparatus, without perturbing the rotating stone in any way, to look through an astronomical telescope whose "*eyepiece is supported on the end of the arm, there being no tube for the telescope…direct reading with the eye was very satisfactory*" ([13], p 220, column 1).

Since Miller continued anchored to Michelson's idea that the expected fringeshift was small, the significant fringeshifts observed at Mount Wilson were entirely attributed to "*temperature drift*". This led Miller to eliminate the (presumably unwanted) fringeshit drift in two steps, both of them visible in the datasheet for September 23/1925 at 03:17A.M. (see figure 8 in ([13], p 213)):

(1) A (questionable, in several senses) on-line modification of one arm of the apparatus, whose length was changed by hanging a small weight at its end, thus flexing it. Since rotation was not stopped, the observer continued collecting data without interruption, despite the obvious fact that flexing would induce vibrations in the metalic arm, thus possibly leading to spurious readings in the position of the reference fringeshift (at the very least during the turn of the apparatus immediately after the flexing). Such modification of the hardware was euphemistically identified as "adjust" in figure 8. In Miller's words: "*the adjustments are maintained so that the central fringe of the field of view… is never more than two fringe widths from the fiducial point*" underlining added ([13], p 212, column 1). In passing, this means that Miller did observe fringeshifts larger than one fringe-width. In the particular case shown in figure 8 there were four adjustments in 16 minutes. And,

(2) During data processing, the readings in every single turn lasting 48 seconds were linearly corrected for the presumed temperature variations during that 48-second-time span. The calculations are shown in the lower part of the datasheet in figure 8, and are further illustrated in figure 9 ([13], p 213). Such corrections were applied despite the fact that temperature in the laboratory was almost constant to an accuracy of 0.1˚ as attested by four thermometers, whose readings were taken at 02:57 and 03:19 (see top part of datasheet in Miller's figure 8).

From the data corrected for temperature drift, Miller calculated Earth's speed using Equation (1), often called the "*elementary theory of the experiment*" ([13], p 227, column 1).

As discussed in Section 2.5 below, without the "adjustments" and without the correction for temperature drift, the datasheet for September 23, 1925 at 03:17 A.M. would show a cumulative net fringeshift to the left of 6.1 fringe-widths in 16 minutes ([8], pp 33-34). By any standard, this was a significantly large fringeshift!

The original datasheets of the MMM-experiment (about three hundred pages) were recently unearthed by James De Meo at the Physics Department of Case Western Reserve University (CWRU) and moved to the general CWRU archive ([29], p 308). They all show "adjustments" similar to those discussed above for September 23/1925. Present writer was tempted to reverse Miller's "*adjustments*" in the 300 data sheets. Instead, it was preferred to undertake our MMMM-expe-

riment, summarized in next Section 3.

For further comments on other systematic errors in Miller's experiment see ([9], Section 2.1) and [10]. In particular, as seen in **Figure 2**, the curves of V_I and fringeshift versus time are not sinusoidal in general, and their shape depends on the direction (α, δ) of solar motion. This leads to a 24-hr component in the orientation of V_I upon the plane of the interferometer as a function of angle ω, the direction from local east. Instead of Michelson's Equation (1) above, fringeshift Δf is given in first approximation by Equation (2) here (see equations 2 and 3 in [9] or eq. 2 in ([10], p 192), and for additional details Section 3 in ([14], p 472-478) and equation 20 in Sections 2.2 and 2.3 in ([15], p 75-79)):

$$\Delta f = \frac{2L\beta_I^2}{\lambda}\cos 2\omega \text{ where } \tan\omega = \frac{V(\text{north})}{V(\text{east})}, \beta_I = \frac{V_I}{c} \tag{2}$$

Wavelenght of light used in the interferometer is λ, and length of the arm is L. In the relativistic context of the "negative" experiments, there are phase effects somewhat similar to Equation (2), see Sfarti's equation 3.1 in [30].

Despite all shortcomings, Miller's experiment was "positive": "*these experiments had given conclusive evidence of a real effect which was systematic but which was small in magnitude and was inexplicable as to its azimuth*" underlinings added ([13], p 228, column 1). To get realistic values for solar speed from his experiment, Miller had to introduce by hand a factor of reduction k "*which has so far remained inexplicable*" ([13], p 234, column 2). It is our contention that without the "adjustments" the MMM-experiment would have been succesful.

In our opinion, a given fringeshift is due in part to true motion of Earth relative to a preferred frame and partially to atmospheric variations due to changes in temperature, pressure and air composition (water vapour, CO_2 and other contaminating gases, dust, etc.). In contrast, the possible effect of variations of atmospheric pressure was not explicitly mentioned by Michelson, MM or Miller. The importance of the index of refraction along the light path has been stressed also by the group led by Consoli in Italy [6]. They additionally suggest a possible non-zero refractivity of the vacuum. If the latter is confirmed by experiment it could be interpreted, in my opinion, as the refractivity of a non-material energy-like aether.

Summarizing and frankly speaking, in the short three-second interval between readings in the MMM-experiment, the observer barely had time to raise his head from the eye piece, jump from one reading position to the next, turn and lower again his head towards the eyepiece, identify and shout to the scribe an approximate value (in tenths of a fringe-width) for the position of the central fringeshift relative to the pointer. Also, from the rightside photograph in figure 7 ([13], p 211) showing six black fringes in the field of view (without any scale), it seems hard to achieve the reported 0.1 fringe-width accuracy. It is not credible that a human observer can walk in circles during sixteen (16) minutes with his head sideways and attached to the eyepiece continuously watching a given reference

fringe. Despite these caveats, Miller's data is taken at face value in the analysis carried out in next Section 2.5.

In the same vein, Sir Oliver Lodge wrote a century ago: "*it is rather surprising that the readings were made by a peripatetic observer, with the instrument in constant and not very slow rotation…one would have thought that a stoppage of the frame and a reading of the fringes by a seated observer in many azimuths, would have been more satisfactory*" underlining added ([31], p 854, column 2). In fairness to Miller, he did consider the possibility of having a photographic register of fringeshift position, idea abandoned because luminosity did not suffice for good quality photographs in the rotating interferometer ([13], p 220, column 1).

2.5. A Reinterpretation of MMM Daily Data as a Sequence of 16 Interferometers at Rest

Professor Lodge's suggestion amounts to an interferometer at rest in the laboratory, with the "*many azimuths*" provided by earth's rotation, idea used in our MMMM-experiment (see next Section 3). Instead of Miller's "temperature drift" interpretation, let us reinterpret the drifts in the raw data of the MMM-experiment as real fringeshifts in a group of 16 stationary interferometers at different orientations relative to the laboratory.

Neglecting the effect of the (very small) speed of rotation of the interferometer relative to the laboratory, each one of the 17 columns in anyone of Miller's datasheets may be viewed as a set of 20 readings taken at intervals of 48 seconds in an interferometer at rest in the laboratory. Each column corresponds to a different orientation of the apparatus relative to the laboratory, namely: column 1 is an interferometer oriented with the telescope towards local north. Column 2 is an interferometer with the telescope towards local north plus 22.5˚ counterclockwise, and so on for the other columns. For instance, column 5 is a 90˚ rotation that places the telescope towards local west. Last column 17 is a 360˚ rotation that returns the apparatus to the original orientation towards north.

Let us focus here on the interferometer with the telescope oriented north. Columns 3 and 4 in **Table 1** correspond to columns 1 and 17 in the datasheet for September 23/1925 at 03:17 A.M. local mean time ([13], fig 8, p 213). Values are positive/negative according to the right/left position of the reference fringe relative to the pointer. Column 2 in **Table 1** is time t in seconds, elapsed since the beginning of the first turn, for a total of 960 s at the end of the twentieth turn.

Note that column 17 in Miller's figure 8 contains the last value of a turn, which also is the first value for the next turn in column 1. This should occur for all values within a given session. However, as already noted in previous Section 2.4, this is not the case here because Miller (incorrectly) modified in three occassions the length of one of the arms of the interferometer during the 20 turns of the session. The word "adjust" in turn 5 means that at the end of the turn one arm of the interferometer was flexed, in such a manner that the reading "−15" in

Table 1. Miller's readings for the interferometer at rest with telescope pointing north at Mount Wilson on September 23/1925, 03:17A.M. local mean time ([13], figure 8, page 213).

1	2	3	4	5	6	7	8	9
Turn j	$t(j)$, elapsed time, s	Y = reference fringe position		Comment	Y = reference fringe position			
					Interferometer			
		Column 1 (figure 8)	Column 17 (figure 8)		1	2	3	4
1	0	+10	+7		+10			
2	48	+7	+1		+7			
3	96	+1	−4		+1			
4	144	−4	−13		−4			
5	192	−13	−15	Adjust	−13			
6	240	0	+8		−15	0		
7	288	+8	−2			+8		
8	336	−2	−11			−2		
9	384	−11	−10	Adjust		−11		
10	432	+8	−1			−10	+8	
11	480	−1	0				−1	
12	528	0	+9				0	
13	576	+9	+7				+9	
14	624	+7	+10				+7	
15	672	+10	0				+10	
16	720	0	−4				0	
17	768	−4	−10				−4	
18	816	−10	−12				−10	
19	864	−12	−21	Adjust			−12	
20	912	+1	+4				−21	+1
	960							+4

column 17 was changed into "0" which now appears at the beginning of turn 6. Table 1 also shows similar modifications of the apparatus at the end of turns 9 and 19.

The net effect of Miller's "adjustments" is that, as a matter of fact, there are four different apparatuses during the set of readings under consideration. Apparatus 1 was used for turns 1 to 5, apparatus 2 for turns 6 to 9, apparatus 3 for turns 10 to 19, and apparatus 4 for last turn 20. Individual readings for the reference fringe position in each apparatus appears in columns 6 to 9 in Table 1, and in graphic form in Figure 3 (left panel in top row).

From the direct experience obtained during our MMMM-experiment with an interferometer at rest, present writer may attest that without the "adjustments"

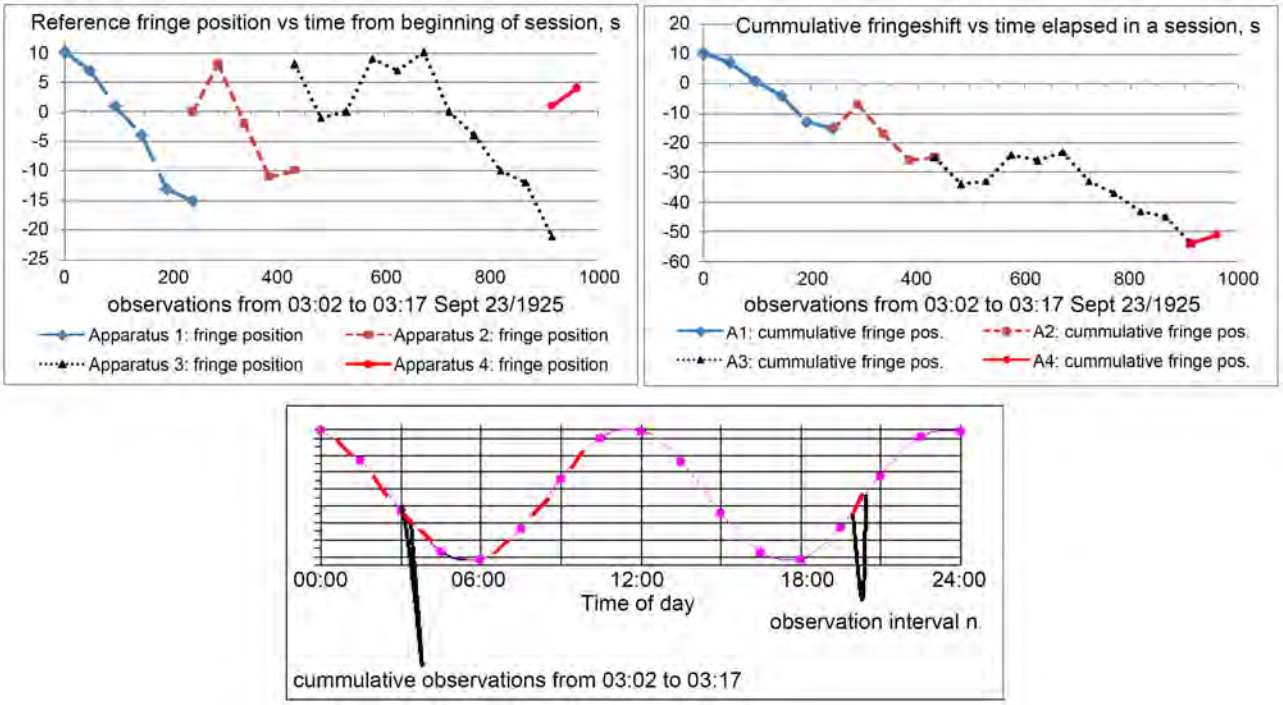

Figure 3. Reinterpretation of Miller's raw data as fringeshifts in an interferometer at rest at some well defined orientation. Top row: position of central black fringe on September 23/1925 at 03:17A.M. Vertical axis is in 0.1 fringe-widths. Horizontal axis shows elapsed time in seconds since beginning of the set of readings. Left graph shows individual readings for each apparatus (see text). Right graph shows the cummulative fringeshift that would be observed without "adjustments". Bottom row: qualitative graph of fringe position versus time of day in an interferometer at rest. Miller obtained N set of readings in a day (see text). Each 16-minute set of readings contributes a 16-minute interval (at the corresponding time of day) towards the 24-hr fringeshift curve.

the interference fringe pattern (which is the real object being observed shown in Miller's figure 7 ([13], p 211)) always keeps a steady drift, *i.e.*, without jumps. Evidently, discrete jumps are introduced by the "adjustments". Then, an approximate estimate for the readings to be observed without "adjustments" is provided by the cummulative fringeshifts registered by the four apparatuses, as shown in right panel, top row in **Figure 3**, where a steady non-random downward trend depicts the usual variations in experimental work.

Total fringeshift amounts to 6.1 fringe-widths during the 16 minute duration of this session, in Miller's interferometer with a 32 meter long optical path. In a smaller interferometer as the 2-meter long apparatus used in our MMMM-experiment, Miller's shift is equivalent to $6.1 \times 2/32 = 0.38$ fringe-widths. Such shift is visually observable and is consistent with our own experience in Bogota: "*During the setup process the first semester of* 2002, *we started with measurements every* 15 *minutes… The interference pattern from one observation to the next showed differences that could be appreciated by the naked eye*" ([15], p 80, column 2); similar remarks appear in another earlier paper ([10], p 198). This supports our contention that Miller's fringeshifts are (possibly to a large extent) due to true solar motion, rather than mere artifacts of "temperature drift".

During the Mount Wilson campaign, there were at least least two sets of readings per hour (see previous Section 2.4) over one working day, for a total of

N per day. Each set of readings provides an estimate for the response of the interferometer at rest during 16 minutes, at a given time of the day, as illustrated in the bottom part of **Figure 3**. The N sets of readings yield a first-order approximation to the response of Miller's interferometer in rest mode during one day.

An interested reader could easily carry out the whole exercise described in this subsection using Miller's original datasheets kept at the CWRU archive ([29], p 308).

3. Our 2002-2005 "Positive" Experiment with a Stationary Interferometer at CIF, Bogota

To begin with, let us state that in contrast to Michelson, Morley, Miller and almost every one else, present writer never mentions the words "ether", "ether wind" or "entrained ether" in the design and analysis of his interferometric data. On the contrary, all translational and rotational motions of earth and interferometer are referred to an inertial or preferred, strictly geometrical, frame Σ ("strictly" geometrical means without material or material-like properties).

Analysis in previous section of Michelson, MM and MMM-experiments suggests that the gathering of data in any interferometric experiment should be modified to insure that, instead of assuming that there is only a fraction of one-fringeshift from one reading to the next, the number of fringeshifts can be actually counted! To achieve this goal a slow rotation of the interferometer is required. The simplest, cheapest and most reliable slow rotation mechanism is the spinning Earth herself, so that we opted for an interferometer at rest relative to the ground floor laboratory at the International Center for Physics (CIF) in the National University Campus in Bogota (Colombia) [10] [15] [17] [18] [19] [20].

3.1. Conceptual Design of the MMMM-Experiment

The slow terrestrial rotation insures that in an interferometer with appropriate arm length the actual number of fringeshifts may be easily counted. The most important theoretical input for designing our experiment was the detailed calculation of expected fringeshifts in a stationary interferometer horizontally placed in a laboratory at a known longitude ϕ and latitude θ on a spinning Earth that tangentially moves in solar orbit at V_O = 29.8 km/s, while Sun moves with unknown velocity V_S relative to preferred frame Σ [14] [15], see **Figure 1**. Light propagates isotropically in Σ with constant speed c.

3.2. Details of the Design during 2002 of the MMMM-Experiment

Two lower rows in central panel of **Figure 2** show that long optical paths are not a necessity in the interferometer, thus avoiding (questionable and troublesome) multiple reflections, as in the 11 meter apparatus used in the 1887 MM-experiment. So, our apparatus had only one reflection at the end of each two-meter

long arm—this is similar to Michelson's 1881 one-meter apparatus. Operational experience gathered by Michelson [2], MM [3], and Miller [13] suggests to avoid metal and wood components. Thus a setup similar to the MM-experiment was selected: a stationary (relative to the laboratory) interferometer was mounted directly upon a thirteen metric ton concrete block supported by a simple pneumatic system to decrease vibrations. Arm A1 was oriented towards local east and orthogonal arm (A2) towards local geographical north (*i.e.*, not towards the magnetic north).

Instead of white light as in MMM-experiment, we used monocromatic coherent laser light. During 2002 we tested two available laser sources (red and green), and selected the green one as the most reliable for our experiment.

The most important and hardest part of our design was to insure that we could actually measure magnitude of the expected fringeshift. As discussed in previous section, all classical experiments failed regarding this aspect.

At the beginning of 2002 we carried out several three-day long sessions, day and night, with a human observer permanently checking the pattern of interference-fringes appearing over a frost-glass screen. To decrease vibrations, this was done from Friday afternoon to Monday morning when the campus of National University is almost empty. The objective was to find the optimum time span between readings. For this the observer recorded the succession of positions and times (in hour, minutes and seconds) at which the observer could discern by the naked eye a motion towards left or right of a selected fringe. The same fringe was followed throughout the whole weekend session. It was found that the interference-pattern was quite stable, and that the eye could only distinguish changes in the position of the reference fringe at the scale of a few minutes, typically five to ten. To be on the safe side we chose to register the whole reference pattern every minute, leading to 1440 frames over a 24-hr rotation of the interferometer.

During 2002 Professor Manuel G. Forero and his Owaha group (Department of Systems Engineering, National University of Colombia) developed software to automatically store at every minute the image appearing in the video camera, and to convert the image into digital colour-level profiles, that were smoothed using Fourier transforms with a low pass filter.

3.3. Our High Orientational Resolution versus the Low Resolution in All MM-Type Experiments

Let us stress the most significant difference between our MMMM-experiment and all classical MM-type experiments: our high orientational resolution in the process of data gathering. Let us explain. Both in MM and in all Miller's experiments, data was collected when one of the arms was oriented to one of sixteen local directions: north, northeast, east, etc. That is, there was an angular distance of 22.5˚ between two consecutive readings. From the central panel in **Figure 2** it is evident that the expected fringeshift would be small (*i.e.*, less than one fringe-width) if the the speed of solar motion were slow, but the fringeshift would be

large (*i.e.*, more than one fringe-width) if solar speed were around 200 km/s. Since current estimates of solar speed [5] [23] [24] [25] [26] are larger than 200 km/s the expected fringeshifts are certainly larger than one fringe-width when measurements are made every 22.5˚. Thus, the design of the MM-experiment was faulty from this contemporary view-point. Note that an angular step of 22.5˚ in a rotating interferometer is the same as taking a reading every 90 minutes in an interferometer at rest, as in our MMMM-experiment.

Instead, we used a video camera at rest in the laboratory to record every minute a photograph of the interference pattern. Thus our angular resolution is ninety times better than the 22.5˚ in MM [3], Miller [13] experiments, and in all classical MM-type experiments [9].

In other words, in a single 360˚ turn of our stationary interferometer lasting 24 hours we obtained 1440 readings (many more than in the whole 1887 MM-experiment). To attain the same angular resolution in any experiment using a rotating interferometer, measurements have to be made every 0.25˚ (=360˚/1440).

Our high angular resolution allowed us to follow the position of the very same fringe throughout the duration of a session, which sometimes lasted several weeks.

3.4. Results of Our 2003-2005 MMMM-Experiment

The MMMM-experiment itself ran over more than two years from January 2003 to February 2005, plus June 2005. Typically, there were several sessions each month, with the exception of May and June 2004 (when the video camera was stolen). Collected data [15] [17] [18] [19] [20] support our theoretical predictions. The raw data are stored in more than 300 flexible disks, which are available for any interested person to copy.

As usual in second-order experiments ([13], p 231, column 1), two velocities of sun relative to a preferred frame Σ were obtained from our data: 1) CIF-N in the northern galactic hemisphere: speed 365 km/s, $\alpha = 81^\circ$, $\delta = 79^\circ$ [19]. And, 2) CIF-S in the southern galactic hemisphere: speed 500 km/s, $\alpha = 250^\circ$, $\delta = -75^\circ$ [18]. Magnitude of our solar speeds is larger than Miller's, but it is in the same range of solar speeds reported in astronomy and astrophysics [5] [23] [24] [25] [26], although direction is not necessarily the same [32].

3.5. Compatibility of CIF-S Solar Velocity and the 2002 Experiment at Stanford University

With the objective of confirming once again the conventional "negative" interpretation of the MM-experiment, in 2002 a hightech experiment was carried out at Stanford University with a duration of several months [21]. Variations in the difference of frequency in two microwave cavities oriented along the local East-West and along the vertical direction were obtained at different times of day. Temperature of the cavities was controlled to an extremely high accuracy, within ±5 micro Kelvin. The experimenters observed unexpected periodical variations

in the frequencies. The authors tried to find physical or astronomical explanations for such periodicity. Since no reasonable explanation was found, the observed periodical variations were dismissed as unexplained "*mechanical disturbances*", and were subtracted from the signal. The resulting white noise was interpreted as a new and more accurate confirmation of the conventional "null" interpretation of MM-type experiments.

In some senses, the Stanford setup is similar to a vertical interferometer with one arm parallel to the floor of the laboratory and the other arm perpendicular to the floor. The periodical structure of the unexplained "*mechanical disturbances*" is amazingly similar to the structure of the "positive" results obtained in our MMMM-experiment. This means that the raw data underlying Stanford's "*mechanical disturbances*" may have the same structure as the raw data underlying our MMMM-experiment at Bogota.

As a preliminary quantitative test we reported at PIRT-2017 [20] the correlation between the magnitude and direction of the "*mechanical disturbances*" observed in Palo Alto (California) on May 30/2002 and the magnitude and direction of terrestrial velocity on the floor of a laboratory located in Palo Alto the same day. Earth's motion was calculated with the solar velocity CIF-S reported in previous subsection. The unpublished graphs are included here as top row in Figure 4. Both correlations are extremely high: 0.998 for Earth's speed, and 0.991

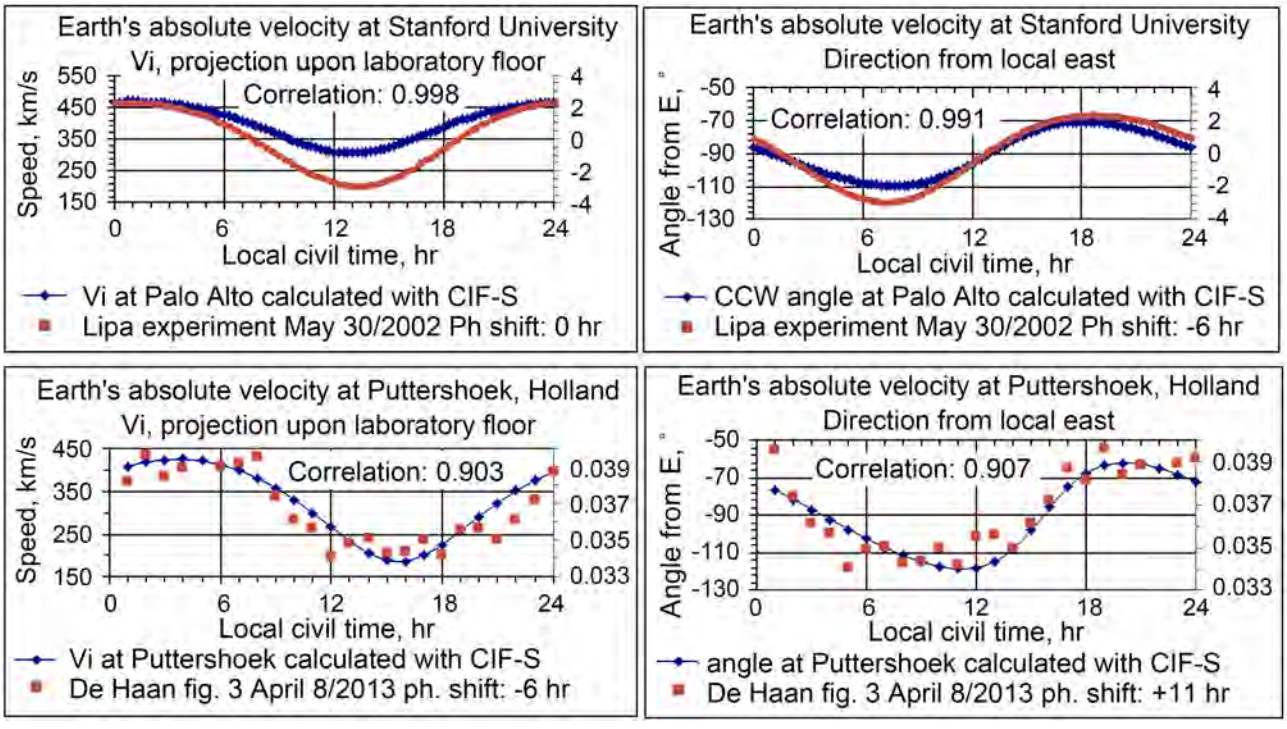

Figure 4. Modern interferometer-like experiments compared to absolute velocity of earth's center of mass calculated with our CIF-S absolute solar velocity. Top row: amplitude of unexplained "mechanical distrurbances" observed in 2002 at Stanford University [21] versus magnitude (correlation = 0.998) and direction (correlation = 0.991) of V_I (=projection of V_{CM} upon the floor of the laboratory). Bottom row: amplitude of signal observed in 2013 in Victor de Haan's Fabry-Perot cavity [22] versus magnitude (correlation = 0.903) and direction (correlation = 0.907) of V_I.

for direction of terrestrial velocity. The authors of the Stanford experiment may easily calculate correlations for other dates. Present writer is available for joint work.

3.6. Compatibility with 2012-2014 Experiments by Victor de Haan in the Netherlands

In his laboratory at Puttershoek, The Netherlands, in April 2012 Victor de Haan compared the phase of a standing wave to the phase difference in a Mach-Zehnder interferometer. Similar experiments were carried out from April/2013 to September/2014 involving Fabry-Perot cavities. De Haan found well-defined periodic responses in amplitude, and less-defined periodicities in azimuth [22]. Bottom row in **Figure 4** compares de Haan's amplitudes for April 8/2013 to magnitude (correlation 0.903) and direction (correlation 0.907) of terrestrial absolute velocity (calculated with CIF-S) projected onto the floor of the laboratory at Puttershoek. Similar correlations appear if terrestrial velocity is calculated with CIF-N. However, correlations with de Haan's azimuth are poor.

4. Closing Remarks: MM-Type Experiments Are Not Crucial

From our MMMM-experiment we obtained by optical means, for the first time ever in a closed laboratory, quantitative estimates for the value of solar velocity relative to a preferred frame. This success contradicts Poincaré's principle stating the impossibility of measuring absolute motion in a closed laboratory. We succeeded, without additional ad hoc assumptions, where Michelson, Morley, Miller and many others failed: we witnessed the slow drift of the reference fringe during the slow terrestrial rotation of our interferometer, and counted the net number of fringe-widths as the reference fringe drifted back and forth.

Given the "positive" results of the MMMM-experiment [15] [17] [18] [19] [20], this writer considers that the notion of a preferred frame of reference Σ should be re-instated [32]. This notion is equivalent to Newton's absolute space, operationally identified by him as a frame at rest relative to the fixed stars. Of course, existence of Σ is compatible with the currently accepted anisotropy of the CMB radiation as observed from the moving Earth.

By the same token, all "negative" experiments, say the Stanford experiment [21], claim that they obtained confirmation of Lorentz-invariance to a high accuracy. The foundational basis of the theory for such experiments was only recently completed by Sfarti who analysed the effect of rotation of earth upon an interferometer on its surface in tangential motion relative to an inertial frame: "*We present the derivation of the Sagnac, Michelson-Morley, Kennedy-Thorndike and the Hammar experiments as viewed from the Earth-bound uniformly rotating frame, that is, the frame of the laboratory where the experiment is taking place. To our best knowledge such an attempt has never been made before, possibly due to its mathematical difficulty, so no precedents exist, this is a first*", underlinings added ([30], p 1). By the way, twenty years ago present writer pub-

lished a similar analysis in a pre-relativistic context [14]—work inspired by Miller [13] and Nassau and Morse [16].

So, proponents of "positive" experiments claim that observation supports their hypothesis that solar velocity can be measured with an interferometer. Likewise, supporters of "negative" experiments claim that similar observations support their hypotesis of Lorentz-contraction. Can these two (apparently) contradictory statements be both true?

Our answer is positive. Furthermore, the reason is simple, and is implicit in the distinction made in Section 1 between "positive" and "negative" experiments. In both cases the object under observation is the same: an interference pattern. However, the "thing" being observed is (in general) different. "Positive" experiments focus on the complete fringeshift of a reference fringe, while "negative" experiments only focus on the fractional component of the said fringeshift. In the case of very small interferometers there is no difference between the two cases.

However, in all cases the end products from "positive" and "negative" experiments are different: a value for solar velocity in "positive" experiments, and a support for Lorentz-contraction in "negative" experiments.

From a pragmatical view point: that's it. Both experiments are correct within their bounds. Correlations in **Figure 4** are to be expected because the physical object (*i.e.*, the interference pattern) being observed in both cases is the same. The difference is in the data recording and reduction.

The difficulty arises when interpetations outside the scope of the tested hypothesis are offered. For instance, the "negative" experiment was not designed to test the hypothesis that "absolute motion does not exist", or to test the hypothesis that "a preferred frame does not exist".

In plain words, we may say that "positive" and "negative" experiments cannot distinguish between pre-relativistic and relativistic theories. This runs contrary to many beliefs! In some sense, we have wasted our time for more than a century...Just sterile discussion! A dialogue between deaf people!

Nonetheless, there are deeper, and related among them, questions that were not addressed, let alone tested, in the "positive" and "negative" experiments: what is the nature of light? How does light propagate? How is light connected to electromagnetic force? What is the origin of electromagnetic force? What is the origin of other fundamental forces? How do fundamental forces propagate?

Ether may be a possible common component in the answer to all previous questions. Such a subject is beyond the scope of present paper, and it is not further considered here. However, let us mention that if ether exists, it has to exist somewhere, for instance it may populate the geometrical space called "preferred frame".

Beyond the "positive" and "negative" experiments, there are arguments of a different class that calls for the existence of a preferred frame. Two conservation

principles of classical physics (energy and linear momentum) implicitly require a preferred frame to define the meaning of the speed that is conserved. Let me ask, if there is no preferred frame, what is the value of the speed that is conserved when Einstein and a Maxwell demon are together in a vehicle comoving with a light ray?

To end, let us mention that present writer has also worked during the last thirty years on a unified theory of nature that may fulfill Einstein's dream, see [33] and references therein. In that context there are Q-solutions to the classical wave equation that are isomorph under all relativistic transformations (Lorentz, Poincaré, Einstein) and under the pre-relativistic Doppler-Voigt [34] transformation. They constitute the new group of D'Alembertian isomorph transformations [33] and page 111 in [35]. In that context the apparently contradictory outcomes of both the "positive" and "negative" experiments are to be expected. Thus, the paradoxical results discussed here constitute observational evidence supporting the existence of the theoretically predicted Q-functions. After all, our MMMM-experiment was not a waste of time! This subject is developed elsewhere.

Conflicts of Interest

The author declares no conflicts of interest regarding the publication of this paper.

References

[1] Prilepskikh, N.N. (2021) Michelson's Experiment, Dopler's Effect and Cosmic Microwave Background in One Context. https://www.researchgate.net/publication/357117965_MICHELSON'S_EXPERIMENT_DOPLER'S_EFFECT_AND_COSMIC_MICROWAVE_BACKGROUND_IN_ONE_CONTEXT

[2] Michelson, A.A. (1881) *American Journal of Science (Third Series)*, **22**, 120-129. https://doi.org/10.2475/ajs.s3-22.128.120

[3] Michelson, A.A. and Morley, E.W. (1887) *American Journal of Science* (*Third Series*), **34**, 333-345. https://doi.org/10.2475/ajs.s3-34.203.333

[4] Penzias, A.A. and Wilson, R.W. (1965) *Astrophysical Journal*, **142**, 419. https://doi.org/10.1086/148307

[5] Planck Collaboration (2013) *Astronomy and Astrophysics A*, **27**, 571. https://doi.org/10.1119/1.2342876

[6] Consoli, M. and Pluchino, A. (2021) *Universe*, **7**, 311. https://doi.org/10.3390/universe7080311

[7] Nolte, D.D. (2020) *Physics Today*, **73**, 30-35. https://doi.org/10.1063/PT.3.4429

[8] Munera, H.A. (2020) *Apeiron*, **20**, 1-45.

[9] Munera, H.A. (1998) *Apeiron*, **5**, 371-376.

[10] Munera, H.A., Alfonso, J.E. and Arenas, G. (2002) *Journal of New Energy*, **6**, 185-211.

[11] Munera, H.A. (2006) The Evidence for Length Contraction at the Turn of the 20th Century: Non-Existent. In: Dvoeglazov, V.V., Ed., *Einstein and Poincaré: The Physi-*

cal Vacuum, Apeiron Press, Montreal, 87-102.

[12] Munera, H.A. (2005) The Missing Statistical Analysis in the Original 1887 Michelson-Morley Experiment. *ICPE*2005 *International Conference on Physics Education*: *World View on Physics Education* 2005: *Focusing on Change*, New Delhi, 21-26 August 2005, 20.

[13] Miller, D.C. (1933) *Reviews of Modern Physics*, **5**, 203-242. https://doi.org/10.1103/RevModPhys.5.203

[14] Munera, H.A. (2002) *Annales de la Fondation Louis de Broglie*, **27**, 463-484.

[15] Munera, H.A., Hernández-Deckers, D., Arenas, G. and Alfonso, E. (2006) *Electromagnetic Phenomena* (*Kharkov*, *Ukraine*), **6**, 70-92.

[16] Nassau, J.J. and Morse, P.M. (1927) *Astrophysical Journal*, **65**, 73-85. https://doi.org/10.1086/143026

[17] Munera, H.A., Alfonso, J.E. and Arenas, G. (2003) *Journal of New Energy*, **7**, 101-105.

[18] Munera, H.A., Hernández-Deckers, D., Arenas, G. and Alfonso, E. (2007) *Proceedings of SPIE*, **6664**, 66640K.

[19] Munera, H.A., Hernández-Deckers, D., Arenas, G., Alfonso, E. and López, I. (2009) Observation of a Non-Conventional Influence of Earth's Motion on the Velocity of Photons, and Calculation of the Velocity of Our Galaxy. *Proceedings of Progress in Electromagnetics Research Symposium*, *PIERS* 2009, Beijing, 23-27 March 2009, 113-119. https://www.piers.org

[20] Munera, H.A. (2017) Absolute Velocity of Earth from Our Stationary Michelson-Morley-Miller Experiment at CIF, Bogota, Colombia. *Abstracts—International Scientific Conference Physical Interpretations of Relativity Theory PIRT* 2017, Moscow, 3-6 July 2017, 109-110. (In Russian)

[21] Lipa, J.A., Nissen, J.A., Wang, S., Stricker, D.A. and Avaloff, D. (2003) *Physical Review Letters*, **90**, Article ID: 060403. https://doi.org/10.1103/PhysRevLett.90.060403

[22] De Haan, V.O. (2015) Experiments to Test Special Relativity. *Proceedings of International Scientific Meeting PIRT*, Moscow, 29 June-2 July 2015, 131-139. (In Russian)

[23] Smoot, G.F., Gorenstein, M.V. and Miller, R.A. (1977) *Physical Review Letters*, **39**, 898-901. https://doi.org/10.1103/PhysRevLett.39.898

[24] Courvoisier, L. (1953) *Experientia*, **9**, 317-356. https://doi.org/10.1007/BF02155829

[25] De Vaucouleurs, G. and Peters, W.L. (1968) *Nature*, **220**, 868-874. https://doi.org/10.1038/220868a0

[26] Conklin, E.K. (1969) *Nature*, **222**, 971-972. https://doi.org/10.1038/222971a0

[27] Morley, E.W. and Miller, D.C. (1905) *Philosophical Magazine* (*Series* 6), **9**, 680-685. https://doi.org/10.1080/14786440509463317

[28] Miller, D.C. (1928) *Astrophysical Journal*, **68**, 352-367. https://doi.org/10.1126/science.68.1763.352

[29] De Meo, J. (2011) Dayton C. Miller Revisited. In: Munera, H.A., Ed., *Should the Laws of Gravitation Be Reconsidered?—The Scientific Legacy of Maurice Allais*, C. Roy Keys Inc., Montreal, 285-315.

[30] Sfarti, A. (2019) *HSOA Journal of Light & Laser*: *Current Trends*, **2**, 4.

[31] Lodge, O. (1926) *Nature*, **117**, 854. https://doi.org/10.1038/117854a0

[32] Munera, H.A. (2009) *ICFAI University Journal of Physics*, **2**, 9-24.

[33] Munera, H.A. (2022) *Journal of Physics*: *Conference Series*, **2197**, Article ID: 012021.

https://doi.org/10.1088/1742-6596/2197/1/012021

[34] Voigt, W. (1887) *Nachrichten von der Königlichen Gesellschaft der Wissenschaften und der Georg-Augusts Universität zu Göttingen*, **2**, 41-51.

[35] Munera, H.A. (2017) *Journal of Physics*: *Conference Series*, **1051**, Article ID: 012024. https://doi.org/10.1088/1742-6596/1051/1/012024

Journal of Modern Physics, 2022, 13, 761-767
https://www.scirp.org/journal/jmp
ISSN Online: 2153-120X
ISSN Print: 2153-1196

Probing Nuclei with High-Energy Hadronic Probes at Inverse Kinematics

Julian Kahlbow[1,2], Maria Patsyuk[3], Vasilisa Lenivenko[3], Efrain P. Segarra[1], Göran Johansson[2], Dmitriy I. Klimanskiy[3], Anna Maksymchuk[3]

[1]Massachusetts Institute of Technology, Cambridge, USA
[2]School of Physics and Astronomy, Tel Aviv University, Tel Aviv, Israel
[3]Joint Institute for Nuclear Research, Dubna, Russia
Email: jkahlbow@mit.edu

How to cite this paper: Kahlbow, J., Patsyuk, M., Lenivenko, V., Segarra, E.P., Johansson, G., Klimanskiy, D.I. and Maksymchuk, A. (2022) Probing Nuclei with High-Energy Hadronic Probes at Inverse Kinematics. *Journal of Modern Physics*, **13**, 761-767.
https://doi.org/10.4236/jmp.2022.135044

Received: February 27, 2022
Accepted: May 28, 2022
Published: May 31, 2022

Abstract

Proton knockout reactions are a widely used tool to study nuclear ground-state distributions. While the interpretation of traditional experiments in direct kinematics has to account for initial and final state interactions, experiments in inverse kinematics can overcome such limitations. We discuss results of an experiment at the BM@N setup at JINR using a ^{12}C beam at 48 GeV/c to study quasi-elastic scattering reactions, single proton distributions, and short-range correlated nucleon-nucleon pairs. The inverse kinematics allows for the direct measurement of the nucleon-nucleon pair center-of-mass motion and provides first experimental evidence for scale separation of such pairs. Based on these results, we will in the future study neutron-rich nuclei in inverse kinematics in the context of short-range correlations and neutron stars.

Keywords

Nuclear Ground-State Distributions, High-Energy Hadronic Scattering, Inverse Kinematics, Short-Range Correlations, Neutron-Rich Nuclei, Neutron stars

1. Introduction

From superconductors to atomic nuclei, strongly-interacting many-body systems are ubiquitous in nature. Understanding the emergent macroscopic properties of such systems in terms of the underlying microscopic particle correlations is an outstanding challenge with wide ranging implications. In the case of nuclear systems, significant experimental and theoretical efforts are being devoted towards understanding the dynamics of protons and neutrons in both stable and radioac-

tive nuclei, and its implications for the dynamics of dense matter in neutron stars, and astrophysical nucleosynthesis processes.

Measurements of high-energy scattering reactions are a time-honored method to study nucleons in nuclei. In such cases high-energy projectiles are shot at a stationary nucleus, the scattered projectile and knocked-out nucleons are detected, and the initial momentum of the struck nucleon in the nucleus is reconstructed. While such measurements are fundamental for mapping the structure of atomic nuclei, their interpretation is often complicated by Initial-State Interactions/Final-State Interactions (ISI/FSI) of the incoming and scattered particles. Such interactions reduce the scattered particle flux (attenuation) and distort their kinematics, complicating the relation between the measured reaction cross-sections and the inferred ground-state nuclear momentum distribution.

2. Experiment

Here we report on a recent study by the Baryonic Matter at Nuclotron (BM@N) collaboration at the Joint Institute for Nuclear Research (JINR) that overcame this fundamental limitation and extracted the distributions of nucleons and correlated nucleon pairs in nuclei. The experiment measured high-energy inverse-kinematics scattering, where a relativistic ion beam was scattered from a stationary proton target, see Figure 1. Large-angle quasi-elastic proton-proton scattering was measured in coincidence with a bound residual nuclear fragment. The detection of the residual nucleus was shown to choose the transparent part of the reaction, excluding the otherwise large kinematic distortions due to ISI/FSI that would also break the fragment apart.

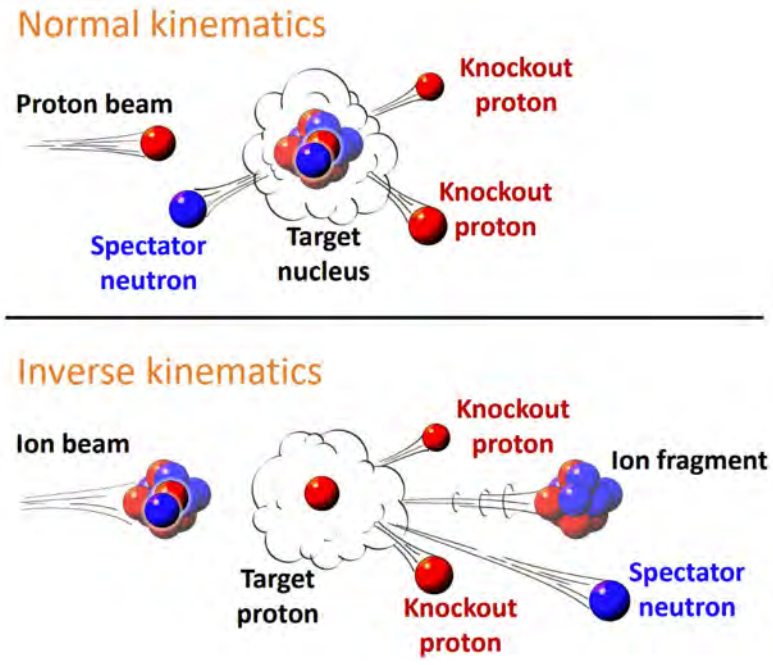

Figure 1. Study of SRC pair in nuclei by normal (above the line) and inverse (below the line) kinematics reactions. In this picture protons are shown in red, neutrons in blue.

While much more complex than traditional "normal-kinematics" measurements, such "inverse-kinematics" measurements also allow us to study radioactive nuclei with large neutron excess that are too short-lived to be used as a fixed target in the laboratory, cf. Figure 1. Understanding the structure and properties of radioactive nuclei is fundamental for our understanding of nucleosynthesis processes in astrophysics.

The experiment took place at the JINR using a 48 GeV/c ^{12}C ion beam from the Nuclotron accelerator, a stationary liquid hydrogen target, and a modified BM@N experimental setup as shown in Figure 2. A two-arm spectrometer was placed downstream of the target to detect the two protons from the quasi-elastic (QE) (p,2p) scattering at ~90˚ in the pp center-of-mass (c.m.). The residual nuclear fragments (^{11}B, ^{10}B, or ^{10}Be) were identified in coincidence, and their momenta were determined, based on their energy deposition in two thin scintillators and their measured trajectories as they passed through a large-acceptance dipole magnet. The data was first published in [1], here we wish to show the results in the context of previous data obtained by different measurement methods.

3. Results and Discussion

The suppression of ISI/FSI was demonstrated by comparing the reconstructed knocked-out proton initial momentum distribution for QE ^{12}C(p,2p) events with and without the coincidence detection of a bound ^{11}B fragment. The results are shown in Figure 3 (adapted from [1]) compared with Plane-Wave Impulse Approximation (PWIA) calculations for knockout of p-shell protons from the ^{12}C that assumes no distortion due to ISI/FSI. As can be seen, the ^{11}B fragment detection significantly suppresses ISI/FSI effects, especially above the nuclear Fermi momentum (k_F ~ 250 MeV/c), where the kinematical distortion of the scattered nucleons due to secondary processes becomes significant.

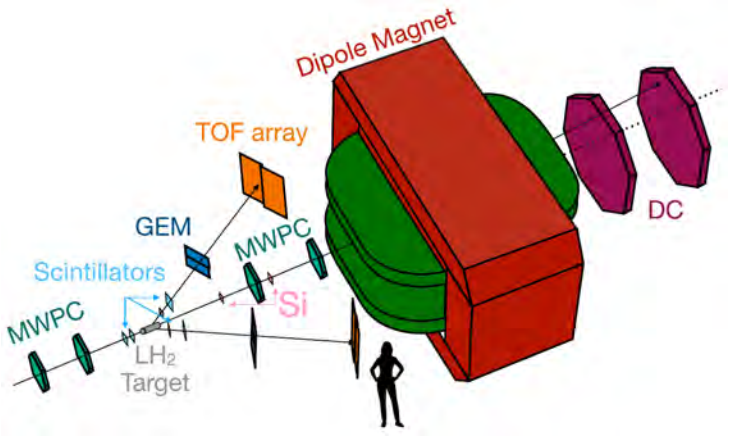

Figure 2. Illustration of the SRC@BMN experimental setup at the JINR in Dubna, Russia. A 48 GeV/c ^{12}C beam is incident from the left on a liquid hydrogen target. The (p,2p) reaction is measured using a non-magnetic time-of-flight spectrometer. The residual nuclear fragment is measured using a magnetic spectrometer downstream the target.

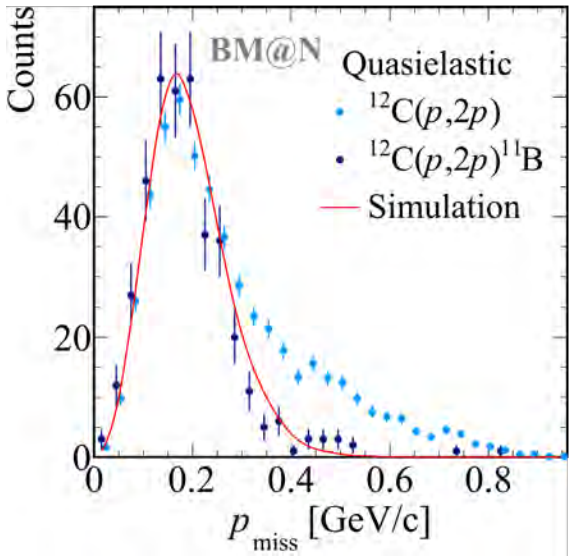

Figure 3. Measured missing-momentum distribution in the ^{12}C rest-frame for the quasi-elastic inclusive $^{12}C(p,2p)$ and exclusive $^{12}C(p,2p)^{11}B$ reactions. The data are compared with a PWIA-based simulation of proton knockout from the ^{12}C p-shell. The ^{11}B tagging clearly suppresses ISI/FSI distortions at high momenta. Figure adapted from [1].

Next we studied short-range correlated (SRC) nucleon pairs by measuring two-nucleon knockout $^{12}C(p,2p^{10}B)n$ and $^{12}C(p,2p^{10}Be)p$ reactions. SRCs are fluctuations of strongly interacting nucleon pairs at short distances [2] [3] [4]. Their formation and properties are sensitive to the many-body dynamics of nuclear systems, properties of the short-distance nucleon-nucleon interaction, nucleon structure, and properties of cold dense nuclear matter such as in the outer core of neutron stars [5] [6].

In SRC breakup reactions, ^{10}B and ^{10}Be nuclei are produced when a proton-neutron (pn) or proton-proton (pp) pair in the projectile interacts with a proton in the target. We measured 23 $^{12}C(p,2p^{10}B)n$ and two $^{12}C(p,2p^{10}Be)p$ events. The other isospin-symmetric nn pairs are not accessible here because neutron knockout was not measured. The large ^{10}B to ^{10}Be event-yield ratio is consistent with the previously observed dominance of pn- over pp-SRC pairs [7] [8] [9], and fully agrees with predictions based on ab-initio many-body calculations. Contributions from inelastic reactions and from reactions due to mean-field QE scattering followed by FSI are negligible.

Beyond the suppression of ISI/FSI, the fragment momentum distribution is equal to the SRC pair c.m. momentum distribution. This distribution is consistent with that of a Gaussian.

In **Figure 4** we compare the Gaussian width measured directly by BM@N with previous indirect extractions from electron scattering measurements at the Thomas Jefferson National Accelerator Facility (JLab) done in "normal kinematics" and with several theoretical predictions [10]. All measurements agree with each other and with the theoretical calculations, showcasing the probe-independence of SRC measurements and the success of its theoretical description.

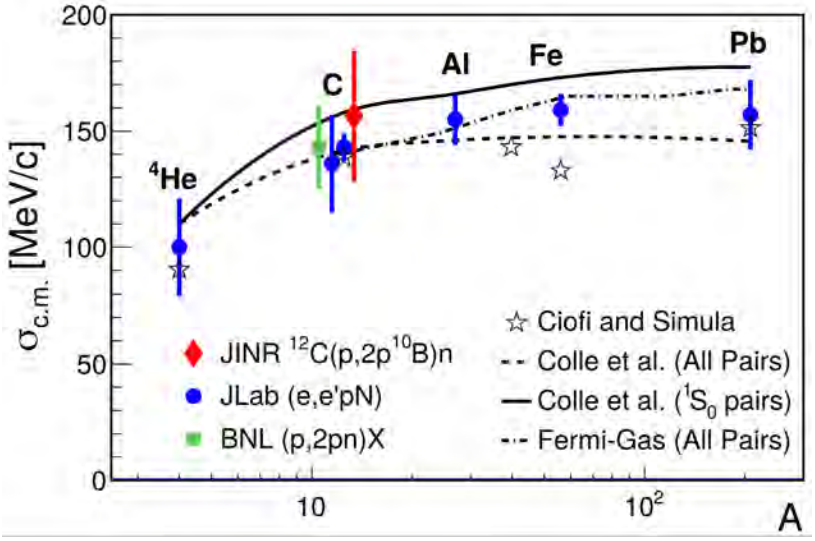

Figure 4. The width of the SRC pair c.m. momentum distributions extracted from the direct fragment detection in inverse kinematics and from normal-kinematics electron and proton scattering measurements, cf. [10].

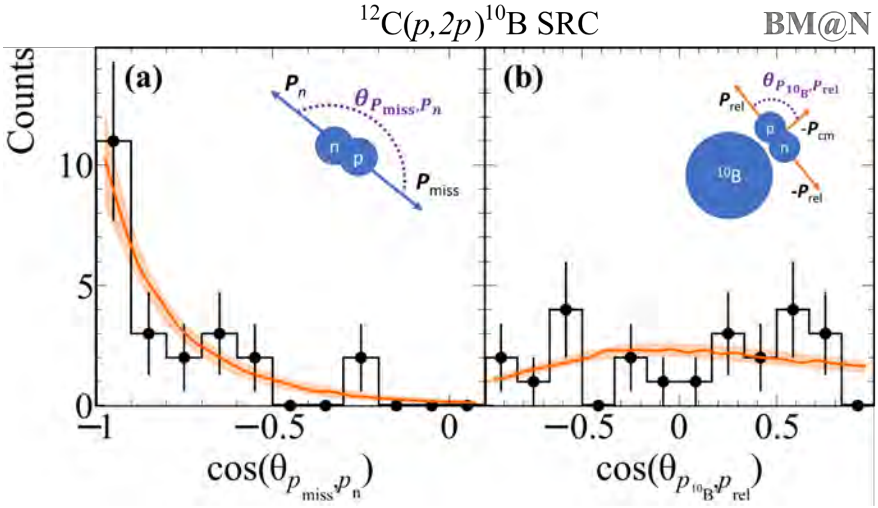

Figure 5. Angular correlation between the two nucleons in the SRC pair (a) and between the SRC pair c.m. and relative momenta (b). Data are compared with theoretical calculations using the nuclear Generalized Contact Formalism (GCF), assuming full factorization of SRC wave function from the residual nuclear system. Figure adapted from [1].

Lastly, detecting the residual nucleus allows, also for the first time, measuring the interaction between the SRC pair and the residual nuclear system. From a theoretical standpoint, the strong two-body interaction between the nucleons in SRC pairs is expected to be significantly stronger than the average mean-field nuclear interaction [11] [12]. Therefore, the pair interaction should be scale separated from that of the residual nuclear system, allowing us to model the distributions of SRC pairs by independent functions of the pair c.m. and relative momenta that do not depend on the angle between the two.

This is shown in **Figure 5** (adapted from [1]). A clear back-to-back correla-

tion between the momenta of the nucleons in the SRC pair is observed, as expected for strongly-correlated nucleons. The width of the distribution is driven by the pair c.m. motion and agrees with the Generalized Contact Formalism (GCF) simulation [11] [12]. In contrast, no correlation is observed between the angles of SRC c.m. momentum (*i.e.* ^{10}B) and the relative momentum between the nucleons in the pair, providing the first direct experimental evidence for the factorization of SRC pairs from the many-body nuclear medium.

4. Summary

To conclude, we demonstrated the feasibility of directly accessing properties of single nucleons and SRC nucleon pairs in nuclei using a 48 GeV/c ion beam from the JINR Nuclotron accelerator and a stationary liquid hydrogen target to measure high-energy inverse kinematics scattering. We identified SRC pairs and performed the first direct measurement of their c.m. momentum distribution. We used this to experimentally verify the SRC factorization assumption which leads to a universal description of the high-momentum tail in all nuclei. This measurement opens the way for SRC studies in radioactive nuclei at the forthcoming FAIR and FRIB facilities, focusing on the dynamics of high-density nucleon-pair fluctuations in very neutron-rich systems. These studies will be pivotal for developing a microscopic understanding of the structure and properties of nuclei far from stability and the formation of visible matter in the universe.

5. Outreach

The study of the structure of radioactive nuclei and its relation to nucleon correlations is a growing frontier of nuclear physics, motivated by the importance of neutron-rich nuclei for modeling astrophysical processes. Measurements have shown that nuclear shell occupations (magic numbers) evolve with nuclear asymmetry where for neutron-rich nuclei "known" shells disappear and new shells appear. This evolution of shells has dramatic astrophysical implications as "magic number nuclei" serve as a waiting point for element formation in the r-process. Extending the study to radioactive nuclei using the new experimental approach reported here, based on measurements of hard nucleon-knockout reactions in inverse kinematics, is paramount for a ground-breaking experimental and theoretical program to understand very asymmetric cold dense nuclear systems from unstable nuclei to neutron stars.

From an ab-initio theory perspective, understanding the manner by which two-body correlations impact the emergence of collective phenomena such as shell closure in neutron-rich nuclei is a significant challenge, undertaken by nuclear EFT calculations using many-body numerical techniques such as lattice, coupled-cluster, and Quantum Monte-Carlo calculations. Measuring the ground-state distributions of particles and particle-pairs in such exotic systems is crucial to improving our understanding of such correlation effects in other strongly interacting many-body systems.

Acknowledgements

We acknowledge the efforts of the BM@N Collaboration, staff of the Nuclotron-NICA Accelerator Division, and Veksler and Baldin High Energy Physics Laboratory at JINR that made this experiment possible. The research was supported by the Israel Science Foundation, the Pazy Foundation, and the BMBF via project no. 05P15RDFN1, through the GSI/TU Darmstadt cooperation agreement, by the US DoE under grant no. DE-FG02-08ER41533 and by the Deutsche Forschungsgemeinschaft (DFG, German Research Foundation), project ID 279384907, SFB 1245, and the RFBR under grant numbers 18-02-40046 and 18-02-40084/19.

Conflicts of Interest

The authors declare no conflicts of interest regarding the publication of this paper.

References

[1] Patsyuk, M., Kahlbow, J., Laskaris, G., Duer, M., Lenivenko, V., Segarra, E.P., Atovullaev, T., Johansson, G., Aumann, T., Corsi, A., Hen, O., Kapishin, M., Panin, V., Piasetzky, E. and the BM@N Collaboration (2021) *Nature Physics*, **17**, 693-699. https://doi.org/10.1038/s41567-021-01193-4

[2] Subedi, R., *et al.* (2008) *Science*, **320**, 1476-1478. https://doi.org/10.1126/science.1156675

[3] Hen, O., Miller, G.A., Piasetzky, E. and Weinstein, L.B. (2017) *Reviews of Modern Physics*, **89**, 045002. https://doi.org/10.1103/RevModPhys.89.045002

[4] Tang, A., *et al.* (2003) *Physical Review Letters*, **90**, 042301. https://doi.org/10.1103/PhysRevLett.90.042301

[5] Frankfurt, L., Sargsian, M., Strikman, M. (2008) *International Journal of Modern Physics A*, **23**, 2991-3055. https://doi.org/10.1142/S0217751X08041207

[6] Schmidt, A., *et al.* (2020) *Nature*, **578**, 540-544. https://doi.org/10.1038/s41586-020-2021-6

[7] Piasetzky, E., Sargsian, M., Frankfurt, L., Strikman, M. and Watson, J.W. (2006) *Physical Review Letters*, **97**, 162504. https://doi.org/10.1103/PhysRevLett.97.162504

[8] Duer, M., *et al.*(2018) *Nature*, **560**, 617-621. https://doi.org/10.1038/s41586-018-0400-z

[9] Hen, O., *et al.* (2014) *Science*, **346**, 614-617. https://doi.org/10.1126/science.1256785

[10] Cohen, E.O., Hen, O., Piasetzky, E., Weinstein, L.B., Duer, M., Schmidt, A., Korover, I., Hakobyan, H. and the CLAS Collaboration (2018) *Physical Review Letters*, **121**, 092501. https://doi.org/10.1103/PhysRevLett.121.092501

[11] Weiss, R., Bazak, B. and Barnea, N. (2015) *Physical Review C*, **92**, 054311. https://doi.org/10.1103/PhysRevC.92.054311

[12] Cruz-Torres, R., Lonardoni, D., Weiss, R., *et al.* (2021) *Nature Physics*, **17**, 306-310. https://doi.org/10.1038/s41567-020-01053-7

Journal of Modern Physics, 2022, 13, 768-775
https://www.scirp.org/journal/jmp
ISSN Online: 2153-120X
ISSN Print: 2153-1196

Anderson Localization Light Guiding in a Two-Phase Glass

Nicholas F. Borrelli, Thomas P. Seward, Karl W. Koch, Lisa A. Lamberson

Corning Inc. Sullivan Park Research Laboratory, New York, USA
Email: Borrellinf@Corning.com, Sewardtp@gmail.com, Kochkw@Corning.com, Lambersola@corning.com

How to cite this paper: Borrelli, N.F., Seward, T.P., Koch, K.W. and Lamberson, L.A. (2022) Anderson Localization Light Guiding in a Two-Phase Glass. *Journal of Modern Physics*, **13**, 768-775.
https://doi.org/10.4236/jmp.2022.135045

Received: February 25, 2022
Accepted: May 28, 2022
Published: May 31, 2022

Abstract

Anderson localization has been realized in several different systems over the years. In this paper we describe a rather unique manifestation of the phenomenon occurring in a two-phase glass composition that guides light. The glasses are a borate or alkali borosilicate composition that when heated separates into two distinct phases of different compositions, a high index phase and a low index phase. When the glass is heated with a specific thermal schedule to develop the phase separation it is then drawn into a rod or fiber, the particulate phase forms elongated strands resulting in a random cross-sectional refractive index pattern. This pattern of refractive index is maintained along the length producing a light guiding behavior over a significant distance that we propose is a manifestation of an Anderson localization phenomenon.

Keywords

Anderson Localization, Imagining Optical Fiber, Phase Separated Glass

1. Introduction

The following paper is an attempt to connect what, at first glance, appears to be an unrelated phenomenon in glass to an example of Anderson localization using the common themes involving waves and disorder. This common behavior of localization in all cases results from wave interference. The unique insight of Anderson [1] was utilizing the Schrodinger equation to treat the diffusion of defects in crystals. What was the natural approach for treating the behavior of photons and phonons was now used for electrons to explain how localized states could occur as a consequence of structural disorder. The physical description of disorder is different for electrons with dopants in an otherwise perfect lattice than for photons where the disorder would correspond to fluctuations of the refractive index; for acoustic phonons it would be regions of different velocities of

sound. (Equation (3)) Clearly, the specific wave equations governing the different wave phenomena are not the same as well as the resulting incorporation of the disorder. For these two examples the disorder is incorporated from the refractive index and the sound velocity, respectively. For the electron case the Hamiltonian is altered either by letting the defect have a broad distribution of energies or letting the potential function $V(r)$ vary spatially. As we will see in the case of electrons for the Anderson treatment to be operative requires that there is ignorable interaction between sites so that the wavefunction of the defect can be uniquely defined. For photons and phonons this is always the case. A simple statement can be made; Waves + Disorder = Localization.

Localized states for photons become localized propagating modes. It appears that one could have arrived at this directly from Maxwell's equations because interference phenomena is inherent in light propagation in a medium with a spatially varying refractive index as we will see below, but here we interpret as an example of Anderson localization.

$$\nabla\times\nabla\times E+\frac{\varepsilon}{c^2}\frac{\partial^2 E}{\partial t^2}=\frac{4\pi}{c^2}\frac{\partial^2 P^{NL}}{\partial t^2} \tag{1}$$

For the 2-D case one can write the nonlinear wave equation (Equation (1)) with an intensity dependent refractive index but now one replaces this term with a static spatial refractive index variation shown here in Equation (2).

$$\frac{i\partial E}{\partial z}=\left(\frac{1}{2k}\right)\nabla_T^2 E+\left(\frac{\int_2}{n_0^2}\right)k\left|E^2\right|E=0 \tag{2}$$

$$\frac{i\partial A}{\partial z}+\left(\frac{1}{2k}\right)\nabla_T^2 A+\left(\frac{k}{n_0}\right)\Delta n(x,y)A=0 \tag{3}$$

Equation (3) appears similar to the Schrodinger equation [2] [3] shown below in Equation (4); where the disorder is represented in the potential wells, $V(r)$ of the electrons on the various sites.

$$ih\frac{\partial\varphi}{\partial t}+\left(\frac{ih^2}{2m}\right)\nabla^2\varphi+\Delta V(r)\varphi(r,t)=0 \tag{4}$$

From the similarity one can work it backward; viz. localized optical modes from disorder by analogy implies localized electronic states as "a wave is a wave".

2. Optical Material Examples

1) Mixed polymers

Below is shown an example of redrawing a mix of two polymer optical fibers of differing refractive index [4]. This can be interpreted as propagating modes via the Anderson localization phenomenon as long the light is not confined to the higher index fiber. The first picture in **Figure 1** shows an SEM image resulting from the co-drawing of the 50 - 50 mix of two 0.25-mm polymer fibers with different refractive indices, thus resulting in a refractive index pattern through which light guiding occurs from the Anderson localization phenomenon.

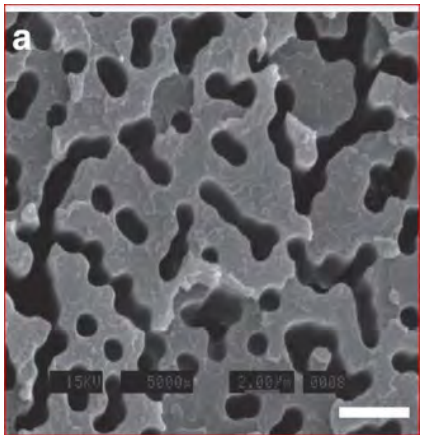

Figure 1. Polymer fiber constructed from 40k PMMA filaments and 40k PS filaments; SEM of the fused and drawn mixture, where one composition has been differentially etched to provide surface relief between the two compositions to enhance the visibility of the compositional structure [4].

2) Glass

The next example of a fiber made from the elongation of phase separated glass [5] [6]. This glass undergoes a liquid-liquid phase separation on heating, (see **Figure 2**). The elongation of the droplets seen in **Figure 2** is produced in the present case by what is termed a down-draw method. Here, by gravity, the glass flows out of a hole in the bottom of the crucible at the appropriate viscosity (temperature) and is formed into a fiber. The observation of image transport in these fibers is indicative of Anderson localization. Light launched into an arbitrary point at the input face of the fiber, emerges in the same transverse location on the output face. The processing method used to create these fibers is more adaptable to a manufacturing process than one based on stacking filaments of different compositions.

The elongated regions are continuous thoughout the length of the fiber as shown in **Figure 2(a)** and a cross sectional view in shown in **Figure 2(b)** showing the random refractive index pattern.

One can obtain an estimate of the relationship between the initial phase droplet size and the ultimate length of the continuous fiber that can result. We utilize the volume conservation of the particles in the blank with radius, R as it relates to the filament radius, r over a length, L. Then, by conservation of volume, we have the following.

$$\frac{4}{3}\pi R^3 = \pi r^2 L\,. \tag{5}$$

Solving for the initial particulate radius we have

$$R = \left(\frac{3r^2 L}{4}\right)^{1/3} \cong 0.909\left(r^2 L\right)^{1/3} \tag{6}$$

One can see from **Figure 3** that for a 10-μm droplet that the fiber radius would be ~0.1 μm for the fiber length of 30 cm and ~0.5 μm for a 2-cm length.

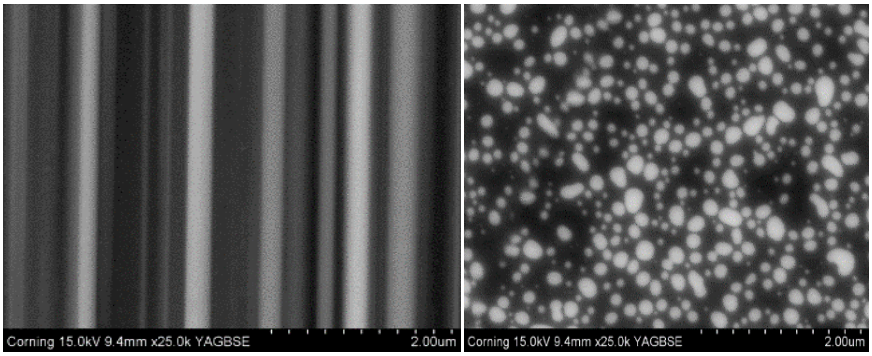

(a)

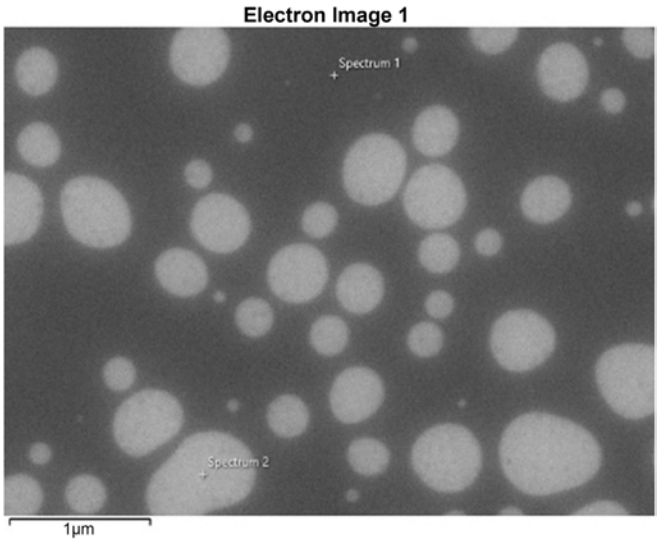

(b)

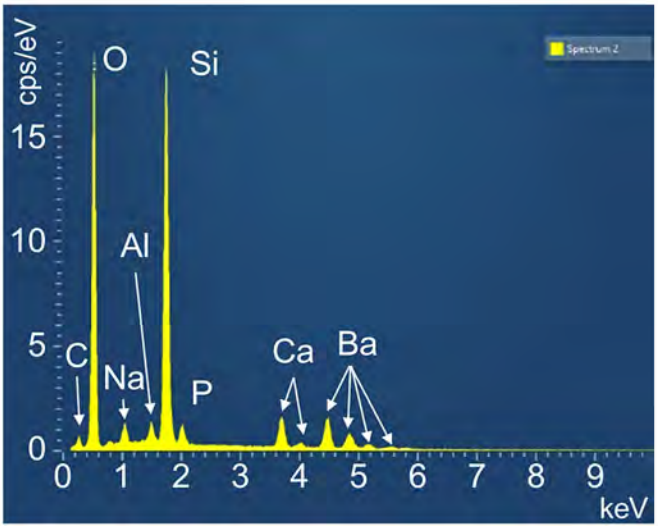

(c)

Figure 2. (a) SEM of a borosilicate composition fiber viewed parallel to the fiber axis (left) and viewed in cross section (right); white regions are the higher index particulate (discontinuous) phase. (b) SEM of the fiber shown in (a), but at higher magnification to show the areas from which chemical element identifications were made. (c) Compositional analysis of the particulate (discontinuous) phase obtained from the SEM images.

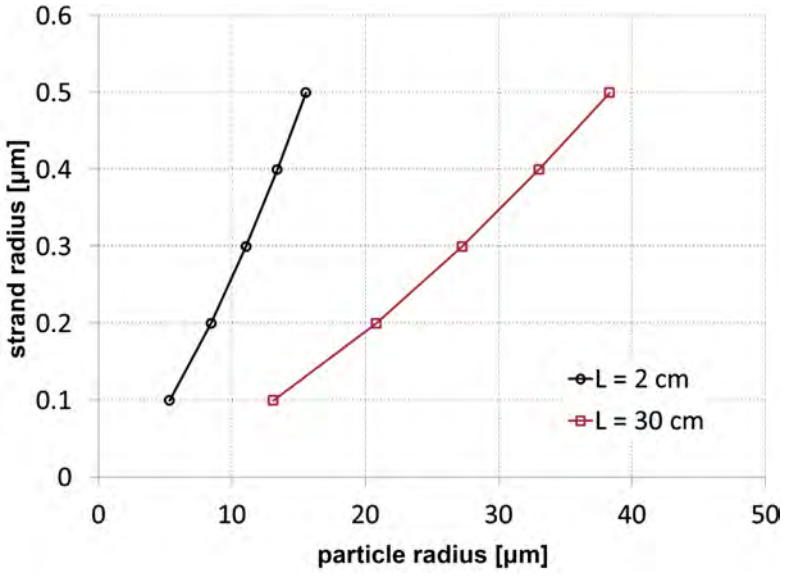

Figure 3. Computed fiber radius as a function of the droplet radius for two different redrawn lengths.

3. Light Guiding Mechanism

It is useful at this point to be more specific about the proposed light guiding mechanism. The light is not guided by the elongated particles (strands) per se, this would not represent Anderson localization. The light guiding is by regions of the index pattern where *regions* of high index are surrounded by *regions* low index. The actual delta *n* is not that of the refractive of respective phases, rather by the difference of the effective indices of the two respective regions. Therefore, this results in a distribution of the values of delta *n* and effective light guiding radii. This is consistent with why we see the guiding behavior irrespective of whether the droplets are the high (borosilicate glass case) or low index phase (borate glass). So truly the light propagation is determined by Equation (2), namely Anderson localization.

4. Mode Calculation

In this section a calculation of the possible propagating modes is accomplished by using the SEM result shown in **Figure 4(b)** to make a map of the refractive and then numerically solving Equation (2) for the modes, realizing that the spatial inhomogeneity remains substantially axially invariant over large distances. This was done for the two cases where the elongated droplet phase was the higher index phase and then the lower index phase. From **Figure 4(a)** one observes the multiplicity of modes that can propagate. This represents a true example of Anderson localization.

5. Examples of Imaging

In the picture below in **Figure 5** is shown the image transfer property in a sample that is in a larger diameter cane form.

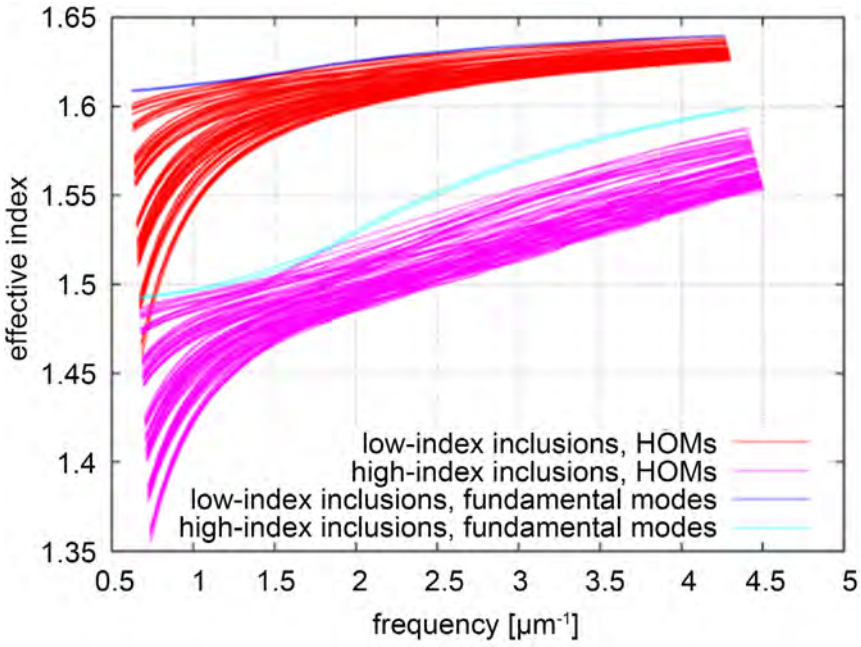

(a)

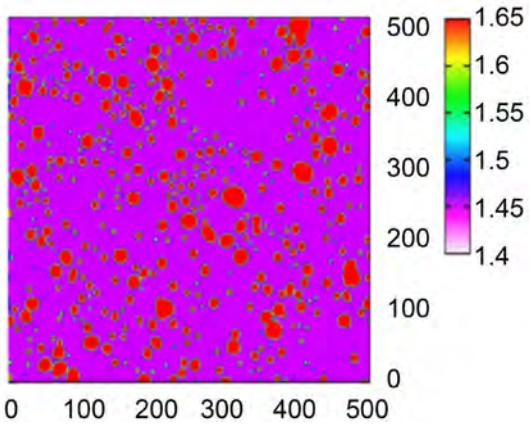

(b)

Figure 4. (a) Calculation of modes obtained from the refractive index map estimated from SEM image on RHS using numerical solution of Equation (2); (b) refractive index distribution used for the results in (a).

Figure 5. Example of image transfer from a much larger diameter bulk sample.

In the following two Figures, pictures are shown of images from 0.5-mm fiber samples; Figure 6 indicating the resolution and Figure 7 indicating the longest length where an image can be transmitted.

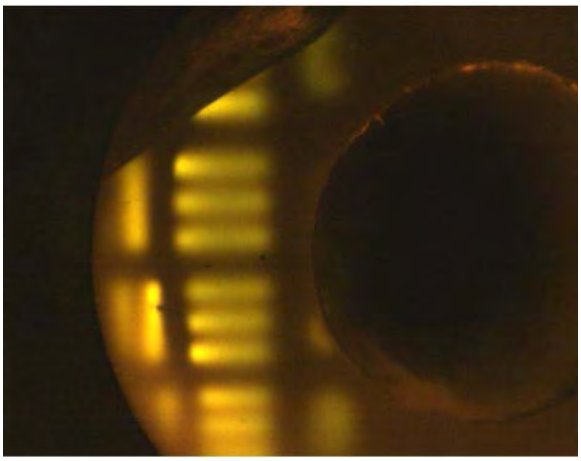

Figure 6. Image transfer from input face to exit face a 19 lp/mm resolution chart element from phase-separated borosilicate cane fiber 0.5-mm diameter 2-cm long.

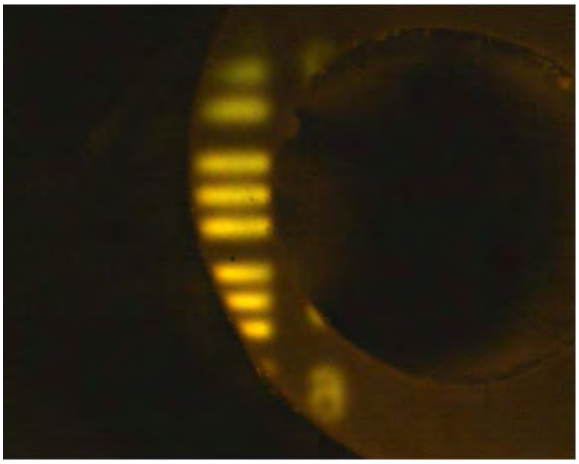

Figure 7. Image transfer of a bar pattern from a 13-cm long, 0.5-mm diameter, phase-separated Pb-borate fiber.

Compositions of the two fibers of Figure 6, Figure 7 (wt%).

compound	Figure 6	Figure 7
SiO_2	62.1	0.05
B_2O_3	13.3	69.45
PbO	0	30
Al_2O_3	2.2	0.5
Na_2O	2.7	0
P_2O_5	2.1	0
CaO	4.1	0
BaO	13.5	0

6. Conclusion

Imaging via an Anderson localization mechanism in an optical fiber can be produced from a particle-elongated, phase-separated glass medium. The approach suggests a more manufacturable approach to producing such fibers.

Acknowledgements

We wish to thank Joseph Schroeder, Derek Webb, and Heath Filkins for technical support in the processing of the glasses reported in this paper.

Conflicts of Interest

The authors declare no conflicts of interest regarding the publication of this paper.

References

[1] Anderson, P.W. (1958) *Physical Review*, **109**, 1492-1505. https://doi.org/10.1103/PhysRev.109.1492

[2] Segev, M., Silberberg, Y. and Christodoulides, D.N. (2013) *Nature Photonics*, **7**, 197-204. https://doi.org/10.1038/nphoton.2013.30

[3] Wiersma, D., Bartolini, P., Lagendijk, A., *et al.* (1997) *Nature*, **390**, 671-673. https://doi.org/10.1038/37757

[4] Karbasi, S., *et al.* (2014) *Nature Communications*, **5**, 3362. https://doi.org/10.1038/ncomms4362

[5] Randall, L.J. and Seward III, T.P. (1975) US Patent 3,870,399, "Pseudo-Fiber Optic Devices," March 11.

[6] Seward III, T.P. (1977) Proceedings of the Physics of Non-Crystalline Solids, Fourth International Conference. Transtech Publications, Aedermannsdorf, Switzerland, 342-347.

Journal of Modern Physics, 2022, 13, 776-838
https://www.scirp.org/journal/jmp
ISSN Online: 2153-120X
ISSN Print: 2153-1196

Demystifying the Lorentz Force Equation

André Michaud

Service de Recherche Pédagogique, Québec, Canada
Email: srp2@srpinc.org

How to cite this paper: Michaud, A. (2022) Demystifying the Lorentz Force Equation. *Journal of Modern Physics*, **13**, 776-838.
https://doi.org/10.4236/jmp.2022.135046

Received: April 19, 2022
Accepted: May 28, 2022
Published: May 31, 2022

Abstract

The Lorentz force equation $F = q(\boldsymbol{E} + \boldsymbol{v} \times \boldsymbol{B})$, which has been used by the engineering community since the early 20th century to control the motion of electrons on free trajectories, in a wide range of technical applications, is a generalized equation that was originally developed by Hendrik Antoon Lorentz at the beginning of the 20th century, and which treats, in a single formulation, two very different aspects of the behavior of free-moving electrons. This article aims to put into perspective the historical context in which the equation was developed, and to clarify how its two different aspects can be clearly separated for practical computational purposes and used in fundamental research in physics, to help reconcile classical/relativistic mechanics and quantum mechanics with electromagnetism, and in particular how its first term can be related to gravitation while its second term can be related to measurable mass from the electromagnetic perspective.

Keywords

Electron Resonance States, Elementary Electromagnetic Particles, Electromagnetism, Hydrogen Atom

1. Introduction

In 1904, H.A. Lorentz published an article that revolutionized two major aspects of fundamental physics, one pertaining to classical/relativistic physics as applicable at our macroscopic level of magnitude, and one pertaining to the electromagnetic behavior of free moving electrons at the subatomic level of magnitude. His article is largely referenced in the literature in relation with his proposal applicable to relative motion at our macroscopic level, but his analysis of the free moving electron behavior that emerges from the experimental data previously collected by Walter Kaufmann remains mostly obscured behind the popularity and universal reach of his proposal regarding relative motion [1].

The revolutionary development that he proposed regarding relative motion

was meant to account for physical processes observed at the astronomical level that seemed to deviate from classical mechanics as established by Newton, at a time when general knowledge about these issues was much less extensive than what we know today.

His proposition was a set of mathematical transformations meant to address the issue of relative motion of macroscopic masses with respect to each other, as a solution to the apparent impossibility at the time of identifying an absolute reference in the universe, relative to which the motion of all massive bodies could be calculated, a conclusion that resulted from the apparent failure of the Michelson and Morley experiments to demonstrate the existence of such an absolute reference [2].

This development, although meant to resolve issues not addressed by Newton's classical mechanics, was still grounded on the double assumption that the existence of kinetic energy that sustains momentum is caused by the motion of massive bodies and that the total amount of this energy is conservative, in the sense that when a body slows down, this kinetic energy is deemed to progressively convert to potential energy, so that when the body stops completely, all of its kinetic energy has converted to potential energy, and that at all times, the sum of the kinetic energy and of the potential energy remains constant—a concept mandated by the classical Principle of energy conservation ([3], p.217).

The Newtonian mechanics equation that did not seem able to completely address some astronomical observations is precisely related to the relation between the kinetic energy of a moving mass $K = 1/2mv^2$ and its momentum $p = mv$, both equations being related via the relation $K = p^2/2m$. Briefly summarized, Lorentz brought in the picture the idea that the correction required could be addressed by the introduction of the γ-factor in Newton's kinetic energy equation $K = 1/2\gamma m_0 v^2$ and in his momentum equation $p = \gamma m_0 v$, thus defining with symbol m_0 the *rest mass* of a body when its velocity is zero, both equations still being related via the amended relation $K = p^2/2\gamma m_0$, the γ factor now relating the motion of bodies to the perception of an observer in the absence of an absolute reference, by means of the mathematical transformations that he was proposing.

As soon as Henri Poincaré recognized the mathematical validity of the *Lorentz transformations*—term that he coined in his June 5 of 1905 note [4]—Albert Einstein published his major article on relative motion, now known as the Special Relativity Theory (SRT) [5], that integrated the Lorentz transformations as a means by which the relative motion of massive bodies with respect to each other could be mechanically explained, involving the concepts of time dilation and mass length contraction, as well as the γ-factor controlled non-rectilinear increase of the momentum kinetic energy of massive bodies with their increasing velocity toward the speed of light, now established as an asymptotic velocity limit for massive bodies, as a refinement to Newton's original assumption, that assumed a rectilinear increase of their momentum energy with velocity, with no ultimate velocity limit.

The second revolutionary development established by Lorentz in his 1904 article [1] was the confirmation of the validity of the first equation of electromagnetic mechanics initially developed by himself to control the motion of free moving—electrically charged—electrons at the subatomic level, now known as the Lorentz force equation, from experimental data collected by Walter Kaufmann using this equation [6] [7]; free moving electrons whose trajectories could now be controlled by a combination of electric and magnetic $\boldsymbol{E}$ and $\boldsymbol{B}$ fields of separately controllable intensities, which acted directly on the charge of the electron rather than on its mass, contrary to the concept of force imagined by Newton as acting on mass. We will see later that Einstein assumed the two concepts to be equivalent.

But contrary to classical mechanics, that assumed that the amount of momentum energy of an electron depends on the velocity of its mass, the Lorentz electromagnetic mechanics equation involved that the amount of momentum energy of the moving electron does not depend on its velocity, but rather that the opposite relation was involved, that is, that it was the velocity of the electron that depended on the amount of momentum energy communicated to its charge by the variable intensity $\boldsymbol{E}$ and $\boldsymbol{B}$ fields that controlled its trajectory; an energy adiabatically induced in the moving electron as a function of the inverse of the distances that separated the moving electron from other charged particles whose mutual interaction established the controlling $\boldsymbol{E}$ and $\boldsymbol{B}$ fields, as clarified in Reference [8] and in its expanded final republication [9].

But at that time, the concepts of force fields were rather grounded on the conservative duality of kinetic energy versus potential energy as defined in classical mechanics, as Aram d'Abro clearly explained in the 1930s in his excellent synthesis ([3], p. 217). However, according to this perspective, the concept of potential energy in a force field would only appear if the field is derived from a potential:

"*Consider a particle in a conservative field, and two arbitrary points* $\boldsymbol{A}$ *and* $\boldsymbol{B}$ *in the field. The relationship between the potential energy and the particle a*t **A** and at **B** is fur*nished by the following definition*:"

"*Potential energy at* $\boldsymbol{B}$ *minus potential energy at* $\boldsymbol{A}$ = *work* (*positive or negative*) *expended by the field of force when the particle is made to pass from* $\boldsymbol{B}$ *to* $\boldsymbol{A}$"

"*For instance, if we agree that the potential energy at the point* $\boldsymbol{A}$ *is zero, the potential energy at any arbitrary point* $\boldsymbol{B}$ *is given by the work* (*positive or negative*) *expended by the force when the particle is moved from* $\boldsymbol{B}$ *to* $\boldsymbol{A}$…"

So, while a stone is falling from point $\boldsymbol{B}$ *to point* $\boldsymbol{A}$, "*...its potential energy would be decreasing and its kinetic energy increasing at an equal rate, so that the sum of the two kinds of energy would remain constant.*"

"*This rule is general. Whenever a particle is released from a position of rest in a conservative field, it will always start moving towards regions of decreasing potential energy...*"

"*The conservation of energy would not hold in a non-permanent field*; *nor would it be realized in a permanent field which is not derived from a potential*."

This last condition is precisely the case for the ***E*** and ***B*** fields controlled by the Lorentz force equation. Neither field is permanent. And they are not derived from a potential, but depend on specific and modifiable configurations of electric wire windings in which electric current is made to circulate—a current made of electrons moving along the wires—and of ferromagnetic material or permanent magnets, whose magnetic fields depend on non-permanent configurations of electrons captive of atoms in these materials.

The velocity of the electrons flowing in a wire (determined by the voltage) determines the intensity of the Coulomb interaction between the charges related ***E*** field controlled by the first term of Lorentz equation while the related magnetic ***B*** field of his second term is generated about the wire according to the Biot-Savart equation due to the forced magnetic parallel spins alignment of the electrons flowing in the same direction in the wire, complemented, to control the curvature of the free moving electrons trajectories by the controllable ***B*** fields of nearby ferromagnetic material and/or permanent magnets, whose macroscopic magnetic fields are due to forced parallel alignment of the magnetic spins of unpaired electrons in these materials [10] [11].

Let us note that the Coulomb equation $F = q_1 q_2 / 4\pi\varepsilon_0 d^2$ is the means by which the energy adiabatically induced in all charged particles according to the underlying Coulomb interaction can be calculated strictly as a direct function of the inverse of the distances separating them $E = d \cdot F = q_1 q_2 / 4\pi\varepsilon_0 d$, as clarified in Reference [12] and its expanded final republication [13].

Given that the macroscopic ***E*** and ***B*** fields generated by current flowing in wires disappear when the current is made to stop flowing in the wire, that the macroscopic ***B*** field of electromagnets disappears when the current in their wire is cut, and that even the macroscopic ***B*** field of so-called permanent magnets disappears when heated, and is not restored upon cooling when overheated past a critical temperature, d'Abro's condition that "conservation of energy would not hold in a non-permanent field" is realized.

So, when we consider a charged particle in such non-conservative fields, and two arbitrary points in space ***A*** *and* ***B***, the relationship between the energy and the *charged particle* at ***A*** *and at* ***B*** is then provided by the following definition:

"*The energy at* ***B*** *minus the energy at* ***A*** (*positive or negative*) *provided by the non-conservative field of force when the charged particle is made to pass from* ***B*** *to* ***A*** *can only be adiabatic in nature*"

Let us note in passing, that at the beginning of the 20th century, the general consensus was not that elementary charged particles induce energy into each other as a function of the distances separating them as just mentioned, but that energy was induced in each elementary charged particle by an all pervading underlying supposedly conservative electromagnetic field, which muddled the issue of energy induction in elementary charged particles for the rest of the 20th century and a good chunk of the twenty first century.

This relation was clearly described by Einstein in his 1910 article [14]. (The German original of this article having been lost, the quotes in English are made from its initial French translation made the same year by E. Guillaume, which is the only existing translation made from the lost original German version. The formal English translation published in 2021 of the Guillaume version is available from the Minkowski Institute [15]):

"*…the electric and magnetic fields eventually came to be considered to be entities whose mechanical interpretation was superfluous. This led to the view of these fields in vacuum as being particular states of the aether that did not require further analysis.*

A charged particle in motion relative to the aether is like an element of current; the actions of the electromagnetic field on the particle and the reactions of the latter on the field are the only bonds that bind matter to the aether. In the latter, where space is not already occupied by a particle, the intensities of the electric and magnetic field are expressed by Maxwell's equations for the free aether, assuming that the equations are related to a system of axes which is immobile relative to the aether."

By carefully calibrating the intensity of ambient macroscopic electric and magnetic fields, subatomic scale local electric and magnetic $\boldsymbol{E}$ and $\boldsymbol{B}$ fields are consequently locally adiabatically generated in the immediate vicinity of each electron in electron beams, that locally guide each electron on its trajectory according to equation $\boldsymbol{v} = \boldsymbol{E}/\boldsymbol{B}$, equal densities of the $\boldsymbol{E}$ and $\boldsymbol{B}$ fields defining straight line motion of the charged particle, while unequal densities of these induced fields define curved trajectories, each electron being propelled by a local momentum energy which is simultaneously adiabatically induced in each of them [16], that is, a combination of local $\boldsymbol{E}$ and $\boldsymbol{B}$ field energy, the sum of which is equal by structure to the momentum energy which is simultaneously induced, these two induced components constituting the carrier-energy whose momentum component propels the electron [12] [13].

This control method that Lorentz initially proposed in a previous article [17], that involved combining the Coulomb equation to calculate the total $\boldsymbol{E}$ field energy of the electron, to the transverse $\boldsymbol{B}$ field energy relation established by Heaviside [18], to control its velocity and the curvature of its trajectory was then used by Kaufmann [6] to collect data from accelerating free moving electrons in a bubble chamber.

After Abraham in 1902 [19], Lorentz also succeeded in his 1904 article [1] in relating the total amount of $\boldsymbol{E}$ field energy provided by the Coulomb equation to the exact classical/relativistic longitudinal inertia of the free moving electron by introducing the γ-factor—"k" in his paper—(see mass m_1 of his first Equation (30) and related explanations), and by also introducing the same γ-factor to account for the total transverse electromagnetic/relativistic inertia of the electron being deflected—that turned out to be different from the total m_1 longitudinal inertia—(see mass m_2 of his second Equation (30)), the latter value corresponding to the velocity related increase in the total transverse magnetic $\boldsymbol{B}$ field of the

moving electron.

This method, experimentally confirmed by the Kaufmann data as analyzed by Abraham and Lorentz, was immediately adopted by the engineering community to deal with all applications requiring precise control of the trajectories of free moving electrons, typical current applications of which being precise control of the trajectories of electron beams in all CRT screens applications and precise control of charged particle beams in all high energy particle accelerators.

2. The Adoption of the Special Relativity Theory

When Einstein published his article on relativistic motion and non-rectilinear momentum energy increase with velocity towards c, established as a speed limit for massive bodies [5], directly grounded on the Lorentz transformations [1], he had already astonished the physics community with two other groundbreaking articles published only a few months earlier that made the whole community pay heightened attention to his third paper.

The first article, from March of 1905, explained his quantum theory of light [20], grounded on Max Planck's conclusions [21] about the black-body experiments recently carried out by Wilhelm Wien [22], the main conclusion of which can be summarized with this quote:

"*In fact, it seems to me that the observations on "black-body radiation", photoluminescence, the production of cathode rays by ultraviolet light and other phenomena involving the emission or conversion of light can be better understood on the assumption that the energy of light is distributed discontinuously in space. According to the assumption considered here, when a light ray starting from a point is propagated, the energy is not continuously distributed over an ever increasing volume, but it consists of a finite number of energy quanta, localized in space, that move without being divided and that can be absorbed or emitted only as a whole.*"

This conclusion is what led him to the photoelectric effect mechanical explanation that confirmed that the energy of localized electromagnetic photons, as he hypothesized them to be emitted, to propagate and to be absorbed individually, has measurable longitudinal inertia—inertia in the direction of their motion, which eventually earned him the Nobel Prize in 1921.

This discovery also led, in correlation with his soon to be published conclusion that the momentum energy that propelled moving masses has to be a physically existing substance [23]—see further on—and the later proposed double-particle photon hypothesis regarding the possible inner dynamic electromagnetic structure of these localized photons by Louis de Broglie published in the 1930's [24], to the establishment of the LC equation and the related $\boldsymbol{E}$ and $\boldsymbol{B}$ fields equation that mechanically describe their internal electromagnetic structure in an article initially published in 2016 [25], republished in expanded final version in 2021 [26], in complete agreement with Maxwell's equations, describing them as moving separately without spherically expanding from their point-

source, but being emitted, propagating and being absorbed only as a individual separate quanta as concluded by Einstein [20], that is, mechanical absorption, propagation and emission processes that were analyzed and published in 2020 [12] [13].

In May of 1905, another major paper of his was published, drawing attention to a possible explanation to the Brownian motion observed in liquids, according to which the erratic motion of microscopic particles visible with microscopes in liquids could be explained by stochastic collisions with molecules too small to be seen, of which the liquid had to be made, which he concluded could lead to the possibility of calculating the physical dimensions of these molecules [27], a process that was independently discovered and explained by Marian von Smoluchowski one year later [28]. Their conclusions were experimentally confirmed by Jean Perrin en 1912 [29]. The relation between Brownian motion and electromagnetism will be analyzed in Section 13, in which will be explained the reason why these molecules, that Einstein sensed the existence of, keep naturally moving in liquids, which is what makes them collide with the particles visible with microscopes.

So when Einstein's third significant paper was published within a few months of the first two on September 26 of 1905—received June 30—this one grounded on the recently mathematically confirmed Lorentz transformation [1] [4], proposing a logical solution that apparently reconciled electromagnetism as observable at our macroscopic level with classical mechanics, that seemed to resolve the issues not addressed by Newton's classical mechanics regarding the behavior of massive bodies in a comprehensive theory that came to be known as the Special Relativity Theory [5], Einstein's stature as a leading edge theoretician was already overwhelming the community.

Finally, when Einstein published a fourth paper November 21 of 1905—received September 27 [23] as an extension of his June 30 paper [5]—the revolution of physics was completed with the introduction of his conclusion that the energy in excess of a body's rest mass which is transferred to the environment when a body is stopped in its motion had to be a physically existing substance [12] [13], since it was proven to have inertia just like the body's rest mass and just like the energy of localized electromagnetic photons as they hit electrons in massive bodies as demonstrated by the photoelectric effect as described in his previous March 1905 article [20], given that inertia can hardly be expected to be manifested by something that did not have physical existence as a ponderable substance:

"*When a body emits energy L in the form of radiation, its mass decreases by* L/V^2*… The mass of a body is a measure of its energy content; if the energy changes by L, the mass changes in the same manner by* $L/9.10^{20}$*, if the energy is measured in erg and the mass in grams.*"

Obviously, Einstein had in mind here the momentum energy of a macroscopic body that can be measured in addition to the energy making up its rest mass, as conceived in classical mechanics when this energy is communicated to the envi-

ronment when a body is stopped in its motion [8] [9]. The case of a 1 kg mass falling to the ground from a height of 1 meter, to clearly put in perspective what can be experimentally ascertained from our macroscopic level perspective, is analyzed in References [8] [9].

Let us note at this point that his correlation in his September 1905 article of the *inertia* of moving bodies with the "physically-existing-substance" aspect of the energy released when they are stopped in their motion did not attract attention at the time, given that the whole community and Einstein himself immediately became utterly engrossed into endless discussions and further analyses of the "relative-motion aspect" of his SR theory.

One century later, this aspect of the SR theory is still the object of constant arguments and further publications in the community, given the difference between the observable behavior of masses at our macroscopic level and that of the electron mass at the subatomic level as revealed by the Kaufmann experiments, that the same 1904 Lorentz paper also put to light [1], and that we will now examine.

3. Adoption of the First Electromagnetic Mechanics Equation by the Engineering Community

Before getting into the analysis of the 1904 Lorentz conclusions [1] regarding the Kaufmann data [6] [7], that confirmed the first equation that allows complete control of the trajectory and the velocity of a charged and massive elementary particle at the subatomic level, thus establishing the first bridge between classical mechanics, that deals with the control of massive bodies at our macroscopic scale, and electromagnetic mechanics that deals with the control of charged particles at the subatomic level, thanks to the electron simultaneously possessing both an invariant rest mass (m_0 = 9.10938188E−31 kg) and a charge at all times invariant (e = 1.602176462E−19 C), let us briefly put in perspective the knowledge previously established on which his research was grounded.

The mutually perpendicular interaction between the electric $\boldsymbol{E}$ and magnetic $\boldsymbol{B}$ aspects of light moving in vacuum in a direction that can only be perpendicular to both $\boldsymbol{E}$ and $\boldsymbol{B}$ fields, was understood by Maxwell as being the reason why light could move at invariant velocity c in vacuum, as demonstrated by the second partial derivatives of electromagnetic equations drawn from experiments previously carried out by earlier experimentalists [30]. Maxwell came to this conclusion after Faraday informed him in 1845 that he had observed that light passing through a glass plate becomes polarized when he locates the plate between the magnetic poles of his electromagnet, a behavior that was given the name of Faraday Effect.

This information convinced Maxwell that light had to be some form of free moving energy that could only be electromagnetic in nature, propagating in vacuum at the velocity revealed by his second partial derivative calculations, a velocity that was maintained by the interaction of these two separate fields, one

electric, and one magnetic, interacting perpendicularly to each other, and perpendicularly to the direction of motion of the light energy. He was in fact, the first to mathematically associate a velocity to light, that is, to free moving electromagnetic energy, by means of direct calculation [31].

$$c = \frac{\boldsymbol{E}}{\boldsymbol{B}} \tag{1}$$

About 20 years after Maxwell's publication of his conclusions in 1865, Heaviside, simplified Maxwell's 20 equations into the 4 equations that have since been in universal use [17], and also established for the first time that a magnetic field would apply a force, manifested as a pressure on the infinitesimal *ds* surface of the fulcrum of a point-like behaving charged particle in free motion that would determine its velocity—see Section 13 on this particular issue—and that this pressure, or force, could be calculated when the charge of the particle and the strength of the ambient magnetic $\boldsymbol{B}$ field are known:

$$F = q(\boldsymbol{v} \times \boldsymbol{B}) \tag{2}$$

Given that pressure is defined as a *force* being applied perpendicularly to the surface of an object per unit area (A) over which that force is distributed, the dimensions of a pressure in the SI system come out as "*Newtons per meter squared*" ($P_A = F_A$ = Newtons/m^2). In the case of a point-like behaving charged particle, this surface tends by structure to mathematically reduce to an "infinitesimal surface" meant to represent at the limit the practically dimensionless point-like fulcrum of the point-like behaving particle [26] that can be mathematically represented by an infinitesimal ds surface for calculation purposes, to which the pressure will be applied ($P_{A\to ds} = F_{A\to ds} = F$ = Newtons).

If such a point-like behaving charged particle is immobilized in some stationary electromagnetic equilibrium state, a force applied to this idealized *ds* surface that would be insufficient to overcome this stationary state can only result in the velocity of the particle remaining at zero (v_0) even if the pressure remains fully applied—see Section 13 for further development of this relation between pressure and force:

$$P_{A=ds} = q(\boldsymbol{v}_0 \times \boldsymbol{B}) \tag{3}$$

But if the *pressure*/*force* ($P_{A=ds} = F_{A=ds}$) exerted on the particle's fulcrum by the magnetic field $\boldsymbol{B}$ is sufficient to overcome the stationary electromagnetic state that immobilizes the charged particle, then the *pressure* applied and constantly maintained on the particle by the magnetic $\boldsymbol{B}$ field will cause the particle to start moving at the corresponding velocity, that can be calculated with the equation previously mentioned, established by Heaviside:

$$P_{A=ds} = F_{A=ds} = F = q(\boldsymbol{v} \times \boldsymbol{B}) \tag{4}$$

Ten years later, Lorentz had the intuition that if electric and magnetic fields in mutual transverse interaction, as Maxwell conceived them, could propel light energy at velocity c in vacuum, then perhaps they could also be combined to

precisely control the motion of charged particles, such as the electron. So the idea came to him that combining the Coulomb force equation, that allows controlling the intensity of the $\boldsymbol{E}$ fields in the vicinity of an electron $F = e \cdot \boldsymbol{E} = k\left(e \cdot q/d^2\right)$—$q$ being the sum of charges in the vicinity that establish the $\boldsymbol{E}$ field as a function of the inverse square of the mean distances d separating them from the electron e, et $k = 1/4\pi\varepsilon_0$ being the Coulomb constant—to control its acceleration, to the Heaviside force equation $F = e(\boldsymbol{v} \times \boldsymbol{B})$, that provides its velocity as a function of the intensity of the related magnetic $\boldsymbol{B}$ field, all aspects of the motion of the electron could be addressed, resulting in his famous general equation:

$$F = q\left(\boldsymbol{E} + \boldsymbol{v} \times \boldsymbol{B}\right) \tag{5}$$

Kaufmann then proceeded to experiments with free moving electrons, using interacting electric and magnetic fields in the manner suggested by Lorentz, observing and measuring their trajectories in a bubble chamber, and collected the data that Abraham and Lorentz then analyzed, confirming that not only momentum energy was induced in electrons by the Coulomb interaction to explain their longitudinal motion, but that transverse energy was also simultaneously induced in them, that could be measured longitudinally as well as transversely contrary to the momentum energy that could be measured only longitudinally, a transverse energy that added momentary velocity related additional measurable mass to the invariant rest mass of the electron.

In his famous 1904 article [1], in which Lorentz was commenting and correlating the experimental data collected by Kaufmann from 1901 to 1903 [6] [7] [32] [33], previously analyzed by Abraham [19], that confirmed the validity of the force equation that he had established in 1895 [17], he clearly concluded with reference to Equations (30) of his development that:

"*Consequently, in processes in which acceleration occurs in the direction of motion, the electron behaves as if it had mass* m_1, *and in acceleration in a direction perpendicular to the motion, it behaves as if it had mass* m_2. *These quantities* m_1 *and* m_2 *are therefore appropriately named the* '*longitudinal*' *and* '*transverse*' *electromagnetic masses. I will assume that, in addition, there is no* '*real*' *or* '*material*' *mass.*"

Lorentz represents these two measurable perpendicular states of acceleration of the electron, that is, acceleration in the direction of its trajectory, and acceleration perpendicular to it, with the following two equations ([1], Equations (30)):

$$m_1 = \frac{e^2}{6\pi c^2 R}\frac{\mathrm{d}\left(kl\omega\right)}{\mathrm{d}\omega} \quad \text{for longitudinal acceleration} \tag{6}$$

and

$$m_2 = \frac{e^2}{6\pi c^2 R}kl \quad \text{for transverse acceleration} \tag{7}$$

And finally, for negligible velocities that reduce the v^2/c^2 ratio of the γ-fac-

tor—represent as k in his equations (explained further down)—to an infinitesimal value, which in turn reduces the value of the γ-factor to 1, the mass of the electron is considered to remain at its rest mass value, that is, the initial mass used in the $F = ma$ acceleration equation as defined in Newtonian mechanics (defined according to our modern notation as m_0), he equates both m_1 and m_2 with the electromagnetic definition of this rest mass, when the electron velocity is theoretically zero:

$$m_0 = m_1 = m_2 = \frac{e^2}{6\pi c^2 R} \tag{8}$$

Also commenting the experiments carried out by Kaufmann [7] by means of the force equation developed by Lorentz, and the calculation also carried out by Abraham from the same Kaufmann data [19], Henri Poincaré concluded in 1905 ([34], p. 137):

"*Abraham's calculations and Kaufmann's experiments have shown that mechanical mass itself is zero and that the mass of electrons, or at least of negative electrons, is exclusively of electrodynamic origin. This forces us to change the definition of mass; we can no longer distinguish mechanical mass from electrodynamic mass, because then the former would disappear; there is no other mass than electrodynamic inertia; but in this case the mass can no longer be constant, it increases with the velocity; and even, it depends on the direction, and a body animated by a notable velocity will not oppose the same inertia to the forces which tend to deviate it from its course, and to those which tend to accelerate or to delay its forward motion.*"

4. The 1907 Turning Point

By his own admission, Einstein had worked in isolation at the elaboration of his Special Relativity Theory for more than 7 years before producing his historical June 30 article [5], just a few weeks after Poincaré published his June 5 note about the Lorentz transformation [4], that was immediately widely distributed as was the habit of the French *Académie des sciences*, and that seemed to confirm what he had been suspecting all along, which is that absolute motion apparently could not be proven to exist in physical reality.

It seems that Einstein's attention was drawn more specifically to this specific conclusion of Lorentz before he published his 1905 paper [1], momentarily paying less attention to the behavior of electrons as analyzed in the Lorentz article, that had been under scrutiny since 1887, initiated by Heaviside [18], then Voigt [35], Lorentz in 1895 [17], and experimentally by Kaufmann in 1901, 1902 and 1903 [6] [7] [32] [33], whose results were analyzed by Abraham in 1902 [27] and by Lorentz himself in 1904, as finally reported by Poincaré in his book *La valeur de la science* published in 1905 [34].

The problem with this situation is that this observed difference between the variation rate of the transverse inertia of the accelerating electron and its differently varying rate of longitudinal inertia now made obvious at the subatomic

level, corresponding to the m_1 and m_2 terms of the Lorentz analysis, had never been observed in any experiment carried out with macroscopic masses, and resulted in Einstein having concluded that the transverse mass of macroscopic masses do not similarly increase with velocity, so the confirmed Lorentz m_1 and m_2 terms were not incorporated into the Special Relativity theory, leaving only the longitudinal momentum energy increasing as a function of the γ-factor to be integrated into SR, since applying it only to momentum energy seemed to satisfy the observable behavior of masses at our macroscopic level.

This apparent contradiction between the behavior of electrons and the behavior of macroscopic masses of course quickly attracted general attention in the community, and a whole series of experiments were carried out, mainly by Bucherer and Neumann [36] [37] all confirming the Kaufmann data. Planck, for example, re-analyzed the Kaufmann data [38] and found no flaw in Kaufmann's analysis, and the same for Poincaré's re-analysis [39]. From Lorentz's own admission, none of the experiments seemed to confirm the length contraction that he had himself introduced with his concept of relative transformations in the same 1904 article [1] on which Einstein's had grounded his 1905 theory, and suggested that more analysis should be carried out [40].

But Einstein did not change his mind [41] [42]:

"*Herr Kaufmann has determined the relation between [electric and magnetic deflection] of β-rays with admirable care... Using an independent method, Herr Planck obtained results which fully agree with Kaufmann... It is further to be noted that the theories of Abraham and Bucherer yield curves which fit the observed curve considerably better than the curve obtained from relativity theory. However, in my opinion, these theories should be ascribed a rather small probability because their basic postulates concerning the mass of the moving electron are not made plausible by theoretical systems which encompass wider complexes and phenomena.*"

Considering that all of his scientific production shows that during his whole life, Einstein was convinced that the key to resolving the gravitation issue involves only interaction between astronomical-sized macroscopic masses, and although he perfectly understood that the electron behaves at the subatomic level in accordance with the Kaufmann data, he could not see how such behavior of the subatomic level could have any bearing in the search for an explanation to gravitation, a pursuit that resulted in his November 4 of 1915 article that describes the main aspects of his General Relativity Theory (GRT), that indeed addresses the gravitation issue only from the astronomical magnitude perspective, but completely dismisses the possibility that the behavior of subatomic masses such as that of the electron could contribute to the final solution.

Einstein's opinion with regard to the Kaufmann data was indeed met with the approval of his colleagues, as revealed by this quote from Abraham Pais ([42], p.159):

"*Special Relativity killed the classical dream of using the energy-momentum-velocity relations of a particle as a means of probing the dynamic origin of its*

mass. The relations are purely kinematic. The classical picture of a particle as a finite little sphere is also gone for good. Quantum field theory has taught us that particles nevertheless have structure, arising from quantum fluctuations. Recently, unified field theories have taught us that the mass of the electron is certainly not purely electromagnetic in nature. But we still do not know what causes the electron to weigh."

The unfortunate outcome of this general opinion in the theoretical physics community at the beginning of the 1900's is that for the past century, although the engineering community has successfully been using the confirmed Lorentz force equation to control free-moving electron trajectories with the highest degree of accuracy in the whole set of functional applications developed to date, including high-energy particle accelerators [43], most in the fundamental physics and astrophysics communities, who rather gave credence to Special Relativity and General Relativity became less and less aware of the confirmed behavior of electrons at the subatomic level, due to all literature pertaining to SR and GR never referencing and explaining the now almost forgotten Heaviside-Lorentz-Kaufmann perspective—except in the engineering community, fortunately—and progressively became convinced without requestioning that the mass of the accelerating electron remains constant at all velocities and that only their γ-factor dependent momentum varies with said velocities, which largely explains why so little theoretical progress has been made in fundamental electromagnetism during the past century.

Given that no further reference was ever made after 1907 in SR an GR textbooks of the collective agreement in the early 1900's physics community that the Abraham and Lorentz analyses of Kaufmann's data was correct, this explains why generation after generation of physicists never heard about this agreement and also why one hundred years later numerous senior physicists, who obviously are not aware of the 1907 collective agreement, strongly assert, grounded on the too restrictive knowledge base provided by these SR and GR reference works, that "*mass gain with velocity is an illusion*".

We will now see that the physics community's general opinion of the early 1900's summarized by Pais was quite premature in light of what was subsequently discovered in the 1930's about the electromagnetic nature of the energy of which the electron rest mass is made, and in the 1960's about the elementary charged and massive subcomponents that make up the inner scatterable structure of protons and neutrons, and finally about the discovery in 2003 that the local transverse $\boldsymbol{B}$ field of a free moving electron increases with its velocity synchronously with its increasing transverse mass as measured by Kaufmann one hundred years earlier.

We will see that it is not the energy-momentum-velocity relations of a particle that can be useful in probing the dynamic origin of the electron mass, but the general Lorentz force equation.

Or course, the naive classical picture of elementary particles as finite little spheres is gone for good. But in light of the more extensive knowledge pool now

available, the notion that the relations between masses could be purely kinematic is contrariwise quite illusory and turns out to effectively be purely electromagnetic in nature.

Moreover, although Quantum field theory (QFT) grounded on the Ludwig Lorenz interpretation, that treats $\boldsymbol{E}$ and $\boldsymbol{B}$ fields as a single unified field, does not lead to conclude that electromagnetic particles may have an internal structure, Electromagnetic Mechanics grounded on Maxwell's initial interpretation, that treats both $\boldsymbol{E}$ and $\boldsymbol{B}$ fields as separate and mutually inducing each other in alternance, does it quite naturally, as we will soon see.

Finally, Contrary to what unified field theories seem to teach us, due to the discoveries made in the 1930's, we know now for certain that the mass of the electron is purely electromagnetic in nature, and that it is the omnidirectional inertia of the energy making up its rest mass plus the additional contribution of the omnidirectional inertia of the adiabatically induced transverse magnetic $\boldsymbol{B}$ field of its carrying energy in addition to its also adiabatically induced momentum energy, that causes the electron to weigh.

5. Mathematical Notation Synchronization

Historically, a trend progressively developed in the physics community according to which the ultimate understanding of Nature should result in the eventual development of a general equation that would summarize all of our knowledge about Nature and from which all useful equations could then be derived.

For a number of idealists in the orthodox physics community, the Friedmann equations developed in 1922 from Einstein's theories are considered to embody this ultimate accomplishment. But of course, as always through history, more and more information about Nature is gathered as time goes by, and much more has now been learned about Nature over the course of the past century, so there is little doubt that a new set of more ideal yet "ultimate equations", so to speak, are likely to be developed on our way to this hypothesized final equation from the now more extensive current pool of accumulated knowledge.

In the specific domain of electromagnetism, the Lorentz force equation is such an idealized equation that summarizes all of what was understood by the end of the 19th century about the nature and behaviour of electrons at the subatomic level. It is in fact an idealized regrouping of the two mathematical developments that for the first time allowed precise control of the motion of free moving electrons trajectories by precise combinations of electric and magnetic field, which was confirmed by the Kaufmann experiments, and by the successful development of many types of high energy accelerators all through the 20th century, from the first cyclotron conceived and built by Lawrence in 1932 [44] to the *CERN Large Hadrons Collider* (LHC) that entered service in 2008.

Being a generalized equation, seemingly summarizing and combining two different equations, it gives by default the impression that a single force results from resolving it. It is indeed generally referred to in the community as "The"

Lorentz force, when in reality two different forces are calculated, one related to the electric field $\boldsymbol{E}$ of the first term and the other related to the magnetic field $\boldsymbol{B}$ of the second term. They act in opposition to each other on the charge of the moving electron, and force it to move in a straight line when they are equal [31].

In this author's opinion, the various aspects of high energy accelerators operation and charged particle beams control are best introduced by Stanley Humphries Jr.'s outstanding reference work titled *Principles of Charged Particle Acceleration* [43].

Note that the symbols used by Lorentz in Equations (6) and (7) to represent velocity and the gamma factor were respectively ω and k, the latter now better known as the Lorentz factor. In the present work, the modern symbols v for velocity and γ for the Lorentz factor will be used.

Coefficient l on its part was function of the velocity, and resolves to 1 when velocity is zero, as does the γ-factor, such as in Equation (8). Let us note also, that coefficient l was meant by Lorentz to relate the electron velocity to the state of motion of an observer. But since we will be studying the Lorentz force equation in relation with the absolute velocity of the electron strictly according to the amount of its instantaneous amount of momentum energy, this coefficient resolves to 1 in all equations and will be ignored.

In his article [1], Lorentz defines the γ factor with his Equation (3):

$$\frac{c^2}{c^2-w^2}=k^2 \quad \text{that is:} \quad k=\frac{c}{\sqrt{c^2-w^2}} \tag{9}$$

Expanding this form to the limit reveals the more familiar modern form:

$$\gamma=k=\frac{c}{\sqrt{c^2-v^2}}=\frac{1}{\sqrt{\frac{c^2-v^2}{c^2}}}=\frac{1}{\sqrt{1-\frac{v^2}{c^2}}} \tag{10}$$

But although this last form is generally mentioned in reference works, calculations with scientific pocket calculators are hugely simplified when the following form is used, that leaves only one fraction in the expression:

$$\gamma=\frac{c}{\sqrt{c^2-v^2}}$$

The historical notation used by Lorentz in his 1904 article having now become unfamiliar to most, we will now convert Equations (6), (7) and (8) to their equivalent modern notation before proceeding to their analysis.

The electron rest mass is now symbolized by m_0. This is its well understood invariant mass when its velocity is theoretically zero, that is, when classically assuming that its momentum energy is also zero. This rest mass is established as a physical constant with value m_0 = 9.10938188E−31 kg. Equation (8) will now be resolved as follows when calculated from the Coulomb equation perspective:

$$m_0=m_{1(v=0)}=m_{2(v=0)}=\frac{e^2}{6\pi c^2 R}=\frac{e^2}{4\pi\varepsilon_0 r_e c^2}$$

Resolving to:

$$m_0 = \frac{e^2}{4\pi\varepsilon_0 r_e c^2} = 9.10938188\text{E}-31\,\text{kg} \tag{11}$$

In which r_e is the physical constant known as the classical electron radius (r_e = 2.817940285E−15 m), used with the Coulomb equation to calculate the invariant rest mass of the electron.

Equation (7) represents what Lorentz identified as the varying mass of an electron accelerating in a direction perpendicular to its direction of motion on its trajectory in space, and that he describes as behaving "as if" it was larger than its rest mass m_0 represented by Equation (11), and that corresponds to the rest mass of the electron m_0 plus a mass increment $\Delta m = \gamma m_0 - m_0$, the latter corresponding to the velocity related transverse mass increment whose energy was identified in 2003 by Paul Marmet as causing the increase of the electron magnetic $\boldsymbol{B}$ field as its velocity increases on its trajectory [12] [45], and that corresponds to the second term of the Lorentz force equation $F = e(\boldsymbol{v} \times \boldsymbol{B})$, as will be clarified further on:

$$m_2 = \frac{e^2}{6\pi c^2 R} kl = \gamma m_0 = \gamma \frac{e^2}{4\pi\varepsilon_0 r_e c^2}$$

Resolving for transverse acceleration to:

$$m_2 = \gamma m_0 = m_0 + \Delta m = \gamma \frac{e^2}{4\pi\varepsilon_0 r_e c^2} \tag{12}$$

And finally, Equation (6), representing what Lorentz identified as the varying longitudinal "mass" of the accelerating electron, that is, its measurable inertia in its direction of motion, and that he describes behaving "as if" it was higher for the same velocity than mass $m_2 = m_0 + \Delta m$ represented by Equation (12), itself larger than m_0 represented by Equation (11). The only additional energy that can be identified as acting longitudinally on a moving electron happens to be its momentum energy ΔK.

Note that the term "mass" to which Lorentz refers to, represented by the term m_1, includes the ΔK momentum energy of the electron as a mass increment because in his era, it still was not clearly established that its momentum energy component $\Delta K = \gamma m_0 v^2/2$ did not become part of its actual varying mass $m_2 = \gamma m_0 = \Delta m + m_0$ [12], although it behaves longitudinally—but not transversely—with the same inertia as if it was part of the longitudinal varying mass, which allows, pending further clarification moving on, to momentarily assume that ΔK converts to a "theoretical mass increment", by dividing it by c^2 to clearly establish Lorentz's logical development:

$$m_1 = \frac{e^2}{6\pi c^2 R}\frac{\mathrm{d}(kl\omega)}{\mathrm{d}\omega} = \left(\frac{\gamma m_0 v^2}{2c^2} + \gamma m_0\right) = m_0 + \frac{\Delta K}{c^2} + \Delta m$$

$$= \gamma m_0\left(\frac{v^2}{2c^2} + 1\right) = \gamma \frac{e^2}{4\pi\varepsilon_0 r_e}\left(\frac{v^2}{2c^2} + 1\right)$$

Resolving for longitudinal acceleration to

$$m_1 = \left(\frac{\gamma m_0 v^2}{2c^2} + \gamma m_0 \right) = m_0 + \frac{\Delta K}{c^2} + \Delta m = \gamma \frac{e^2}{4\pi\varepsilon_0 r_e c^2} \left(\frac{v^2}{2c^2} + 1 \right) \quad (13)$$

Of course, equation conversions without numerical confirmation are never guaranteed to be error free, so before proceeding further, we will verify the resulting equations with a well known relativistic velocity to confirm that the modernized forms of Lorentz's equations have been correctly established and remain conform to Lorentz's intent.

The reference relativistic velocity that we will use is the typical reference relativistic velocity related to the mean energy E = 4.359743085E−18 j of the electron when stabilized in the stationary action ground state of the hydrogen atom v = 2187647.561 m/s, whose wavelength is λ = 4.556335261E−8 m and frequency is f = 6.579683909E15 Hz, one cycle of which was discovered by de Broglie in 1924 to correspond to exactly one unit of energy represented by Planck's constant h as clarified in a 2017 article [46] and its 2021 expanded final republication [47], which explains why the frequency of all photons emitted by electrons de-exiting as they return to their stable rest state orbital in atoms are resonance harmonics of this fundamental resonance state.

Of course, the fact that this mean amount of carrying energy E = 4.359743085E−18 j adiabatically induced in the electron when captive in the least action stationary resonance orbital of the hydrogen atom means in no way that the electron is moving on a closed orbit about the proton at this relativistic velocity, as put in clear perspective in Reference [48] and its expanded final republication [49]. This particular issue will be clarified in Section 10.

When so stabilized, the momentum energy component $\Delta K = m_0 c^2(\gamma - 1)$ = 2.179871903E−18 j of this carrying energy can be understood as applying a constant pressure in its vectorial direction of application, if its velocity is impeded, to the fulcrum identified in Reference [26] of the point-like behaving electron, mathematically representable as an infinitesimal ds area, a pressure which is equal in numerical value to the force calculated with the first component the Lorentz force equation, that is, the force calculated with the Coulomb equation for the electron in motion, a_0 being the Bohr radius:

$$P = F = e\boldsymbol{E} = \frac{e^2}{4\pi\varepsilon_0 \alpha_0^2} \quad (14)$$

But it was clearly established in all electron acceleration experiments ever since the first experiments carried out by Kaufmann [7] that when such an amount of carrying energy—momentum energy ΔK plus an equal amount of transverse magnetic field energy corresponding to $\Delta \boldsymbol{B}$ or Δm_m is induced in free moving electrons, they will effectively move at this velocity on their individual trajectories, as verified and confirmed by Planck, Poincaré, Bucherer, Newman and Einstein himself [42], as previously put in perspective. The $\Delta \boldsymbol{B}$ form will be explained further on.

We will now compare the increased amount of mass displayed by a moving

electron with respect to the reference m_0 rest mass formulated as Equation (11), as a measurable longitudinal mass m_1 and a measurable transverse mass m_2 according to Lorentz's conclusions about Kaufmann's experimental data for the chosen test reference relativistic velocity of $v = 2187647.561$ m/s.

The m_0 mass equation of the electron at rest is reposted here for convenience:

$$m_0 = \frac{e^2}{4\pi\varepsilon_0 r_e c^2} = 9.10938188\text{E}-31\ \text{kg} \tag{11}$$

The m_2 transverse mass when the electron is moving at velocity $v = 2187647.561$ m/s—resolving the γ-factor with this velocity—will be:

$$m_2 = \gamma m_0 = \gamma \frac{e^2}{4\pi\varepsilon_0 r_e c^2} = 9.109624417\text{E}-31\ \text{kg} \tag{15}$$

The m_2 mass provided by Equation (15) involves that the transverse magnetic energy of the electron increases by an amount corresponding to the Δm_m mass increase measurable transversely [48] [49], that will be equal to:

$$\Delta m_m = \frac{\mu_0 e^2 v^2}{8\pi r_e c^2} = 2.425337715\text{E}-35\ \text{kg} \tag{16}$$

Then:

$$\begin{aligned} m_0 + \Delta m_m &= 9.10938188\text{E}-31\ \text{kg} + 2.425434194\text{E}-35\ \text{kg} \\ &= 9.109624423\text{E}-31\ \text{kg} \end{aligned}$$

The measurable longitudinal m_1 "mass" of the electron moving at velocity $v = 2187647.561$ m/s will then be:

$$m_1 = \left(\frac{\gamma m_0 v^2}{2c^2} + \gamma m_0\right) = 9.109866957\text{E}-31\ \text{kg} \tag{17a}$$

That can also be calculated by addition:

$$\begin{aligned} m_1 &= m_0 + \left(\Delta K/c^2 + \Delta m_m\right) \\ &= 9.10938188\text{E}-31\ \text{kg} + 4.850868388\text{E}-35\ \text{kg} \\ &= 9.109866957\text{E}-31\ \text{kg} \end{aligned} \tag{17b}$$

We observe that longitudinal "mass" m_1 is higher than transverse mass m_2 by an amount of 2.425402292E−35 kg, and that transverse mass m_2 is higher than rest mass m_0 by a practically equal amount of 2.425434576E−35 kg, for a total amount in excess of rest mass m_0 of 4.850836867E−35 kg. Converting this amount to energy in joules resolves to 4.359714795E−18 j, which is the amount of energy adiabatically induced in the electron when stabilized at the mean ground state distance from the proton in a hydrogen atom, and that can be directly calculated with the Coulomb equation to be applying a pressure of $P = e^2/4\pi\varepsilon_0 a_0^2$ = 8.238721806E−8 Newtons oriented towards the proton against the infinitesimally small *ds* area of the fulcrum of the electron stabilized in axial resonance state at this mean distance of the proton, or alternatively, to the infinitesimally small *ds* area of the fulcrum of an electron moving on a free trajectory at relativistic velocity $v = 2187647.561$ m/s.

In summary, when transposed to modern classical/relativistic notation in replacement of Lorentz's era archaic classical/relativistic notation, this is what Lorentz calculated from the data provided by Kaufmann, calculations that were subsequently confirmed as valid by the leading edge physicists of his era, including Einstein ([42], p.159), and whose electromagnetic calculation equation—the Lorentz force equation—has been in use ever since by the engineering community, but that the decision to ignore it in the establishment of the Special Relativity Theory that these leading edge physicists made in 1907, in agreement with Einstein's opinion, caused it not to be referred to nor to be taken into consideration afterwards in the subsequent search to resolve the gravitational issue.

6. Discoveries Made after the Fateful 1907 Turning Point

In 1923, Louis de Broglie came to the conclusion that the only way that the electromagnetic spectra of the different atoms could be explained was that all electrons must be stabilized in a series of resonance states by observing that the frequencies of their electromagnetic spectra were all ordered according to a sequence of integers similar to the known macroscopic resonance states, and discovered that this sequence was related to the energy of one cycle of the energy of the electron stabilized in the Bohr orbit of the hydrogen atom, a cycle whose energy value is exactly equal to Planck's constant [46] [47] [48] [49] [50].

Three years later, end of 1926, Erwin Schrödinger introduced the wave equation that he meant to account for the resonance states and resonance volumes hypothesized by de Broglie [51].

One year earlier, end of 1925, Werner Heisenberg had published the first paper on his matrix mechanics, meant to account for the distribution of the energy within the limits of the resonance volumes that de Broglie hypothesized and that Schrödinger's wave equation was to shortly define [52]. Both methods were then merged into what was to become Quantum Mechanics, later completed by Feynman's path integral method [53]. The very idea that electronic orbitals were supposed to be resonance volumes of a permanently localized electron as understood by de Broglie and Schrödinger was eventually neglected and forgotten.

The common purpose of de Broglie and Schrödinger was to eventually succeed in establishing the emission mechanics of the electromagnetic photons that constitute the electromagnetic spectra of atoms when electrons stabilize in the various stationary action resonance states that they become captive into when captured by ionized atoms, and the absorption mechanics of such photons that cause electrons to be ejected from these stationary states [48] [49] [54] [55]. More on this emission and absorption mechanics further on.

But given the fact that Heisenberg's method seemed to locate the electron with greater probability in the vicinity of the Bohr radius, his method was preferred in the community, and the search to identify the mechanics of emission and absorption of electromagnetic photons by electrons in their capture and ejection processes from stationary resonance states in atoms did not raise any real interest in the community, as put in perspective in References [48] [49]. This me-

chanics has now been established [12] [13].

In 1932, Cockcroft and Walton succeeded in converting some nucleon mass into energy by bombarding Lithium$_{7,3}$ nuclei with protons (Hydrogen$_{1,1}$), that resulted in the fusion of protons with Lithium nuclei, momentarily producing unstable Beryllium$_{8,4}$ nuclei that immediately fissioned into two Helium$_{4,2}$ nuclei, releasing a large amount of electromagnetic energy during the process. Einstein considered this experiment as proof that the mass of elementary particles was made of energy, meaning that it proved the validity of equation $E = mc^2$ [56], proving by the same token that the mass of atomic nuclei was made of electromagnetic energy.

A further step was taken a year later, in 1933, when Carl Anderson proved experimentally that photons of energy of 1.022 MeV or more emitted as electromagnetic by-products of cosmic radiation spontaneously convert into massive electron/positron pairs when they graze massive atomic nuclei [57], a process that came to be known as "materialization". Expanding our understanding of the relationship between "energy" and "mass", Anderson's discovery confirmed that the energy of which the "mass" of electrons and positrons is made was also "electromagnetic" in nature, prompting de Broglie to formulate in 1937 a first hypothesis on a possible internal electromagnetic structure of free-moving photons consistent with Maxwell's equations [24], which led to the subsequent establishment of the LC and field equations of electromagnetic photons [25] [26] (see Equations (27) and (28) further on).

In the last years of a whole life of relentless continued research, at the beginning of the 1950's, Einstein had become more and more doubtful about his SR and GR theories and finally communicated the opinion that gravitation likely follows the pattern of electromagnetism. However, the whole orthodox community apparently immediately rejected his recommendation without a second look, as reported in 1995 by Archibald Wheeler, a major physics community opinion leader ([58], p.391):

"*A distinguished physicist even published in his very last years' works, the main point of which is to claim that gravitation follows the pattern of electromagnetism. This thesis, we cannot accept, and the community of physics, quite rightly, does not accept.*"

In 1969 was published the outcome of the experimental exploration of the internal volumes of protons and neutrons, carried out by means of electron beams energetic enough to penetrate the volume occupied by individual protons and neutrons to non-destructively scatter against whatever could be physically existing inside their volumes, at the freshly activated Stanford Linear Accelerator (SLAC).

Martin Breidenbach and his colleagues reported that some of the electrons had been back scattered in a highly inelastic manner from inner scatterable components of protons and neutrons, that were thus physically detected [59], which revealed that these particles had to be electrically charged and also had to have

masses in the same range as that of the electron, this latter characteristic revealed by the highly inelastic character of the electron rebounds observed. Deep analysis revealed that two types of such inner elementary components physically existed with masses different from each other, both close to the electron rest mass, that were named up and down quarks, in relation with the theories of Gell-Mann and Zweig that had previously predicted their existence.

In 1997, Kirk McDonald *et al.* succeeded at the SLAC facility to produce electron/positron pairs by focusing two beams of photons towards a single point in space, one beam involving photons of energy in excess of the 1.022 MeV decoupling threshold, with no heavy nucleus present in the vicinity, which established that electromagnetic energy could convert to mass by mere photons interactions without any mass present in the vicinity [60].

In the same year, although the results of the experiment were not published until 2013, an important seminal experiment was performed with magnetic fields whose two poles coincide geometrically with the center of the field [10], which by similarity must be the case for the electron's magnetic field, since it always behaves in a punctual way during experiments of mutual collisions, a behavior which was confirmed one year later, in 2014, by an experiment carried out with real electrons [61], which confirms that such fields interact according to the inverse of the cube of the distances separating them, and that their two poles cannot be simultaneously present at this punctual location.

7. Resumption of Fundamental Research in Electromagnetism

In fact, it was the realization that no fundamental research had been conducted in electromagnetism since at least the 1950s, as revealed by Wheeler in 1995 ([58], p.391), despite Einstein's recommendation, that triggered the resumption of such research in the late 1990s. This section presents a brief overview of the different aspects of electromagnetism discussed in a series of articles published between 2000 and 2013, aiming at drawing more attention to the electromagnetic aspect of physical reality.

Investigation of the historical record clearly showed that all research carried out in electromagnetism for the past century had been attempts at reconciling electromagnetism as established from the Ludwig Lorenz gauge perspective with the classical concepts of the Lagrangian and the Hamiltonian, themselves grounded on the classical principle of universal conservation of energy.

Further investigation revealed that Maxwell disagreed with the Lorenz gauge concept because it negated the possibility of the existence of the displacement current that was built-in into the Gauss equation for the electric $\boldsymbol{E}$ field, which is in fact the Coulomb equation minus one of its built-in double charges, since that in the Coulomb equation, as analyzed in References [62] [63], the force, and consequently the energy $E = d \cdot F = q^2/4\pi\varepsilon_0 d$ induced by the force into each charge depends on no other criterion than on the inverse of the distance d sepa-

rating both charges, a distance that can only vary in an infinitesimally progressive manner between all moving charged particles, which is inconsistent with the very principle of universal conservation of energy that underlies the classical concepts of the Lagrangian and the Hamiltonian when applied to charged particles, but are in direct harmony with Maxwell's initial interpretation and most importantly, with de Broglie's hypothesis about a possible inner structure of free moving electromagnetic photons [24]:

$$F = q\boldsymbol{E} = q_1 \frac{q_2}{4\pi\varepsilon_0 d^2} = \frac{q_1 q_2}{4\pi\varepsilon_0 d^2} \tag{18}$$

Let us note here that Equation (18) is the fully expanded form of the first term of the Lorentz force equation (see Equation (5) analyzed earlier).

In July of 2000, after 160 years of neglect, attention was drawn again at CONGRESS-2000 to Maxwell's initial interpretation from which emerged the trispatial geometry that offered a new potential development perspective in the exploration of the subatomic level of magnitude, that is, a perspective that was out of reach of the Lorenz gauge approach [64].

Three years later, in 2003, Paul Marmet, probably the most advanced experimenter and theoretician in electromagnetism of the late 20th century, brilliantly established the following equation, by means of a flawless derivation from the Biot-Savart equation, that revealed that the increasing energy of the transverse magnetic field of the accelerating electron is the same energy measurable as an increase in the transverse mass of the electron, that Kaufmann had measured 100 years earlier as increasing with the velocity of the electron [45], *i.e.* the energy that Lorentz had related to the transverse mass m_2 of the electron (see Equations (7) and (12) analyzed previously), *i.e.* an identity relation that had not been noticed at the time:

$$\frac{\mu_0 e^2}{8\pi r_e}\frac{v^2}{c^2} = \frac{m_e}{2}\frac{v^2}{c^2} \tag{19}$$

In 2007, a first wave of derivations from this revolutionary equation was published in the same *Kazan State University* engineering journal that had previously published Marmet's article [65], that separated for the first time the invariant magnetic $\boldsymbol{B}$-field of the invariant rest mass of the electron, from the variable magnetic $\Delta\boldsymbol{B}$-field of its carrying-energy, the sum of both turning out to be the $\boldsymbol{B}$-field of the second term of the Lorentz force equation (see Equation (2) previously analyzed).

The invariant magnetic field of the rest mass of the electron being:

$$\boldsymbol{B} = \frac{\mu_0 \pi e c}{\alpha^3 \lambda_C^2} \tag{20}$$

in which λ_C is the electron Compton wavelength, and the variable magnetic field of the electron carrying-energy being:

$$\boldsymbol{B} = \frac{\mu_0 \pi e c}{\alpha^3 \lambda^2} \tag{21}$$

in which λ is the wavelength of the carrying energy of the electron. The sum of Equations (20) and (21) provides the combined $\boldsymbol{B}$-field of the second term of the Lorentz force equation:

$$\boldsymbol{B} = \frac{\pi\mu_0 ec\left(\lambda^2 + \lambda_C^2\right)}{\alpha^3\lambda^2\lambda_C^2} \tag{22}$$

Similarly, Marmet's derivation allowed separating the invariant electric $\boldsymbol{E}$-field of the invariant rest mass of the electron:

$$\boldsymbol{E} = \frac{\pi e}{\varepsilon_0\alpha^3\lambda_C^2} \tag{23}$$

from the variable $\boldsymbol{E}$-field of its carrying-energy:

$$\boldsymbol{E} = \frac{\pi e}{\varepsilon_0\alpha^3\lambda^2} \tag{24}$$

The vectorial product of which provides the combined $\boldsymbol{E}$-field of the first term of the Lorentz force equation:

$$\boldsymbol{E} = \boldsymbol{E} \times \Delta\boldsymbol{E} = \frac{\pi e}{\varepsilon_0\alpha^3}\frac{\left(\lambda^2 + \lambda_C^2\right)\sqrt{\lambda_C\left(4\lambda + \lambda_C\right)}}{\lambda^2\lambda_C^2\left(2\lambda + \lambda_C\right)} \tag{25}$$

In the case of the $\boldsymbol{E}$-field of the electron in motion, the vectorial product approach is required due to the fact that the trispatial geometry reveals that the invariant $\boldsymbol{E}$-field of the electron rest mass is perpendicular to the variable $\Delta\boldsymbol{E}$-field of its carrying energy within electrostatic Y-space [16].

Simultaneously varying wavelength λ of the electron carrying-energy of both Equations (22) and (25) over the whole range of possible values effectively yields the very same relativistic velocity curve obtained by Abraham and Bucherer, that Einstein candidly admitted "fit the observed curve considerably better than the curve obtained from relativity theory" previously quoted from Abraham Pais' book ([42], p.159) by means of this equation for straight line motion of the electron:

$$v = \frac{\boldsymbol{E}}{\boldsymbol{B}} \tag{26}$$

It can be noted that Equations (20) and (23) establishing the precise invariant $\boldsymbol{E}$ and $\boldsymbol{B}$ fields corresponding to the rest mass of the electron are only specific cases of the general Equations (21) and (24) that can be used to calculate the whole possible range of $\boldsymbol{E}$ and $\boldsymbol{B}$ fields for free moving photons.

Equations (21) and (24) also allowed converting the photon LC equation previously developed [66] to the corresponding fields equation [25] [26]:

$$E\vec{I}\vec{i} = \left(\frac{hc}{2\lambda}\right)_X \vec{I}\vec{i} + \left[2\left(\frac{e^2}{4C}\right)_Y \left(\vec{J}\vec{j}, \vec{J}\vec{j}\right)\cos^2(\omega t) + \left(\frac{Li^2}{2}\right)_Z \vec{K}\sin^2(\omega t)\right] \tag{27}$$

$$E\vec{I}\vec{i} = \left(\frac{hc}{2\lambda}\right)_X \vec{I}\vec{i} + \left[2\left(\frac{\varepsilon_0\boldsymbol{E}^2}{4}\right)_Y \left(\vec{J}\vec{j}, \vec{J}\vec{j}\right)\cos^2(\omega t) + \left(\frac{\boldsymbol{B}^2}{2\mu_0}\right)_Z \vec{K}\sin^2(\omega t)\right]V \tag{28}$$

A second outcome of this first wave of derivations from the Marmet Equation (19) is the following variation on the Coulomb equation that allows calculating the energy of any free moving photon by use of its wavelength, without any need to use the Planck constant:

$$E = hf = \frac{e^2}{2\varepsilon_0 \alpha \lambda} \tag{29}$$

After it had become obvious that the LC and fields equations of the carrying-energy of the electron were identical to the LC and fields equations of free moving photons, and that even the actual invariant rest mass of the electron could be represented by such LC and Fields equations [16] [66] [67]:

$$E\vec{\mathbf{0}} = m_e c^2 \vec{\mathbf{0}} = \left[\frac{hc}{2\lambda_C}\right]_Y \vec{J}\vec{i} + \left(2\left[\frac{(e')^2}{4C_C}\right]_X \left(\vec{I}\vec{j}, \vec{J}\vec{j}\right)\cos^2(\omega t) + \left[\frac{L_C i_C^2}{2}\right]_Z \vec{K}\sin^2(\omega t)\right) \tag{30}$$

and

$$m_0\vec{\mathbf{0}} = \frac{V_m}{c^2}\left\{\left[\frac{\varepsilon_0 \boldsymbol{E}^2}{2}\right]_Y \vec{J}\vec{i} + \left[2\left(\frac{\varepsilon_0 v^2}{4}\right)_X \left(\vec{I}\vec{j}, \vec{J}\vec{j}\right)\cos^2(\omega t) + \left(\frac{\boldsymbol{B}^2}{2\mu_0}\right)_Z \vec{K}\sin^2(\omega t)\right]\right\} \tag{31}$$

it became possible to upgrade Newton's non-relativistic kinetic energy equation to full relativistic electromagnetic status and to develop equations that required only the energies or the wavelengths of the electron and of its carrier-photon to trace by this means the very same relativistic velocity curve as Equation (26) and those of Abraham and Bucherer [68]:

$$v = c\frac{\sqrt{4EK + K^2}}{2E + K} \tag{32}$$

and

$$v = c\frac{\sqrt{\lambda_C(4\lambda + \lambda_C)}}{2\lambda + \lambda_C} \tag{33}$$

This development allowed for the first time in history to derive the Lorentz γ-factor equation (Equation (9)) from an electromagnetic equation in an article published in 2013 [68], that is, from Equation (33) previously mentioned, thus confirming the relativistic nature of the adiabatic energy induced in all elementary charged particles by the Coulomb interaction, classically represented via the first term of the Lorentz force equation $F = e\boldsymbol{E}$ or directly by the Coulomb equation (see analysis of Section 5).

Then, by means of the general form of the Coulomb Equation (29) and of this other form developed even further, considering that ($\varepsilon_0 = 1/(4\pi c^2 \cdot 10^{-7})$ [69],

$$F = \frac{1}{4\pi\varepsilon_0}\frac{e^2}{d^2} = \frac{4\pi c^2 \cdot 10^{-7}}{4\pi}\frac{e^2}{d^2} = e^2 \cdot 10^{-7}\frac{c^2}{d^2} \tag{34}$$

it became possible to unify all classical force equations by deriving the fundamental force equation $F = ma$ from each of them [69], which mathematically demonstrates that all classical force equations, even Newton's so fundamental F

= *ma* acceleration equation, all are variations of the Coulomb force equation.

$$F = G_p \frac{M_p \cdot m_e}{r_o^2} = k\frac{e^2}{r_o^2} = ev\boldsymbol{B} = e\alpha\boldsymbol{E} = m_e a \tag{35}$$

The trispatial geometry that naturally emerges from Maxwell's initial interpretation then allowed establishing a coherent decoupling mechanics of electromagnetic photons of energy exceeding the minimal decoupling threshold of 1.022 MeV into massive electron/positron pairs when the required circumstances are met [16].

The mechanics of the Einstein-de Haas and Barnett effects could then be explained [11] in context of the trispatial geometry, as well as the difference between permanently compensated stable orbital or resonance stationary action states and uncompensated metastable orbital or resonance states at the astronomical magnitude level as well as at the subatomic magnitude level.

The electron magnetic moment anomaly was then analyzed and explained [70] by revealing the existence of a gyroradius related drift of the electron carrier-photon energy from the $\Delta\boldsymbol{E}$ electric state to the $\Delta\boldsymbol{B}$ magnetic state that was found to match Julian Schwinger's calculations [71] about this so-called anomaly that he carried out in 1948, thus providing in an unexpected way the first clue leading to the explanation of the fractional charges of the up and down quarks.

Actually, when adapting Equations (32) and (33) to establish the gyroradius at the mean ground state distance of the electron in its stationary action orbital in the hydrogen atom, the electron g factor first established by Schwinger as $\alpha/2\pi$ for this orbit naturally falls out of both of these equations:

$$\text{Magnetic drift} = \frac{\delta\mu}{\mu_B} = \frac{\sqrt{4EK + K^2}}{2\pi(2E + K)} = \frac{\alpha}{2\pi} = 1.161386535\text{E}-3 \tag{36}$$

E = 8.18710414E−14 j being the rest mass energy of the electron and K = 4.359743805E−18 j being the carrying energy of the electron in the Hydrogen atom ground state, and

$$\text{Magnetic drift} = \frac{\delta\mu}{\mu_B} = \frac{\sqrt{\lambda_C(4\lambda + \lambda_C)}}{2\pi(2\lambda + \lambda_C)} = \frac{\alpha}{2\pi} = 1.161386535\text{E}-3 \tag{37}$$

λ_C = 2,426310215E-12 m being the electron Compton wavelength and λ = 4,556335256E-8 m being the wavelength of the energy induced at the Bohr radius of the hydrogen atom.

For the first time in history, vacuum constants ε_0 and μ_0 were derived from first principles in Reference [31], and it was demonstrated that Equation (34), on top of allowing all classical force equations to be derived from each other, also is at the heart of all electrodynamics equations, that is, that they all involve charges being accelerated.

Indeed, the inverse product term for term—to take into account the mutual orthogonality of the electrostatic and magnetostatic states—of the two vectorial equations derived from first principles in Reference [31], that account for the

mutually opposite electric and magnetic transverse forces that apply to a moving electron in the trispatial geometry, in agreement with Maxwell's theory:

$$\frac{\overrightarrow{\boldsymbol{F}_{\boldsymbol{B}}}}{\overrightarrow{\boldsymbol{F}_{\boldsymbol{E}}}}=\frac{\overrightarrow{4\pi c^2}}{\overrightarrow{4\pi c^2}}\frac{10^{-7}}{10^{-7}} \tag{38}$$

could be related to the constant expression that emerges from the second partial derivatives equations of the instantaneous magnetic and electric fields of a propagating electromagnetic wave in vacuum with respect to distance and time initially derived by Maxwell, that is,

$$\frac{\partial^2 \boldsymbol{B}}{\partial x^2}=\mu_0\varepsilon_0\frac{\partial^2 \boldsymbol{B}}{\partial t^2} \quad \text{and} \quad \frac{\partial^2 \boldsymbol{E}}{\partial x^2}=\mu_0\varepsilon_0\frac{\partial^2 \boldsymbol{E}}{\partial t^2} \tag{39}$$

Given that this constant is the product of ε_0 and μ_0, which product is equal to $1/c^2$ by structure [31], and also that $\varepsilon_0 = 1/4\pi c^2 \cdot 10^{-7}$ and that $\mu_0 = 4\pi \cdot 10^{-7}$, by converting Equation (38) to its scalar form and substituting these values for their standard symbols ε_0 and μ_0, the constant velocity relation that emerges from Maxwell's second partial derivative Equations (39) can be directly obtained from Equation (38):

$$1=\frac{4\pi c^2 10^{-7}}{4\pi c^2 10^{-7}}=\left(\frac{1}{4\pi c^2 10^{-7}}\right)\left(4\pi 10^{-7}\right)c^2=\varepsilon_0\mu_0 c^2 \tag{40}$$

With regard to the calculation of the speed of light for individual photons, using the wavelength of any photon as the only variable required to establish their $\boldsymbol{E}$ and $\boldsymbol{B}$ fields with Equations (21) and (24), the invariant speed of light can systematically be calculated with the following standard equation:

$$c=\frac{\boldsymbol{E}}{\boldsymbol{B}} \tag{41}$$

From the trispatial fields equation that could be established for the muon particle in Reference [72],

$$m_\mu=\left\{\left[\frac{\varepsilon_0 \boldsymbol{E}_e^2}{2}\right]_Y+\left[2\left(\frac{\varepsilon_0\left(\nu_e+\nu_\mu\right)^2}{4}\right)_X\cos^2(\omega t)+\left(\frac{\left(\boldsymbol{B}_e+\boldsymbol{B}_\mu\right)^2}{2\mu_0}\right)_Z\sin^2(\omega t)\right]\right\}\frac{V_m}{c^2} \tag{42}$$

A coherent mechanics of separation of neutrino pairs that reduces the metastable muon mass to the electron rest mass could be established.

And final development regarding the nature of stable elementary particles at the subatomic level from the trispatial perspective, Einstein's conclusion that energy has to be a physically existing substance, and the fact that the Coulomb interaction turns out to be the physical agent that induces this *physically existing substance* in the form of electromagnetic carrying-energy into each charged particle as a function of the inverse square of the distance separating them, the mechanics of the adiabatic establishment of the least action highest intensity stationary action energy states in the universe, that is, the proton and neutron structures, has been analyzed, resulting in the establishment in Reference [73] of the up and down quarks electromagnetic mass fields equations,

$$m_U = \frac{E}{c^2} = \frac{V_{m_U}}{c^2}\left\{S_U\left[\frac{\varepsilon_0 \boldsymbol{E}_U^2}{2}\right]_Y + \left(2 - S_U\right)\left[2\left(\frac{\varepsilon_0 v_U^2}{4}\right)_X \cos^2\left(\omega t\right) + \left(\frac{\boldsymbol{B}_U^2}{2\mu_0}\right)_Z \sin^2\left(\omega t\right)\right]\right\} \quad (43)$$

and

$$m_D = \frac{E}{c^2} = \frac{V_{m_D}}{c^2}\left\{S_D\left[\frac{\varepsilon_0 \boldsymbol{E}_D^2}{2}\right]_Y + \left(2 - S_D\right)\left[2\left(\frac{\varepsilon_0 v_D^2}{4}\right)_X \cos^2\left(\omega t\right) + \left(\frac{\boldsymbol{B}_D^2}{2\mu_0}\right)_Z \sin^2\left(\omega t\right)\right]\right\} \quad (44)$$

that turn out in the trispatial geometry to be normal electrons and positrons whose mass and charge characteristics are warped into these altered states due to the extreme stresses imposed on them by the intensity of their mutual interactions at such short distances when they reach the ultimate electromagnetic equilibrium states in which they are forced to stabilize as they establish the stable internal structure of protons and neutrons.

Ultimately, the trispatial geometry provides a mechanical explanation to the creation of protons and neutrons from triads of the two possible mixes of electrons and positrons when the local electromagnetic circumstances cause them to be thermal enough to have insufficient energy to escape each others' interaction, which causes them to accelerate and end up ultimately stabilizing as protons and neutrons [73].

This summarily completes the general overview of the main conclusions drawn in the first set of articles published from 2000 to 2013 to establish the internal structure and individual interactions of photons and of the set of stable charged elementary electromagnetic particles of which all atoms are made, from the perspective given by Maxwell's initial interpretation, in light of Einstein's conclusion about the physical nature of energy as a substance, de Broglie's hypothesis about the inner electromagnetic structure of photons, that Einstein understood have to be continuously localized, and of Marmet's discovery that the increase of the transverse mass of accelerating electrons observed by Kaufmann can only be related to a simultaneous increase of their transverse magnetic field.

8. Immediate Implications for the Atomic, Macroscopic and Astronomical Orders of Magnitude

Two other articles were published in 2013, that put in perspective the immediate implications that emerge, at the atomic, macroscopic and astronomical levels, of the conclusions drawn at the subatomic level about the internal electromagnetic structure and the interactions of the set of stable elementary charged particles, in light of the trispatial perspective [74] [75].

In particular, the intensity of the energy released in the form of three highly energetic bremsstrahlung photons—each estimated to be in the vicinity of 155 MeV—that must be emitted upon the evacuation of the momentum kinetic energy of each accelerating charged particle when each electron-positron-electron or positron-electron-positron triad stabilizes in stable stationary action states as neutron and proton at the end of their acceleration sequence [73], has clearly provided a possible explanation for the still unexplained sustained temperatures of 2

to 3 million degrees Kelvin that are often observed with higher peaks in the solar corona.

These temperatures exceeding one million degrees in the corona of the sun are about 200 times those of the photosphere and chromosphere of the sun. This extreme average temperature in the corona turns out to be an equilibrium temperature [76], which is revealed by the fact that it remains constant in spite of the enormous energy losses that the corona undergoes through the constant inwards exchanges with the chromosphere on one hand, and the constant outward ejections of matter via coronal mass ejections (CMEs) on the other, which means that these energy and mass losses must necessarily be compensated for by a yet to be understood constant internal coronal process.

It turns out that according to the mechanics of adiabatic energy increase provided by the Coulomb interaction, which is a function of the inverse of the decreasing distances between charged particles [8], the trio of bremsstrahlung photons of about 155 MeV each, emitted at the moment of ultimate stabilization of each of the two possible initial triads in their final high energy proton or neutron configuration, happens to correspond to a 227-fold increase in the ambient energy level, which falls precisely within the range of excess ambient energy observed in the solar corona, and could sustain these temperatures consistently if nucleons were continuously generated in the corona in a continuous low-level chain reaction that remains to be understood [74].

Such a permanent low level chain reaction nucleon generation process that would have been active since the Sun ignited even opens the door to the possibility that all of the matter making up the planetary system and other lesser bodies in the solar system could have been generated locally, and also opens the door to the possibility for us to learn to control this nucleon generation process as a source of reaction mass for propulsion requirements and as a source of unlimited energy for other purposes, as will be put in clearer perspective in Section 12.

The adiabatic nature of the progressive energy increases of all electrons captive of the orbitals that define the volume of each atom, as they are progressively forced closer to each their central atomic nucleus due to the mutual increasing pressure that atoms exert on each other as the depth increases within celestial bodies, also brings an explanation to the adiabatic increase in temperature with increasing depth in the Earth, which is estimated to reach 5100 degrees Kelvin in the center of the planet [77], and also brings a mechanical explanation to the actual cause of ignition of stars and subsequent high intensity chain reaction fusion for proto-stellar masses as they reach the ignition threshold pressure in their center during their initial phase of primordial hydrogen accumulation [75].

What leads to this conclusion is that the adiabatic compression suffered by the electronic escorts of all atoms as pressure increases with depth in large celestial bodies such as stars masses, becomes sufficient when critical ignition temperature is reached in their central areas for the unreleasable adiabatic energy induced in the electrons of hydrogen atoms for these electrons carrier-photon to

reach the 1.022 MeV threshold decoupling level at a distance of less than 0.2E−15 meter from their proton nucleus, which is the radius of the volume within which protons and neutrons structures reach the highest energy stationary state of least action that can be established in the universe by natural application of the Coulomb force, that is, the volume within which the pressure axially applied by the ΔK momentum energy of their charged sub-components falls into equilibrium against the mutually repulsive counter-pressure exerted between these subcomponents by their magnetic energy.

Now, the energy in excess of that of the rest mass of a moving elementary charged particle such as an electron, has clearly been established from the Kaufmann data and the Lorentz analysis, combined with Marmet's discovery in light of de Broglie's hypothesis regarding the possible inner electromagnetic structure of free moving photons, as having the very same electromagnetic characteristics as those of such free moving photon, as analysed in References [25] [26] [68], the only difference being that in the case of a moving electron, this excess energy has to "carry", so to speak, the intrinsically inert massive electron to which it is related, hence the name carrier-photon adopted to qualify the electron carrying energy.

It can then be fully expected that this carrier-photon, if it were to reach the 1.022 MeV threshold, would also be susceptible to decoupling into an electron-positron pair, which, being totally thermal, given that all of its 1.022 MeV of energy converts to the two 0.522 MeV/c^2 masses of the newly decoupled pair, will be unable to evade maximum interaction with the formerly carried electron now also totally thermal given that its carrying energy has now disappeared, the threesome will immediately start accelerating due to their mutual Coulomb interactions into converting to neutron state, releasing the 3 highly energetic bremsstrahlung photons inherent in the neutron creation process, a neutron that would then immediately form a deuterium nucleus with the close by proton [75].

Thus would be initiated the high energy chain reaction that ignites a proto-star mass, a self-sustaining chain reaction due to the now increasing pressure at the center of the star being born, that will then create more and more neutrons as the mass of the new star increases.

One particular aspect of the compression of the electronic orbitals of atoms larger than the hydrogen atom, due to mutual increasing pressure of atoms against each other with the increasing depth in celestial bodies, is that, contrary to the shrinking of the distances between the electronic escorts and the central nucleus of each atom involved, the nucleons (protons and neutrons) making up their nuclei are so relatively far inside their electronic escorts that this adiabatic pressure applied from outside to their individual electronic escorts is insufficient to force a similar contraction of the nucleon triads located far inside their electronic escorts.

Considering that if the proton in a hydrogen atom was theoretically enlarged

to reach the size of the Sun, its electron would stabilize as far as Neptune if its mean ground state distance was extended in the same proportion. Then contrariwise, as the pressure increases with depth in celestial bodies against the electronic escorts of neighboring atoms, the nuclei of these atoms will obviously drift closer to each other as the overall volume of each electronic escort shrinks.

The logical outcome can only be a progressive "outward pull" on the internal charged structure of each nucleon of all nuclei now getting closer to each other, with the Coulomb force increasing between them as the distances separating the nuclei decrease, since the force induces an increasingly large outwardly directed momentum kinetic energy amount in each charged quark of each triad. As each triad increases its internal interaction radius, their relativistic-velocity/energy-level can only decrease in proportion, reducing their total rest mass accordingly.

Reference [75] analyzes all aspects of this adiabatic variation of atomic and nucleon volumes—and relativistic masses in the latter case—as a function of the local state of the Coulomb interaction dependent gravitational gradient. Particularly informative are the 3D graphs in Section VIII of Reference [75].

Another unexpected and somewhat surprising outcome of the immediate reactivity of all charged elementary particles captive in atomic structures to any variation in the unidirectional pressure applied by their momentum energy, is that when small masses are taken away from a large mass such as that of the Earth, the "outward pull" exerted on their electronic escorts as well as on the internally charged subcomponents of their nuclei by the sum of the charged particles constituting the atoms of the large Earth mass will decrease as the small mass gains altitude, causing the internal mutual Coulombian interaction between the charged particles within each atom of the small mass moving away to contract their electronic orbitals towards their respective nuclei, as well as those of the nucleons of which their nuclei are made, thus causing more momentum kinetic energy directed towards the nucleus of each atom to be induced in each captive electron of the orbitals being brought closer to their respected nuclei.

The consequence, easily observable in some cases, such as in the case of atomic clocks whose periodicity depends on the specific frequency of 9,192,631,770 Hz—measured at ground level—of the bremsstrahlung photon emitted when an electron jumps to its reference hyperfine electronic rest orbital after having been excited to jump to the other reference metastable electronic orbital, located further away from the nucleus of the caesium 133 atom, is that the frequency of this bremsstrahlung photon will increase with altitude due to the fact that the two reference orbitals move closer to the caesium nuclei as the distance between the earth's mass and the clock increases, a behavior that, from the point of view of the special relativity theory is interpreted as if time was running faster at higher altitudes, while in reality the increased frequency of the photon emitted during the reference jump is obviously due, from the electromagnetic point of view, only to the fact that the reference jump is now performed between reference levels that are now closer to the nucleus of each caesium atom. This issue is also analyzed in Reference [75].

Another related outcome is the as yet unresolved issue of the of the so-called "*anomalous residual acceleration directed towards the Sun*" of the Pioneer 10 and 11 spacecrafts on their hyperbolic trajectories leading them out of the solar system, which is an issue that was observed to also affect other spacecrafts [78]. All of these spacecrafts behave exactly as if they were slightly more massive as they run their trajectories than was measured at the surface of the Earth before launch, which is also consistent with the analysis that we have just summarized, and which was completely analyzed in Reference [75].

Many other "apparently unexplained" observations are also addressed and analyzed in Reference [75], that also proposes an easy to carry out experiment that could confirm the dependence of nucleon masses to the local intensity of the gravitational gradient. See Subsection 11.1 further on in this regard.

It must be mentioned in context that the rest mass of the electron on its part is not dependent on any variation of the gravitational gradient since it is a confirmed elementary particle—in the sense that it is clearly established that it is not made of smaller subcomponent particles in mutual interaction like protons and neutrons, that are not elementary particles, but systems of elementary particles captives of their mutual electromagnetic interactions, just like the solar system is not a heavenly body, but a system of heavenly bodies captive of their mutual electromagnetic interactions. The rest mass of the electron turns out to be universally invariant, whatever the local intensity of the gravitational gradient.

9. Other Developments at the General Level

Seven more articles were published from 2016 to 2020, all selected for republication in final form from 2017 to 2021 as chapters in specialized collections that preselect articles deemed worthy of interest from the global offer that few researchers and doctoral students find the time to investigate in depth to locate all new developments relevant to their respective disciplines. A brief overview of the issues addressed in each of these articles will be provided in this section.

The first of these articles explains the seminal considerations that initially led to the development of the expanded Maxwellian space geometry that naturally emerges from Maxwell's initial interpretation, and to the establishment of the LC and fields equations of the free-moving photon according to Louis de Broglie's hypothesis about the double-particle photon [24], that Marmet's derivation had led to understand mandatorily had to possess the same internal electromagnetic structure as the carrier energy of free-moving electrons [45] [65], originally published in 2016 [25], republished in final version in 2021 [26].

Then followed in 2016 a second article [8] that was republished in final version in 2021 [9], analyzing in depth the adiabatic nature of the physically existing energy which is continuously induced by Coulomb interaction in all charged particles as a function of the inverse of the distances that separate them, and whose quantities vary in an infinitesimally progressive manner as the distances vary, in addition when they are in the process of approaching each other, or in

subtraction when they are in the process of moving away from each other. This article also proposes a high-tech experiment meant to demonstrate the adiabatic nature of the energy that would result from the acceleration of the electron-positron-electron or positron-electron-positron thermal triads that would lead to the creation of neutrons and protons according to the trispatial perspective [73]. See Subsection 11.2.

A synthesis article was then published in 2017 [62], republished in final version in 2020 [63], to put into perspective the sum of the separate analyses presented in the series of articles published since 2000, to serve as a guide in the 2017 monograph that laid the foundation of an electromagnetic mechanics grounded on Maxwell's initial interpretation, by regrouping all of these articles [79]. This article also analysed in depth the concept of "force" as applicable to the subatomic level in light of the possibility that electromagnetic energy could be a physical substance as concluded by Einstein [23]—see Section 2 on this issue—and presents a first glimpse of the universal gravitational gradient that emerges from these considerations. See Section 13 for a final analysis of the gravitational issue from this perspective.

In 2017 article [46] was published, republished in a final version in 2021 [47], that puts in perspective the sum of what all experimental scattering experiments revealed about stable and metastable elementary particles. It also gives an overview of the past attempts to expand the spatial geometry in view of solving the currently unresolved issues that 3D-4D spatial geometry seemed insufficient to solve, and explains how the trispatial geometry leads to a first possible mechanical explanation of the existence of charges. Then follows an overview of the set of new electromagnetic mechanics equations that now come in complement to the first equation of electromagnetic mechanics, that is, the Lorentz force equation, subject of this in-depth analysis.

In 2018 was published article [48], republished in final version in 2020 [49], that analyzes how electromagnetic mechanics, classical/relativistic mechanics and quantum mechanics can be reconciled. For example, the very first definition of mass strictly from electromagnetic parameters is proposed:

$$\Delta m_m = \frac{\mu_0 e^2}{8\pi r_e}\frac{\left(\boldsymbol{E}/\boldsymbol{B}\right)^2}{c^2} = 2.425337726\text{E}-35\ \text{kg} \tag{45}$$

which is in fact Equation (16) in which parameter v is replaced by its electromagnetic version $v = \boldsymbol{E}/\boldsymbol{B}$—Equation (26)—that defines the moving electron velocity, taking as usual the standard example of the energy induced in the electron when stabilized in the hydrogen atom ground state (relativistic velocity v = 2187647.566 m/s is used to resolve the γ-factor), Δm_m being the relativistic mass contribution of the transversely oscillating electromagnetic energy of the electron carrier-photon, which, when combined with the following equation to calculate the related momentum energy:

$$\Delta K = m_0 c^2\left(\gamma - 1\right) = 2.179784832\text{E}-18\ \text{j} \tag{46}$$

allows establishing the following equation to describe the total electron carrier-photon energy:

$$\text{Electron carrier-photon} = \Delta K + \Delta m_m c^2 = 4.359743805\text{E}-18 \text{ j} \quad (47)$$

which is the direct classical/relativistic equivalent of LC Equation (27) and fields Equation (28), and when adapted as follows, provides the longitudinal m_1 mass measured by Kaufmann as established by Lorentz:

$$m_1 = \Delta K / c^2 + \Delta m_m + m_0 \quad (48)$$

while m_2 resolves to:

$$m_2 = \Delta m_m + m_0 \quad (49)$$

The first mechanical explanation of the stability of the hydrogen atom is also proposed in this article in context of the trispatial geometry, as it puts in perspective how the momentum energy of the electron applies a constant pressure on the infinitesimal surface of the electron's fulcrum to maintain in a stable resonance state the constantly oscillating magnetic energy spheres of the electron and of the subcomponents of the proton, which are in permanent mutual repulsion due to the fact that their magnetic spins are in constant parallel alignment by structure, as established in Reference [10].

The simultaneous invariant electron oscillation frequency and the varying carrier-photon oscillation frequency that need to be considered in establishing the electromagnetic mechanics compliant varying beat wave equation of a free moving electron and the additional varying proton oscillation frequency that must be added to the varying beat wave equation of the free moving electron when the electron is captive in axial resonance state in atomic orbitals are described, although the related varying beat wave equations have not yet been developed.

Two years later, in 2020 was published article [12], selected the same year for republication in final version [13], that summarizes all aspects of the electromagnetic mechanics of the set of stable elementary electromagnetic particles at the subatomic level, that emerges from Maxwell's initial interpretation. The considerations previously put in perspective in References [62] and [63] are also elaborated on in greater details, including the establishment of the trispatial energy-momentum equation:

$$E_e = \Delta K + \Delta m_m c^2 + m_0 c^2 \quad (50)$$

The main feature of references [12] and [13] is the introduction of the emission mechanics of a bremsstrahlung electromagnetic photon when an electron becomes captive in orbital resonance state in an ionized atom, and also the absorption mechanics of an incoming electromagnetic photon that energizes a captive electron sufficiently for it to jump to a further away metastable orbital from which it instantly jumps back to its rest orbital, releasing the bremsstrahlung photon that we record as part of this atom's spectrum, or is completely ejected from the atom, which is the photon emission and absorption mechanics

that Schrödinger and de Broglie had been looking to establish in the 1920's [54] as put in perspective in References [48] [49].

In 2020 also was published a second monograph [80] regrouping and synthesizing these last three articles [12] [48] [62], as an introduction to electromagnetism according to Maxwell's initial interpretation.

Reference [80] also relates the 4 first level electromagnetic equations for the subatomic order of magnitude that were developed during the first wave of derivations after Paul Marmet's discovery, published in 2007 [65], with the 4 Maxwell equations that were synthesized by Heaviside for application at the atomic, macroscopic and astronomical levels of magnitude.

Finally, an article was republished in final version [81] that was initially published in 2016 [82] that proposed the hypothesis of the progressive establishment and growth of the Universe strictly from electromagnetic considerations, as suggested by Einstein towards the end of his life, describing the possibility of the progressive adiabatic energy increase in the universe from a hypothetical zero energy level in vacuum at the beginning of the universe inspired by Maxwell's initial interpretation, as an alternate solution to the Lorenz gauge grounded Quantum Field Theory (QFT) postulated stable conservative zero-point energy level in vacuum and to the conservative Big Bang theory that emerges from Einstein's General Relativity theory.

The function of time in the universe is also analyzed from this new perspective, and going a step further than References [12] into addressing the gravitational issue, Reference [81] summarily describes the universal trispatial vector field that emerges from Maxwell's initial interpretation, as a possible alternative to the universal Hilbert vector field that emerges from the Lorenz interpretation. See also Section 13.

10. Gyroradius vs Mean Distance of Electromagnetic Resonance

In the Special and General Relativity Theory, the concept of force does not exist as such and is completely replaced by inertial motion due to the axiomatically hypothesized space-time curvature in which astronomical masses are deemed to always follow the least action slope of the space-time curvature. From this perspective, inertial motion can occur only if a body has not reached some stationary action state along the slope of some geodesic line, which establishes any variation of the longitudinal inertia of massive bodies as being due to its motion, thus to its instantaneous velocity during its acceleration along such a geodesic line. The transverse inertia of moving bodies seems not to be addressed from this perspective except for local rotational inertia variation of a moving body.

For charged and massive particles in electromagnetism on the other hand, the kinetic energy induced by the underlying Coulomb interaction is fundamental and does not depend on the motion of the particle, but strictly on its distance from other charged particles. It is the momentum half of the physically present

energy induced in excess of the energy of which the inert mass of the particle is made, that causes the particle to move if its motion is not hindered in some way by local electromagnetic circumstances, in which case this momentum energy will instead apply an equivalent pressure in the vectorial direction in which it would force the electron to move if not hindered.

When a "charged" electron is moving freely, its momentary "relativistic" mass, made of its rest mass m_0 plus the Δm_m mass increment provided by the other half of the energy induced in excess of that of which its rest mass is made, can at face value be interpreted as being velocity dependent, but it must be emphasized that its instantaneous velocity at any given moment is dependent only on the instantaneous amount of ΔK carrying-energy momentum that the electron is adiabatically induced with at this moment. See Reference [68].

It must also be made clear that when a "charged" electron ends up captive in resonance state in an atom's orbital, even if the local electromagnetic equilibrium may not allow it to actually translate about the nucleus, both ΔK and Δm_m components of its carrying energy remain physically present, increasing its mass in the case of the Δm_m electromagnetic component, and applying pressure in the direction of the nucleus in the case of its ΔK momentum component, against the resistance offered by the mutually repelling parallel spin aligned magnetic energy spheres of the electron and of the elementary subcomponents of the atomic nucleus [48] [49].

It is on account of their incompatibility with the permanent physical presence of the adiabatically varying energy with distance of the momentum ΔK of the electron and of its transverse electromagnetic complement Δm_m that the traditional classical conservative concepts of momentum, of the Lagrangian and of the Hamiltonian become unable to properly account for the stability of the hydrogen atom, because they are grounded on the traditional concept that momentum depends on velocity, and which is supposed to vanish in favor of a non-existent "potential energy" when the motion of the particle is impeded. Reference [62] analyzes this issue in depth. In an electromagnetic context, an expressed velocity is not a cause, but an effect whose expression depends on the freedom of motion allowed to a "charged" mass by the local electromagnetic equilibrium state. See Section 10.8 in Reference [79] on this particular issue.

One other example of what more clearly perceiving that the carrying energy of elementary charged particles is a physically existing substance allows understanding is the following. In frozen water, for example, the momentum energy of individual molecules is obviously completely hindered, but when its melting point is reached, some motion of the individual molecules becomes possible and the pressure applied by their momentum energy can now be expressed as motion against the now weakened resistance of the surrounding molecules, causing the molecules to easily move about with respect of each other in the now liquid mass. This brings a mechanical explanation to the motion of microscopic particles observed in liquids, known as the Brownian motion, as these microscopic particles—relative giants compared to the individual molecules of which the liquid

is made—are now repeatedly collided against by the now more freely moving molecules of the surrounding liquid [27] [28]. When in gaseous state, each molecule is now freed from any hindrance, and the ΔK momentum energy of each molecule can be fully expressed as a velocity.

Another example of the cause/effect reversal involved in a well-known physical process as considered from the electromagnetic perspective, is the case of the adiabatic compression of gases. Adiabatic compression is classically defined as causing an increase in the temperature of a gas, whereas it can be understood from an electromagnetic point of view that it is the reduction of the volume in which a gas is captive that causes the increase in temperature, by making the gas molecules—all made of charged elementary particles—getting closer to each other, each of them consequently undergoing an adiabatic increase of their carrying energy, which increases their momentum, therefore their speed and their longitudinal inertia, which in turn causes the increase in the pressure that they exert on the walls of the enclosure.

Whenever the term "translating" is used in this article for simplicity's sake with regard to electrons or up and down quarks captive in stable electromagnetic resonance states in orbitals inside atoms and nuclei, it must be kept in mind that such translation motion is at best theoretical, and that the term only implies that the energy required to potentially sustain such translating motion is permanently induced in the particle, and can just as well sustain an axial resonance oscillation of the particle about the mean distance of its orbital resonance volume with respect to the center of the atom, an axial oscillation maintained by the pressure exerted by its momentum energy towards the nucleus that prevents the mutually repelling oscillating parallel-aligned magnetic spin energy spheres of the electron and nucleus from flying away from each other (see References [48] or [49]).

So, given that the same amount of energy is induced adiabatically in a charged electron, whether it is actually orbiting the proton in an isolated hydrogen atom, as de Broglie assumed, or simply oscillating locally in axial resonance, as the electromagnetic perspective reveals, no conceptual or mathematical error is introduced by referring to the electron as oscillating on a closed orbit, on which the momentum energy is expressed as a velocity, or simply oscillating locally axially towards the nucleus, during which oscillation the momentum energy is expressed as a pressure towards the nucleus of the atom, both cases being the two limiting cases of the same process. See Reference [70].

So, in context, even if the Lorentz force equation was successfully developed to account for and control the actual relativistic velocities and trajectories of moving electrons, it can just as well account for the axial resonance motion of electrons and nucleon charged subcomponents if they are prevented from actually moving on closed orbits inside atoms.

Reference ([43], Equation (3.38)) provides the standard equation used in all existing closed circuit high energy accelerators, including the recently activated LHC, to calculate the radius of a closed orbit for a charged particle (see also Reference [70] for complementary developments). This equation was established by

equating the second term of the Lorentz force equation, that is, Equation (2) developed by Heaviside, with the fundamental acceleration equation $F = ma$:

$$F = q(\boldsymbol{v} \times \boldsymbol{B}) = ma = \frac{\gamma m_0 v^2}{r} \tag{51}$$

In which, when isolating the radius of the orbit to be established and simplifying provides the following equation:

$$r = \frac{\gamma m_0 v}{q\boldsymbol{B}} \tag{52}$$

In which the magnetic $\boldsymbol{B}$ field of the moving particle can be calculated with Equation (22). The interesting feature about this standard equation that was meant to calculate actual circular orbits for moving charges, is that it is directly adaptable to calculate the mean distance of the resonance volumes of electronic orbitals with respect to their central nuclei, whether the electron happens to be possibly orbiting the nucleus as in the case of an isolated hydrogen atom [83] or is simply captive locally in axial resonance, by using the invariant rest mass and invariant charge of the electron:

$$d = \frac{\gamma m_0 v}{e\boldsymbol{B}} \tag{53}$$

As an example of the potential usefulness of using this equation for this purpose, **Appendix A** provides the method to be used to obtain the estimated atomic radii for isolated atoms, as calculated by means of Equation (53), a few examples of which are provided in Table 1.

11. Confirming Experiments

Of course, an analysis leading to the conclusion that even macroscopic masses increase with velocity in sheer contradiction with the observed fact that no experiment with macroscopic masses ever carried out at the surface of the Earth ever gave any clue to this possibility due to their too slow velocities, even if, despite the unawareness in the current physics community—due to lack of referencing—that all physicists of the beginning of the 20th century verified, understood and agreed that the mass of the electron indeed increased with velocity according to the data collected by Kaufmann, requires more proof than only such logical reasoning and references to the formal historical accounts of these events that occurred more than a century ago.

All the more so since the same logical reasoning reveals that the rest mass of macroscopic bodies can only vary with the intensity of the local gravitational gradient, and that such variation, if confirmed, would definitely disqualify the conclusion of the 1972 Hafele and Keating experiments [84] that asserts that the increasing frequency of the caesium atoms reference photons with increasing altitude proves that the "velocity" of the "flow of time" increases as the distance increases between the clock and the large mass of the Earth, but would rather prove that this increase in frequency of the reference photons simply is due to

the perfectly natural mass increase of the caesium nucleons with increasing distance from the Earth, which in turns draws in reaction all electronic orbitals closer to the caesium nuclei of the clock, causing the energy, thus the frequency, of the reference photons to consequently increase, leaving the time element completely out of the picture.

It is entirely understandable that such doubts would dominate in the community, given that any measurable macroscopic mass increase with velocity could not begin to be measurable unless velocities achievable with macroscopic masses were way higher than those possible at our macroscopic level, since they would have to reach the 2000 km/sec range to even become measurable, which is easy for electrons at the subatomic level, as revealed by the Kaufmann data. Just like it is understandable, that the physicists of the beginning of the 20th century could have concluded that such mass increase concerned only the subatomic level, given the impossibility to detect any such mass increase for macroscopic bodies.

But we now have such clues even at our macroscopic level that were unavailable 100 years ago, that were provided by the behavior of space probes Pioneer 10 and 11 on their escape trajectories from the solar system [85] [86] [87] [88], due in part to their velocities much higher than those that are possible here on Earth, in relation with the fact that their mass was measured before launch here on Earth before they were raised in altitude to then travel in deep space, far from any large planetary mass. It is to be noted that the behavior observed with the Pioneer 10 and 11 spacecrafts also characterizes the behavior of all spacecrafts, and even of natural bodies in the solar system [78].

A very low tech and easy to carry out experiment was proposed in 2013 [75], mentioned again in 2016 [8] and in 2021 [9], that could simultaneously demonstrate that the rest masses of atoms m_0 increase when the intensity of the local gravitational gradient diminishes, such as when small macroscopic masses are taken up in altitude away from the Earth's surface, and that the velocity of the time flow is unrelated to the process, since it is impossible that the masses of the two types of atoms to be used as test masses in the experiment would increase according to different time rates as they are simultaneously lifted in altitude.

Note that this experiment was also proposed in an article submitted to the *Bureau International des Poids et Mesures* (BIPM) and to the *National Institute of Standards and Technology* (NIST) at the beginning of March of 2011 [89].

11.1. The Equal-Arms Balance Experiment

If protons and neutrons are in reality triads of electrons and positrons that accelerated until they reached a stable stationary action electromagnetic equilibrium state within a volume whose radius is in the 1.2E−15 m range, that would warp their mass and charge characteristics into those observed after they stabilized in up and down quark state, this would mean that the better part of nucleon's masses can only be relativistic in nature since the verified possible mass ranges of the up and down quarks making up their scatterable inner structure have been

experimentally confirmed to amount to barely 2% of the total mass of the proton and 2.4% of the total mass of the neutron. See References [73] and [90].

This relativistic mass must then be related to the highly relativistic velocities or carrying-energy levels—see Section 10—that the up quarks (presumably accelerated positrons) and down quarks (presumably accelerated electrons) have to maintain at the very short mean axial resonance gyroradii at which this electromagnetic equilibrium state forces them to stabilize. These velocities/carrying-energy-levels and all other related parameters are analyzed in Reference [73].

Given that the relativistic velocities—or energy levels—of their internal charged and massive subcomponents would be involved, this means that the measurable masses of protons and neutrons are directly dependant on the local intensity of the Coulomb field gradient that establishes and maintains the level the carrying energy of their charged subcomponents.

Consequently, if a small quantity of atoms is taken away from a large mass such as that of the Earth, these distances between the charged quarks within the nucleons of the small quantity are bound to shorten somewhat as the distance increases between this small quantity and the Earth, due the "diminishing outward pull" of the charged quarks of the atoms making up the large mass of the Earth as a function of the increasing distance, which will unavoidably cause the relativistic-velocities/carrying-energy-levels to increase within the nucleons of the small mass in process of moving away, which in turn will cause an increase of the relativistic energy component of this smaller mass, and thus its measurable mass.

This also means that the less densely packed nuclei of lithium or magnesium for example, are likely to have a nucleon contraction gradient towards their maximum density in deep space—far from any large mass—that would be more pronounced than that of denser elements such as uranium or osmium, as the intensity of the ambient Coulomb field gradient decreases if they are simultaneously lifted in altitude away from the surface of the Earth, given that they contain much fewer nucleons in volumes of about the same order. The diameter of denser atoms being estimated to be only about 3 times that of hydrogen, so the volumes ratio between the lowest density and highest density metals will be lower yet. See **Table 1**.

This can be verified in a very simple manner. Only an equal arms balance would be required to conduct the experiment, in which two equal masses of elements of widely different densities would be set in perfect equilibrium at ground level, or better yet, at the bottom of the deepest mine shaft possible. This assembly would then be lifted in altitude.

Why not 10 km, as was done with the first caesium atomic clocks experiment by Hafele and Keating [84]? If the nucleon contraction gradients really are different for low and high density elements, as hypothesized here, then the side holding the low density element should go down for a moment at least as altitude increases, showing that it is becoming more massive than the higher density element. Proof would then be obtained that the rest masses of nucleons do vary

in accordance with local variations of the gravitational gradient, the consequence of this increase in nucleon density as altitude increases will obviously be a tightening of all electronic orbitals about the now more massive nuclei.

The fact that two types of atoms of two different density display different rest mass increase rates with increasing distance from the Earth mass would also confirm that the velocity of the time flow can in no way be involved, since both types of atoms display these different rest mass increase rates while being simultaneously raised in altitude.

This experiment would also prove out of any possible doubt that varying relativistic velocities and/or varying carrying-energy levels are involved inside nucleons, which would definitely give substance to the possibility that nucleons could come into being by means of the apparently irreversible adiabatic acceleration process allowed from Maxwell's initial interpretation perspective [73].

11.2. Reversing the Adiabatic Process of Nucleon Creation

Other than the previously described low-tech experiment, a high-tech experiment could also be conducted that would directly confirm that up and down quarks actually are simple electrons and positrons whose mass and charge characteristics are warped into these altered states by the extreme stresses imposed on them by these most energetic stationary action equilibrium states that they can potentially be forced into by their mutual electromagnetic interaction, that is, the proton and neutron stable states.

Of course, since protons and neutrons are stable states, the adiabatic acceleration process that causes the increase in energy that ultimately add up to constitute their rest mass seems not to be reversible. But, given that the establishment of a hydrogen atom involves the stabilization of an electron into its least action orbital about a proton according to the adiabatic process described in References [8] [9], accompanied by the ejection of a 13.6 eV bremsstrahlung photon that we can detect, and that this process can be reversed by forcing the ejection of this electron when the same amount of energy of 13.6 eV is communicated to the electron, it can be surmised that the establishment of nucleon structures from triads of the two possible mixes of thermal electrons and positrons could be subject to the same reversible adiabatic process.

This could theoretically be realized by causing an immobilized proton to simultaneously absorb 3 photons of energy slightly higher than 154.8696007 MeV [73], which is the momentum energy that each incoming electron and positron was adiabatically induced with at the moment of final stabilization, and that would have been liberated as three bremsstrahlung photons, as the triad stabilized as the inner charged subcomponents that established the proton stable structure.

Similarly for the neutron, the theoretical simultaneous absorption of 3 photons of energy slightly higher than 155.2289185 MeV [73] should free in this case also the captive positron and the 2 electrons, causing the non-releasable adiabat-

ic energy that they accumulated during their initial acceleration to adiabatically reduce to zero.

In practice however, considering the difficulty inherent in producing and precision guiding such high energy photons, it is possible to consider using more numerous lesser energy photons amounting to or exceeding the required 465 MeV liberation energy being simultaneously absorbed by an immobilized target proton, coming from arrays of high power lasers.

If successful, such an experiment that would simultaneously eject the three inner scatterable subcomponents of a proton as detectable a free moving electron and two free moving positrons, accompanied by the disappearance of the adiabatically induced unreleasable energy that made up the major part of the proton rest mass, which would constitute the physical proof out of any possible doubt of the reality of the processes described in the present analysis, and that up and down quarks really are only normal positrons and electrons whose mass and charge characteristics are warped into these altered states by the stresses imposed on them by these most energetic electromagnetic stationary action axial equilibrium states that electrons and positrons can reach in nature, and by the same token, would bring the proof that the energy induced by the Coulomb interaction is of adiabatic nature.

12. Potential New Sources of Energy

Coming back to the summary description of what occurs in the solar corona presented in Section 8, the possibility that the million + temperatures ambient in the solar corona plasma could be due to some sort permanent slow chain reaction that would continuously generate nucleons as analyzed in Reference [74], the establishment of each of which would release the energy that maintains these temperatures, of course brings to mind the possibility that this process, if confirmed, could possibly be controlled to our benefit [75].

12.1. The Corona Engine

It is not difficult to imagine what could become possible if we were able to consistently manufacture highly massive protons and neutrons from way less massive electron-positron pairs generated from the decoupling of simple massless 1.022 MeV electromagnetic photons [73], that the 3-spaces model clearly hints as being a definite possibility in explaining the corona's extreme temperatures as analyzed in Reference [74], which amounts to manufacturing matter from energy, instead of painstakingly extracting energy from matter as has been our only possibility up to now.

To put it bluntly, and not even taking into account the 227 fold increase in free energy that would results from each nucleon creation, controlling as a first stage such a conversion process of two 1.022 MeV photons into 2.044 MeV/c^2 of mass (two electron-positron pairs), and then as a second stage, adiabatically converting these 2 MeV/c^2 of mass to about 938 MeV/c^2 of effective mass (one

hydrogen atom, that is one proton with its associated electron, or alternatively one neutron with a free positron to spare) through an entirely natural and irreversible acceleration process, would provide us with about 470 times our stake mass wise.

From all probabilities, the solution would fundamentally involve bombarding thin targets of still to be identified materials with massive amounts of highly focused photons of exactly 1.021998 MeV energy, so that the decoupling pairs are immediately thermal and have no momentum energy to spare to escape each other while being produced in sufficiently high concentrations and proximity for the triads to have a chance to engage the mutual interaction acceleration process.

Regarding space exploration, it becomes possible to envision propulsion systems fuelled by such massless photons, some sort of "corona engine" that would eject matter fundamentally created from pure energy in such huge quantities that constant acceleration possibly up to 1 g could possibly be envisioned, in spaceships whose masses would no longer be a factor, as put in perspective in Reference [75].

It would become possible to design hulls as thick as required, profile and magnetize them to efficiently protect crews against cosmic radiation and other particles, mostly produced as cosmic radiation high energy protons collide with the hull, at the huge relative velocities that could be achieved.

Travel to the farthest reaches of the solar system could be reduced to months while trips to Mars for colonization purposes would be reduced to weeks. The nearest stars could be round-trip reached within a time frame compatible with the duration of a human life.

Interestingly, the new generation of Free Electron Laser wigglers (FEL wigglers) already is a type of accelerator that could possibly be modulated to generate precise coherent beams of bremsstrahlung photons of the right threshold frequency required for eventual pair production when directed to appropriate target material.

In 2009 already, experimentalists succeed in accelerating coherent electrons beams in a stable manner to energies of ~0.8 MeV by bombarding a silicon dioxide target with a system of highly collimated double laser pulses at a 500 times per second frequency [91].

This means that if the conclusions which, according to this analysis, emerge from Maxwell's initial interpretation, correspond to reality, the day is not far when the magical carrier-photons 1.021998 MeV energy threshold will be reached, generated by coherent electron beams with such simplified devices that will be more easily adaptable for miniaturization and spacecraft motorization, and provide us with a source of energy available in unlimited quantities when completely controlled.

12.2. The Star Ignition Process

The present analysis reveals that only two stable stationary action resonance in-

tensities of the fundamental electromagnetic energy can be related to mass at the subatomic level, the electron mass energy intensity level and the nucleon mass energy intensity level.

The first stable energy intensity level, involving the establishment of electron and positron masses from free moving photon energy is entirely reversible and involves no adiabatic component [16]. The second one however, involving the establishment of protons and neutrons, also seems to be theoretically reversible, and involves an adiabatic component, unsuspected up to now, that opens up a very promising perspective [73].

With regard to the star ignition process also discussed in Section 8, related to the critical level of compression of hydrogen atoms located at the very center of proto-star mass accumulations, that causes the carrier-photons of the hydrogen atom electrons to come close enough to the central proton of each of these atoms for them to reach the precise decoupling triggering energy level of 1.021998 MeV, that causes the carrier-photon to immediately destabilize into converting to the required totally thermal electron-positron pair, which can immediately trigger the neutron creation process for each atom involved by combining with the now thermal carried electron, it is doubtful that such pressure could be maintained at the exact value required for successive occurrences of such decoupling events to remain totally thermal except fleetingly in any attempt to reproduce this process as a continuous sequence.

There exists however a two step process already well within our current technological capabilities, which consists in first accelerating coherent electron beams to the required precise velocity that would cause their carrier-photons to reach the critical 1.021998 MeV energy decoupling level, which in joules amounts to 1.637420828E−13 J.

As analyzed in Reference [75], this level of energy of the electron carrier-photon is reached at the fantastic critical velocity of 259,627,884 m/s, which is 86.6% of the speed of light. If these electrons are then caused to interact with catalyzing materials that will simulate the proximity of the hydrogen proton nuclei in the central area of stars, the outcome should be crowds of deuterium nuclei that could be used to sustain hydrogen fusion if coupled with the process analyzed for the corona.

Readers familiar with high energy accelerators are well aware that such velocities are easily reached and even exceeded by far up to 99.99…% of the speed of light for beams of collimated electrons in the storage rings of synchrotron accelerators and in betatron accelerators, and this since the 1960's for synchrotrons and since the 1940's for the Betatron design [92].

The following question now comes to mind: Shouldn't we have observed this neutron generating phenomenon quite often for such critical and supercritical velocities? Random occasional nucleon production were quite probably often observed as a fleeting by-product of scattering experiments carried out to observe the outcome of unrelated other elementary particles scattering processes!

It must be clearly understood at this point that the decoupling into pairs of high velocity electron carrier-photons does not depend only on the electrons having reached the critical velocity. Some destabilizing condition must be present to trigger the process at the precise triggering velocity required, otherwise this velocity will be exceeded, which will immediately prevent any pair generated from remaining thermal enough for triads to mutually capture and start accelerating. It is well understood that electrons can be pushed as far into the supercritical range that technology will allow without any decoupling of their carrier-energy to occur.

At the precise critical velocity required however, the least interference in the path of an electron beam by any other particle in the immediate vicinity of the beam, be it stray or planned, is likely to trigger decoupling. The explosive traces of such occurrences must have been recorded for the past 5 decades and these records remain available for eventual re-study.

But since the traditional purpose of all experiments carried out in high energy accelerators have been attempts at detecting ever more massive partons that technology allowed, these collisions have traditionally been carried out at the highest possible velocities. The carrier-photons' energy of the particle beams then systematically exceed the precise amount of 1.021998 MeV that must be maintained for the process to trigger, which makes it doubtful that more than a few stray neutrons would have been directly produced, which seems to be precisely what was observed [93]. See also Reference ([66] Section 20.2).

13. Gravitation

Now that all aspects of the Lorentz force equation have been clearly explained with respect to the direction of motion in which the electron is propelled by its carrier-photon momentum energy, a momentum energy that applies its pressure perpendicularly against the quasi-punctual *ds* surface of the fulcrum that connects it with its longitudinally inert transversely oscillating $\boldsymbol{E}$ and $\boldsymbol{B}$ fields energy complement, on top of against the electron also longitudinally inert invariant rest mass energy, the issue of gravitation in the universe can finally be addressed from this perspective.

Actually, Einstein himself set the stage for this issue to be resolved from the electromagnetic perspective when he concluded in his fourth 1905 article [23] that when a body emits energy in the form of radiation, its mass decreases as a consequence (see Section 2).

Given, according to simple common sense, that if the mass of a macroscopic body is made of a physically existing substance, which is proven by the fact that it verifiably occupies a volume in space that no amount of experimentation allows denying, it can also be concluded that if any amount of this *physically existing substance* is removed from this body, that results in this body's mass diminishing, this removed amount has to continue existing as a *physically existing substance* after removal.

Einstein's conclusion in this regard must be related to a conclusion from his previously published article on the creation and transformation of light into kinetic energy [20]:

"*According to the view that the incident light consists in energy quanta of energy* $(R/N)\beta v$, *the generation of cathode rays by light can be understood as follows. Energy quanta penetrate into the surface layer of the body and their energy is transformed at least partially into the kinetic energy of electrons. The simplest assumption is that a light quantum transfers all of its energy to a single electron; we shall assume that this is the case. However, it shall not be excluded that electrons absorb the energy of light quanta only partially.*"

Obviously, he was considering that the incoming energy quanta convert to momentum energy in a manner that simply adds it to whatever momentum energy the electrons may have previously possessed, that is, a mechanical absorption process that was analyzed and explained in References [12] [13] as previously put in perspective. This means that incoming photon kinetic energy can only be of the same nature as this previously existing momentum energy previously possessed by the electron.

It is quite clear by now that this previously existing momentum energy of the electron is induced by the Coulomb interaction, given that electrons are charged particles. And this is what establishes the difference between the classical concept of momentum energy, and the electromagnetic concept of electromagnetic momentum energy, an electromagnetic momentum energy that we know now makes up only half of the total energy amount induced by the Coulomb interaction, and that "when emitted by a body in the form of radiation causes its [longitudinal] mass to decrease" as Einstein concluded in his fourth 1905 article [23].

This means in turn that this electromagnetic momentum energy can only be a "physically existing substance" that keeps on existing while electrons are captive within atomic structures prior to the moment when it is emitted in the form of radiation, a condition that Einstein identified with respect to macroscopic bodies as causing a decrease in the mass of the body [23], and that when this electromagnetic momentum energy is unable of manifesting its existence as a velocity of the electron, can consequently only exert a corresponding pressure in the same vectorial direction.

The question now is: Exerting a *pressure* against what exactly?

In the case of the point-like behaving electron, this pressure will obviously be exerted against the point-like location that the electron is known to occupy in space whenever it is recorded as scattering point-like against any other elementary particle, a point-like location that must logically coincide with the center of the energy quantum of which the measurable rest mass of the electron is made.

This point-like location can be mathematically represented as an infinitesimal *ds* surface, as first introduced in Section 3, an idealized infinitesimal surface deemed to represent the actual fulcrum, or "point of application" on which the momentum energy exerts its pressure against the center of the electron energy quantum.

Let us now consider how this point of application of the momentum energy pressure of a photon or carrier-photon can be represented in the trispatial geometry.

With reference to **Figure 1**, the vector cross-product of the ***E*** and ***B*** fields, resulting in a third vector perpendicular to the first two is a quite familiar reference in the physics community (**Figure 1(a)**). To establish the trispatial geometry, each of these three linear vectors needs to be expanded into a full 3D vector space of its own (**Figure 1(b)** and **Figure 1(c)**), Y-space representing an idealized "*electrostatic space*", in which the energy displays electric characteristics, while Z-space represents an idealized "magnetostatic space", that will be the seat of all magnetic characteristic of energy, and finally X-space representing the idealized "normal space" within which momentum energy remains located in constant unidirectional mode, applying a *pressure* to the central point-like location at which the three mutually perpendicular vector spaces meet at the center of any physically existing electromagnetic energy quantum [12] [13] [25] [26].

Conceptually speaking, the universal vacuum as defined in Quantum Field Theory (QFT) can be overlaid by a vectorial Hilbert space that establishes an overall continuous vector field [94] [95] [96], each individual vector of which requires two point-like objects to be defined.

Similarly, in the alternative electromagnetic concept of an absolute void with zero energy as it could theoretically have existed at the beginning of the universe, a zero energy that would have increased adiabatically to the level which is ambient in the universe today, a minimum of two point-like behaving trispatial electromagnetic photons must have appeared simultaneously for the first electromagnetic relationship to have existed, since the individual existence of each of the two photons depends on the simultaneous existence of the other, since this existence depends on their mutual interaction. In the case of point-like behaving electromagnetic particles, pairs of electric charges of opposite signs are mandated by structure.

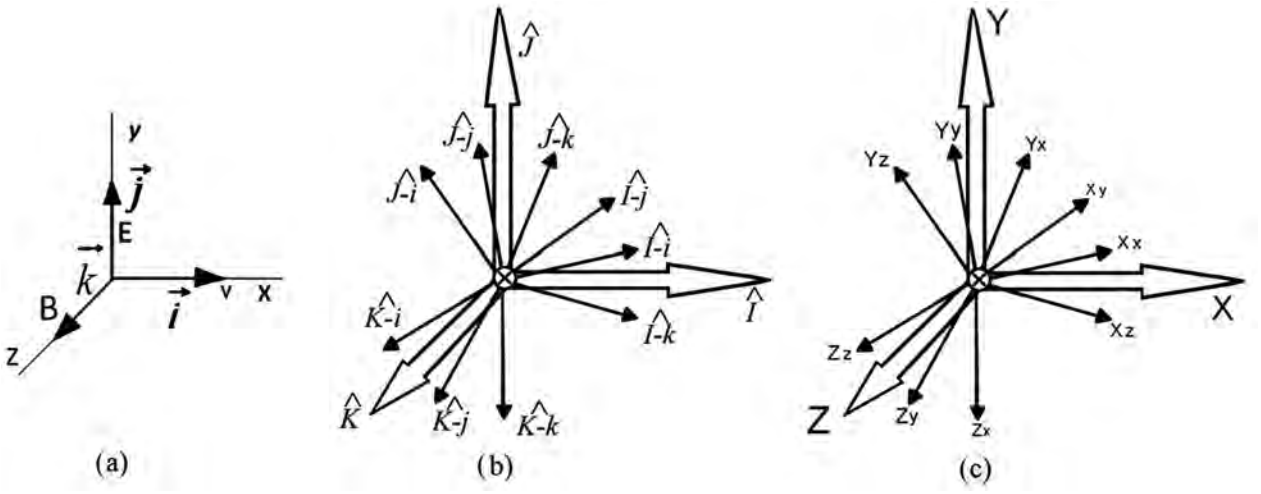

Figure 1. The Major and minor vector sets applicable to the trispatial geometry.

So, a pair of opposite signs charges would give rise in X-space to a pair of oppositely oriented vectors representing the momentum energy of each member of the pair, oriented so as to map their tendency to move towards each other with a progressively increasing adiabatic energy, function of the inverse of the diminishing distance separating them, while a pair of like signs charges would give rise to a pair of oppositely oriented vectors representing the momentum energy of each member of the pair, oriented so as to map their tendency to progressively decrease their adiabatic energy as they move away from each other as a function of the same inverse of the distance rule.

For the vectorial and energy symmetry to be maintained, two more pairs of opposite vectors are established in standing mode at the level of each point-like behaving particle, perpendicularly to the momentum vector, within Y-space for one pair, and within Z-space for the other, each pair being perpendicular to the other by structure, each pair cyclically reversing direction and inducing the other perpendicular pair in alternance in stationary standing mode with respect to the particle's point-like location at the frequency of the energy of the particle represented in the trispatial orthogonal vector structure.

What is interesting about this thee-way mutually perpendicular vector structure is that if the amount of energy represented by the two oscillating transverse pairs is made equal by structure to the energy represented by the momentum vector [81], since they represent a physically existing energy substance cyclically moving from one maximum to another oriented perpendicularly, then by structure, the energy oscillating transversely is subjected to two acceleration sequences perpendicular to each other, whose maximum velocity will reach but cannot exceed the speed of light, when half of the energy *substance* has transferred from one orientation to the other, if the velocity of the *substance* is to return to zero when at maximum in either perpendicular orientation [12] [13]; the half-half equilibrium between the momentum energy half and the transversely oscillating energy half being what ensures that the momentum energy of the particle establishes the invariant speed of light of the photon in vacuum, which was mathematically confirmed in References [31] and [67] for both transverse and longitudinal velocities.

First will now be presented a series of figures that were developed to illustrate the internal oscillation of the energy within elementary electromagnetic particles in the trispatial geometry. Then will be addressed the relation between the charges of the elementary particles of which all atoms are made and gravitation.

The representation of **Figure 2** is an exploded sequence of the successive transverse states that the oscillating half of an electromagnetic photon's energy travels through during one of its transverse oscillating cycles, first introduce in Reference [67], and of the unidirectional momentum energy half-quantum that propels the transversely oscillating half at the speed of light in vacuum.

The same description applies to the carrier-photon of an electron in free motion, with the difference that in addition to propelling its transverse oscillating

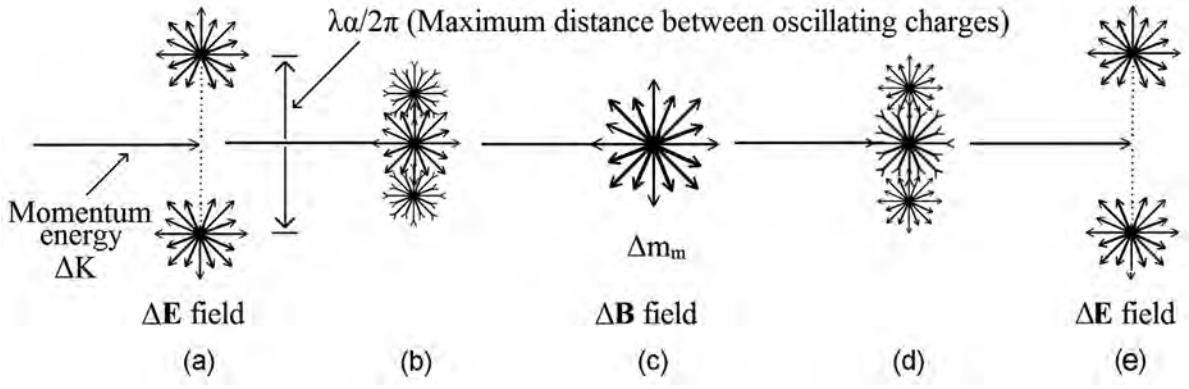

Figure 2. Representation of the transverse oscillation cycle of the electromagnetic half-quantum of a photon or of an electron carrier-photon.

inert other half, the momentum energy of the carrier-photon also has to propel the inert transverse rest mass energy of the electron—not illustrated in **Figure 2**, causing the ratio propelling-momentum-energy/propelled-transverse-energy to limit the momentum component to forever account for less than half of the sum total of the energy of which the carrier-photon and the carried-electron are made, thus preventing the electron from ever reaching the speed of light, as analyzed in Reference [68].

The representation of **Figure 3** shows the same sequence with the successive aspects of the transverse oscillation cycle regrouped on the same transverse plane with respect to the momentum energy of the quantum, both the longitudinal momentum half and transverse oscillating half of the carrier-photon energy being united into a single quantum through the central quasi-punctual location within each photon or carrier-photon that also acts as the fulcrum against which the momentum energy is applying its pressure, in this plane wave treatment representation.

The representation of **Figure 4** describes the internal oscillating field energy structure of the rest mass of the electron, of the up quark state and of the down quark state, corresponding to Equation (31) for the electron rest mass, to Equation (43) for the up quark rest mass state and to Equation (44) for the down quark rest mass state. Equation (31) was established in Reference [16] and the neutrinic field was analyzed in Reference [72]. Equations (43) and (44) were established in Reference [73].

Let us note that the carrying-energy of the electron is not represented in **Figure 4**. The combined energy of the electron rest mass and of its carrier-photon can be calculated with Equation (32) from their separate energy values, and with Equation (33) from their separate wavelengths. The combination of their trispatial fields equations is available as Table I in Reference [16].

The $\boldsymbol{E}$ fields of the electron, of the up quark and of the down quark correspond to their respective electric charges, which are the only charges that exist inside the hydrogen atom. By structure, the electron stabilized in the hydrogen atom ground state has a charge of C_e = 1.602176462E−19 Coulomb, and the three

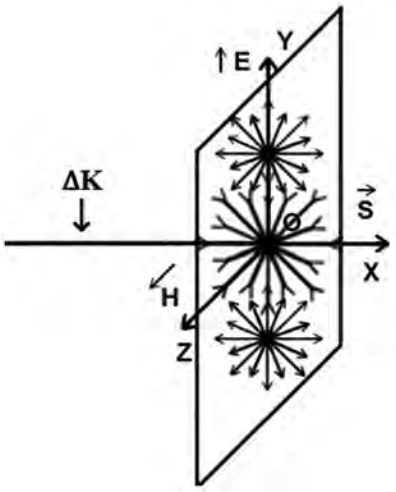

Figure 3. The plane wave concept being applied to a permanently localized photon or carrier-photon.

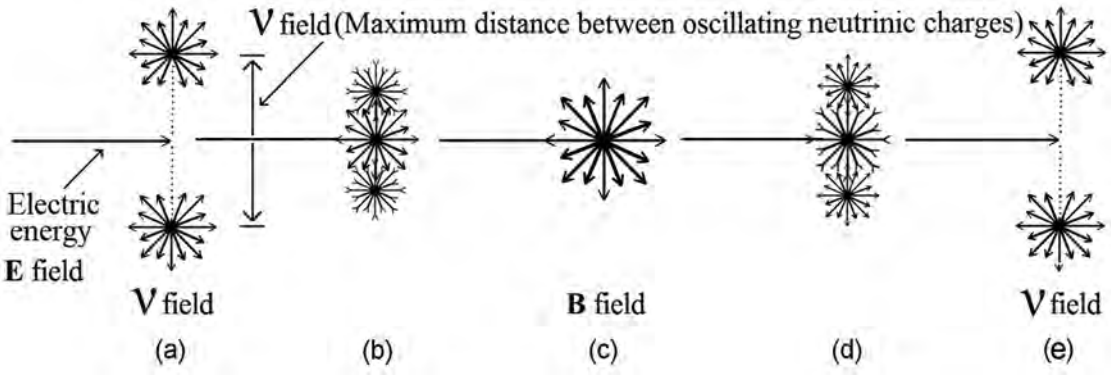

Figure 4. Representation of the transverse oscillation cycle of the invariant magnetic field corresponding to half of an electron invariant rest mass and of the invariant electric field of the other half of its invariant rest mass.

charges of the proton are two up quark charges C_u = 1.068117641E−19 Coulomb, and one down quark charge C_d = 5.340588207E−20 Coulomb, for a total of 4 charges making up the internal structure of the hydrogen atom. They are being constantly induced carrying energy by the permanently present underlying Coulomb interaction as a function of the inverse of the distances separating them, and these energy levels are subject to vary according to any variation in intensity of the local gravitational gradient that determines these distances.

Consequently, from the electromagnetic perspective, the hydrogen atom is not a system of two massive bodies in mutual interaction as still currently considered in classical/relativistic mechanics, but is rather a system of four charged electromagnetic elementary particles in mutual interaction, stabilized in electromagnetic resonance stationary action state [62].

The same transposition from the traditional perspective of interacting masses to the perspective of interacting electromagnetic charged elementary particles seems to be required for all existing atoms as well as for all macroscopic and astronomical sized masses, so that it becomes possible to clearly understand how

the gravitational gradient is dependent on the Coulomb interaction.

This in no way implies that calculations carried out according to the masses interaction perspective are inappropriate or inexact, only that the strict masses interaction perspective does not allow relating the universal Coulomb interaction to the universal gravitational gradient, due to the absence of any reference to the known intimate relation that physically exists between the invariant charge of the electron and its invariant rest mass in all current theories, and this, despite the fact that this relation was clearly established by Einstein himself in his 1910 article [14], as analyzed in References [80] and [81]:

"*We can, for example, obtain in this way the equations of motion of a material point of mass m carrying an electric charge e* (*for example an electron*) *and subjected to the action of an electromagnetic field. We know, in fact, the equations of motion of a material point at the moment when its velocity is zero. According to Newton's equations and the definition of the electric field strength, we have*."

$$(2)\quad m\frac{\mathrm{d}^2x}{\mathrm{d}t^2}=e\boldsymbol{E}_x \quad ([14], \text{p. } 143)$$

To analyze a tentative first draft procedural example to realize this transposition operation from the traditional perspective of interacting masses towards the perspective of interacting charges at the general level, we will use both the hydrogen atom internal mass structure and its internal charges structure as a test case.

From this perspective, the hydrogen atom mass involves adding the standard mass of the electron to the standard mass of the proton (m_e = 9.10938188E−31 kg and m_p = 1.67262158E−27 kg), that is, m_h = 1.673532518E−27 kg.

Let us now calculate the force applied to a hydrogen atom at ground Earth level by means of the established acceleration value due to gravity at mean Earth ground level [11]:

$$a=\omega^2 r=\frac{v^2}{r}=g=9.80665\ \mathrm{m/s^2} \tag{54}$$

Let us note that this standard acceleration value is the mean acceleration value between the precise acceleration of 9.83208 m/s^2 at the poles and the precise acceleration of 9.78036 m/s^2 at mean sea level at the equator [90]. The force obtained with the mean acceleration value for a hydrogen atom at the surface of the Earth is:

$$F=m_h\cdot g=1.641174767\mathrm{E}-26\ \mathrm{N} \tag{55}$$

Given that this is the mean force at the surface of the Earth, multiplying this force value by the estimated mean radius of the Earth r = 6378140 meters [90] will give us the amount of adiabatic carrying energy induced in the hydrogen atom at ground level:

$$E=F\cdot r=1.641174767\mathrm{E}-26\times 6378140=1.046764243\mathrm{E}-19\ \mathrm{j} \tag{56}$$

Converting this value into electronvolts for comparison purposes by dividing it by the unit charge of the electron (e = 1.602176462E−19 Coulombs) gives

0.653338922 eV. As established for the energy induced by the Coulomb interaction in the electron stabilized at the mean orbital distance of the ground state of the hydrogen atom, half of this energy self-orients perpendicular to the other half to oscillate between the electric and magnetic states, increasing the measurable mass of the hydrogen atom, while the other half remains unidirectionally oriented toward the center of the Earth as momentum energy, applying its pressure on the hydrogen atom oriented towards the center of the Earth.

Now, given that the hydrogen atom inner structure involves 4 elementary charged particles, and that only two of them are interacting in attraction with the other two, only the possible attraction between these two charges and the charges of opposite sign of the Earth will be considered, since as analyzed in Reference [75] the repelling relations between same sign charges become infinitesimal at very close range and can be ignored, while the attractive relations between opposite signs charges constantly increases with the diminishing distances between them, so the amount of energy calculated with Equation (56) will be shared in equal parts by both attractive charges of the hydrogen atom.

Now, as established in Reference [69], all classical force equations have been proven to be derivable from each other and from the $F = ma$ fundamental acceleration equation—see Equation (35) in Section 7—including the Coulomb force equation. This means that the force just calculated with Equation (55) can be directly related to the Coulomb force equation, in agreement with Einstein's conclusion in his 1910 article previously quoted [14].

It is at this point that the jump can be made from the interacting masses perspective to the interacting charges perspective between bodies lying at the surface of the Earth and the Earth itself. Given that the two charges of the hydrogen atom that will interact in attraction with the opposite sign charges of the Earth can be assumed to be at the same distance from the center of the Earth, given the infinitesimal parallax angle that the diameter of the hydrogen atom offers when considered from the center of the Earth, we will also assume, for simplicity's sake in this demonstration that both have the same electric charge, that is, the charge of the electron. Multiplying then this charge of the electron by 2 gives us the charge of the hydrogen atom that can be put in charges-pairs attractive relations with opposite charges of the Earth:

$$q_1 = 1.602176462\text{E}-19 \times 2 = 3.204352924\text{E}-19\ \text{C} \tag{57}$$

The composite attractive charge of the Earth can then be calculated by isolating q_2 in the standard Coulomb equation (see Equation (14)), using the force calculated with Equation (55), the composite attractive charge of the hydrogen atom calculated with Equation (57) and the radius of the Earth previously given:

$$q_2 = \frac{F 4\pi\varepsilon_0 r_e^2}{q_1} = 2.318254855\text{E}-04 \quad \text{Coulomb} \tag{58}$$

If we then divide q_2 by the unit charge, we obtain the number of attractive charges that theoretically account for half the mass of the Earth:

$$A_E = \frac{q_2}{e} = 1.446941027\text{E}15 \quad \text{attractive elementary charges} \tag{59}$$

Multiplying this value by 2 will then give the estimated number of elementary charges of which the whole mass of the Earth is made (A_E·2 = 2.893882054E15).

Similarly, the attractive force exerted on the Earth mass by the Sun can be calculated with the traditional gravitational equation [69], in which M represents the estimated mass of the Sun (M = 1.9891E30 kg), r represents the mean radius of the Earth orbit (r = 1.4959787E11 m), m represents the estimated mass of the Earth (m = 5.9742E24 kg), G is the gravitational constant (G = 6.673E−11 Newton·m^2/kg^2) [90]:

$$F = G\frac{Mm}{r^2} = 3.543289846\text{E}22 \text{ N} \tag{60}$$

Knowing the composite attractive charge of the Earth established with Equation (58) and using it as charge q_1 in the Coulomb equation, the attractive force of the Sun calculated with Equation (60), and the radius of the Earth orbit, the composite attractive charge of the Sun can be calculated by isolating charge q_2 in the Coulomb equation:

$$q_2 = \frac{F 4\pi\varepsilon_0 r_e^2}{q_1} = 3.805878467\text{E}38 \quad \text{Coulomb} \tag{61}$$

Dividing q_2 by the unit charge, we obtain the number of attractive charges that theoretically account for half the mass of the Sun:

$$A_S = \frac{q_2}{e} = 2.375442754\text{E}57 \quad \text{attractive elementary charges} \tag{62}$$

Multiplying this value by 2 will then give the estimated number of elementary charges of which the whole mass of the Sun is made (A_S·2 = 4.750885508E57).

The same procedure can be applied to all atoms of the periodic table that make up all masses lying at the surface of the Earth and of any other heavenly body, to all masses in orbits in the Solar system and to all masses in the universe, to calculate the number of charges of which they are made and calculate the gravitational force exerted on each of them by means of the Coulomb equation.

Regarding massive bodies resting at the surface of the Earth, that provide our first clues to the reality of gravitation, the weight of an object as measured at the Earth's surface can only be a measure of this pressure exerted by the sum of the individual momentum energies vectorially oriented towards its centre of mass, belonging to half of the whole set of separate charged particles of the atoms that constitute the measurable mass of this object [12] [13]. For example, when we climb on a bathroom scale to verify our "*weight*", it is this pressure that the sum of the momentum energies that this half of the crowd of elementary charged particles, of which our body is made, exerts toward the ground that we are measuring. In other words, what we name "*the force of gravity*" can be seen as an "*impeded velocity*" expressed as a "*pressure*" due to the fact that the unidirectional momentum energy induced in bodies oriented towards the ground cannot

be expressed as motion.

At the astronomical level, the celestial bodies of the solar system seem to be captive in stable stationary action resonance states at mean distances from the Sun similar to that which de Broglie assumed to apply to the electron in the hydrogen atom [48] [49], *i.e.* a state of axial resonance of celestial bodies on closed orbits, limited by very precise minimum and maximum stable distances from the central star, which are their perihelion and aphelion. These two boundary distances combined with the mean radius of the elliptical orbit of each celestial body constitute the three stable references that allow clearly defining the volumes of space visited over time by each celestial body about the central star.

On the other hand, unlike the case of the hydrogen atom, as analyzed in References [48] [49], for which the intensity of the momentum energy level induced in the electron at the mean Bohr radius distance from the proton with respect to the electron mass, that clearly favors a local high frequency axial resonance motion rather than a translational motion on a closed resonance orbit at the same average distance from the proton, the ratio of the adiabatic energy induced in each charged particle of the Earth's mass at the average distance of the Earth's orbit from the Sun, with respect to the energy making up the mass of the Earth, being insufficient to generate such a high frequency axial oscillation, given the inertia of the macroscopic mass of which each charged particles is captive, rather favors the stabilization of celestial bodies in the observed stationary action closed orbital motion.

The volume of space visited over time by each celestial body about a central star can evolve into fairly complex shapes for celestial bodies that have satellites, which induces beat frequencies that cyclically modify the otherwise regular volumes visited by bodies that do not have satellites. In fact, all bodies stabilized in such axial resonance systems mutually influence each other's trajectories and the shape of the resonance volumes that they visit. It is this type of interaction, combined with the occultation process of the central star as these bodies pass between this star and our position in space that allowed the identification of the many planets orbiting nearby stars that have recently been discovered.

14. The Analysis Method

The analysis method used all through the *Electromagnetic Mechanics of Elementary Particles* project is described in Reference [97], republished in final version as Reference [98], and the mathematical method used is described in Section 27 of Reference [99], republished in final version as Reference [100].

15. Conclusions

One major aspect of Lorentz's 1904 article was mentioned but not discussed in this work because it was out of direct context, since it pertains to the reason why Lorentz was proposing his transformations, that is, the apparent impossibility to prove absolute motion. This issue was analyzed as part of this project, but would

require a too lengthy introduction to be addressed as a side issue in this already long article. The pertaining final analysis is available in Subsection 3.5.1 of Reference [80], and in Subsection 17.8 of Reference [26], following a preliminary analysis in Reference [25].

As mentioned in Section 9, the trispatial wave equations of this model remain to be developed. They minimally comprise the varying wave equation required to describe the resonance volume visited by a free moving photon, the varying single beat wave equation required to describe the resonance volume of an electron moving freely, and the varying double beat wave equation required to describe the motion of an electron captive in axial resonance state in an electronic orbital.

A recently published example of wave function development that exemplifies the recent evolution of ideas in new directions in fundamental physics, that the trispatial approach presented in this article is part of, is the development by Declan Trail of interesting wave functions for the electron and the positron, which are stable solutions to the Schrödinger's wave equation [101].

Coming back to the trispatial model, as mentioned in the conclusions of References [8] and [9], considering the relative simplicity of implementation of the experiments described in Section 11, that could confirm whether the initial irreversible acceleration sequence of newly created elementary charged particles is subject or not to the Principle of conservation, and the potentially unlimited energy source that could become available from controlling the process as described in Section 12, if this conclusion emerging from the trispatial model is confirmed, it is to be hoped that the physics community will become interested in having these experiments carried out sooner than later.

Conflicts of Interest

The author declares no conflicts of interest regarding the publication of this paper.

References

[1] Lorentz, H.A. (1937) Electromagnetic Phenomena in a System Moving with any Velocity Smaller than That of Light. In: *Collected Papers*, Springer, Dordrecht, 172-197. https://doi.org/10.1007/978-94-015-3445-1_5 https://en.wikisource.org/wiki/Electromagnetic_phenomena

[2] Michelson, A.A. and Morley, E.W. (1887) *The American Journal of Science*, **34**, 332-345. https://history.aip.org/exhibits/gap/PDF/michelson.pdf

[3] D'Abro, A. (1951) The Rise of the New Physics. Dover Publications, New York.

[4] Poincaré, H. (1905) *Comptes rendus d l'Académie des Sciences*, **140**, 1504-1508. https://www.academie-sciences.fr/pdf/dossiers/Poincare/Poincare_pdf/Poincare_CR1905.pdf

[5] Einstein, A. (1905) *Annalen der Physik*, **322**, 891-921. https://doi.org/10.1002/andp.19053221004 https://onlinelibrary.wiley.com/doi/epdf/10.1002/andp.19053221004

[6] Kaufmann, W. (1901) Die magnetische und electrische Ablenkbarkeit der Bequerelstrahlen und die Scheinbare Masse der elektronen. zvdd—Zentrales Verzeichnis Digitalisierter Drucke.
https://www.deutsche-digitale-bibliothek.de/item/JY5VJK77FHEBMHQXC2DWOPGNPWPMXH4A

[7] Kaufmann, W. (1903) Über die, Elektromagnetische Masse" der Elektronen, Kgl. Gesellschaft der Wissenschaften Nachrichten. In *Mathematisch-Physikalische Klasse aus dem Jahre 1903*, Vandenhoeck & Ruprecht, Deutsch, 91-103.
https://gdz.sub.uni-goettingen.de/id/PPN252457811_1903

[8] Michaud, A. (2016) *Journal of Physical Mathematics*, **7**, 1-15.
https://projecteuclid.org/journals/journal-of-physical-mathematics/volume-7/issue-2/On-Adiabatic-Processes-at-the-Elementary-Particle-Level/10.4172/2090-0902.1000177.full

[9] Michaud, A. (2021) On Adiabatic Processes at the Subatomic Level. In: Purenovic, J., Ed., *Newest Updates in Physical Science Research*, Vol. 4, BP International, London, 30-62. https://doi.org/10.9734/bpi/nupsr/v4/1978F
https://stm.bookpi.org/NUPSR-V4/article/view/1641

[10] Michaud, A. (2013) *International Journal of Engineering Research and Development*, **7**, 50-66. http://www.ijerd.com/paper/vol7-issue5/H0705050066.pdf

[11] Michaud A. (2013) *International Journal of Engineering Research and Development*, **6**, 7-11. http://ijerd.com/paper/vol6-issue12/B06120711.pdf

[12] Michaud, A. (2020) *Journal of Modern Physics*, **11**, 16-80.
https://doi.org/10.4236/jmp.2020.111003
https://www.scirp.org/pdf/jmp_2020010915471797.pdf

[13] Michaud, A. (2020) Emphasizing the Electromagnetism According to Maxwell's Initial Interpretation. In: George, T.F., Ed., *New Insights into Physical Science*, Vol. 10, Book Publisher International, West Bengal, Chapter 4, 35-96.
https://bp.bookpi.org/index.php/bpi/catalog/book/350

[14] Einstein, A. (1910) *Archives des sciences physiques et naturelle*, **29**, 5-28+125-144.
https://einsteinpapers.press.princeton.edu/vol3-doc/169
https://einsteinpapers.press.princeton.edu/vol3-doc/193

[15] Einstein, A. (1910) The Principle of Relativity and its Implications in Modern Physics. Translated by André Michaud and Fritz Lewertoff, In: Petkov, V., Ed., *Relativity: Meaning and Consequences for Modern Physics and for Our Understanding of the World*, Minkowski Institute Press, Montreal, 73-96.
http://www.minkowskiinstitute.org/mip/books/einstein2.html

[16] Michaud, A. (2013) *International Journal of Engineering Research and Development*, **6**, 36-49. http://ijerd.com/paper/vol6-issue10/F06103649.pdf

[17] Lorentz, H.A. (1895) Versuch einer Theorie der electrischen und optischen Erscheinungen in bewegten Körpern, Leiden—E. J. Brill. B.G. Teubner, Leiden.
https://archive.org/details/versucheinerthe00loregoog
https://de.wikisource.org/wiki/Versuch_einer_Theorie_der_electrischen_und_optischen_Erscheinungen_in_bewegten_K%C3%B6rpern
https://en.wikisource.org/wiki/Translation:Attempt_of_a_Theory_of_Electrical_and_Optical_Phenomena_in_Moving_Bodies

[18] Heaviside, O. (1889) XXXIX. On the Electromagnetic Effects Due to the Motion of Electrification through a Dielectric. The London, Edinburgh, and Dublin Philosophical Magazine and Journal of Science, London, 324-339.
https://zenodo.org/record/1431195#.YR-God9KthF

[19] Abraham, M. (1902) Dynamik des Elektrons. Nachrichten von der Gesellschaft der Wissenschaften zu Göttingen, Mathematisch-Physikalische Klasse. 20-41. https://gdz.sub.uni-goettingen.de/id/PPN252457811_1902

[20] Einstein, A. (1905) *Annalen der Physik*, **322**, 132-148. https://doi.org/10.1002/andp.19053220607 https://onlinelibrary.wiley.com/doi/epdf/10.1002/andp.19053220607 http://users.physik.fu-berlin.de/~kleinert/files/eins_lq.pdf

[21] Planck, M. (1900) *Annalen der Physik*, **309**, 553-563. https://doi.org/10.1002/andp.19013090310 https://onlinelibrary.wiley.com/doi/pdf/10.1002/andp.19013090310

[22] Wien, W. (1898) *Annalen der Physik*, **65**, 1-18. https://de.wikisource.org/wiki/Translatorische_Bewegung_des_Licht%C3%A4thers

[23] Einstein, A. (1905) *Annalen der Physik*, **323**, 639-641. https://doi.org/10.1002/andp.19053231314 https://onlinelibrary.wiley.com/doi/epdf/10.1002/andp.19053231314 http://www.fourmilab.ch/etexts/einstein/E_mc2/www/

[24] De Broglie, L. (1993) La physique nouvelle et les quanta. Flammarion, France, 1937, 2nd Edition 1993, with New 1973 Preface by Louis de Broglie.

[25] Michaud, A. (2016) *Journal of Physical Mathematics*, **7**, Article No. 153. https://www.hilarispublisher.com/open-access/on-de-broglies-doubleparticle-photon-hypothesis-2090-0902-1000153.pdf

[26] Michaud, A. (2021) De Broglie's Double-Particle Photon. In: Purenovic, J., Ed., *Newest Updates in Physical Science Research*, Vol. 4, BP International, London, 63-102. https://doi.org/10.9734/bpi/nupsr/v4/1979F https://stm.bookpi.org/NUPSR-V4/article/view/1642

[27] Einstein, A. (1905) *Annalen der Physik*, **322**, 549-560. https://doi.org/10.1002/andp.19053220806 https://onlinelibrary.wiley.com/doi/10.1002/andp.19053220806

[28] Smoluchowski, M. (1906) *Annalen der Physik*, **326**, 756-780. https://doi.org/10.1002/andp.19063261405 https://gallica.bnf.fr/ark:/12148/bpt6k15328k/f770.chemindefer

[29] Perrin, J. (1912) Les Preuves de la réalité moléculaire (Étude spéciale des émulsion). Rapport lu au Congrès Solvay en novembre 1911, in La théorie du rayonnement et des quanta (Gauthier-Villards, 1912, 153-251).

[30] Maxwell, J.C. (1965) *Philosophical Transactions of the Royal Society of London*, **155**, 459-512. http://www.bem.fi/library/1865-001.pdf

[31] Michaud, A. (2013) *International Journal of Engineering Research and Development*, **7**, 32-39. http://ijerd.com/paper/vol7-issue4/G0704032039.pdf

[32] Kaufmann, W. (1902) *Göttinger Nachrichten*, No. 5, 291-296. https://de.wikisource.org/wiki/Die_elektromagnetische_Masse_des_Elektrons

[33] Kaufmann, W. (1902) *Physikalische Zeitschrift*, **4**, 54-57. https://wikilivres.org/wiki/Die_elektromagnetische_Masse_des_Elektrons

[34] Poincaré, H. (1905) La valeur de la science. 1994 Edition, Flammarion, Paris.

[35] Ernst, A. and Hsu, J.P. (2001) *Chinese Journal of Physics*, **39**, 211-230 http://adsabs.harvard.edu/cgi-bin/nph-data_query?bibcode=2001ChJPh..39..211E&link_type=ARTICLE&db_key=PHY&high=

[36] Bucherer, A.H. (1908) *Physikalische Zeitschrift*, **9**, 755-762.

[37] Neumann, G. (1914) *Annalen der Physik*, **350**, 529-579.
https://doi.org/10.1002/andp.19143502005
https://onlinelibrary.wiley.com/doi/10.1002/andp.19143502005

[38] Planck, M. (1906) *Physikalische Zeitschrift*, **7**, 753-761.
https://de.wikisource.org/wiki/Die_Kaufmannschen_Messungen_der_Ablenkbarkeit_der_%CE%B2-Strahlen_in_ihrer_Bedeutung_f%C3%BCr_die_Dynamik_der_Elektronen
https://en.wikisource.org/wiki/Translation:The_Measurements_of_Kaufmann

[39] Poincaré, H. (1908) *Revue général des Sciences pures et appliquées*, **19**, 386-402.
http://henripoincarepapers.univ-lorraine.fr/chp/hp-pdf/hp1908rg.pdf

[40] Holton, G.J. and Elkana, Y. (1980) Albert Einstein, Historical and Cultural Perspectives. *Proceedings of Einstein Centennial Symposium*, Princeton, 14-23 March 1979, 106.
https://catalog.library.vanderbilt.edu/discovery/fulldisplay/alma991006105249703276/01VAN_INST:vanui

[41] Einstein, A. (1907) Über das Relativitätsprinzip und die aus demselben gezogenen Folgerungen. *Jahrbuch der Radioaktivität und Elektronik*, **4**, 411.
https://link.springer.com/chapter/10.1007/978-3-322-83770-7_6

[42] Pais, A. (2008) Subtle is the Lord: The Science and the Life of Albert Einstein. Oxford University Press, Oxford.

[43] Humphries Jr., S. (1986) Principles of Charged Particle Acceleration. John Wiley & Sons.
http://citeseerx.ist.psu.edu/viewdoc/download?doi=10.1.1.382.7882&rep=rep1&type=pdf

[44] Lawrence, E.O. and Livingston, M.S. (1932) *Physical Review*, **40**, 19-35.
https://doi.org/10.1103/PhysRev.40.19
https://journals.aps.org/pr/abstract/10.1103/PhysRev.40.19
https://journals.aps.org/pr/pdf/10.1103/PhysRev.40.19

[45] Marmet, P. (2003) *International IFNA-ANS Journal*, **9**, 120-145.
http://www.newtonphysics.on.ca/magnetic/index.html

[46] Michaud, A. (2017) *Journal of Physical Mathematics*, **8**, Article No. 217.
https://www.hilarispublisher.com/open-access/the-last-challenge-of-modern-physics-2090-0902-1000217.pdf

[47] Michaud, A. (2021) The Last Challenge of Modern Physics: Perspective to Concept and Model Analysis. In: Purenovic, J., Ed., Newest Updates in Physical Science Research, Vol. 4, BP International, London, 1-29.
https://doi.org/10.9734/bpi/nupsr/v4/1977F
https://stm.bookpi.org/NUPSR-V4/article/view/1640

[48] Michaud, A. (2018) *Journal of Modern Physics*, **9**, 1052-1110.
https://doi.org/10.4236/jmp.2018.95067
https://www.scirp.org/journal/paperinformation.aspx?paperid=84158

[49] Michaud, A. (2020) An Overview of The Hydrogen Atom Fundamental Resonance States. In: Rafatullah, M., Ed., *New Insights into Physical Science*, Vol. 6, Book Publisher International, West Bengal, Chapter 5, 54-109.
http://bp.bookpi.org/index.php/bpi/catalog/book/265

[50] De Broglie, L. (1923) *Comptes Rendus*, **177**, 507-510.
http://www.academie-sciences.fr/pdf/dossiers/Broglie/Broglie_pdf/CR1923_p507.pdf

[51] Schrödinger, E. (1926) *Physical Review*, **28**, 1049-1070.

https://doi.org/10.1103/PhysRev.28.1049
https://journals.aps.org/pr/abstract/10.1103/PhysRev.28.1049

[52] Heisenberg, W. (1925) *Zeitschrift für Physik*, **33**, 879-893. https://doi.org/10.1007/BF01328377 https://link.springer.com/article/10.1007/BF01328377

[53] Brown, L.M. (2005) Feynman's Thesis—A New Approach to Quantum Theory. World Scientific, Singapore. https://doi.org/10.1142/5852

[54] Einstein, A., Schrödinger, E., Pauli, W., Rosenfeld, L., Born, M., Joliot-Curie, I.F., Heisenberg, W., Yukawa, H., *et al.* (1953) Louis de Broglie, physicien et penseur. Éditions Albin Michel, Paris.

[55] Schrödinger, E. (1952) *The British Journal for the Philosophy of Science*, **3**, 233-242. https://philpapers.org/rec/SCHATQ-3

[56] Cockcroft, J.D. and Walton, E.T.S. (1932) *Nature*, **129**, 649. https://doi.org/10.1038/129649a0 https://www.nature.com/articles/129649a0

[57] Anderson, C.D. (1933) *Physical Review*, **43**, 491-498. https://doi.org/10.1103/PhysRev.43.491 https://journals.aps.org/pr/pdf/10.1103/PhysRev.43.491

[58] Ciufolini, I. and Wheeler, J.A. (1995) Gravitation and Inertia, Princeton University Press, Princeton. https://doi.org/10.1515/9780691190198

[59] Breidenbach, M., Friedman, J.I., Kendall, H.W., Bloom, E.D., Coward, D.H., DeStaebler, H., *et al.* (1969) *Physical Review Letters*, **23**, 935-939. http://www.slac.stanford.edu/pubs/slacpubs/0500/slac-pub-0650.pdf

[60] Burke, D.L., Field, R.C., Horton-Smith, G., Spencer, J.E., Walz, D., Berridge, S.C., *et al.* (1997) *Physical Review Letters*, **79**, 1626-1629. https://doi.org/10.1103/PhysRevLett.79.1626 http://www.slac.stanford.edu/exp/e144/ http://journals.aps.org/prl/abstract/10.1103/PhysRevLett.79.1626

[61] Kotler, S., Akerman, N., Navon, N., Glickman, Y. and Ozeri, R. (2014) *Nature*, **510**, 376-380. https://doi.org/10.1038/nature13403 https://www.nature.com/articles/nature13403.epdf?referrer_access_token=yoC6RXrPyxwvQvi-ChYrG0tRgN0jAjWel9jnR3ZoTv0PdPJ4geER1fKVR1YXH8GThqECstdb6e48mZm0qQo2OMX_XYURkzBSUZCrxM8VipvnG8FofxB39P4lc-1UIKEO1

[62] Michaud, A. (2017) *Journal of Astrophysics & Aerospace Technology,* **5**, Article No. 152. https://www.hilarispublisher.com/open-access/gravitation-quantum-mechanics-and-the-least-action-electromagneticequilibrium-states-2329-6542-1000152.pdf

[63] Michaud, A. (2020) Gravitation, Quantum Mechanics and the Least Action Electromagnetic Equilibrium States. In: Lopez, A., Ed., *Prime Archives in Space Research*, Vide Leaf, Hyderabad, 1-70. https://doi.org/10.37247/PASR.1.2020.1 https://videleaf.com/gravitation-quantum-mechanics-and-the-least-action-electromagnetic-equilibrium-states/

[64] Michaud, A. (2000) On an Expanded Maxwellian Geometry of Space. *Proceedings of Congress*-2000—*Fundamental Problems of Natural Sciences and Engineering*, Vol. 1, St. Petersburg, 3-8 July 2000, 291-310. https://www.researchgate.net/publication/357527119_On_an_Expanded_Maxwellian_Geometry_of_Space

[65] Michaud, A. (2007) *International IFNA-ANS Journal*, **13**, 123-140.

https://www.researchgate.net/publication/282646291_Field_Equations_for_Localized_Photons_and_Relativistic_Field_Equations_for_Localized_Moving_Massive_Particles

[66] Michaud, A. (2012) Expanded Maxwellian Geometry of Space. SRP Books, Smashwords. https://www.smashwords.com/books/view/163704

[67] Michaud, A. (2013) *International Journal of Engineering Research and Development*, **6**, 31-45. http://ijerd.com/paper/vol6-issue8/G06083145.pdf

[68] Michaud, A. (2013) *International Journal of Engineering Research and Development*, **6**, 1-10. https://www.researchgate.net/publication/282353551_From_Classical_to_Relativistic_Mechanics_via_Maxwell

[69] Michaud, A. (2013) *International Journal of Engineering Research and Development*, **6**, 27-34. http://www.ijerd.com/paper/vol6-issue6/F06062734.pdf

[70] Michaud, A. (2013) *International Journal of Engineering Research and Development*, **7**, 21-25. http://ijerd.com/paper/vol7-issue3/E0703021025.pdf

[71] Schwinger, J. (1948) *Physical Review*, **73**, 416-417. https://doi.org/10.1103/PhysRev.73.416 https://journals.aps.org/pr/abstract/10.1103/PhysRev.73.416

[72] Michaud, A. (2013) *International Journal of Engineering Research and Development*, **7**, 1-8. http://www.ijerd.com/paper/vol7-issue7/A07070108.pdf

[73] Michaud, A. (2013) *International Journal of Engineering Research and Development*, **7**, 29-53. http://ijerd.com/paper/vol7-issue9/E0709029053.pdf

[74] Michaud, A. (2013) *International Journal of Engineering Research and Development*, **7**, 1-9. http://www.ijerd.com/paper/vol7-issue11/A07110109.pdf

[75] Michaud, A. (2013) *International Journal of Engineering Research and Development*, **8**, 10-33. http://ijerd.com/paper/vol8-issue1/B08011033.pdf

[76] Aschwanden, M. (2006) Physics of the Solar Corona. Springer, Berlin.

[77] Lowrie, W. (2007) Fundamentals of Geophysics. 2nd Edition, Cambridge University Press, Cambridge. https://doi.org/10.1017/CBO9780511807107

[78] Kühne, R.W. (1998) Remark on "Indication, from Pioneer 10/11, Galileo, and Ulysses Data, of an Apparent Anomalous, Weak, Long-Range Acceleration. arXiv: gr-qc/9809075v1. https://arxiv.org/pdf/gr-qc/9809075.pdf

[79] Michaud, A. (2017) Electromagnetic Mechanics of Elementary Particles. 2nd Edition, Scholar's Press, Saarbrücken. https://www.morebooks.de/store/gb/book/electromagnetic-mechanics-of-elementary-particles/isbn/978-3-330-65345-0

[80] Michaud, A. (2020) Introduction to Electromagnetism According to Maxwell: (Electromagnetic Mechanics). Generis Publishing, Chișinău. http://generis-publishing.com/book.php?title=introduction-to-electromagnetism-according-to-maxwell-electromagnetic-mechanics

[81] Michaud, A. (2021) Our Electromagnetic Universe. In: Rafatullah, M., Ed., *Newest Updates in Physical Science Research*, Vol. 12, BP International, London, 64-82. https://doi.org/10.9734/bpi/nupsr/v12/11459D

[82] Michaud, A. (2016) *American Journal of Modern Physics*, **5**, 44-52. http://article.sciencepublishinggroup.com/pdf/10.11648.j.ajmp.s.2016050401.17.pdf

[83] Stodolna, A.S., Rouzée, A., Lépine, F., Cohen, S., Robicheaux, F., Gijsbertsen, A., *et al.* (2013) *Physical Review Letters*, **110**, Article ID: 213001. http://prl.aps.org/abstract/PRL/v110/i21/e213001

[84] Hafele, J.C. and Keating, R.E. (1972) *Science*, **177**, 166-168. https://doi.org/10.1126/science.177.4044.166 http://www.personal.psu.edu/rq9/HOW/Atomic_Clocks_Experiment.pdf

[85] Anderson, J.D., Laing, A., Lau, E.L., Liu, A.S., Nieto, M.M., *et al.* (1998) Indications from Pioneer 10/11, Galileo, and Ulysses Data, of an Apparent Anomaleous, Weak, Long-Range Acceleration. gr-qc/9808081, v2. http://arxiv.org/pdf/gr-qc/9808081v2.pdf

[86] Nieto, M.M., Goldman, T., Anderson, J.D., Lau, E.L. and Perez-Mercader, J. (1994) Theoretical Motivation for Gravitation Experiments on Ultra low Energy Antiprotons and Antihydrogen. hep-ph/9412234. http://arxiv.org/pdf/hep-ph/9412234.pdf

[87] Anderson, J.D., Campbell, J.K. and Nieto, M.M. (2006) The Energy Transfer Process in Planetary Flybys. Astro-ph/0608087v2. http://arxiv.org/pdf/astro-ph/0608087.pdf

[88] Anderson J.D., Laing, P.A., Lau, E.L., Liu, A.S., Nieto, M.M. and Turyshev, S.G. (2005) *Physical Review D*, **65**, Article ID: 082004. https://doi.org/10.1103/PhysRevD.65.082004 https://arxiv.org/abs/gr-qc/0104064

[89] Michaud, A. (2011) *International Journal of Engineering Research and Development*, **8**, 10-33. https://www.researchgate.net/publication/359227304_Proposal_of_an_invariant_mass_reference_for_the_kilogram

[90] Lide, D.R. (Editor-in-chief) (2003) CRC Handbook of Chemistry and Physics. 84th Edition 2003-2004, CRC Press, New York.

[91] Mordovanakis, A.G., Easter, J., Naumova, N., Popov, K., Masson-Laborde, P.-E., Hou, B., *et al.* (2009) *Physical Review Letters*, **103**, Article ID: 235001. https://journals.aps.org/prl/abstract/10.1103/PhysRevLett.103.235001

[92] Blewett, J.P. (1946) *Physical Review*, **69**, 87-95. https://doi.org/10.1103/PhysRev.69.87 https://journals.aps.org/pr/abstract/10.1103/PhysRev.69.87

[93] Hanson, G., Agrams, G.S., Boyarski, A.M., Breidenbach, M., Bulos, F., Chinowsky,, W., Feldman, G.J., *et al.* (1975) *Physical Review Letters*, **35**, 1609-1612. https://journals.aps.org/prl/abstract/10.1103/PhysRevLett.35.1609

[94] Hassani, S. (1999) Mathematical Physics. Springer-Verlag, New York.

[95] Van Leunen, J. (2021) The Standard Model of Particle Physics and the Hilbert Repository. The Hilbert Book Model Project. https://vixra.org/abs/2103.0188

[96] Van Leunen, J. (2021) Elemental and Structured Spaces. The Hilbert Book Model Project. https://vixra.org/abs/2102.0087

[97] Michaud, A. (2017) *Journal of Biometrics & Biostatistics*, **8**, Article No. 331. https://www.hilarispublisher.com/open-access/on-the-relation-between-the-comprehension-ability-and-the-neocortexverbal-areas-2155-6180-1000331.pdf

[98] Michaud, A. (2021) Relating the Comprehension Ability to the Neocortex Verbal

Areas: A Brief Study. In: Borek, S., Ed., *New Visions in Biological Science*, Vol. 1, BP International, London, 136-164. https://doi.org/10.9734/bpi/nvbs/v1/1787C
https://stm.bookpi.org/NVBS-V1/article/view/3183

[99] Michaud, A. (2019) *Creative Education*, **10**, 353-406.
https://doi.org/10.4236/ce.2019.102028
http://www.scirp.org/pdf/CE_2019022016190620.pdf

[100] Michaud, A. (2020) Advancement on the Mechanics of Conceptual Thinking. In: Jain, S.K. and Mag, A.G., Eds., *New Horizons in Education and Social Studies*, Vol. 6, Book Publisher International, West Bengal, 81-124.
https://bp.bookpi.org/index.php/bpi/catalog/book/338

[101] Trail, D. (2022) *Applied Physics Research*, **14**, 59-99.
https://doi.org/10.5539/apr.v14n1p59
https://ccsenet.org/journal/index.php/apr/article/view/0/47058

[102] Slater, J.C. (1964) *The Journal of Chemical Physics*, **41**, 3199-3204.
https://doi.org/10.1063/1.1725697
https://aip.scitation.org/doi/10.1063/1.1725697

[103] Clementi, E., Raimondi, D.L. and Reinhardt, W.P. (1967) *The Journal of Chemical Physics*, **47**, 1300-1307. https://doi.org/10.1063/1.1712084
https://aip.scitation.org/doi/10.1063/1.1712084

Appendix A

This Appendix establishes the procedure to calculate the atomic radii for unbound atoms by means of the second term of the Lorentz force equation traditionally used to calculate the radius of circular orbits for charged particles in high-energy accelerators, considering that the same amount of energy is required to maintain an electron on a closed resonant orbit about the nucleus of an isolated hydrogen atom, or to maintain it in an axial resonance state at the same mean distance from the nucleus without it necessarily moving on a closed orbit as explained in Section 10, by calculating the mean distance between the nucleus and the outermost orbital of atoms using the wavelength of the first ionization energy of each atom (Column A). Some of these radii for atoms mentioned in this paper are shown in Table 1 (Columns D and E).

A.1. Calculation Procedure

Calculation of the values of Column E was carried out with a Texas Instrument TI-89 Titanium calculator.

Taking the Helium atom first ionization energy value of 24.58741 eV (Column A in Table 1) as an example, here is how each atomic radius of Column E can be calculated by means of Equation (53), repeated here for convenience (see Section 10):

$$d = \frac{\gamma m_0 v}{e\boldsymbol{B}} \tag{53}$$

First, the first ionization value in eV of the atom—here that of the helium atom—is converted to joules by multiplying it by the invariant charge of the electron (1.602176462E−19 C):

$$E = 24.58741 \cdot e = 3.939336956\text{E}-18 \text{ j} \tag{A.1}$$

This value is then doubled to account for both components of the carrying energy induced by the Coulomb interaction at the corresponding mean distance from the helium nucleus, corresponding to the first two terms of Equation (50), corresponding in fact to Equation (47), reproduced here for convenience:

$$2E = \Delta K + \Delta m_m c^2 = 3.939336956\text{E}-18 \times 2 = 7.878673913\text{E}-18 \text{ j} \tag{47}$$

The related wavelength is then calculated by means of the standard equation:

$$\lambda = \frac{hc}{2E} = 2.521284145\text{E}-8 \text{ m} \tag{A.2}$$

Making use of the electron Compton wavelength (λ_c = 2.426310215E−12 m), the corresponding relativistic velocity is calculated by means of Equation (33):

$$v = c\frac{\sqrt{\lambda_C\left(4\lambda + \lambda_C\right)}}{2\lambda + \lambda_C} = 2940812.243 \text{ m/s} \tag{33}$$

The term $\gamma m_0 v$ of Equation (53) can then be resolved as follows, resolving the γ-factor with the velocity obtained from Equation (33):

$$\gamma m_0 v = \frac{2E}{v} = 2.679080901\text{E}-24 \tag{A.3}$$

The value of the magnetic field $\boldsymbol{B}$ corresponding to wavelength λ calculated with Equation (A.2) is then obtained with the following equation:

$$\boldsymbol{B}_{(\lambda)} = \frac{2\pi(2E)}{ce\alpha^2\lambda} = 7676725.6829\ \text{T} \tag{A.4}$$

Then, given that the variable values of Equation (53) have been resolved, it can in turn be resolved for the first ionization energy of the helium atom with the values provided by Equations (A.3) and (A.4) to provide the related atomic radius:

$$d = \frac{\gamma m_0 v}{e\boldsymbol{B}_{(\lambda)}} = 2.178341596\text{E}-11\ \text{m} \tag{53}$$

in which d would be the approximate radius of the isolated helium atom as estimated via the second term of the Lorentz force equation. This value is listed rounded in picometers in column D of **Table 1** for direct comparison with the values of Columns B and C, and listed in meters in column E in standard physics notation with the radii of other atoms of the periodic table.

Column A provides the list of the first ionization values for each atom of the periodic table, taken from Reference ([90]. p.10-178).

For comparison purposes with other atomic radii calculation methods, columns B and C respectively list the values for the Empirical Bound Ionic Method [102] and the Calculated Atomic method [103].

Table 1. Table of atomic radii—not bound.

		A	B	C	D	E
	Symbol	Ionization energy in eV	Empirical bound ionic	Calculated atomic	Calculated not bound $\gamma m_0 v/e\boldsymbol{B}$ rounded	Calculated not bound $\gamma m_0 v/e\boldsymbol{B}$
1	H	13.59844	25	53	53	5.296111314E−11
2	He	24.58741	120	31	22	2.178354555E−11
3	Li	5.39172	145	167	212	2.121269975E−10
12	Mg	7.64624	150	145	125	1.256073509E−10
76	Os	8.4382	130	185	108	1.083459614E−10
92	U	6.19405	175	No data	172	1.722756745E−10

Call for Papers

Journal of Modern Physics

ISSN: 2153-1196 (Print) ISSN: 2153-120X (Online)
https://www.scirp.org/journal/jmp

Journal of Modern Physics **(JMP)** is an international journal dedicated to the latest advancement of modern physics. The goal of this journal is to provide a platform for scientists and academicians all over the world to promote, share, and discuss various new issues and developments in different areas of modern physics.

Editor-in-Chief

Prof. Yang-Hui He City University, UK

Subject Coverage

Journal of Modern Physics publishes original papers including but not limited to the following fields:

Biophysics and Medical Physics
Complex Systems Physics
Computational Physics
Condensed Matter Physics
Cosmology and Early Universe
Earth and Planetary Sciences
General Relativity
High Energy Astrophysics
High Energy/Accelerator Physics
Instrumentation and Measurement
Interdisciplinary Physics
Materials Sciences and Technology
Mathematical Physics
Mechanical Response of Solids and Structures
New Materials: Micro and Nano-Mechanics and Homogeneization
Non-Equilibrium Thermodynamics and Statistical Mechanics
Nuclear Science and Engineering
Optics
Physics of Nanostructures
Plasma Physics
Quantum Mechanical Developments
Quantum Theory
Relativistic Astrophysics
String Theory
Superconducting Physics
Theoretical High Energy Physics
Thermology

We are also interested in: 1) Short Reports—2-5 page papers where an author can either present an idea with theoretical background but has not yet completed the research needed for a complete paper or preliminary data; 2) Book Reviews—Comments and critiques.

Notes for Intending Authors

Submitted papers should not have been previously published nor be currently under consideration for publication elsewhere. Paper submission will be handled electronically through the website. All papers are refereed through a peer review process. For more details about the submissions, please access the website.

Website and E-Mail

https://www.scirp.org/journal/jmp **E-mail: jmp@scirp.org**

What is SCIRP?

Scientific Research Publishing (SCIRP) is one of the largest Open Access journal publishers. It is currently publishing more than 200 open access, online, peer-reviewed journals covering a wide range of academic disciplines. SCIRP serves the worldwide academic communities and contributes to the progress and application of science with its publication.

What is Open Access?

All original research papers published by SCIRP are made freely and permanently accessible online immediately upon publication. To be able to provide open access journals, SCIRP defrays operation costs from authors and subscription charges only for its printed version. Open access publishing allows an immediate, worldwide, barrier-free, open access to the full text of research papers, which is in the best interests of the scientific community.

- High visibility for maximum global exposure with open access publishing model
- Rigorous peer review of research papers
- Prompt faster publication with less cost
- Guaranteed targeted, multidisciplinary audience

Scientific Research Publishing

Website: https://www.scirp.org

Subscription: sub@scirp.org

Advertisement: service@scirp.org